

**Formation of the Immunoglobulin
Repertoire in Precursor-B-cell Development**

Magdalena Beata Rother



The studies described in this thesis were performed at the Department of Immunology, Erasmus MC, University Medical Center, Rotterdam, The Netherlands and collaborating institutions.

The studies were financially supported by ZonMW Veni grant 916.116.090. The research of this thesis was performed within the framework of the Erasmus Postgraduate School Molecular Medicine.

The printing of this thesis was supported by Erasmus MC, Erasmus Postgraduate School Molecular Medicine and BD Biosciences.

ISBN: 978-94-91811-10-4

Illustrations: Magdalena B. Rother

Cover and Lay-out: Mariusz Krawitowski & Magdalena B. Rother

Printing: Ridderprint B.V., Ridderkerk

Copyright © 2015 by Magdalena B. Rother.

All rights reserved. No part of this book may be reproduced, stored in a retrieval system or transmitted in any form or by any means, without prior permission of the author.

**Formation of the Immunoglobulin
Repertoire in Precursor-B-cell Development**

De vorming van het immunoglobuline
repertoire tijdens voorloper-B-celontwikkeling

Doctoral dissertation

For the purpose of being admitted to the degree of Doctor at
Erasmus University Rotterdam
on the authority of the Rector Magnificus

Prof.dr. H.A.P. Pols

and in accordance with the decision of the Doctorate Board

The public defense ceremony shall take place on
Wednesday 11 November 2015 at 13.30 hours by

Magdalena Beata Rother

born in Bytom, Poland

Erasmus University Rotterdam



Doctoral Committee

Promoter: Prof.dr. J.J.M. van Dongen

Other members: Prof.dr. C. Murre
Prof.dr. R.W. Hendriks
Dr. T. Cupedo

Co-promoter: Dr. M.C. van Zelm

mojemu mężowi

CONTENTS

Chapter I	General Introduction	8
Chapter II	Pre-B cell receptor signaling induces immunoglobulin κ locus accessibility by functional redistribution of enhancer-mediated chromatin interactions	40
Chapter III	Nuclear positioning rather than contraction controls ordered rearrangements of immunoglobulin loci	76
Chapter IV	Increased ID2 levels in adult precursor-B cells as compared with children is associated with impaired Ig locus contraction and decreased bone marrow output	100
Chapter V	Altered V(D)J recombination underlies the skewed immunoglobulin repertoires in normal and malignant B-cell precursors from fetal origin	126
Chapter VI	The human thymus is enriched for autoreactive B cells	164
Chapter VII	General Discussion	190
Addendum	List of abbreviations Summary Samenvatting Acknowledgements PhD Portfolio Curriculum Vitae List of publications	212



Chapter I

General Introduction

The vertebrate immune system detects and eliminates a wide spectrum of pathogens including viruses, bacteria and parasites to protect against infection. In mammals, such as humans, the immune system contains three lines of defense against invading pathogens: 1) physical and chemical barriers formed by the skin and mucous membranes,^{1, 2} 2) immune cells and molecules that promote innate responses³ and 3) adaptive responses mediated by B and T lymphocytes. All immune cells originate from hematopoietic stem cells (HSC) that reside in the bone marrow (BM). During hematopoiesis, HSC-derived progenitor cells are progressively restricted into distinct cell lineages controlled by specific transcription programs (**Figure 1**).⁴ Innate immune cells are crucial for fast host responses. They recognize general foreign structures and eliminate pathogens through phagocytosis (granulocytes and macrophages) or cytotoxicity (natural killer cells).³ B and T lymphocyte responses take more time. They bind to pathogens with highly specific antigen receptors. The few cells that specifically recognize the pathogens proliferate to enhance the response, thereby adapting the antigen receptor affinity to improve the recognition of pathogens. This improved response is subsequently maintained in the form of immunological memory, i.e. long-lived memory B and T cells that provide a faster response to the same pathogen during next encounter.

The capability of B and T lymphocytes to recognize the enormous diversity of pathogens is underlined by the unique antigen-specific receptors generated during early stages of B and T-cell development. The antigen receptors are encoded by immunoglobulin (Ig) and T-cell receptor (TR) loci that contain various coding elements. Random assembly of these elements provides the broad and diverse repertoire of antigen-specific receptors. The assembly occurs via somatic V(D)J recombination and requires a tight control. Alterations at any step of these processes may lead to formation of different or abnormal antigen-receptor repertoire.

This thesis is focused on the mechanisms underlying the stage-specific regulation of V(D)J recombination and the generation of a diverse antigen-receptor repertoire during precursor-B-cell development.

B-CELL DEVELOPMENT IN BONE MARROW

B cells create the humoral part of the adaptive response and contribute to the clearance of pathogens through production of immunoglobulins (Ig). Ig can be secreted as soluble molecules (antibodies) or expressed on the B-cell surface as B-cell antigen receptors (BCR). The ultimate goal of precursor-B-cell differentiation in bone marrow (BM) is to generate a unique BCR, whereby all B cells together provide an enormous Ig repertoire diversity.

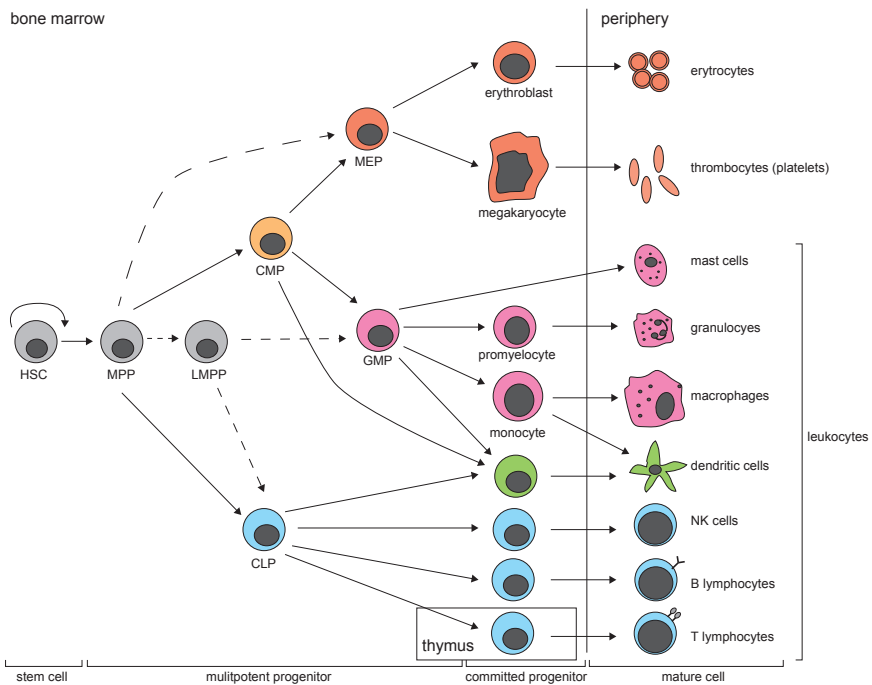


Figure 1. Schematic representation of hematopoiesis. Hematopoiesis occurs in bone marrow and occurs throughout the life. Long-lived and self-renewing hematopoietic stem cells (HSC) give rise to a number of different progenitor stages that become progressively restricted towards a specific cell lineage.⁴ The dotted arrows represent an alternative model of hematopoiesis which postulate existence of LMPP giving rise to CLP and GMP, and direct formation of MEP from MPP.³ MPP, multipotent progenitor; LMPP, lymphoid-primed multipotent progenitor; CLP, common lymphoid progenitor; CMP, common myeloid progenitor; GMP, granulocyte/monocyte progenitor; MEP, megakaryocyte/erythrocyte progenitor; NK, natural killer. The Figure was adapted from Bryder *et al.*, 2006, *Am J Pathol.*⁴

B-cell commitment

After birth, B cells are continuously generated throughout life from hematopoietic stem cells (HSC) that reside in BM and are long-lived with self-renewing capacity. In mouse models, it has been established that B-cell precursors differentiate through several consecutive stages controlled by a tight balance between various transcription factors (**Figures 1 and 2**).^{6,7} First, HSC give rise to multilineage progenitors. Subsequently, the expression of PU.1, Ikaros and growth factor receptor FLT3 restrict the multilineage progenitors to either the lymphoid or myeloid lineage. High levels of Ikaros and low levels of PU.1 direct the cells to lymphoid lineage, while high PU.1 expression induces myeloid cell fate. Next, common lymphoid progenitors induce expression of IL-7R which antagonizes myeloid development and supports lymphoid development.⁸⁻¹¹ Subsequently,

upregulation of E2A further blocks the myeloid cell fate and promotes formation of lymphoid progenitors that can differentiate into B cells, T cells or NK cells (**Figure 2**).^{7, 12} E2A is one of the most important transcription factors in developing B cells. It belongs to the basic helix-loop-helix (bHLH) family of transcription factors and exists in two splice variants: E12 and E47. Similar to the other bHLH proteins, E2-2 and HEB, E2A can bind specific DNA sequences, E-boxes, as homo- or heterodimers.^{13, 14} B cells mainly express E47 homodimers.¹⁵ Inhibition of E2A by ID2 protein at this stage of development may recruit the cells to the NK lineage.¹⁶⁻¹⁸

Next, PU.1, E2A and FOXO1 further upregulate expression of EBF transcription factor. EBF specifies the B-cell fate and directs differentiation of lymphoid progenitors into pre-pro-B cells.¹⁹⁻²² These cells are not yet fully committed to the B-cell lineage and show a high degree of T-cell lineage plasticity.¹² Notch signaling may still skew the pre-pro-B-cell development into T-cell lineage.²³ Finally, E2A, EBF and FOXO1 promote expression of multiple B-cell specific factors, including the most crucial Pax5. Pax5 ensures irreversible commitment of pre-pro-B cells to pro-B cells through upregulation of EBF and downregulation of Notch signaling and ID2. Moreover, Pax5 directs expression of B-cell specific molecules such as CD19.^{21, 22, 24} Pax5 and EBF transcription factors are expressed only in B-lineage cells and have the ability to silence non-B-cell genes and to activate B-cell genes. This gives the B-cell program its tight coherence and provides full commitment (**Figure 2**).^{25, 26}

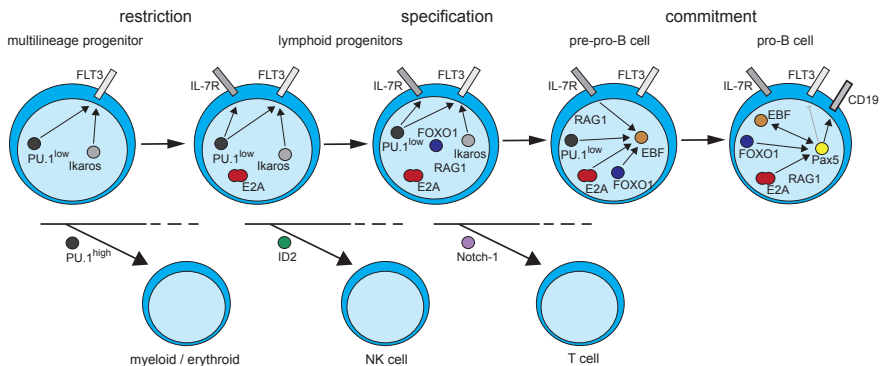


Figure 2. Hematopoietic stem cells (HSC) commitment to the B-cell lineage. HSC in bone marrow give rise to multilineage progenitors able to differentiate into all blood cells. Restriction, specification and commitment to each blood cell lineage depends on a tight balance between various transcription factors. High levels of Ikaros and low levels of PU.1 restricts the multilineage progenitors into lymphoid progenitors, which further upon induction of IL-7R signaling, E2A, FOXO1 and RAG1 are specified to the B-cell lineage. ID2 and Notch-1 proteins may still re-direct the cell plasticity into NK-cell and T-cell fate. Upon expression of EBF the pre-pro-B cells differentiate into pro-B cells and finally Pax5 ensures full commitment to the B-cell lineage. Arrows indicate positive interactions and \perp indicates repression. The Figure was adapted from Nutt *et al.*, 2007, *Immunity*⁷ and Berkowska *et al.*, 2011, *Ann NY Acad Sci.*²⁷

B-cell differentiation and ordered immunoglobulin gene rearrangements

B-cell differentiation in BM takes place in 5 consecutive differentiation stages (**Figure 3A**).^{4, 28-33} This differentiation is similar between man and mice and ensures the generation of unique Ig molecules composed of two Ig heavy chains (IgH) and two Ig light chains (Igκ or Igλ) encoded by rearranged Ig loci. In lymphoid progenitor cell Ig loci lack a functional first coding exon and instead they contain multiple coding elements. The first functional coding exon is generated through somatic rearrangement of these elements during B-cell differentiation process (**Figure 3B**),^{34, 35} which is paralleled by an ordered upregulation and downregulation of lineage-specific markers (**Figure 3C**).^{36, 37} Two common precursors-B cell nomenclature system by Osmond^{28, 38} (adapted for mice) and by Melchers and Rolink³⁹ (adapted for man) distinguish the B-cell developmental stages based on the Ig gene rearrangement processes and expression of specific markers.

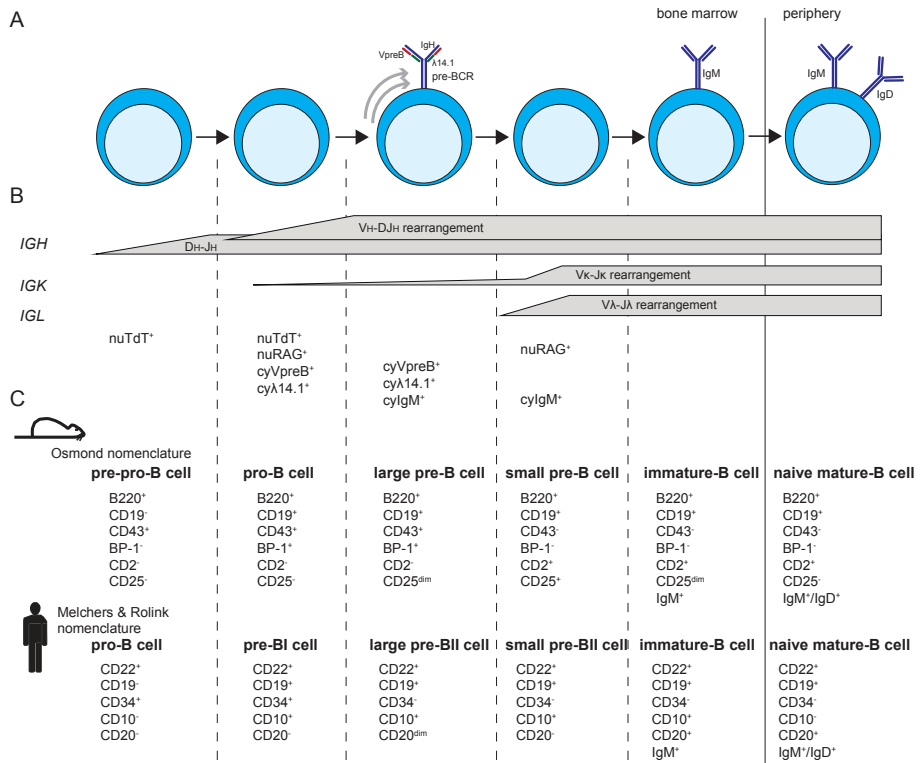


Figure 3. B-cell differentiation in bone marrow. (A) Precursor-B cells differentiate in bone marrow through 5 distances stages. (B) During the differentiation, precursor-B cells rearrange Ig genes to finally create functional and diverse B-cell receptors expressed on mature cells migrating out of bone marrow. (C) The distinct stages of differentiation can be distinguished through surface and intracellular expression of several markers. The nomenclature of B-cell-differentiation stages and usage of expression marker varies between mouse and human. Two

commonly used precursor-B cell nomenclature systems are these by Osmond^{28,38} and by Melchers and Rolink.³⁹ The Figure was adapted from Hardy *et al.*, 2001, *Annu Rev Immunol*³⁷ and van Zelm *et al.*, 2005, *J Immunol*.³⁶

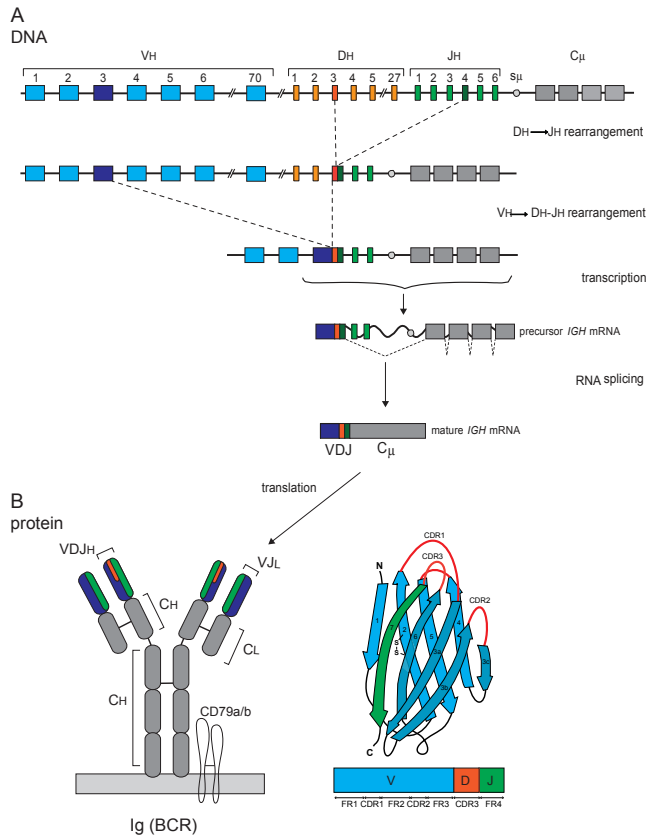


Figure 4. *IGH* gene rearrangement and immunoglobulin structure. (A) VDJ recombination in *IGH* locus initiates through DH to JH rearrangement and proceeds with coupling of VH gene to the DJH joint. Subsequently, the VDJH exon is transcribed and spliced to the *IGHM* exon followed by translation to Ig μ protein. Similar recombination events within *IGL* loci lead to formation of functional IgL protein. Finally, IgH and IgL chains are paired into complete Ig (BCR) which is expressed on the B-cell membrane with CD79a and CD79b proteins (B, left panel). (B, right panel) The IgH variable domain is composed of 4 framework regions (FR) separated by 3 complementary determining regions (CDR) forming loops responsible for antigen binding. The Figure was adapted from thesis of Prof. dr. J.J.M. van Dongen, from thesis of Dr. M.C. van Zelm and from thesis of Dr. M.A. Berkowska.

Ig gene rearrangements occur in a stepwise manner, i.e. Ig heavy chain locus (*IGH*) is rearranged before Ig light chain loci (*IGK* or *IGL*). *IGH* assembly begins with DH to JH rearrangement initiated in pro-B cells (mouse: pre-pro-B cells). This is followed in pre-BI cells (mouse: pre-B cells) with genomic coupling of one of the VH genes to the already formed incomplete DH-JH joint to generate a complete VH-DJH rearrangement (Figures 3A-B and 4A).^{32, 36, 40} DH-JH rearrangements occur generally on both *IGH* alleles^{31, 41} and

are not exclusive for B cells, as up to 48% of common lymphoid progenitors carry these $DH-JH$ rearrangements.¹² The $VH-DJH$ rearrangements, however, are specific for B cells and are initially induced only on one allele. The second *IGH* allele is poised for rearrangement only if the first rearrangement was unsuccessful. If the rearrangement attempt was successful on one allele, the second non-rearranging allele undergoes allelic exclusion. Subsequently, the rearranged genes are transcribed, spliced and translated into IgH protein (**Figure 4B**). Because V and J genes can be read only in one reading frame and stop codons can be introduced in the coding joints, only less than one-third of rearrangements leads to a functional protein.

Following the successful assembly of IgH, Ig light chain gene rearrangements are induced in pre-BII small cells (mouse: pre-B small cells) (**Figure 3A-B**). Still, a minor fraction of B cells rearranges Ig light chain loci before formation of productive IgH.⁴² Because the Ig light chain loci do not contain D genes, the Ig light chain gene rearrangements occur through joining of one of the V with one of the J genes. The V-J rearrangements are first induced on one *IGK* allele and only if both *IGK* alleles render a non-functional rearrangement, the *IGL* alleles will be recombined. In addition, the presence of many V and J genes and only single step of rearrangement allows for multiple attempts on the same allele, known as receptor editing: if a non-functional rearrangement is formed, an upstream V and a downstream J gene can rearrange and thereby removes the preexisting V-J rearrangement from the genome.

IL-7R and pre-B-cell receptor signaling

IL-7R and pre-BCR signaling are key mediators of the order in Ig gene rearrangements. In pro-B cells, the IL-7R signaling opens the *IGH* locus for rearrangements by facilitating the locus contraction.⁴³ The IL-7R signaling also modifies the histone code through activation of STAT5. In pro-B cells, STAT5 regulates germline transcription and histone acetylation of the distal VH region,⁴⁴ whereas within the *IGK* locus, IL-7R signaling recruits STAT5 tetramers to $iE\kappa$ which further induces Ezh2 methyltransferase and thereby silences the *IGK* locus through H3K27me3 modifications.⁴⁵ In pre-B cells, the primary function of IL-7R is to maintain and expand the cells (**Figure 5**). IL-7R activates STAT5⁴⁶⁻⁴⁸ which further induces transcription of cell-cycle checkpoint protein cyclin D3^{49, 50} and anti-apoptotic factors such as BCL2, BCLXL and MCL1.⁵¹⁻⁵³ Complementary signaling through the phosphoinositide 3-kinase (PI3K)-AKT pathway represses FOXO1, an inducer of RAG1 and RAG2 gene transcription.^{54, 55}

By contrast, the pre-BCR inhibits proliferation and induces Ig light chain gene rearrangement (**Figure 5**).^{33, 56-58} The pre-BCR is formed after functional $VDJH$ rearrangement through assembly of the $Ig\mu$ with the surrogate light chain molecules $VpreB$ and

λ 14.1. Aggregation of the pre-BCR and auto-crosslinking of the surrogate light chains is sufficient to induce the signaling which is mediated by basic amino acids in the non-immunoglobulin tail of λ 14.1.⁵⁹⁻⁶¹ Upon pre-BCR cross-linking, the protein-tyrosine kinase LYN phosphorylates immunoreceptor tyrosine-based activation motifs (ITAMs) in CD79a and CD79b. Recruitment of LYN and activation of BLNK promotes the RAS-RAF-MEK-ERK pathway,^{62, 63} which represses cyclin D3 and ID3, while induces E2A.⁶⁴ Increasing levels of free nuclear E2A together with IRF4, downstream of BLNK, coordinately enhance Ig light chain gene accessibility and rearrangements.⁶⁵ Allelic exclusion of the second non-rearranged *IGH* allele is established via SYK and PLC γ signaling.^{66, 67}

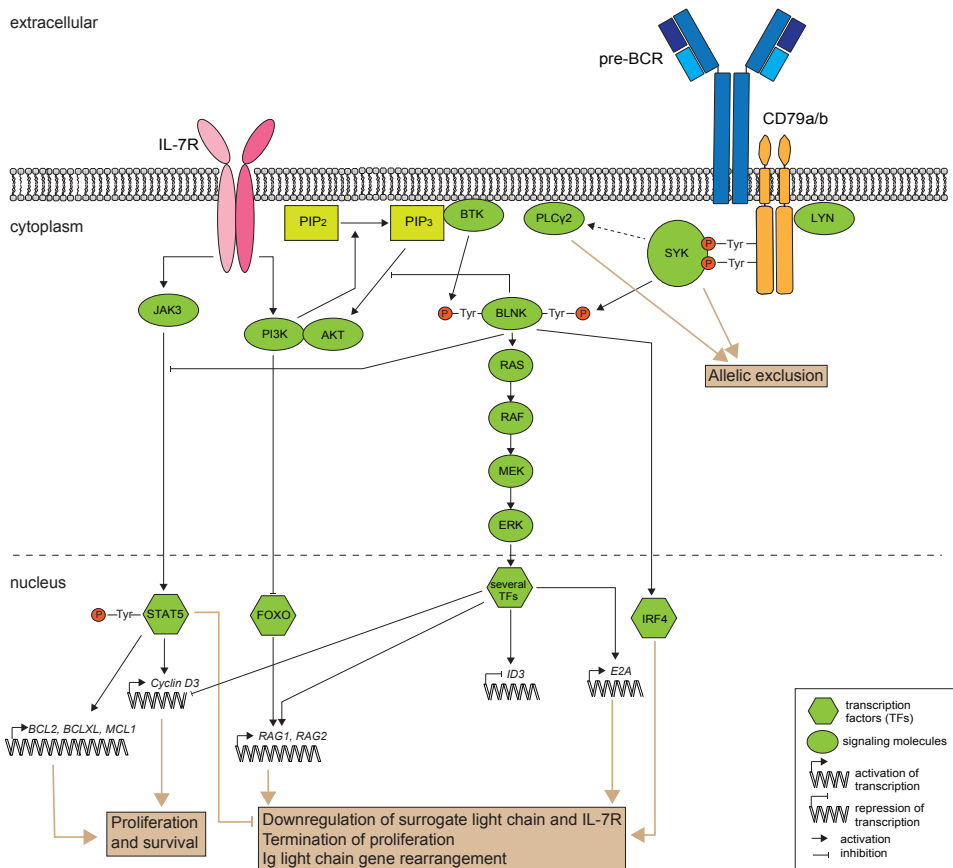


Figure 5. IL-7R and pre-B-cell receptor signaling. IL-7R and pre-BCR provide distinct downstream signaling pathways which ensure that proliferation and immunoglobulin recombination are mutually exclusive. Signaling through IL-7R activates STAT5 and PI3K-AKT pathway which induce cell proliferation and survival, while repress Ig light chain gene rearrangements. Pre-BCR signaling by contrast via SYK and BLNK activates RAS-ERK pathway thereby attenuating cell cycling and promoting Ig light chain gene rearrangements. Downstream

signaling of pre-BCR via PLC γ 2 and SYK ensures allelic exclusion of the second non-rearranged *IGH* allele. The Figure was adapted from Clark *et al.*, 2014, *Nat Rev Immunol*⁵⁷ and Rickert, 2013, *Nat Rev Immunol*.⁵⁸

Preferential coupling of the PI3K pathway to the IL-7R, and not to the pre-BCR, ensures that each receptor has opposing and antagonistic functions.⁶⁸ Thus, in the presence of IL-7, the pre-BCR cannot fully act. After a pre-B cell has attenuated or escaped IL-7R signaling, likely through Ikaros,^{69, 70} the SYK–BLNK represses PI3K–AKT which augments FOXO1 activity and commits to the Ig light chain gene rearrangements (**Figure 5**).^{54, 55}

Early B-cell tolerance checkpoints

Upon successful rearrangement of an Ig light chain gene, at the immature-B cell stage complete Ig molecules are formed which are composed of two IgH and two IgL chains (**Figure 4B, left panel**). Each Ig chain contains a variable domain that determines the antigen-specificity and a constant domain, which is responsible for the Ig functionality. The Ig variable domain is composed of 4 conserved framework regions (FR) interspersed by 3 complementary determining regions (CDR) (**Figure 4B, right panel**). The FRs form a solid Ig structure, while the 3 diverse CDRs create loops recognizing pathogens. CDR3 is the most polymorphic because it is encoded by the junction between rearranged V, (D) and J genes and thereby crucial for antigen binding specificity.

Upon generation of a BCR, developing B cells expressing the receptors at the immature-B cell stage are selected for recognition of antigens followed by negative selection for self-reactivity. Approximately 75% of Ig generated in BM is autoreactive and approximately 55% is polyreactive.⁷¹ To ensure proper immune tolerance, negative selection allows to remove these receptors from the repertoire via apoptosis, anergy or receptor editing.⁷²⁻⁷⁵ Removal of the autoreactive and polyreactive Ig first occurs at the immature-B cells stage (**Figure 6**).^{71, 76} During differentiation from early immature-B-cell to immature-B-cell in BM, central tolerance mechanisms reduce both the autoreactive and polyreactive Ig repertoire to ~45% and less than 10%, respectively. In addition, there is a peripheral tolerance checkpoint after migration of the B cells out of the BM which further reduces autoreactive Ig repertoire to ~20%.^{71, 76}

THE V(D)J RECOMBINATION PROCESS

The Ig heavy chain and Ig light chain loci contain multiple variable (V), diverse (D) and joining (J) coding elements which must be assembled to create the functional first coding exon. During generation of Ig, only one V, one D and one J genes are randomly

chosen and rearranged in a process of somatic V(D)J recombination.^{35,77} V(D)J recombination mechanism is the same for all Ig loci and occurs in a stepwise manner.

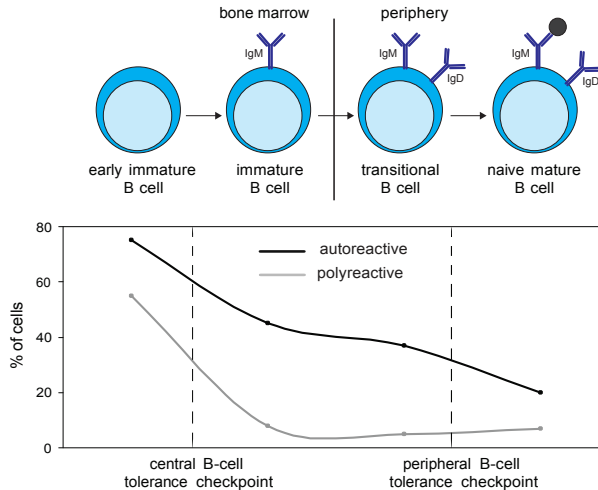


Figure 6. Early B-cell tolerance checkpoints. Immunoglobulins created in bone marrow are counterselected for autoreactivity and polyreactivity at two tolerance checkpoints. First, central B-cell tolerance in bone marrow reduces the ~75% autoreactive and ~55% polyreactive receptors to ~45% and less than 10%, respectively. Subsequently, during the cell transition from bone marrow to periphery, peripheral B-cell tolerance checkpoint further removes autoreactive immunoglobulin to ~20% present in naive mature B-cell repertoire. The Figure was adapted from Wardemann *et al.*, 2003, Science⁷¹ and Meffre, 2011, Ann NY Acad Sci.⁷⁶

Molecular mechanism of V(D)J recombination

The V(D)J recombination starts with induction of double stranded DNA breaks (DSBs) by the heterodimeric complex of recombinase activating gene protein products RAG1 and RAG2 (**Figure 7**). RAG proteins specifically recognize recombination signal sequences (RSS) flanking all Ig genes. RSS are composed of conserved heptamer and nonamer sequences separated by a less conserved spacer region of 12 or 23 base pairs (bp).⁷⁸⁻⁸⁰ Rearrangements always occur between Ig genes flanked by a 12-bp RSS and a 23-bp RSS, commonly referred to as 12-23 rule.⁷⁹

The RAG complex brings together the two genes poised for rearrangement and introduces single stranded DNA breaks at the border of each gene and its flanking RSS.⁸¹⁻⁸³ Next, DNA hairpins are created at the site of the gene breaks (coding ends) and blunt ends are created at the side of RSS (signal ends). Before ligation of the two coding ends by the non-homologous end joining pathway (NHEJ), the MRN complex consisting of NBS, MRE11 and RAD50 proteins tethers the DNA ends to ensure they remain in close proximity.^{84,85} In addition, the MRN complex activates the ataxia-telangiectasia-mutated

protein (ATM), which results in cell cycle arrest, activation of DNA repair pathways and initiation of apoptosis in cells that fail to repair.⁸⁶⁻⁸⁹ The DNA repair is initiated by loading of Ku70 and Ku80 proteins onto the break and recruitment of the catalytic subunit of DNA-dependent protein kinase (DNA-PKcs) and Artemis.^{90, 91} DNA-PKcs stabilizes the protein-DNA complex, protects against exonuclease activity and stimulates juxtaposition of DNA ends.⁹² Subsequently, Artemis opens the hairpins within coding ends preferentially at the tip or 1-2 bp 5' of the tip.^{93, 94} If the hairpins are opened 5' of the tip, complementary nucleotides can be added to generate blunt ends which results in formation of palindromic (P-) nucleotides. Nucleotides can be also deleted by exonucleases or non-template (N-) nucleotides can be added by terminal deoxynucleotidyl transferase protein (TdT).⁹⁵⁻⁹⁷ Finally, the DNA coding ends are ligated by a protein complex including XRCC4, DNA ligase IV and XLF.⁹⁸⁻¹⁰⁰ The signal ends at the side of RSS are joined by the NHEJ and remain in the cell as a circular excision product.

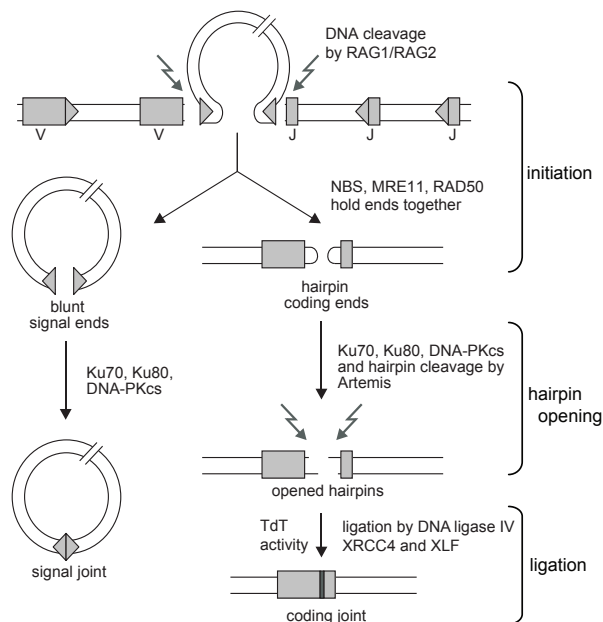


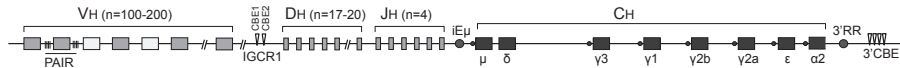
Figure 7. Molecular mechanism of V(D)J recombination. The RAG protein complex cleaves the double stranded DNA at the border of two immunoglobulin genes poised for rearrangement and flanking recombination signal sequences. This results in coding ends and signal ends formation. The signal ends are directly ligated by the non-homologous end joining pathway (NHEJ) and the coding ends with hairpins are tethered in close proximity by MRN complex (NBN, MRE11, Rad50). Subsequently, Ku70, Ku80, DNA-PKcs and Artemis are loaded onto the coding ends and Artemis cleaves the hairpins. The opened ends are further processed by endonucleases and TdT which incorporates the non-template N-nucleotides. Finally, the two coding ends are sealed into the coding joint by complex of DNA ligase IV, XRCC4 and XLF. The Figure was adapted from van der Burg *et al.*, 2009, *Curr Opin Allergy Clin Immunol*¹⁰¹ and Berkowska *et al.*, 2011, *Ann NY Acad Sci*.²⁷

Organization of immunoglobulin loci

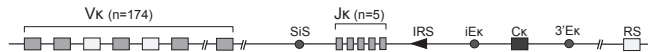
The stepwise manner of Ig gene rearrangements is controlled by various regulatory elements present within Ig loci (**Figure 8**).¹⁰²⁻¹⁰⁵ Each V gene contains individual promoter located upstream of the gene, while D and J gene clusters contain one common promoter for the cluster. Furthermore, each Ig locus contains intron enhancer located between J and C genes and enhancer at the 3' end of the locus. Presence of few additional regulatory elements were recently shown within murine *IGH* locus, i.e. Pax5-activated intergenic elements (PAIR) interspersed in the distal V_H region,¹⁰⁶ intergenic control region (IGCR1) located between V and D genes¹⁰⁷ and CTCF-binding elements (CBE) at the 3' end of the locus. Within murine *IGK*, additional silencer in the intervening sequence (SiS) located between V and J genes was also recently described (**Figure 8**).¹⁰⁸

A mouse

IGH locus (chr12); 2.9 MB



IGK locus (chr6); 3.5 MB

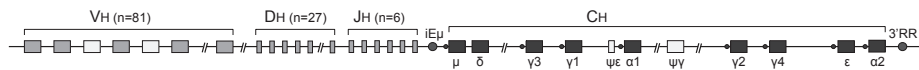


IGL locus (chr16); 0.24 MB

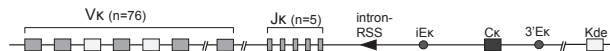


B human

IGH locus (chr14); 1.25 MB



IGK locus (chr2); 1.82 MB



IGL locus (chr22); 1.05 MB



Figure 8. Organization of immunoglobulin loci. (A) Murine and (B) human immunoglobulin loci positioned at different chromosomes show similar organization although differ in size. They are composed of multiple variable (V), diverse (D), joining (J) and constant (C) genes and contain a spectrum of regulatory elements. Intronic enhancers (iE) and enhancers located at the 3' end of the locus were described in all loci. Additionally, within murine *IGH* locus Pax5-activated intergenic elements (PAIR) and intergenic control region (IGCR1) were recently found, while silencer in the intervening sequence (SiS) was detected within murine *IGK*. Each C gene of the *IGH* is preceded by a switch region. Rearrangement within the *IGK* between the IRS (mouse) or intronRSS (human) and the RS (mouse) and Kde (human) elements can make the *IGK*

allele nonfunctional by deleting the C κ exons and the enhancers. CBE, CTCF-binding element, $\Psi\epsilon$ -pseudo epsilon gene; $\Psi\gamma$ -pseudo gamma gene; $\Psi\lambda$ -pseudo lambda gene.

TRANSCRIPTIONAL AND EPIGENETIC REGULATION OF IG GENE REARRANGEMENTS

The formation of Ig during B-cell differentiation is tightly regulated. V(D)J recombination occurs in a stepwise manner where *IGH* rearranges prior *IGK* and *IGL*, and D H -J H joints are formed before V H -D H assembly. Moreover, *IGK* rearranges before *IGL* and functional Ig rearrangements never occur on both Ig alleles. The tight control is partially provided by presence of RSS only within antigen receptor loci and RAG expression only in lymphoid cells. Although the V(D)J recombination machinery is common for lymphoid cells, complete TCR β rearrangements never occur in B cells and complete *IGH* gene rearrangements are absent or very rare in T cells. Thus, the lineage and developmentally restricted manner of V(D)J recombination must be further controlled. The second degree of control is provided by transcriptional regulation. B and T lymphocyte express distinct transcription factors which recognize specific binding sites within promoters and enhancers of antigen receptor loci.

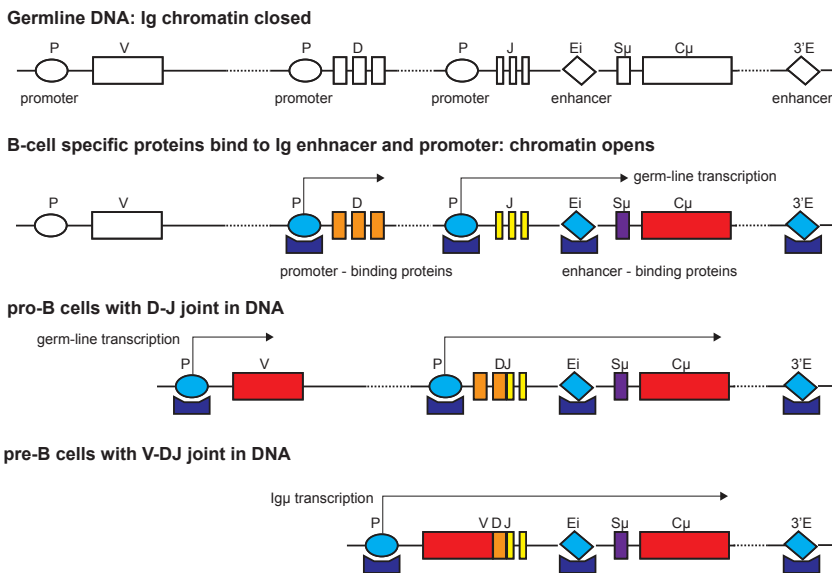


Figure 9. Transcriptional regulation of immunoglobulin loci accessibility. *IGH* locus becomes progressively accessible for transcriptional machinery. Prior to rearrangement, chromatin opens within enhancers and promoters of diversity (D) and joining (J) genes which enables binding of B-cell specific transcription factors. Occupancy of promoters and enhancers by transcription factors initiates germ-line transcription and induces D H -J H rearrangement. After DJ H joint formation, promoters of variable (V) genes become accessible for transcriptional machinery which promotes V H -DJ H rearrangement. The Figure was adapted from Corcoran, 2010, Semin Immunol.¹¹⁰

The binding sites, however, become accessible for transcription factors only at specific stages during development. It is thought that the ordered accessibility of Ig loci is controlled by epigenetic processes such as DNA and chromatin modifications, locus contraction and nuclear positioning.^{29, 77, 109}

Transcriptional regulation of immunoglobulin loci accessibility

The ordered accessibility of Ig genes for V(D)J recombination is underlined by transcriptional control (**Figure 9**). Alt & Yancopoulos formulated the accessibility hypothesis which proposed that the germ-line transcription over unrearranged *IGH* and *IGL* loci regulated the stepwise V(D)J recombination.³¹ In non-rearranging B cells, the chromatin enclosing Ig loci is not accessible for the transcription machinery. Prior to rearrangement, the chromatin opens progressively within Ig promoters and enhancers to enable binding of B-cell specific transcription factors. Occupancy of promoters and enhancers by transcription factors initiates germ-line transcription and induces rearrangement.¹¹⁰ Within the *IGH* locus, chromatin is first opened at the D_H - J_H region, and only after D_H - J_H rearrangement, the V_H region becomes accessible (**Figure 9**).^{111, 112} Within the *IGK* locus, germline transcription is induced after pre-BCR signaling.¹¹³

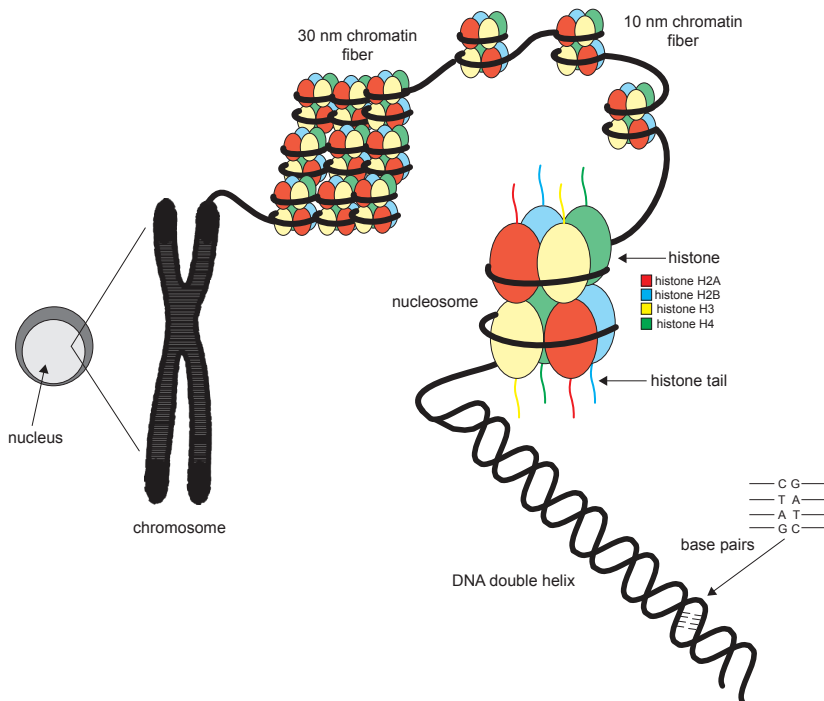


Figure 10. DNA organization in the eukaryotic cell nucleus. DNA is tightly packed in the small volume of nucleus to fit its mass. 146 base pairs of double stranded DNA helix are wrapped around a protein octamer composed of 2 copies of 4 histone molecules: H2A, H2B, H3 and H4. The DNA with histones create the basic

chromatin unit, the nucleosome. Subsequently, the nucleosomes are packed into 10 nm and 30 nm chromatin fiber structures. During mitosis, additional DNA compaction takes place and the 30 nm chromatin fiber is further folded into chromosomes. This Figure was adapted from thesis of Dr. R. Stadhouders.

The histone code determines chromatin accessibility

Ig loci are present in every cell of multicellular organisms such as vertebrates, however, they are transcribed only in B cells, thus their expression is tightly regulated. To fit the small volume of the cell nucleus, around 2 meter-long DNA molecule is tightly packed (**Figure 10**). A stretch of 146 base pairs of double-stranded DNA helix is wrapped around a histone protein octamer (two copies of the four core histones: H2A, H2B, H3, H4) creating nucleosome, which forms the basic unit of chromatin. Further nucleosomes are compacted into 10 nm and 30 nm chromatin fibers which subsequently are folded into chromosomes in proliferating cells.^{114, 115}

When the DNA is tightly wrapped around histones and the nucleosome density is high, chromatin is difficult to access for the transcriptional machinery (referred as heterochromatin), whereas less tight DNA wrapping around histones and lower nucleosome density creates a more accessible form of chromatin (referred as euchromatin). “Closed” vs “open” chromatin conformation is established through several processes such as post-translational histone modifications, chromatin remodeling and DNA modifications. Histones are modified at special amino acids residues present in histone tails. Histone tails are methylated, phosphorylated, acetylated, sumoylated, ubiquitinated and ADP-ribosylated. There are two characterized mechanisms for the function of these modifications. The first is the disruption of contacts between nucleosomes in order to unwrap chromatin and the second is the recruitment of non-histone proteins. For instance, acetylation alters the charge on the histone, which weakens the DNA-histone interaction leading to a less compact chromatin structure (**Figure 11A**).^{114, 116, 117} In general, active chromatin is enriched in acetylated histones H3, H4, H2A and histone H3 methylated at Lys 4 (H3K4), while histone hypoacetylation and methylation of histone H3 Lys 9 (H3K9) are a hallmark of inactive chromatin. Next to the histone modifications, multiprotein complexes such as chromatin (nucleosome) remodelers have the ability to slide or (dis)assemble histone octamers in an ATP-dependent manner which changes the chromatin accessibility (**Figure 11B**).¹¹⁸ Finally, the DNA itself can be modified. CpG methylation is generally associated with the gene silencing.¹¹⁹

Ig genes poised for V(D)J recombination are extensively acetylated at histones H3 and H4, as well as methylated at H3K4.¹²⁰⁻¹²² First methyl and acetyl groups are added to the histones within D_H-J_H region and only after D_H assembly, these are incorporated within V_H genes (**Figure 11C**).¹²³ Within Ig light chain loci, chromatin marks are present only after pre-BCR signaling. Importantly, stage-specific trimethylation of H3K4 (H3K4me3) in Ig genes can directly recruit RAG2.¹²⁴⁻¹²⁶ Incorporation of histone code within Ig loci is

shown to be driven by intron enhancers: germline deletion of $iE\mu$ greatly reduces histone acetylation on DH and JH genes and $H3K4me3$ levels on JH genes.¹²⁷ Consequently, $iE\mu$ deletion reduces the *IGH* gene rearrangements.^{77, 104} $iE\mu$ may also initiate chromatin remodeling by recruiting the chromatin remodeling SWI/SNF complex to the DH - JH region.¹²⁸

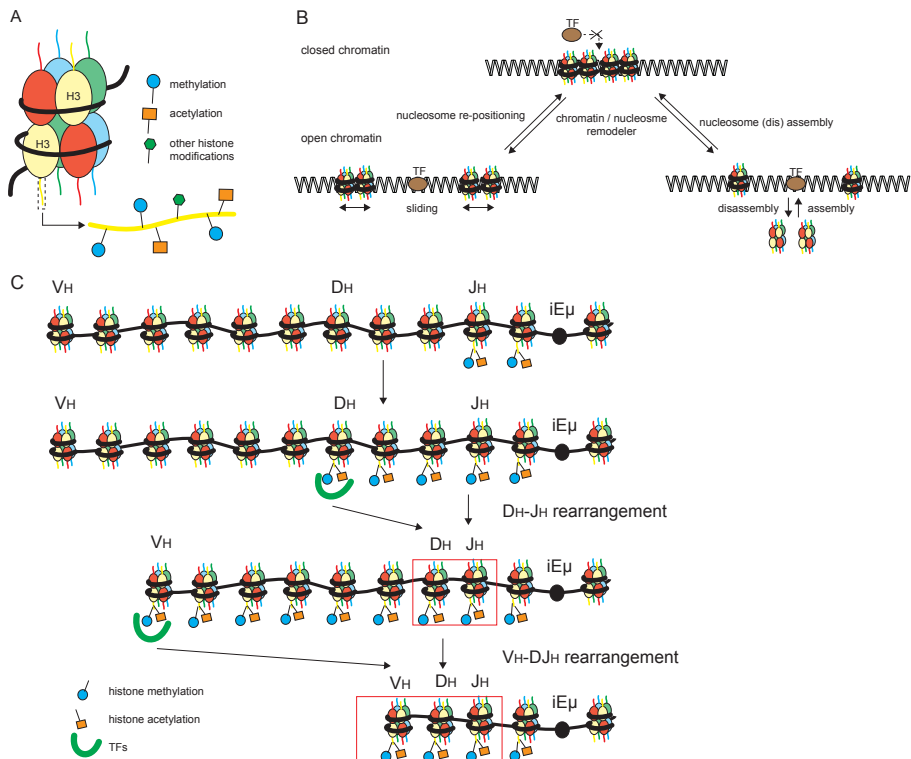


Figure 11. Histone modifications and chromatin remodeling. “Closed” vs “open” chromatin state is established through posttranslational histone modifications and chromatin remodeling. **(A)** Histone marks such as acetyl and methyl groups are added to specific amino acids residues within histone tails. **(B)** Chromatin (nucleosome) remodelers have the ability to slide or (dis) assemble histone octamers in an ATP-dependent manner. TF, transcription factor. **(C)** Stepwise addition of histone marks to the *IGH* locus facilitates the ordered rearrangement process. The Figure was adapted from Kouzarides, 2007, *Cell*¹¹⁷, Saha *et al.*, 2006, *Nat Rev Mol Cell Biol*¹¹⁸ and Feeney, 2011, *Curr Opin Immunol*.¹²⁹

3D chromatin structure and long-range genomic interactions

Activation or suppression of genes depends on multiple regulatory elements such as enhancers, silencers or locus regulatory elements which often act from a distance (**Figure**

12A).¹³⁰ Ig loci create large genetic complexes (**Figure 8**) and V(D)J recombination also requires interactions between Ig regulatory elements and Ig genes over the genomic distance. These long-range genomic interactions are established through chromatin folding.

Mammalian genomes fold into clusters of loops that assemble into topologically associated domains (TADs).¹³¹⁻¹³³ These chromatin loops are established through interactions between ubiquitously expressed global chromatin architecture proteins such as CCCTC-binding factor (CTCF), cohesin and Yin-Yang 1 (YY1).^{134, 135} CTCF recognizes specific bindings sites across the whole genome to mediate the long-range looping,¹³⁶ whereas cohesin interacts with CTCF and forms a ring-like structure around the chromatin loops to maintain them (**Figure 12B**).¹³⁷ The murine *IGH* locus is organized into three major multi-loop domains of rosettes-like shape (**Figure 12C**).¹³⁸ Recent analysis of the pro-B cell genome indicates that the long-range interactions within multi-loop chromatin domains of *IGH* are associated with CTCF and YY1 binding.^{106, 131, 139-141} CTCF and YY1 binding sites are disseminated within the V_H region, they are present in intergenic control region (IGCR1) and 3'CTCF-binding element (3' CBE). YY1 can also bind to $i\mu$. Thus, the long-range interactions between these regulatory elements establish the chromatin loops within *IGH*.^{107, 142}

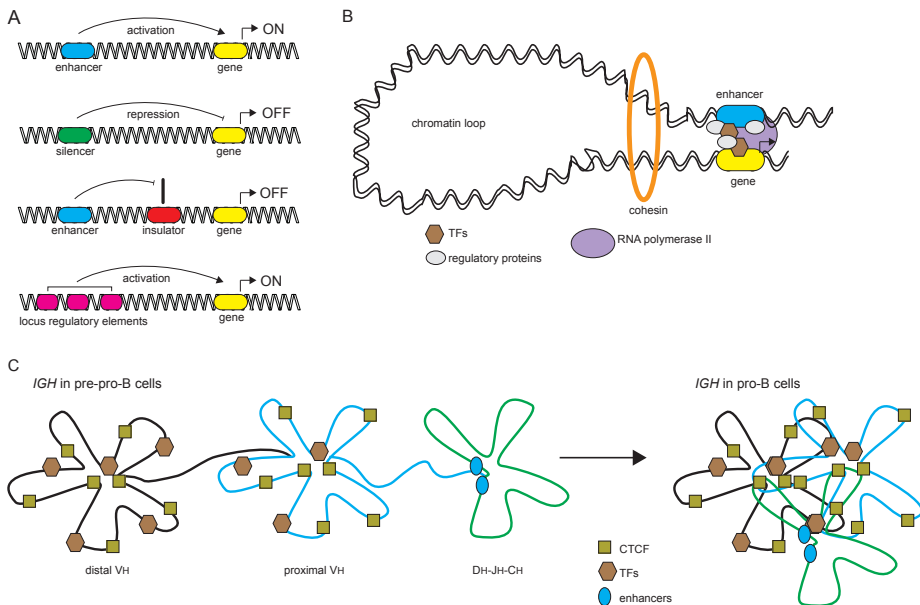


Figure 12. Long-range interactions between genes and gene regulatory elements. Interactions between distal gene regulatory elements and genes are enabled through chromatin folding. (A) Enhancers, silencers and other locus regulatory elements can activate a gene from a distance, while insulators inhibit the long-range interactions. (B) Speculative model of chromatin looping which brings genes and gene regulatory elements in

close spatial proximity. Various global and lineage-specific transcription factors and regulatory proteins cluster together around gene and regulatory elements which facilitates looping. Cohesin likely maintains the chromatin loop. (C) Schematic representation of *IGH* locus organization into three multi-loop domains which contract upon B-cell differentiation from pre-pro-B cells to pro-B cells. Locus contraction brings V_H genes in close proximity of the DJ_H region and provides equal gene usage during recombination. The Figure was adapted from Maston *et al.*, 2006, *Annu Rev Genomics Hum Genet*¹³⁰ and Feeney, 2011, *Curr Opin Immunol*.¹²⁹

However, global genome folding seems to be insufficient to mediate the gene expression. Ig loci must further contract at the stage of rearrangement to bring all genes in close proximity and provide equal opportunities for rearrangement (**Figure 12C**).^{43, 143-145} After complete Ig gene rearrangement, the loci decontract to prevent the rearrangement event at the second allele.¹⁴³ Further locus contraction is likely driven by lineage-specific factors (**Figure 12B**). Recent analysis of the pro-B cell genome indicates that long-range interactions between multi-loop chromatin domains of *IGH* were associated with the binding of B-cell specific transcription factors such as E2A, EBF1, Pax5, Ikaros and PU.1.^{106, 131, 139-141, 146-150} Likely, these factors contract the three multi-loop domains of *IGH* locus upon progenitor-B cell commitment to pro-B cells.^{138, 143, 144} So far the role in locus contraction was proven for E2A, Pax5 and Ikaros which mediate the efficient rearrangements of V_H genes.^{139, 141, 142, 147, 149}

Looping of *IGK* locus yields similar picture to that of *IGH*. First, ubiquitously expressed proteins such as CTCF provide the global chromatin folding and subsequently the multi-loop domains are contracted by B-cell specific factors such as E2A. CTCF-binding sites were located across the V_κ region, within SiS and downstream of the 3'Ek, while E2A binds to the V_κ region and iEk.^{113, 140, 151, 152} *IGK* locus also contracts specifically at the stage of rearrangements in pre-B cells,¹⁴³ however, the locus contraction was also reported in pro-B cells.¹⁵³

Nuclear positioning of genes

Nuclear positioning of Ig loci is involved in transcriptional control of Ig loci accessibility for recombination. In general, regions with euchromatin are associated with increased transcriptional accessibility, while heterochromatin is transcriptionally repressive. The nuclear periphery also represents a repressive region, whereas the nuclear center is enriched with transcription factories. The nuclear lamins, which line the inner membrane of the nucleus, acts as a repository for transcriptionally inactive chromatin domains, known as lamina-associated domains (LADs).^{154, 155}

In the interphase nucleus, chromatin fibers occupy spatially distinct regions, i.e. chromosome territories (**Figure 13A**).¹⁵⁶ Genes can change their nuclear 'neighborhoods' from repressive sites towards transcription factories through extruding of decondensed chromatin loops into interchromosomal space and intermingling with neighboring

chromosome territories (**Figure 13B**).^{116, 157, 158} Many of the genes positioned in LADs are recruited at specific stages of cellular differentiation.^{116, 154, 157, 158} The Ig loci are positioned at the nuclear periphery in non-B cells, while they are centrally located in committed B-cell progenitors.^{155, 159, 160} The molecular mechanisms underlying the changes of gene localization are still obscure, but seem to correlate with histone acetylation.¹¹⁶

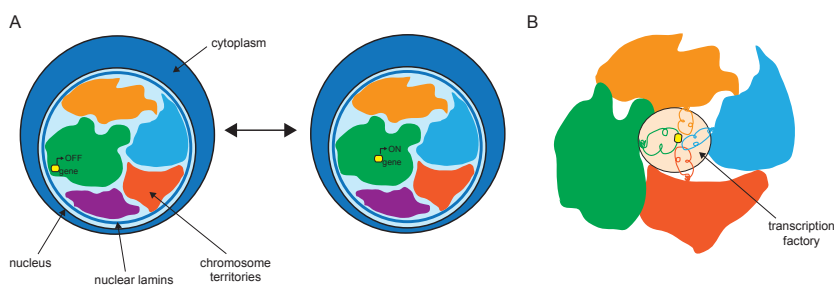


Figure 13. Nuclear positioning of genes. (A) In interphase nucleus, the more “free” chromatin fibers are not positioned randomly but occupy spatially distinct regions named chromosome territories. The nuclear periphery (nuclear lamins which lines the inner nuclear membrane) represents a repressive region, while the nuclear center is enriched with transcription factories, therefore genes change their nuclear localization during cellular maturation. (B) Genes can change their nuclear ‘neighborhoods’ from repressive sites towards transcription factories through extruding of decondensed chromatin loops into interchromosomal space and intermingling with neighboring chromosome territories. The Figure was adapted from Schneider and Grosschedl, 2007, *Genes Dev.*¹¹⁶

AIMS OF THE THESIS

Ig loci recombine in an ordered manner: the *IGH* locus rearranges before the Ig light chain loci, functional Ig rearrangements rarely occur on both Ig alleles, and complete Ig assembly is exclusive for B cells. Still, the exact mechanisms controlling the stage-specific V(D)J recombination remain unknown. In **Chapters II and III**, we aimed to decipher which epigenetic processes control the stepwise Ig loci assembly in mouse models. In **Chapter II**, we studied how pre-BCR signaling influences the *IGK* locus recombination, while **Chapter III** elucidates the role of locus contraction and nuclear positioning in stepwise V(D)J recombination.

B-cell differentiation occurs primarily in BM and starts already before birth in fetal liver and fetal BM. It is also suggested that B cells may develop in postnatal thymus. The ultimate goal of precursor-B-cell differentiation is to generate a diverse Ig repertoire. Still, the mechanisms controlling the generation of a diverse Ig repertoire are poorly understood. In **Chapters IV, V and VI**, we studied the Ig repertoire formation in different niches of B-cell development, other than human postnatal BM, and to what extent this

influences the Ig reactivity. **Chapter IV** contains the analysis of Ig repertoire formation in human postnatal BM during aging. **Chapter V** outlines the mechanism underlying the skewed Ig repertoire formation during prenatal life. Whereas, **Chapter VI** describes the reactivity of fetal B cells and the Ig gene repertoire and reactivity of thymic B cells.

Finally, the **General Discussion** summarizes the basic research results and considers implications of these results for our understanding of precursor-B-cell biology.

REFERENCES

1. Marchiando, A. M., W. V. Graham, and J. R. Turner. 2010. Epithelial barriers in homeostasis and disease. *Annu Rev Pathol* 5:119-144.
2. Turner, J. R. 2009. Intestinal mucosal barrier function in health and disease. *Nat Rev Immunol* 9:799-809.
3. Janeway, C. A., Jr., and R. Medzhitov. 2002. Innate immune recognition. *Annu Rev Immunol* 20:197-216.
4. Bryder, D., D. J. Rossi, and I. L. Weissman. 2006. Hematopoietic stem cells: the paradigmatic tissue-specific stem cell. *Am J Pathol* 169:338-346.
5. Adolfsson, J., R. Mansson, N. Buza-Vidas, A. Hultquist, K. Liuba, C. T. Jensen, D. Bryder, L. Yang, O. J. Borge, L. A. Thoren, K. Anderson, E. Sitnicka, Y. Sasaki, M. Sigvardsson, and S. E. Jacobsen. 2005. Identification of Flt3+ lympho-myeloid stem cells lacking erythro-megakaryocytic potential a revised road map for adult blood lineage commitment. *Cell* 121:295-306.
6. Zandi, S., D. Bryder, and M. Sigvardsson. 2010. Load and lock: the molecular mechanisms of B-lymphocyte commitment. *Immunol Rev* 238:47-62.
7. Nutt, S. L., and B. L. Kee. 2007. The transcriptional regulation of B cell lineage commitment. *Immunity* 26:715-725.
8. DeKoter, R. P., and H. Singh. 2000. Regulation of B lymphocyte and macrophage development by graded expression of PU.1. *Science* 288:1439-1441.
9. Nichogiannopoulou, A., M. Trevisan, S. Neben, C. Friedrich, and K. Georgopoulos. 1999. Defects in hemopoietic stem cell activity in Ikaros mutant mice. *J Exp Med* 190:1201-1214.
10. Kondo, M., I. L. Weissman, and K. Akashi. 1997. Identification of clonogenic common lymphoid progenitors in mouse bone marrow. *Cell* 91:661-672.
11. Akashi, K., D. Traver, T. Miyamoto, and I. L. Weissman. 2000. A clonogenic common myeloid progenitor that gives rise to all myeloid lineages. *Nature* 404:193-197.
12. Rumfelt, L. L., Y. Zhou, B. M. Rowley, S. A. Shinton, and R. R. Hardy. 2006. Lineage specification and plasticity in CD19- early B cell precursors. *J Exp Med* 203:675-687.
13. Murre, C., P. S. McCaw, and D. Baltimore. 1989. A new DNA binding and dimerization motif in immunoglobulin enhancer binding, daughterless, MyoD, and myc proteins. *Cell* 56:777-783.
14. Murre, C. 2005. Helix-loop-helix proteins and lymphocyte development. *Nat Immunol* 6:1079-1086.

15. Bain, G., S. Gruenwald, and C. Murre. 1993. E2A and E2-2 are subunits of B-cell-specific E2-box DNA-binding proteins. *Mol Cell Biol* 13:3522-3529.
16. Kee, B. L. 2009. E and ID proteins branch out. *Nat Rev Immunol* 9:175-184.
17. Ikawa, T., S. Fujimoto, H. Kawamoto, Y. Katsura, and Y. Yokota. 2001. Commitment to natural killer cells requires the helix-loop-helix inhibitor Id2. *Proc Natl Acad Sci U S A* 98:5164-5169.
18. Boos, M. D., Y. Yokota, G. Eberl, and B. L. Kee. 2007. Mature natural killer cell and lymphoid tissue-inducing cell development requires Id2-mediated suppression of E protein activity. *J Exp Med* 204:1119-1130.
19. Kee, B. L., and C. Murre. 1998. Induction of early B cell factor (EBF) and multiple B lineage genes by the basic helix-loop-helix transcription factor E12. *J Exp Med* 188:699-713.
20. Medina, K. L., J. M. Pongubala, K. L. Reddy, D. W. Lancki, R. Dekoter, M. Kieslinger, R. Grosschedl, and H. Singh. 2004. Assembling a gene regulatory network for specification of the B cell fate. *Dev Cell* 7:607-617.
21. Mansson, R., E. Welinder, J. Ahsberg, Y. C. Lin, C. Benner, C. K. Glass, J. S. Lucas, M. Sigvardsson, and C. Murre. 2012. Positive intergenic feedback circuitry, involving EBF1 and FOXO1, orchestrates B-cell fate. *Proc Natl Acad Sci U S A* 109:21028-21033.
22. Welinder, E., R. Mansson, E. M. Mercer, D. Bryder, M. Sigvardsson, and C. Murre. 2011. The transcription factors E2A and HEB act in concert to induce the expression of FOXO1 in the common lymphoid progenitor. *Proc Natl Acad Sci U S A* 108:17402-17407.
23. Ordentlich, P., A. Lin, C. P. Shen, C. Blaumueller, K. Matsuno, S. Artavanis-Tsakonas, and T. Kadesch. 1998. Notch inhibition of E47 supports the existence of a novel signaling pathway. *Mol Cell Biol* 18:2230-2239.
24. O'Riordan, M., and R. Grosschedl. 1999. Coordinate regulation of B cell differentiation by the transcription factors EBF and E2A. *Immunity* 11:21-31.
25. Nutt, S. L., B. Heavey, A. G. Rolink, and M. Busslinger. 1999. Commitment to the B-lymphoid lineage depends on the transcription factor Pax5. *Nature* 401:556-562.
26. Schebesta, M., P. L. Pfeffer, and M. Busslinger. 2002. Control of pre-BCR signaling by Pax5-dependent activation of the BLNK gene. *Immunity* 17:473-485.
27. Berkowska, M. A., M. van der Burg, J. J. van Dongen, and M. C. van Zelm. 2011. Checkpoints of B cell differentiation: visualizing Ig-centric processes. *Ann NY Acad Sci* 1246:11-25.
28. Osmond, D. G., A. Rolink, and F. Melchers. 1998. Murine B lymphopoiesis: towards a unified model. *Immunol Today* 19:65-68.
29. Bossen, C., R. Mansson, and C. Murre. 2012. Chromatin Topology and the Regulation of Antigen Receptor Assembly. *Annu Rev Immunol* 30:337-356.
30. Jung, D., C. Giallourakis, R. Mostoslavsky, and F. W. Alt. 2006. Mechanism and control of V(D)J recombination at the immunoglobulin heavy chain locus. *Annu Rev Immunol* 24:541-570.

31. Alt, F. W., G. D. Yancopoulos, T. K. Blackwell, C. Wood, E. Thomas, M. Boss, R. Coffman, N. Rosenberg, S. Tonegawa, and D. Baltimore. 1984. Ordered rearrangement of immunoglobulin heavy chain variable region segments. *EMBO J* 3:1209-1219.
32. Ghia, P., E. tenBoekel, E. Sanz, A. delaHera, A. Rolink, and F. Melchers. 1996. Ordering of human bone marrow B lymphocyte precursors by single-cell polymerase chain reaction analyses of the rearrangement status of the immunoglobulin H and L chain gene loci. *J Exp Med* 184:2217-2229.
33. Hendriks, R. W., and S. Middendorp. 2004. The pre-BCR checkpoint as a cell-autonomous proliferation switch. *Trends Immunol* 25:249-256.
34. Hozumi, N., and S. Tonegawa. 1976. Evidence for somatic rearrangement of immunoglobulin genes coding for variable and constant regions. *Proc Natl Acad Sci U S A* 73:3628-3632.
35. Tonegawa, S. 1983. Somatic generation of antibody diversity. *Nature* 302:575-581.
36. van Zelm, M. C., M. van der Burg, D. de Ridder, B. H. Barendregt, E. F. de Haas, M. J. Reinders, A. C. Lankester, T. Revesz, F. J. Staal, and J. J. van Dongen. 2005. Ig gene rearrangement steps are initiated in early human precursor B cell subsets and correlate with specific transcription factor expression. *J Immunol* 175:5912-5922.
37. Hardy, R. R., and K. Hayakawa. 2001. B cell development pathways. *Annu Rev Immunol* 19:595-621.
38. Osmond, D. G. 1986. Population dynamics of bone marrow B lymphocytes. *Immunol Rev* 93:103-124.
39. Melchers, F., A. Strasser, S. R. Bauer, A. Kudo, P. Thalmann, and A. Rolink. 1991. B cell development in fetal liver. *Adv Exp Med Biol* 292:201-205.
40. Ghia, P., E. ten Boekel, A. G. Rolink, and F. Melchers. 1998. B-cell development: a comparison between mouse and man. *Immunol Today* 19:480-485.
41. Ehlich, A., S. Schaal, H. Gu, D. Kitamura, W. Muller, and K. Rajewsky. 1993. Immunoglobulin heavy and light chain genes rearrange independently at early stages of B cell development. *Cell* 72:695-704.
42. Novobrantseva, T. I., V. M. Martin, R. Pelanda, W. Muller, K. Rajewsky, and A. Ehlich. 1999. Rearrangement and expression of immunoglobulin light chain genes can precede heavy chain expression during normal B cell development in mice (vol 189, pg 75, 1999). *Journal of Experimental Medicine* 189:1361-1361.
43. Nodland, S. E., M. A. Berkowska, A. A. Bajer, N. Shah, D. de Ridder, J. J. van Dongen, T. W. LeBien, and M. C. van Zelm. 2011. IL-7R expression and IL-7 signaling confer a distinct phenotype on developing human B-lineage cells. *Blood* 118:2116-2127.
44. Bertolino, E., K. Reddy, K. L. Medina, E. Parganas, J. Ihle, and H. Singh. 2005. Regulation of interleukin 7-dependent immunoglobulin heavy-chain variable gene rearrangements by transcription factor STAT5. *Nat Immunol* 6:836-843.
45. Mandal, M., S. E. Powers, M. Maienschein-Cline, E. T. Bartom, K. M. Hamel, B. L. Kee, A. R. Dinner, and M. R. Clark. 2011. Epigenetic repression of the Igk locus by STAT5-mediated recruitment of the histone methyltransferase Ezh2. *Nat Immunol* 12:1212-1220.
46. Corfe, S. A., and C. J. Paige. 2012. The many roles of IL-7 in B cell development; mediator of survival, proliferation and differentiation. *Semin Immunol* 24:198-208.

47. O'Shea, M. J., P. T. Flute, and G. M. Pannell. 1971. Laboratory control of heparin therapy. *J Clin Pathol* 24:542-546.
48. Chou, W. C., D. E. Levy, and C. K. Lee. 2006. STAT3 positively regulates an early step in B-cell development. *Blood* 108:3005-3011.
49. Mandal, M., S. E. Powers, K. Ochiai, K. Georgopoulos, B. L. Kee, H. Singh, and M. R. Clark. 2009. Ras orchestrates exit from the cell cycle and light-chain recombination during early B cell development. *Nat Immunol* 10:1110-1117.
50. Cooper, A. B., C. M. Sawai, E. Sicinska, S. E. Powers, P. Sicinski, M. R. Clark, and I. Aifantis. 2006. A unique function for cyclin D3 in early B cell development. *Nat Immunol* 7:489-497.
51. Malin, S., S. McManus, C. Cobaleda, M. Novatchkova, A. Delogu, P. Bouillet, A. Strasser, and M. Busslinger. 2010. Role of STAT5 in controlling cell survival and immunoglobulin gene recombination during pro-B cell development. *Nat Immunol* 11:171-179.
52. Jiang, Q., W. Q. Li, R. R. Hofmeister, H. A. Young, D. R. Hodge, J. R. Keller, A. R. Khaled, and S. K. Durum. 2004. Distinct regions of the interleukin-7 receptor regulate different Bcl2 family members. *Mol Cell Biol* 24:6501-6513.
53. Bednarski, J. J., A. Nickless, D. Bhattacharya, R. H. Amin, M. S. Schlissel, and B. P. Sleckman. 2012. RAG-induced DNA double-strand breaks signal through Pim2 to promote pre-B cell survival and limit proliferation. *J Exp Med* 209:11-17.
54. Herzog, S., E. Hug, S. Meixlsperger, J. H. Paik, R. A. DePinho, M. Reth, and H. Jumaa. 2008. SLP-65 regulates immunoglobulin light chain gene recombination through the PI(3)K-PKB-Foxo pathway. *Nat Immunol* 9:623-631.
55. Amin, R. H., and M. S. Schlissel. 2008. Foxo1 directly regulates the transcription of recombination-activating genes during B cell development. *Nat Immunol* 9:613-622.
56. Melchers, F. 2005. The pre-B-cell receptor: selector of fitting immunoglobulin heavy chains for the B-cell repertoire. *Nat Rev Immunol* 5:578-584.
57. Clark, M. R., M. Mandal, K. Ochiai, and H. Singh. 2014. Orchestrating B cell lymphopoiesis through interplay of IL-7 receptor and pre-B cell receptor signalling. *Nat Rev Immunol* 14:69-80.
58. Rickert, R. C. 2013. New insights into pre-BCR and BCR signalling with relevance to B cell malignancies. *Nat Rev Immunol* 13:578-591.
59. Ohnishi, K., and F. Melchers. 2003. The nonimmunoglobulin portion of lambda5 mediates cell-autonomous pre-B cell receptor signaling. *Nat Immunol* 4:849-856.
60. Bankovich, A. J., S. Raunser, Z. S. Juo, T. Walz, M. M. Davis, and K. C. Garcia. 2007. Structural insight into pre-B cell receptor function. *Science* 316:291-294.
61. Vettermann, C., K. Herrmann, C. Albert, E. Roth, M. R. Bosl, and H. M. Jack. 2008. A unique role for the lambda5 nonimmunoglobulin tail in early B lymphocyte development. *J Immunol* 181:3232-3242.
62. Fleming, H. E., and C. J. Paige. 2001. Pre-B cell receptor signaling mediates selective response to IL-7 at the pro-B to pre-B cell transition via an ERK/MAP kinase-dependent pathway. *Immunity* 15:521-531.

63. Seckinger, P., and M. Fougereau. 1994. Activation of src family kinases in human pre-B cells by IL-7. *J Immunol* 153:97-109.
64. Kee, B. L., M. W. Quong, and C. Murre. 2000. E2A proteins: essential regulators at multiple stages of B-cell development. *Immunol Rev* 175:138-149.
65. Lu, R., K. L. Medina, D. W. Lancki, and H. Singh. 2003. IRF-4,8 orchestrate the pre-B-to-B transition in lymphocyte development. *Genes Dev* 17:1703-1708.
66. Schweighoffer, E., L. Vanes, A. Mathiot, T. Nakamura, and V. L. Tybulewicz. 2003. Unexpected requirement for ZAP-70 in pre-B cell development and allelic exclusion. *Immunity* 18:523-533.
67. Wen, R., Y. Chen, J. Schuman, G. Fu, S. Yang, W. Zhang, D. K. Newman, and D. Wang. 2004. An important role of phospholipase Cgamma1 in pre-B-cell development and allelic exclusion. *EMBO J* 23:4007-4017.
68. Ochiai, K., M. Maienschein-Cline, M. Mandal, J. R. Triggs, E. Bertolino, R. Sciammas, A. R. Dinner, M. R. Clark, and H. Singh. 2012. A self-reinforcing regulatory network triggered by limiting IL-7 activates pre-BCR signaling and differentiation. *Nat Immunol* 13:300-307.
69. Heizmann, B., P. Kastner, and S. Chan. 2013. Ikaros is absolutely required for pre-B cell differentiation by attenuating IL-7 signals. *Journal of Experimental Medicine* 210:2823-2832.
70. Ferreiros-Vidal, I., T. Carroll, B. Taylor, A. Terry, Z. Liang, L. Bruno, G. Dharmalingam, S. Khadayate, B. S. Cobb, S. T. Smale, M. Spivakov, P. Srivastava, E. Petretto, A. G. Fisher, and M. Merkenschlager. 2013. Genome-wide identification of Ikaros targets elucidates its contribution to mouse B-cell lineage specification and pre-B-cell differentiation. *Blood* 121:1769-1782.
71. Wardemann, H., S. Yurasov, A. Schaefer, J. W. Young, E. Meffre, and M. C. Nussenzweig. 2003. Predominant autoantibody production by early human B cell precursors. *Science* 301:1374-1377.
72. Nemazee, D., and K. Buerki. 1989. Clonal deletion of autoreactive B lymphocytes in bone marrow chimeras. *Proc Natl Acad Sci U S A* 86:8039-8043.
73. Nossal, G. J., and B. L. Pike. 1980. Clonal anergy: persistence in tolerant mice of antigen-binding B lymphocytes incapable of responding to antigen or mitogen. *Proc Natl Acad Sci U S A* 77:1602-1606.
74. Gay, D., T. Saunders, S. Camper, and M. Weigert. 1993. Receptor editing: an approach by autoreactive B cells to escape tolerance. *J Exp Med* 177:999-1008.
75. Tiegs, S. L., D. M. Russell, and D. Nemazee. 1993. Receptor editing in self-reactive bone marrow B cells. *J Exp Med* 177:1009-1020.
76. Meffre, E. 2011. The establishment of early B cell tolerance in humans: lessons from primary immunodeficiency diseases. *Ann NY Acad Sci* 1246:1-10.
77. Perlot, T., and F. W. Alt. 2008. Cis-regulatory elements and epigenetic changes control genomic rearrangements of the IgH locus. *Adv Immunol* 99:1-32.
78. Lieber, M. R. 1992. The mechanism of V(D)J recombination: a balance of diversity, specificity, and stability. *Cell* 70:873-876.
79. van Gent, D. C., D. A. Ramsden, and M. Gellert. 1996. The RAG1 and RAG2 proteins establish the 12/23 rule in V(D)J recombination. *Cell* 85:107-113.

80. Akira, S., K. Okazaki, and H. Sakano. 1987. Two pairs of recombination signals are sufficient to cause immunoglobulin V-(D)-J joining. *Science* 238:1134-1138.
81. McBlane, J. F., D. C. van Gent, D. A. Ramsden, C. Romeo, C. A. Cuomo, M. Gellert, and M. A. Oettinger. 1995. Cleavage at a V(D)J recombination signal requires only RAG1 and RAG2 proteins and occurs in two steps. *Cell* 83:387-395.
82. van Gent, D. C., K. Hiom, T. T. Paull, and M. Gellert. 1997. Stimulation of V(D)J cleavage by high mobility group proteins. *EMBO J* 16:2665-2670.
83. Curry, J. D., J. K. Geier, and M. S. Schlissel. 2005. Single-strand recombination signal sequence nicks in vivo: evidence for a capture model of synapsis. *Nat Immunol* 6:1272-1279.
84. de Jager, M., J. van Noort, D. C. van Gent, C. Dekker, R. Kanaar, and C. Wyman. 2001. Human Rad50/Mre11 is a flexible complex that can tether DNA ends. *Mol Cell* 8:1129-1135.
85. van der Burg, M., M. Pac, M. A. Berkowska, B. Goryluk-Kozakiewicz, A. Wakulinska, B. Dembowska-Baginska, H. Gregorek, B. H. Barendregt, M. Krajewska-Walasek, E. Bernatowska, J. J. van Dongen, K. H. Chrzanowska, and A. W. Langerak. 2010. Loss of juxtaposition of RAG-induced immunoglobulin DNA ends is implicated in the precursor B-cell differentiation defect in NBS patients. *Blood* 115:4770-4777.
86. Rouse, J., and S. P. Jackson. 2002. Interfaces between the detection, signaling, and repair of DNA damage. *Science* 297:547-551.
87. Shiloh, Y. 2003. ATM and related protein kinases: safeguarding genome integrity. *Nat Rev Cancer* 3:155-168.
88. Zhou, B. B., and S. J. Elledge. 2000. The DNA damage response: putting checkpoints in perspective. *Nature* 408:433-439.
89. Matsuoka, S., B. A. Ballif, A. Smogorzewska, E. R. McDonald, 3rd, K. E. Hurov, J. Luo, C. E. Bakalarski, Z. Zhao, N. Solimini, Y. Lerenthal, Y. Shiloh, S. P. Gygi, and S. J. Elledge. 2007. ATM and ATR substrate analysis reveals extensive protein networks responsive to DNA damage. *Science* 316:1160-1166.
90. Gottlieb, T. M., and S. P. Jackson. 1993. The DNA-Dependent Protein-Kinase - Requirement for DNA Ends and Association with Ku Antigen. *Cell* 72:131-142.
91. Nussenzweig, A., C. H. Chen, V. D. Soares, M. Sanchez, K. Sokol, M. C. Nussenzweig, and G. C. Li. 1996. Requirement for Ku80 in growth and immunoglobulin V(D)J recombination. *Nature* 382:551-555.
92. van Gent, D. C., and M. van der Burg. 2007. Non-homologous end-joining, a sticky affair. *Oncogene* 26:7731-7740.
93. Moshous, D., I. Callebaut, R. de Chasseval, B. Corneo, M. Cavazzana-Calvo, F. Le Deist, I. Tezcan, O. Sanal, Y. Bertrand, N. Philippe, A. Fischer, and J. P. de Villartay. 2001. Artemis, a novel DNA double-strand break repair/V(D)J recombination protein, is mutated in human severe combined immune deficiency. *Cell* 105:177-186.
94. Schlissel, M. S. 1998. Structure of nonhairpin coding-end DNA breaks in cells undergoing V(D)J recombination. *Mol Cell Biol* 18:2029-2037.
95. Benedict, C. L., S. Gilfillan, T. H. Thai, and J. F. Kearney. 2000. Terminal deoxynucleotidyl transferase and repertoire development. *Immunol Rev* 175:150-157.

96. Desiderio, S. V., G. D. Yancopoulos, M. Paskind, E. Thomas, M. A. Boss, N. Landau, F. W. Alt, and D. Baltimore. 1984. Insertion of N Regions into Heavy-Chain Genes Is Correlated with Expression of Terminal Deoxytransferase in B-Cells. *Nature* 311:752-755.
97. Landau, N. R., D. G. Schatz, M. Rosa, and D. Baltimore. 1987. Increased frequency of N-region insertion in a murine pre-B-cell line infected with a terminal deoxynucleotidyl transferase retroviral expression vector. *Mol Cell Biol* 7:3237-3243.
98. Ahnesorg, P., P. Smith, and S. P. Jackson. 2006. XLF interacts with the XRCC4-DNA ligase IV complex to promote DNA nonhomologous end-joining. *Cell* 124:301-313.
99. Critchlow, S. E., R. P. Bowater, and S. P. Jackson. 1997. Mammalian DNA double-strand break repair protein XRCC4 interacts with DNA ligase IV. *Curr Biol* 7:588-598.
100. Grawunder, U., M. Wilm, X. T. Wu, P. Kulesza, T. E. Wilson, M. Mann, and M. R. Lieber. 1997. Activity of DNA ligase IV stimulated by complex formation with XRCC4 protein in mammalian cells. *Nature* 388:492-495.
101. van der Burg, M., J. J. van Dongen, and D. C. van Gent. 2009. DNA-PKcs deficiency in human: long predicted, finally found. *Curr Opin Allergy Clin Immunol* 9:503-509.
102. Inlay, M. A., T. X. Lin, H. H. Gao, and Y. Xu. 2006. Critical roles of the immunoglobulin intronic enhancers in maintaining the sequential rearrangement of IgH and Igk loci. *Journal of Experimental Medicine* 203:1721-1732.
103. Inlay, M. A., H. Tian, T. X. Lin, and Y. Xu. 2004. Important roles for E protein binding sites within the immunoglobulin kappa chain intronic enhancer in activating V(kappa)J(kappa) rearrangement. *Journal of Experimental Medicine* 200:1205-1211.
104. Perlot, T., F. W. Alt, C. H. Bassing, H. Suh, and E. Pinaud. 2005. Elucidation of IgH intronic enhancer functions via germ-line deletion. *Proc Natl Acad Sci U S A* 102:14362-14367.
105. Medvedovic, J., A. Ebert, H. Tagoh, I. M. Tamir, T. A. Schwickert, M. Novatchkova, Q. Sun, P. J. Huis In 't Veld, C. Guo, H. S. Yoon, Y. Denizot, S. J. Holwerda, W. de Laat, M. Cogne, Y. Shi, F. W. Alt, and M. Busslinger. 2013. Flexible long-range loops in the VH gene region of the Igh locus facilitate the generation of a diverse antibody repertoire. *Immunity* 39:229-244.
106. Ebert, A., S. McManus, H. Tagoh, J. Medvedovic, G. Salvaggio, M. Novatchkova, I. Tamir, A. Sommer, M. Jaritz, and M. Busslinger. 2011. The distal V(H) gene cluster of the Igh locus contains distinct regulatory elements with Pax5 transcription factor-dependent activity in pro-B cells. *Immunity* 34:175-187.
107. Guo, C., H. S. Yoon, A. Franklin, S. Jain, A. Ebert, H. L. Cheng, E. Hansen, O. Despo, C. Bossen, C. Vettermann, J. G. Bates, N. Richards, D. Myers, H. Patel, M. Gallagher, M. S. Schlissel, C. Murre, M. Busslinger, C. C. Giallourakis, and F. W. Alt. 2011. CTCF-binding elements mediate control of V(D)J recombination. *Nature* 477:424-430.
108. Liu, Z. M., J. B. George-Raizen, S. Li, K. C. Meyers, M. Y. Chang, and W. T. Garrard. 2002. Chromatin structural analyses of the mouse Iggamma gene locus reveal new hypersensitive sites specifying a transcriptional silencer and enhancer. *J Biol Chem* 277:32640-32649.

109. Cobb, R. M., K. J. Oestreich, O. A. Osipovich, and E. M. Oltz. 2006. Accessibility control of V(D)J recombination. *Adv Immunol* 91:45-109.
110. Corcoran, A. E. 2010. The epigenetic role of non-coding RNA transcription and nuclear organization in immunoglobulin repertoire generation. *Semin Immunol* 22:353-361.
111. Yancopoulos, G. D., and F. W. Alt. 1985. Developmentally Controlled and Tissue-Specific Expression of Unrearranged Vh Gene Segments. *Cell* 40:271-281.
112. Yancopoulos, G. D., and F. W. Alt. 1986. Regulation of the assembly and expression of variable-region genes. *Annu Rev Immunol* 4:339-368.
113. Ribeiro de Almeida, C., R. Stadhouders, M. J. de Bruijn, I. M. Bergen, S. Thongjuea, B. Lenhard, W. van Ijcken, F. Grosveld, N. Galjart, E. Soler, and R. W. Hendriks. 2011. The DNA-binding protein CTCF limits proximal V κ recombination and restricts kappa enhancer interactions to the immunoglobulin kappa light chain locus. *Immunity* 35:501-513.
114. Woodcock, C. L., and R. P. Ghosh. 2010. Chromatin higher-order structure and dynamics. *Cold Spring Harb Perspect Biol* 2:a000596.
115. Kornberg, R. D., and Y. Lorch. 1999. Twenty-five years of the nucleosome, fundamental particle of the eukaryote chromosome. *Cell* 98:285-294.
116. Schneider, R., and R. Grosschedl. 2007. Dynamics and interplay of nuclear architecture, genome organization, and gene expression. *Gene Dev* 21:3027-3043.
117. Kouzarides, T. 2007. Chromatin modifications and their function. *Cell* 128:693-705.
118. Saha, A., J. Wittmeyer, and B. R. Cairns. 2006. Chromatin remodelling: the industrial revolution of DNA around histones. *Nat Rev Mol Cell Biol* 7:437-447.
119. Guibert, S., and M. Weber. 2013. Functions of DNA methylation and hydroxymethylation in mammalian development. *Curr Top Dev Biol* 104:47-83.
120. Chowdhury, D., and R. Sen. 2001. Stepwise activation of the immunoglobulin mu heavy chain gene locus. *EMBO J* 20:6394-6403.
121. Goldmit, M., Y. Ji, J. Skok, E. Roldan, S. Jung, H. Cedar, and Y. Bergman. 2005. Epigenetic ontogeny of the I κ k locus during B cell development. *Nat Immunol* 6:198-203.
122. Perkins, E. J., B. L. Kee, and D. A. Ramsden. 2004. Histone 3 lysine 4 methylation during the pre-B to immature B-cell transition. *Nucleic Acids Res* 32:1942-1947.
123. Xu, C. R., and A. J. Feeney. 2009. The Epigenetic Profile of Ig Genes Is Dynamically Regulated during B Cell Differentiation and Is Modulated by Pre-B Cell Receptor Signaling. *Journal of Immunology* 182:1362-1369.
124. Ji, Y., W. Resch, E. Corbett, A. Yamane, R. Casellas, and D. G. Schatz. 2010. The in vivo pattern of binding of RAG1 and RAG2 to antigen receptor loci. *Cell* 141:419-431.
125. Liu, Y., R. Subrahmanyam, T. Chakraborty, R. Sen, and S. Desiderio. 2007. A plant homeodomain in Rag-2 that binds hypermethylated lysine 4 of histone H3 is necessary for efficient antigen-receptor-gene rearrangement. *Immunity* 27:561-571.

126. Matthews, A. G. W., A. J. Kuo, S. Ramon-Maiques, S. M. Han, K. S. Champagne, D. Ivanov, M. Gallardo, D. Carney, P. Cheung, D. N. Ciccone, K. L. Walter, P. J. Utz, Y. Shi, T. G. Kutateladze, W. Yang, O. Gozani, and M. A. Oettinger. 2007. RAG2 PHD finger couples histone H3 lysine 4 trimethylation with V(D)J recombination. *Nature* 450:1106-U1118.
127. Chakraborty, T., T. Perlot, R. Subrahmanyam, A. Jani, P. H. Goff, Y. Zhang, I. Ivanova, F. W. Alt, and R. Sen. 2009. A 220-nucleotide deletion of the intronic enhancer reveals an epigenetic hierarchy in immunoglobulin heavy chain locus activation. *J Exp Med* 206:1019-1027.
128. Osipovich, O. A., R. Subrahmanyam, S. Pierce, R. Sen, and E. M. Oltz. 2009. Cutting edge: SWI/SNF mediates antisense Igh transcription and locus-wide accessibility in B cell precursors. *J Immunol* 183:1509-1513.
129. Feeney, A. J. 2011. Epigenetic regulation of antigen receptor gene rearrangement. *Curr Opin Immunol* 23:171-177.
130. Maston, G. A., S. K. Evans, and M. R. Green. 2006. Transcriptional regulatory elements in the human genome. *Annu Rev Genomics Hum Genet* 7:29-59.
131. Lin, Y. C., C. Benner, R. Mansson, S. Heinz, K. Miyazaki, M. Miyazaki, V. Chandra, C. Bossen, C. K. Glass, and C. Murre. 2012. Global changes in the nuclear positioning of genes and intra- and interdomain genomic interactions that orchestrate B cell fate. *Nat Immunol* 13:1196-1204.
132. Dixon, J. R., S. Selvaraj, F. Yue, A. Kim, Y. Li, Y. Shen, M. Hu, J. S. Liu, and B. Ren. 2012. Topological domains in mammalian genomes identified by analysis of chromatin interactions. *Nature* 485:376-380.
133. Lieberman-Aiden, E., N. L. van Berkum, L. Williams, M. Imakaev, T. Ragoczy, A. Telling, I. Amit, B. R. Lajoie, P. J. Sabo, M. O. Dorschner, R. Sandstrom, B. Bernstein, M. A. Bender, M. Groudine, A. Gnirke, J. Stamatoyannopoulos, L. A. Mirny, E. S. Lander, and J. Dekker. 2009. Comprehensive Mapping of Long-Range Interactions Reveals Folding Principles of the Human Genome. *Science* 326:289-293.
134. Handoko, L., H. Xu, G. Li, C. Y. Ngan, E. Chew, M. Schnapp, C. W. Lee, C. Ye, J. L. Ping, F. Mulawadi, E. Wong, J. Sheng, Y. Zhang, T. Poh, C. S. Chan, G. Kunarso, A. Shahab, G. Bourque, V. Cacheux-Rataboul, W. K. Sung, Y. Ruan, and C. L. Wei. 2011. CTCF-mediated functional chromatin interactome in pluripotent cells. *Nat Genet* 43:630-638.
135. Parelho, V., S. Hadjur, M. Spivakov, M. Leleu, S. Sauer, H. C. Gregson, A. Jarmuz, C. Canzonetta, Z. Webster, T. Nesterova, B. S. Cobb, K. Yokomori, N. Dillon, L. Aragon, A. G. Fisher, and M. Merkenschlager. 2008. Cohesins functionally associate with CTCF on mammalian chromosome arms. *Cell* 132:422-433.
136. Phillips, J. E., and V. G. Corces. 2009. CTCF: master weaver of the genome. *Cell* 137:1194-1211.
137. Wood, A. J., A. F. Severson, and B. J. Meyer. 2010. Condensin and cohesin complexity: the expanding repertoire of functions. *Nat Rev Genet* 11:391-404.
138. Jhunjhunwala, S., M. C. van Zelm, M. M. Peak, S. Cutchin, R. Riblet, J. J. van Dongen, F. G. Grosveld, T. A. Knoch, and C. Murre. 2008. The 3D structure of the immunoglobulin heavy-chain locus: implications for long-range genomic interactions. *Cell* 133:265-279.

139. Degner, S. C., J. Verma-Gaur, T. P. Wong, C. Bossen, G. M. Iverson, A. Torkamani, C. Vettermann, Y. C. Lin, Z. Ju, D. Schulz, C. S. Murre, B. K. Birshstein, N. J. Schork, M. S. Schlissel, R. Riblet, C. Murre, and A. J. Feeney. 2011. CCCTC-binding factor (CTCF) and cohesin influence the genomic architecture of the Igh locus and antisense transcription in pro-B cells. *Proc Natl Acad Sci U S A* 108:9566-9571.
140. Degner, S. C., T. P. Wong, G. Jankevicius, and A. J. Feeney. 2009. Cutting edge: developmental stage-specific recruitment of cohesin to CTCF sites throughout immunoglobulin loci during B lymphocyte development. *J Immunol* 182:44-48.
141. Liu, H., M. Schmidt-Suppran, Y. Shi, E. Hobeika, N. Barteneva, H. Jumaa, R. Pelanda, M. Reth, J. Skok, and K. Rajewsky. 2007. Yin Yang 1 is a critical regulator of B-cell development. *Genes Dev* 21:1179-1189.
142. Guo, C., T. Gerasimova, H. Hao, I. Ivanova, T. Chakraborty, R. Selimyan, E. M. Oltz, and R. Sen. 2011. Two forms of loops generate the chromatin conformation of the immunoglobulin heavy-chain gene locus. *Cell* 147:332-343.
143. Roldan, E., M. Fuxa, W. Chong, D. Martinez, M. Novatchkova, M. Busslinger, and J. A. Skok. 2005. Locus 'decontraction' and centromeric recruitment contribute to allelic exclusion of the immunoglobulin heavy-chain gene. *Nat Immunol* 6:31-41.
144. Sayegh, C. E., S. Jhunjhunwala, R. Riblet, and C. Murre. 2005. Visualization of looping involving the immunoglobulin heavy-chain locus in developing B cells. *Genes Dev* 19:322-327.
145. Jensen, K., M. B. Rother, B. S. Brusletto, O. K. Olstad, H. C. D. Aass, M. C. van Zelm, P. Kierulf, and K. M. Gautvik. 2013. Increased ID2 Levels in Adult Precursor B Cells as Compared with Children Is Associated with Impaired Ig Locus Contraction and Decreased Bone Marrow Output. *J Immunol* 191:1210-1219.
146. Bain, G., E. C. Maandag, D. J. Izon, D. Amsen, A. M. Kruisbeek, B. C. Weintraub, I. Krop, M. S. Schlissel, A. J. Feeney, M. van Roon, and et al. 1994. E2A proteins are required for proper B cell development and initiation of immunoglobulin gene rearrangements. *Cell* 79:885-892.
147. Fuxa, M., J. Skok, A. Souabni, G. Salvagiotto, E. Roldan, and M. Busslinger. 2004. Pax5 induces V-to-DJ rearrangements and locus contraction of the immunoglobulin heavy-chain gene. *Genes Dev* 18:411-422.
148. Lin, H., and R. Grosschedl. 1995. Failure of B-cell differentiation in mice lacking the transcription factor EBF. *Nature* 376:263-267.
149. Reynaud, D., I. A. Demarco, K. L. Reddy, H. Schjerven, E. Bertolino, Z. S. Chen, S. T. Smale, S. Winandy, and H. Singh. 2008. Regulation of B cell fate commitment and immunoglobulin heavy-chain gene rearrangements by Ikaros. *Nature Immunology* 9:927-936.
150. Verma-Gaur, J., A. Torkamani, L. Schaffer, S. R. Head, N. J. Schork, and A. J. Feeney. 2012. Noncoding transcription within the Igh distal V-H region at PAIR elements affects the 3D structure of the Igh locus in pro-B cells. *P Natl Acad Sci USA* 109:17004-17009.
151. Liu, Z., P. Widlak, Y. Zou, F. Xiao, M. Oh, S. Li, M. Y. Chang, J. W. Shay, and W. T. Garrard. 2006. A recombination silencer that specifies heterochromatin positioning and ikaros association in the immunoglobulin kappa locus. *Immunity* 24:405-415.

152. Xiang, Y., X. Zhou, S. L. Hewitt, J. A. Skok, and W. T. Garrard. 2011. A multifunctional element in the mouse Igkappa locus that specifies repertoire and Ig loci subnuclear location. *J Immunol* 186:5356-5366.
153. Fitzsimmons, S. P., R. M. Bernstein, E. E. Max, J. A. Skok, and M. A. Shapiro. 2007. Dynamic changes in accessibility, nuclear positioning, recombination, and transcription at the Ig kappa locus. *Journal of Immunology* 179:5264-5273.
154. Peric-Hupkes, D., W. Meuleman, L. Pagie, S. W. Bruggeman, I. Solovei, W. Brugman, S. Graf, P. Flicek, R. M. Kerkhoven, M. van Lohuizen, M. Reinders, L. Wessels, and B. van Steensel. 2010. Molecular maps of the reorganization of genome-nuclear lamina interactions during differentiation. *Mol Cell* 38:603-613.
155. Reddy, K. L., J. M. Zullo, E. Bertolino, and H. Singh. 2008. Transcriptional repression mediated by repositioning of genes to the nuclear lamina. *Nature* 452:243-247.
156. Cremer, T., and C. Cremer. 2001. Chromosome territories, nuclear architecture and gene regulation in mammalian cells. *Nat Rev Genet* 2:292-301.
157. Osborne, C. S., L. Chakalova, K. E. Brown, D. Carter, A. Horton, E. Debrand, B. Goyenechea, J. A. Mitchell, S. Lopes, W. Reik, and P. Fraser. 2004. Active genes dynamically colocalize to shared sites of ongoing transcription. *Nature Genetics* 36:1065-1071.
158. Simonis, M., P. Klous, E. Splinter, Y. Moshkin, R. Willemsen, E. de Wit, B. van Steensel, and W. de Laat. 2006. Nuclear organization of active and inactive chromatin domains uncovered by chromosome conformation capture-on-chip (4C). *Nature Genetics* 38:1348-1354.
159. Kosak, S. T., J. A. Skok, K. L. Medina, R. Riblet, M. M. Le Beau, A. G. Fisher, and H. Singh. 2002. Subnuclear compartmentalization of immunoglobulin loci during lymphocyte development. *Science* 296:158-162.
160. Skok, J. A., K. E. Brown, V. Azuara, M. L. Caparros, J. Baxter, K. Takacs, N. Dillon, D. Gray, R. P. Perry, M. Merkenschlager, and A. G. Fisher. 2001. Nonequivalent nuclear location of immunoglobulin alleles in B lymphocytes. *Nat Immunol* 2:848-854.



Chapter II

Pre-B cell receptor signaling induces immunoglobulin κ locus accessibility by functional redistribution of enhancer-mediated chromatin interactions

Ralph Stadhouders¹, Marjolein J.W. de Bruijn², Magdalena B. Rother³, Saravanan Yuvaraj², Claudia Ribeiro de Almeida², Petros Kolovos¹, Menno C. Van Zelm³, Wilfred van Ijcken⁴, Frank Grosveld^{1,5}, Eric Soler^{1,5,6} and Rudi W. Hendriks²

(1) Department of Cell Biology, (2) Department of Pulmonary Medicine, (3) Department of Immunology, (4) Center for Biomics, (5) The Cancer Genomics Center, Erasmus MC, University Medical Center, Rotterdam, The Netherlands, and (6) INSERM UMR967 & French Alternative Energies and Atomic Energy Commission (CEA), Fontenay-aux-Roses, France

Manuscript published in PLoS Biol 2014; 12(2): e100179

The online version of this article contains the supplemental material.

ABSTRACT

During B-cell development the precursor B-cell receptor (pre-BCR) checkpoint is thought to increase immunoglobulin κ light chain (*Ig κ*) locus accessibility to the V(D)J recombinase. Accordingly, pre-B cells lacking the pre-BCR signaling molecules Btk or Slp65 showed reduced germline V κ transcription. To investigate whether pre-BCR signaling modulates V κ accessibility through enhancer-mediated *Ig κ* locus topology, we performed chromosome conformation capture and sequencing analyses. These revealed that already in pro-B cells the κ enhancers robustly interact with the ~3.2 Mb V κ region and its flanking sequences. Analyses in wild-type, Btk and Slp65 single and double-deficient pre-B cells demonstrated that pre-BCR signaling reduces interactions of both enhancers with *Ig κ* locus flanking sequences and increases interactions of the 3' κ enhancer with V κ genes. Remarkably, pre-BCR signaling does not significantly affect interactions between the intronic enhancer and V κ genes, which are already robust in pro-B cells. Both enhancers interact most frequently with highly used V κ genes, which are often marked by transcription factor E2A. We conclude that the κ enhancers interact with the V κ region already in pro-B cells and that pre-BCR signaling induces accessibility through a functional redistribution of long-range chromatin interactions within the V κ region, whereby the two enhancers play distinct roles.

INTRODUCTION

B lymphocyte development is characterized by stepwise recombination of immunoglobulin (Ig) variable (V), diversity (D) and joining (J) genes, whereby in pro-B cells the Ig heavy (H) chain locus rearranges before the *Ig κ* or *Ig λ* light (L) chain loci.^{1, 2} Productive IgH chain rearrangement is monitored by deposition of the IgH μ chain protein on the cell surface, together with the pre-existing surrogate light chain (SLC) proteins $\lambda 5$ and VpreB, as the pre-B cell receptor (pre-BCR) complex.³ Pre-BCR expression serves as a checkpoint that monitors for functional *IgH* chain rearrangement, triggers proliferative expansion and induces developmental progression of large cycling into small resting Ig μ^+ pre-B cells in which the recombination machinery is reactivated for rearrangement of the *Ig κ* or *Ig λ* L chain loci.^{3, 4}

During the V(D)J recombination process, the spatial organization of large antigen receptor loci is actively remodeled.⁵ Overall locus contraction is achieved through long-range chromatin interactions between proximal and distal regions within these loci. This process brings distal V genes in close proximity to (D)J regions, to which Rag (recombination activating gene) protein binding occurs⁶ and the nearby regulatory elements that are required for topological organization and recombination.^{5, 7, 8} The

recombination-associated changes in locus topology thereby provide equal opportunities for individual V genes to be recombined to a (D)J segment. Accessibility and recombination of antigen receptor loci are controlled by many DNA-binding factors that interact with local *cis*-regulatory elements, such as promoters, enhancers or silencers.⁷⁻⁹ The long-range chromatin interactions involved in this process are thought to be crucial for the regulation of V(D)J recombination and orchestrate changes in subnuclear relocation, germline transcription, histone acetylation and/or methylation, DNA demethylation and compaction of antigen receptor loci.^{5, 10}

The mouse *Igk* locus harbors 101 functional V κ genes and four functional J κ elements and is spread over >3 Mb of genomic DNA.¹¹ Mechanisms regulating the site-specific DNA recombination reactions that create a diverse *Igk* repertoire are complex and involve local differences in the accessibility of the V κ and J κ genes to the recombinase proteins.¹² Developmental-stage specific changes in gene accessibility are reflected by germline transcription, which precedes or accompanies gene recombination.¹³ In the *Igk* locus germline transcription is initiated from promoters located upstream of J κ (referred to as κ^0 transcripts) and from V κ promoters.¹⁴ Deletion of the intronic enhancer (iE κ), located between J κ and C κ , or the downstream 3' κ enhancer (3'E κ), both containing binding sites for the E2A and Irf4/Irf8 transcription factors, diminishes *Igk* locus germline transcription and recombination.¹⁵⁻¹⁹ On the other hand, the Sis (silencer in intervening sequence) element in the V κ -J κ region negatively regulates *Igk* rearrangement.²⁰ This Sis element was shown to target *Igk* alleles to centromeric heterochromatin and to associate with the Ikaros repressor protein that also colocalizes with centromeric heterochromatin. Sis contains a strong binding site for the zinc-finger transcription regulator CTCF-binding factor (Ctcf).^{21, 22} Interestingly, deletion of the Sis element or conditional deletion of the *Ctcf* gene in the B cell lineage both resulted in reduced κ^0 germline transcription and enhanced proximal V κ usage.^{21, 23} Very recently, a novel Ctcf-binding element located directly upstream of the Sis region was shown to be essential for locus contraction and recombination to distal V κ genes.²³ In addition, the *Igk* repertoire is controlled by the polycomb group protein YY1.²⁴

Induction of *Igk* rearrangements requires the expression of the Rag1 and Rag2 proteins, the attenuation of the cell cycle and transcriptional activation of the *Igk* locus, all of which are thought to be crucially dependent on pre-BCR signaling.^{4, 25} At first, pre-BCR signals synergize with interleukin-7 receptor (IL-7R) signals to drive proliferative expansion of IgH μ^+ large pre-B cells.⁴ In these cells transcription of the *Rag* genes is low and the Rag2 protein is unstable due to cell-cycle dependent degradation.²⁶ Subsequently, signaling through the pre-BCR downstream adapter Slp65 (SH2-domain-containing leukocyte protein of 65 kDa, also known as Blnk or Bash) switches cell fate from proliferation to differentiation.⁴ Importantly, Slp65 (i) induces the transcription

factor Aiolos, which downregulates $\lambda 5$ expression,²⁷ (ii) binds Jak3 and thereby interferes with IL-7R signaling,²⁸ and (iii) reduces inhibitory phosphorylation of Foxo transcription factors.²⁹ All these changes result in attenuation of the cell cycle and thus Rag protein stabilization. Moreover, *Rag* gene transcription is induced by Foxo proteins.³⁰

Although rearrangement and expression of the *Ig κ* locus can occur independently of IgH μ chain expression,^{31, 32} several lines of evidence indicate that pre-BCR signaling is actively involved in inducing *Ig κ* and *Ig λ* locus accessibility and gene rearrangement. First, surface IgH μ chain expression correlates with germline transcription in the *Ig κ* locus.³³ Second, in the absence of Slp65, κ^0 germline transcription is reduced.³⁴ Third, mice deficient for Bruton's tyrosine kinase (Btk), which is a pre-BCR downstream signaling molecule interacting with Slp65, show reduced *Ig λ* L chain germline transcription and reduced Ig λ usage.³⁵ Fourth, transgenic expression of the constitutively active E41K-Btk mutant in IgH μ chain negative pro-B cells induces premature rearrangement and protein expression of Ig κ L chain.³⁴ Based on fluorescence in situ hybridization (FISH) studies, it has been proposed that in pro-B cells distal V κ and C κ genes are separated by large distances and that the *Ig κ* locus specifically undergoes contraction in small pre-B and immature-B cells actively undergoing V κ -J κ recombination.³⁶ However, it remains unknown how pre-BCR-induced signals affect the accessibility, contraction and topology of the V κ region, or how they affect the long-range interactions of the κ regulatory elements involved in organizing these events.

In this study, we identified the effects of pre-BCR signaling on germline V κ transcription and on the expression of transcription factors implicated in the regulation of *Ig κ* gene rearrangement. We found that the decrease in pre-BCR signaling capacity in wild-type, Btk-deficient, Slp65-deficient and Btk/Slp65 double-deficient pre-B cells was paralleled by a gradient of decreased expression of many transcription factors including Ikaros, Aiolos, Irf4 and (to a lesser extent) E2A, as well as by a decreased *Ig κ* locus accessibility for recombination. Several of these factors can mediate long-range chromatin interactions and are known to occupy κ regulatory elements that regulate locus accessibility.³⁷⁻⁴⁰ We therefore sought to analyze the effect of pre-BCR signaling on the higher-order chromatin structure organized by these regulatory sequences at the *Ig κ* locus. To this end, we performed chromosome conformation capture and sequencing (3C-seq) analyses⁴¹ on pro-B cells, and pre-B cells from mice single or double deficient for Btk or Slp65 to evaluate the effects of this pre-BCR signaling gradient on *Ig κ* locus topology. These 3C-seq experiments demonstrated that already in pro-B cells the κ enhancers robustly interact with the ~3.2 Mb V κ region and its flanking sequences, and that pre-BCR signaling induces accessibility by a functional redistribution of enhancer-mediated chromatin interactions within the V κ region.

RESULTS

Identification of genes regulated by pre-BCR signaling

Whereas mice deficient for the pre-BCR signaling molecules Btk and Slp65 have a partial block at the pre-B cell stage,^{42, 43} in Btk/Slp65 double-deficient mice only very few pre-B cells show progression to the immature-B cell stage characterized by functional *IgL* chain gene recombination.⁴⁴ To enable analysis of the effects of pre-BCR signaling on (i) the expression of genes involved in *Igκ* gene rearrangement and on (ii) long-distance chromatin interactions in the *Igκ* locus in pre-B cells in the absence of *Igκ* gene recombination events, we bred Btk and Slp65 single and double-deficient mice on the Rag1^{-/-} background. In these mice, progression of B cell progenitors to the pre-B cell stage was conferred by the transgenic, functionally rearranged VH81X IgH μ chain, which ensures pre-BCR expression and cellular proliferation. The absence of functional Rag1 protein precludes *IgL* chain gene rearrangement and cells are completely arrested at the small pre-B cell stage (**Figure 1A**).

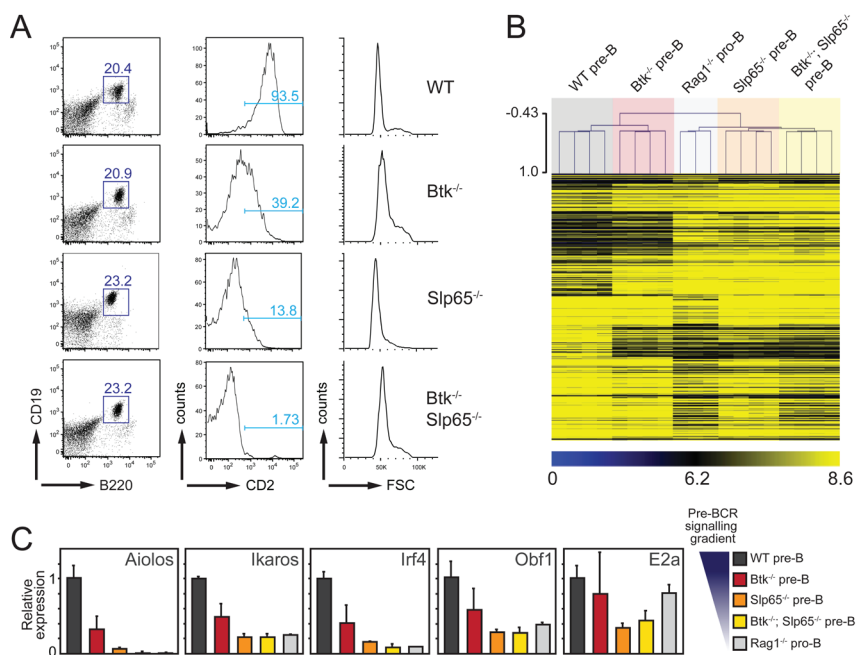


Figure 1. Gene expression profiling strategy for the identification of genes regulated by Btk/Slp65-mediated pre-BCR signaling. (A) FACS Sorting strategy for purification of pre-B cell fractions from the indicated mice on a VH81X transgenic Rag1^{-/-} background. Lymphocytes were gated on the basis of forward/side scatter and B220⁺CD19⁺ pre-B cell fractions were sorted. Virtually all B220⁺CD19⁺ cells were cytoplasmic μ heavy chain positive,³⁴ but showed genotype-dependent levels of expression of the CD2 differentiation marker, in agreement with previous findings.³⁴ (B) DNA microarray analysis of total mRNA from FACS-purified

B220⁺CD19⁺ pre-B/pro-B cell fractions from the indicated mice. One-way ANOVA analysis (p=0.01) identified 266 significantly different genes. MeV hierarchical clustering of gene expression differences are represented in the heatmap. (C) Validation of the expression of transcription factors implicated in *Igκ* gene rearrangement. Total mRNA isolated from FACS-sorted B220⁺CD19⁺ pre-B/pro-B cell fractions from the indicated mice, was analyzed by quantitative RT-PCR for expression of transcription factors. Expression levels were normalized to those of *Gapdh*, whereby the values in WT pre-B cells were set to one. Bars represent mean values and error bars denote standard deviations for 4 independent mice per group.

We performed genome-wide expression profiling of FACS-purified B220⁺CD19⁺ pre-B cell fractions from wild-type (WT), *Btk* and *Slp65* single and double deficient transgenic V_H81X *Rag1*^{-/-} mice (**Figure 1A**). In these experiments non- V_H81X transgenic *Rag1*^{-/-} pro-B cells served as controls. One-way ANOVA analysis using MeV software⁴⁵ (p<0.01) revealed that 266 genes were differentially expressed between the five groups of pro-B/pre-B cells (**Figure 1B**). When compared with WT V_H81X transgenic *Rag1*^{-/-} pre-B cells, 174 genes were up regulated, whereby the average values of the fold-increase were ~1.70, ~3.28, ~3.36 and ~3.47 for *Btk*^{-/-}, *Slp65*^{-/-}, *Btk*^{-/-}*Slp65*^{-/-} V_H81X transgenic *Rag1*^{-/-} pre-B cells and non- V_H81X transgenic *Rag1*^{-/-} pro-B cells, respectively (Table S1). A similar gradient of gene expression changes was apparent from the average values of the fold-change for the 192 significantly down regulated genes, which were ~1.65, ~2.29, ~3.79 and ~4.15 in the four groups of pre-B/pro-B cells, respectively (Table S2). In a hierarchical clustering analysis of the five groups of B cell precursors, the expression profiles of *Btk*^{-/-}*Slp65*^{-/-} V_H81X transgenic *Rag1*^{-/-} pre-B cells and non-V_H81X transgenic *Rag1*^{-/-} pro-B cells were very similar (**Figure 1B**). This implies that expression of the 266 genes is not substantially influenced by pre-BCR-mediated proliferation, which is still induced in pre-B cells lacking both *Btk* and *Slp65*^{44, 46} but not in *Rag1*^{-/-} pro-B cells. Consistent with these findings, gene distance matrix analysis revealed a clear gene expression gradient among the five groups of pre-B/pro-B cells, in which *Btk*^{-/-}*Slp65*^{-/-} pre-B and *Rag1*^{-/-} pro-B cells again showed highly comparably expression signatures (Figure S1).

In agreement with previous findings,^{34, 43, 46} pre-BCR signaling-defective pre-B cells manifested increased expression of *Dntt*, encoding terminal deoxynucleotidyl transferase and the SLC components *Vpre* (*Vpreb1*) and $\lambda 5$ (*Igll1*), as well as decreased expression of the cell surface markers CD2, CD22, CD25(IL-2R) and MHC class II (**Table 1**). *Btk* and *Slp65* single deficient and particularly double deficient pre-B cells failed to upregulate various genes known to be involved in *IgL* chain recombination, such as *Ikzf3* (Aiolos), *Ikzf1* (Ikaros), *Irf4*, *Spib*, *Pou2f2* (Oct2), polymerase- μ ,⁴⁷ as well as *Hivep1* encoding the Mbp-1 protein, which has been shown to bind to the κ enhancers.⁴⁸ In addition, pre-BCR signaling influenced the expression levels of many other DNA-binding or modifying factors that were not previously associated with *IgL* chain recombination, including *Lmo4*, *Zfp710*, *Arid1a/3a/3b*, the lysine-specific demethylases *Aof1* and *Phf2*, *Prdm2* (a H3K9 methyltransferase), the *sik1* gene encoding a histon deacetylase (HDAC)

kinase, *Hdac5*, *Hdac8* and the DNA repair protein gene *Rev1* (Table S2). We did not find significant differences in the expression of several other transcription factors implicated in Ig gene recombination, e.g. *Obf1/Oca-B*, *Pax5*, *E2A* and *Irf8* (Table 1). In addition, in signaling-deficient pre-B cells we found reduced transcription of genes encoding several signaling molecules, (e.g. *Rasgrp1*, *Rapgef1*, *Ralgps2*, *Blk*, *Traf5*, *Hck*, *Nfkbia* ($\text{I}\kappa\text{B}\alpha$), *Syk*, *Csk*), cell surface markers (CD38, CD72, CD74, CD55 and Notch2) or genes regulating cell survival (*Bmf* and *Bcl2l1* encoding Bcl_{XL}) (Table S2). Interestingly, we observed concomitant upregulation of signaling molecules that are also associated with the T cell receptor (*Lat*, *Zap70* and *Prkcq* (PKC θ); Table S1).

Next, we used quantitative RT-PCR to confirm the observed differential expression of several transcription factors. Expression levels of these genes were indeed significantly reduced in a pre-BCR signaling dependent manner, especially for Aiolos, Ikaros and *Irf4*, with residual expression levels in *Btk*^{-/-}*Slp65*^{-/-} VH81X transgenic *Rag1*^{-/-} pre-B cells that were ~1%, ~20% and ~9% of those observed in WT VH81X *Rag1*^{-/-} mice, respectively (Figure 1C). In addition, we found moderate effects on *Obf1* (Oca-B) and *E2A* with residual expression levels of ~28% and ~44%, respectively. In chromatin immunoprecipitation (ChIP) assays we observed in pre-B cells substantial binding of *E2A* protein to the intronic and 3' κ enhancer regions and to the three $\text{V}\kappa$ regions analyzed. Under conditions of reduced pre-BCR signaling activity *E2A* binding to the enhancers was essentially maintained (3' κ) or reduced (i κ), but *E2A* binding to the $\text{V}\kappa$ regions was lost (Table S3). Consistent with the significant reduction of Ikaros expression in *Slp65*^{-/-} pre-B cells, Ikaros binding both κ enhancers and to $\text{V}\kappa$ regions was undetectable in these cells (Table S3).

Taken together, from these findings we conclude that the five groups of pro-B/pre-B cells, representing a gradient of progressively diminished pre-BCR signaling, show in parallel a gradient of diminished modulation of many genes that signify pre-B cell differentiation, including key genes implicated in *Igk* gene recombination.

Progressively diminished $\text{V}\kappa$ and $\text{J}\kappa$ GLTs in *Btk*^{-/-}, *Slp65*^{-/-}, and *Btk*^{-/-}*Slp65*^{-/-} pre-B cells

In these expression profiling studies we only detected limited differences in germline transcription (GLT) over unrearranged $\text{J}\kappa$ and $\text{V}\kappa$ gene segments, which is thought to reflect locus accessibility.¹² However, we previously showed by serial-dilution RT-PCR that the levels of κ^0 0.8 and κ^0 1.1, germline transcripts, which are initiated in different regions 5' of $\text{J}\kappa$ and spliced to the $\text{C}\kappa$ region⁴⁹ are apparently normal in *Btk*^{-/-} pre-B cells, modestly reduced in *Slp65*^{-/-} pre-B cells and severely reduced in *Btk*^{-/-}*Slp65*^{-/-} pre-B cells.³⁴

II. Pre-B Cell Receptor Signaling Induces Immunoglobulin K Locus Accessibility By Functional Redistribution Of Enhancer-Mediated Chromatin Interactions

Table 1. Genes differentially expressed between WT, Btk or Slp65 single or double mutant V μ 8.1X Tg Rag1^{-/-} pre-B cells or Rag1^{-/-} pro-B cells.

ID	Probe set	Accession number	Gene	Description of function	p-value ^(*)	Fold change (Btk KO) ^(b)	Fold change (Slp65 KO)	Fold change (BtkSlp65 KO)	Fold change (Rag1 KO)
Genes known to be upregulated in signaling-deficient pre-B cells									
10463123	NM_009345		Dnrtt	N addition VDJ recombination	4.26E-08	8.46	16.99	22.49	39.19
10438064	NM_016982		Vpreb1	VpreB SLC component	7.58E-06	5.52	6.80	6.32	5.73
10438060	ENSMUST00000100136		Igll1	λ 5 SLC component	2.17E-04	3.38	3.81	4.17	3.69
10427628	NM_008372		Il7r	IL-7 cytokine receptor	n.s. ^(c)	1.08	1.62	1.56	1.91
Genes known to be downregulated in signaling-deficient pre-B cells									
10500677	NM_013486		Cd2	cell adhesion	2.57E-04	-4.82	-5.35	-20.52	-24.26
10469278	NM_008367		Il2ra	IL2 cytokine receptor CD25	1.60E-03	-5.21	-8.79	-15.90	-16.26
10450154	NM_010378		H2-Aa	MHC class II	1.45E-04	-2.04	-5.75	-13.16	-19.80
10562132	NM_001043317		Cd22	Siglec- family receptor	3.32E-05	1.29	1.14	-1.98	-6.06
Transcription regulators & V(D)J recombination									
10390640	NM_011771		Ikzf3	Aiolos DNA binding factor	7.05E-08	-1.66	-3.99	-29.34	-26.09
10384020	NM_017401		Polm	Polymerase mu	2.35E-06	-1.91	-4.17	-10.09	-12.25
10502510	NM_010723		Lmo4	DNA binding factor	1.70E-03	-1.90	-3.56	-5.70	-7.22
10404389	NM_013674		Irf4	DNA binding factor	7.87E-05	-1.60	-2.16	-4.75	-5.29
10438415	ENSMUST00000103752		Igl-V2	Ig V lambda light chain	6.90E-05	-3.41	-3.87	-4.57	-4.81
10438405	M94350		Igl-V1	Ig V lambda light chain	1.58E-06	-3.42	-3.07	-3.98	-6.20
10562812	NM_019866		SpiB	Spi-B DNA binding factor	3.88E-04	-1.57	-1.94	-3.16	-3.22

10364559	NM_007880	Arid3a	Bright DNA binding factor	1.10E-03	-1.80	-2.16	-3.04	-3.18
10594001	NM_019689	Arid3b	DNA binding factor	5.74E-04	-1.79	-2.51	-2.91	-3.53
10554370	NM_175433	Zfp710	DNA binding factor	9.03E-03	-1.50	-1.64	-2.14	-2.99
10374333	NM_001025597	Ikzf1	Ikaros DNA binding factor	5.19E-05	-1.31	-1.77	-1.99	-2.44
10560964	NM_011138	Pou2f2	Oct-2 DNA binding factor	6.20E-03	-1.24	-1.30	-1.84	-2.56
10517090	NM_001080819	Arid1a	DNA binding factor	3.60E-03	-1.05	-1.25	-1.21	-2.16
10371662	NM_011461	Sp1c	Pu.1 Dna binding factor	n.s.	-1.04	-1.05	1.13	1.15
10585276	NM_011136	Pou2af1	OBE/OcaB DNA binding factor	n.s.	-1.10	-1.22	-1.22	-1.53
10359770	NM_011137	Pou2f1	DNA binding factor	n.s.	-1.10	-1.22	-1.22	-1.53
10370837	NM_011548	E2a	helix-loop-helix DNA binding factor	n.s.	-1.18	-1.15	-1.37	-1.68
10399691	NM_010496	Id2	inhibitor hlh DNA binding factor	n.s.	-1.39	-2.78	-3.18	-4.01
10509163	NM_008321	Id3	inhibitor hlh DNA binding factor	n.s.	1.46	1.39	1.29	-1.01
10576034	NM_008320	Irf8	DNA binding factor	n.s.	1.36	1.07	-1.07	-1.63
10512669	NM_008782	Pax5	DNA binding factor	n.s.	1.04	-1.22	-1.32	-1.92
10485372	NM_009019	Rag1	V(D)J recombination	n.s.	-1.45	-1.63	-2.03	-1.50
10485370	NM_009020	Rag2	V(D)J recombination	n.s.	-1.63	-1.21	-1.76	-1.72

^{a)} P-value in ANOVA analysis. ^{b)} Fold change times upregulated or downregulated (-) when compared with WT (VH81X Tg Rag1^{-/-}) pre-B cells. Groups are Rag1^{-/-} pro-B cells; Btk^{-/-} VH81X Tg Rag1^{-/-} pre-B cells; Slp65^{-/-} VH81X Tg Rag1^{-/-} pre-B cells; Btk^{-/-} Slp65^{-/-} VH81X Tg Rag1^{-/-} pre-B cells ^{c)} n.s., p>0.01.

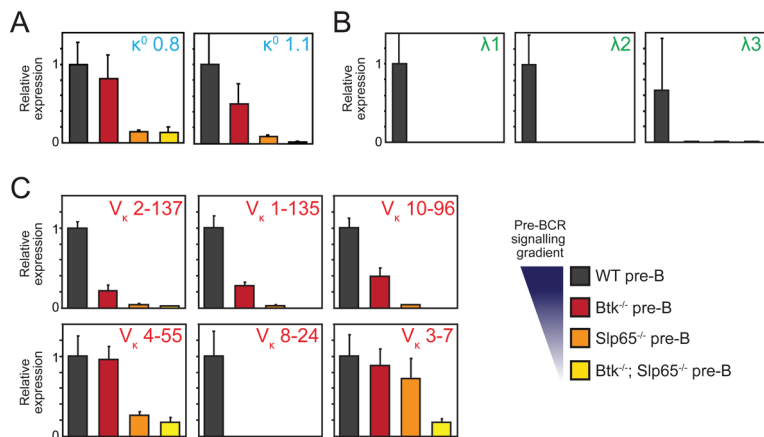


Figure 2. Reduction of Btk/Slp65-mediated pre-BCR signaling is associated with progressive loss of Ighk GLT. Quantitative RT-PCR analysis for κ^0 (A), λ^0 (B) and V_{κ} GLT (C) of FACS-sorted B220⁺CD19⁺ pre-B/pro-B cell fractions from the indicated mice on a V_H81X transgenic Rag1^{-/-} background. Expression levels were normalized to those of *Gapdh*, whereby the values in WT pre-B cells were set to one. Bars represent mean values and error bars denote standard deviations for 4 independent mice per group.

We could confirm these findings for κ^0 GLT by quantitative RT-PCR assays on FACS-purified B220⁺CD19⁺ pro-B/pre-B cell fractions (Figure 2A). In agreement with our reported findings,³⁴ we also found that *Btk*^{-/-} and *Slp65*^{-/-} pre-B cells have defective λ^0 transcription, which is initiated 5' of the J λ segments (Figure 2B).⁴⁹ GLT across the V_{κ} region showed a similar pattern of sensitivity to pre-BCR signaling: decreased transcription of six individual V_{κ} regions tested ($V_{\kappa}3-7$, $V_{\kappa}8-24$, $V_{\kappa}4-55$, $V_{\kappa}10-96$, $V_{\kappa}1-35$ and $V_{\kappa}2-137$) correlated with decreased pre-BCR signaling activity (Figure 2C) in the pre-B cells of the four groups of mice. GLT over unrearranged $V_{\lambda}1$ and $V_{\lambda}2$ segments was strongly reduced in the absence of *Btk* or *Slp65*, as detected by the expression arrays (Table 1). These observations indicate that *Ighk* locus accessibility, a

Figure 3. 3C-Seq analysis of long-range chromatin interactions within the *Ighk* locus and flanking regions. (A) Overview of long-range interactions revealed by 3C-Seq experiments performed on the indicated cell fractions, representing a gradient of pre-BCR signaling, whereby the iE κ element (*top*), the 3'E κ element (*centre*) or the *Sis* element (*bottom*) was used as a viewpoint. Shown are the relative interaction frequencies (average of two replicate experiments) for the indicated genomic locations. The ~8.4 Mb region containing the *Ighk* locus (*yellow shading*) and flanking regions (*cyan shading*) is shown and genes and genomic coordinates are given (*bottom*). The location of the two BAC probes used for 3D DNA-FISH are indicated by a green (distal V_{κ} probe) and red (proximal C κ /enhancer probe) rectangle (*bottom*). Pre-B cell fractions were FACS-purified from the indicated mice on a V_H81X transgenic Rag1^{-/-} background (see Figure 1 for gating strategy). Erythroid progenitor cells were used as a non-lymphoid control. (B) 3D DNA-FISH analysis comparing locus contraction in cultured bone marrow-derived E2A^{-/-} pre-pro-B, Rag1^{-/-} pro-B and V_H81X Rag1^{-/-} pre-B cells (see Figure S6 for phenotype of IL-7 cultured B-lineage cells). Location of the BAC probes used are indicated at the bottom of panel A. Representative images for all three cell types are shown on the left, quantifications (>100 nuclei counted per cell type) on the right. The red lines indicate the median distance between the two probes. Statistical significance was determined using a Mann-Whitney U test (***p<0.001; n.s. = not significant, p≥0.05).

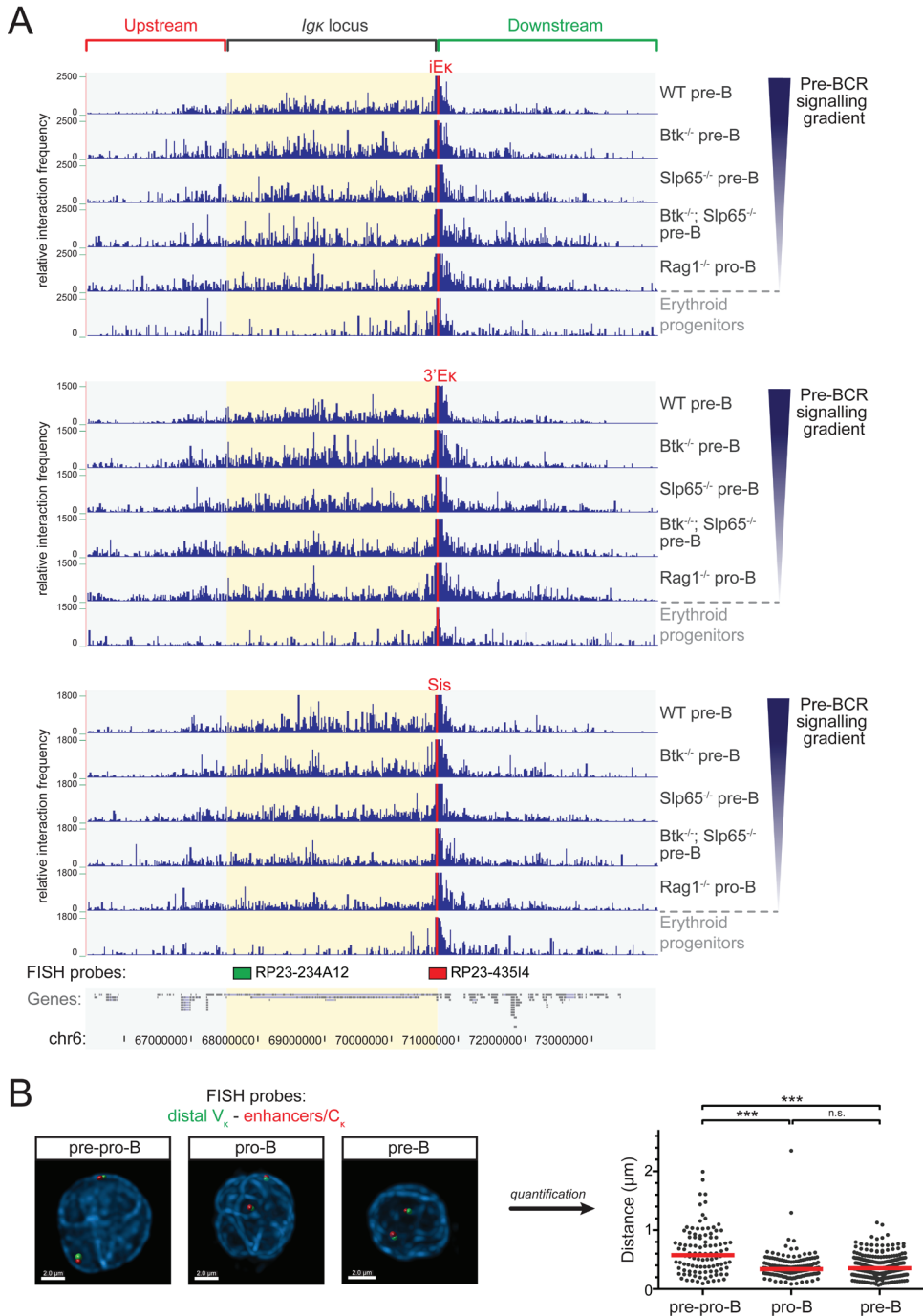


Figure 3. (Legend at the bottom of the previous page)

hallmark of recombination-competent antigen receptor loci, is progressively reduced under conditions of diminishing pre-BCR signaling.

Pre-BCR signaling induces modulation of long-range chromatin interactions at the *Igκ* locus

Accessibility of antigen receptor loci for V(D)J recombination is thought to be initiated by enhancers, in part through long-range chromatin interactions with promoters of non-coding transcription, resulting in the activation of germline transcription.⁸ Because pre-BCR signaling affects the expression of GLT and various nuclear proteins that mediate long-range chromatin interactions and bind the κ enhancers, it is conceivable that pre-BCR signaling induces changes in the enhancer-mediated higher-order chromatin structure of the *Igκ* locus that facilitates V κ gene accessibility.

We therefore performed 3C-Seq analyses on FACS-purified B220⁺CD19⁺ fractions from the same five groups of mice (WT, Btk^{-/-}, Slp65^{-/-} and Btk^{-/-}Slp65^{-/-} V_H81X transgenic Rag1^{-/-} pre-B cells, as well as Rag1^{-/-} pro-B cells). Erythroid progenitors were analyzed in parallel as a non-lymphoid control, in which the *Igκ* locus was not contracted. Genome-wide chromatin interactions were measured for three regulatory elements involved in the control of *Igκ* locus accessibility and recombination: the iE κ and 3'E κ enhancers⁵⁰⁻⁵² and the Sis element,²⁰ which contain binding sites for Ikaros/Aiolos, E2A and Irf4.^{16, 17, 20, 38, 53}

In WT pre-B cells, all three regulatory elements showed extensive long-range chromatin interactions within the V κ region and substantially less interactions with regions up- or downstream of the ~3.2 Mb *Igκ* domain (**Figure 3A**; see Figure S2, Figure S3, Figure S4 for line graphs) confirming previous observations.²¹ Under conditions of reduced pre-BCR signaling activity, the three *Igκ* regulatory elements still showed strong interactions with the V κ region. Surprisingly, even in the complete absence of pre-BCR signaling in Rag1^{-/-} pro-B cells, long-range interactions were still observed at frequencies well above those seen in non-lymphoid cells, suggesting that a contracted *Igκ* locus topology is not strictly dependent on pre-BCR signaling (**Figure 3A** and Figures S2, S3, S4). Next, we used 3D DNA FISH analyses using BAC probes hybridizing to the distal V κ and C κ /enhancer regions to confirm that *Igκ* locus contraction was similar in Rag1^{-/-} pro-B cells and V_H81X transgenic Rag1^{-/-} pre-B cells (both showing a contracted topology, compared with non-contracted pre-pro-B cells deficient for the transcription factor E2A (**Figure 3B**)).

Nevertheless, we did observe that pre-BCR signaling induced clear differences in interaction frequencies. Whereas an increase in pre-BCR signaling was associated with a decrease in the interaction frequencies between the two κ enhancers and regions flanking the *Igκ* locus (as also revealed by more detailed images of selected regions upstream and

downstream of the *Igκ* domain, Figure S5), the overall interaction frequency within the *Igκ* domain appeared unchanged (Figures S3, S4, S5). Remarkably, interactions with the *Sis* element showed quite an opposite pattern: pre-BCR signaling correlated with increased overall interactions within the *Igκ* domain and did not substantially affect interaction frequencies in the *Igκ* flanking regions (Figures S2, S5).

Taken together, these analyses show that (i) the *Igκ* locus is already contracted at the pro-B cell stage and that (ii) pre-BCR signaling induces changes in long-range chromatin interactions, both within the *Igκ* locus and in the flanking regions.

Pre-BCR signaling enhances interactions of 3'Eκ and *Sis*, but not iEκ, with Vκ⁺ fragments

The differential effects of pre-BCR signaling on long-range chromatin interactions of the iEκ, 3'Eκ and *Sis* elements clearly emerged in a quantitative analysis of the 3C-Seq datasets (**Figure 4A**, see Materials and Methods for a detailed description of the quantification methods used). When pre-BCR signaling was absent (*Rag1*^{-/-} pro-B cells) or very low (*Btk*^{-/-}*Slp65*^{-/-} pre-B cells), the average interaction frequencies were similar within the ~3.2 Mb Vκ region and the ~3.2 Mb downstream flanking region, for all three regulatory elements. Interaction frequencies with the upstream flanking region were lower, consistent with the larger chromosomal distance to the three viewpoints. The presence of increasing levels of *Btk*/*Slp65*-mediated pre-BCR signaling was associated with reduced interaction of iEκ and 3'Eκ with the *Igκ* flanking regions and with increased interaction of the *Sis* element and (to a lesser extent) 3'Eκ with the Vκ region (**Figure 4A**). As a result, for all three regulatory elements pre-BCR signaling resulted in a preference for interaction with fragments inside the Vκ region over fragments outside the Vκ region (Figure S7).

We next focused our analysis on the Vκ region and compared fragments that harbor a functional Vκ gene (Vκ⁺ fragment) and those that do not (Vκ⁻ fragment). When pre-BCR signaling was absent (*Rag1*^{-/-} pro-B cells) or very low (*Btk*^{-/-}*Slp65*^{-/-} pre-B cells) the average interaction frequencies of the *Sis* or iEκ elements with Vκ⁺ fragments were higher than with Vκ⁻ fragments. The average interaction frequencies of 3'Eκ with Vκ⁺ and Vκ⁻ fragments, however, were similar (**Figure 4B**). Upon pre-BCR signaling, the *Sis* element showed an increase in interaction frequencies with both Vκ⁺ and Vκ⁻ fragments, with nevertheless an interaction preference for Vκ⁺ fragments. In contrast, interaction frequencies between the iEκ element and Vκ⁺ or Vκ⁻ fragments were not modulated by pre-BCR signaling at all (**Figure 4B**). The 3'Eκ element exhibited yet another profile: pre-BCR signaling induced increased interaction frequencies specifically with Vκ⁻ fragments, while interactions with Vκ⁺ fragments were not notably modulated by pre-BCR signaling

II. Pre-B Cell Receptor Signaling Induces Immunoglobulin K Locus Accessibility By Functional Redistribution Of Enhancer-Mediated Chromatin Interactions

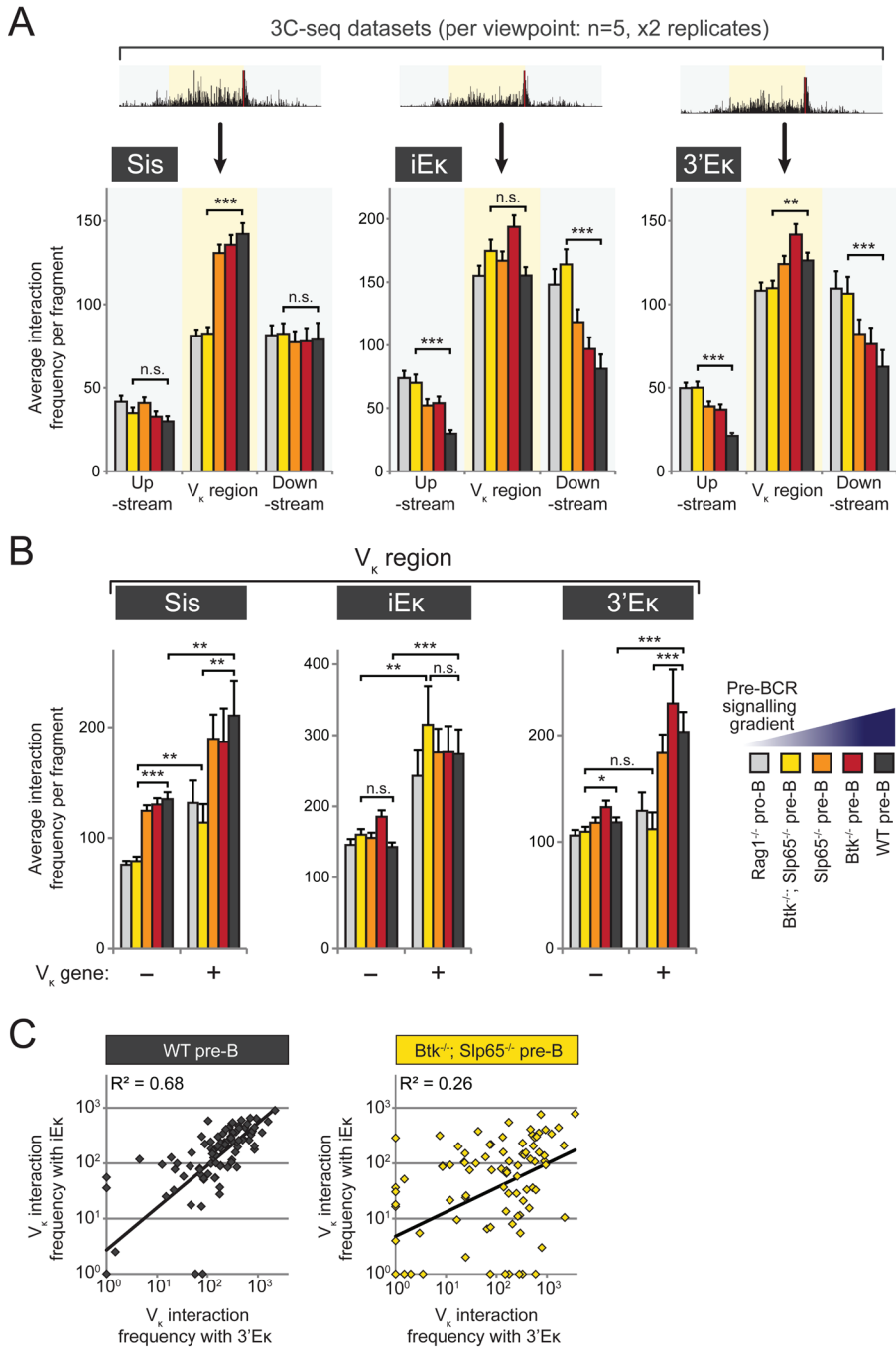


Figure 4. (Legend at the bottom of the next page)

(**Figure 4B**). When we separately analyzed non-functional pseudo-V κ genes, we found for the Sis and 3'E κ elements that the interaction patterns with functional and non-functional V κ genes were similar (Figure S8). In contrast, the iE κ enhancer did show an overall increased interaction frequency with V κ functional genes, compared with non-functional V κ genes, a phenomenon which was again independent from pre-BCR signaling (Figure S8).

The finding that interactions of V κ genes with the intronic enhancer are already robust in pro-B cells, while those with the 3' κ enhancer are dependent on pre-BCR signaling, suggested that for individual V κ genes pre-BCR signaling may result in more similar interaction frequencies with the two enhancers. To investigate this, we examined for all individual V κ genes the correlation between their 3C-Seq interaction frequencies with the iE κ and 3' κ elements, and found that these were highly correlated in WT pre-B cells ($R^2=0.68$; **Figure 4C**). Correlation was severely reduced when pre-BCR signaling was low in Btk⁻/Slp65⁻ pre-B cells ($R^2=0.26$; **Figure 4C**). Similar pre-BCR signaling-dependent correlations were observed between V κ -interactions with the Sis element and those with the two enhancers (Figure S9). As the Sis element particularly suppresses recombination of the proximal V κ 3 family, we investigated interaction correlations specifically for this V κ family. Similar to our findings for all V κ genes, a sub-analysis showed strong correlations for the interactions of V κ 3 family genes with iE κ , 3' κ and Sis in WT pre-B cells, which were diminished when pre-BCR signaling was low, except for iE κ -Sis correlations which were pre-BCR signaling-independent (Figure S9).

In summary, we conclude that pre-BCR signaling induces a redistribution of long-range interactions of the iE κ , 3'E κ and Sis elements, thereby restricting interactions towards the V κ gene region. Moreover, upon pre-BCR signaling the long-range interactions mediated by 3'E κ and Sis - but not those mediated by iE κ - become enriched for fragments harboring a V κ gene, demonstrating increased proximity of 3'E κ and Sis to V κ genes. Finally, for individual V κ genes the interactions with iE κ , 3'E κ and Sis become highly correlated upon pre-BCR signaling, indicating that pre-BCR signals

Figure 4. Modulation of long-range chromatin interactions within the *Ig κ* locus by pre-BCR signaling.

Quantitative analysis of 3C-Seq datasets using the three indicated κ regulatory elements as viewpoints. (A) Average long-range chromatin interaction frequencies (from 2 replicate 3C-Seq experiments) with upstream (-2.0 Mb), V κ (-3.2 Mb) and downstream (-3.2 Mb) regions, as defined in **Figure 3A**, for the five B cell precursor fractions representing a pre-BCR signaling gradient. Average interaction frequencies per region were calculated as the average number of 3C-Seq reads per restriction fragment within that region. See Materials and Methods section for more details. (B) Average interaction frequencies within the V κ region were determined for fragments that do not (-) containing a functional V κ gene and for those that do contain a functional V κ gene (+). (C) Correlation plots of average interaction frequencies of the two enhancer elements with the 101 functional V κ genes for WT pre-B cells (*left*) versus Btk⁻/Slp65⁻ pre-B cells (*right*). On the log scale frequencies <1 were set to 10⁰. Statistical significance was determined using a Mann-Whitney U test (* $p<0.05$; ** $p<0.01$; *** $p<0.001$; n.s. = not significant, $p\geq 0.05$).

result in regulatory coordination between these three elements that govern *Igk* locus recombination. In contrast, interactions between genes of the proximal *Vk3* family, *Sis* and *iEk* - but not *3'k* - appear to be coordinated already in the absence of pre-BCR signaling.

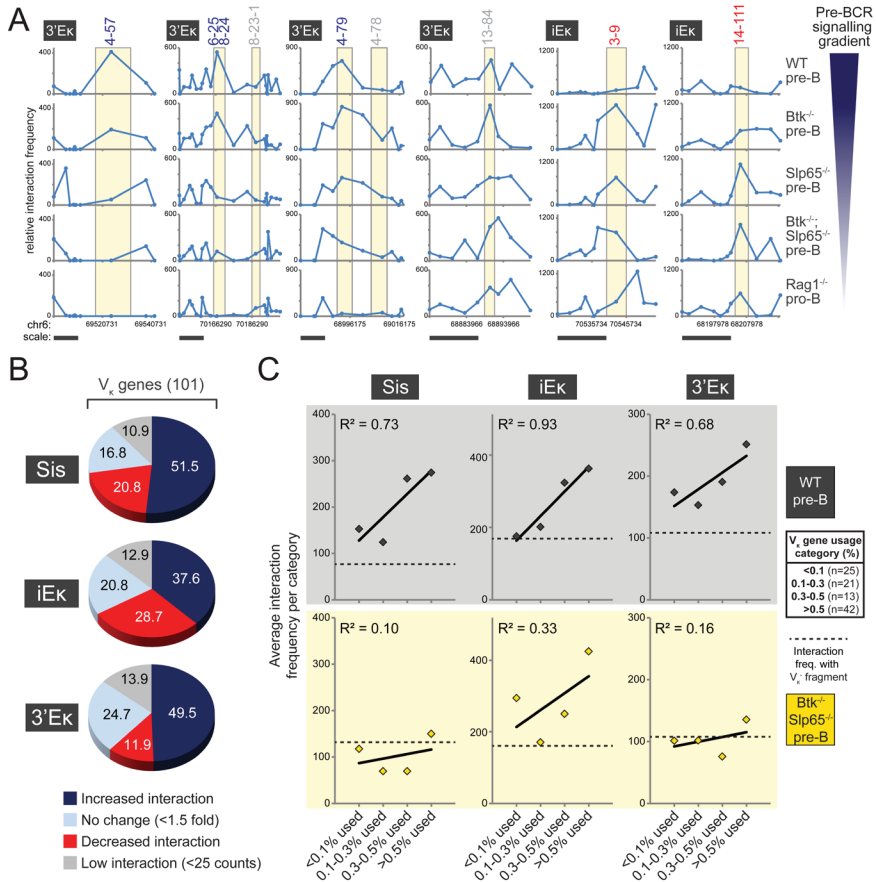


Figure 5. Long-range chromatin interactions of k regulatory elements correlate with *Vk* gene usage. (A) Selected examples of genomic regions containing *Vk*⁺ fragments, showing increased (*Vk*4-57, *Vk*6-25, *Vk*8-24, *Vk*4-79), stable (*Vk*8-23-1, *Vk*4-78, *Vk*13-84) or decreased (*Vk*3-9, *Vk*14-111) 3C-Seq interaction frequencies with *3'Ek* or *iEk* upon pre-BCR signaling. Averaged 3C-Seq signals are plotted as a line-graph, with the individual data points representing the center of the BglII restriction fragments. Yellow shading marks the BglII fragment on which the *Vk* gene(s) is located. *Vk* gene(s) are indicated (*top*) and chromosomal coordinates and scale bars (10 kb) are plotted (*bottom*). (B) Classification of *Vk*⁺ fragments, based on the effect of pre-BCR signaling on their interactions with the three *k* regulatory elements indicated. Increase and decrease were defined as >1.5-fold change of interaction frequencies detected in WT pre-B cells versus Btk^{-/-}Slp65^{-/-} pre-B cells. (C) Correlation of average interaction frequencies (for the three *k* regulatory elements indicated) with four *Vk* usage categories ranging from low (<0.1%) to high usage (>0.5%, listed in the table on the right). Diamonds represent average interaction frequencies for Btk^{-/-}Slp65^{-/-} pre-B cells (yellow) and WT pre-B cells (grey). The

dotted line in each graph depicts the average interaction frequency with fragments that do not contain a functional V κ (V κ -). Primary V κ gene usage data were taken from.⁵⁴

Long-range chromatin interactions of κ regulatory elements correlate with V κ usage

Next, we investigated the effects of pre-BCR signaling on the interaction frequencies of individual functional V κ genes with the three κ regulatory elements (**Figures 5A, 5B**). The 3C-Seq patterns of the majority (~91%) of the 101 individual V κ ⁺ fragments showed evidence for interaction with one or more of the κ regulatory elements (>25 average counts). When comparing Btk^{-/-}Slp65^{-/-} with WT pre-B cells, we observed that for a large proportion (~38-52%) of V κ ⁺ fragments interaction frequencies increased upon pre-BCR signaling (**Figure 5B**). Smaller proportions of V κ ⁺ fragments showed a decrease (~12-29%) or were not significantly affected by pre-BCR signaling (~17-25% with <1.5 fold change). The observed increase or decrease was not related to proximal or distal location of the V κ genes, nor to their sense or antisense orientation (not shown). Distributions of the three different classes of V κ ⁺ fragments showed substantial differences between the κ regulatory elements. For the Sis and 3'E κ elements more V κ ⁺ fragments showed increased than decreased interactions (**Figure 5B**), in agreement with the signaling-dependent increase in average interaction frequencies of all V κ ⁺ fragments (**Figure 4B**). In contrast, for the iE κ viewpoint, V κ ⁺ fragments showing increased and decreased interactions were more equal in number, consistent with the limited effects of pre-BCR signaling on overall iE κ interaction frequencies of all V κ ⁺ fragments (**Figure 4B**).

Although antigen receptor recombination is in principle regarded as a random process, a significant skewing of the primary Ig κ repertoire of C57BL/6 mice was recently reported: one third of the V κ genes was shown to account for >85% of the V κ segments used by B-cells.⁵⁴ To assess whether a correlation exists between usage of V κ genes and their interaction frequencies with κ regulatory elements, we divided the V κ genes into four usage categories (<0.1%, 0.1-0.3%, 0.3-0.5% and >0.5%) and calculated their average 3C-Seq interaction frequencies with Sis, iE κ and 3' κ (**Figure 5C**). In WT pre-B cells, V κ usage showed a strong positive correlation with 3C-Seq interaction frequencies for all three regulatory elements ($R^2 = -0.7-0.9$; **Figure 5C**). These correlations were pre-BCR signaling-dependent, since in Btk^{-/-}Slp65^{-/-} pre-B cells they were reduced (for iE κ ; $R^2 = 0.33$) or absent (for Sis and 3' κ ; $R^2 < 0.10$ and $R^2 < 0.16$, respectively) (**Figure 5C**).

Collectively, our results indicate that specifically the most frequently used V κ genes are the main interaction targets of κ regulatory elements, whereby pre-BCR signaling completely underlies this specificity for the Sis and 3'E κ elements, and to a lesser extent for iE κ .

II. Pre-B Cell Receptor Signaling Induces Immunoglobulin K Locus Accessibility By Functional Redistribution Of Enhancer-Mediated Chromatin Interactions

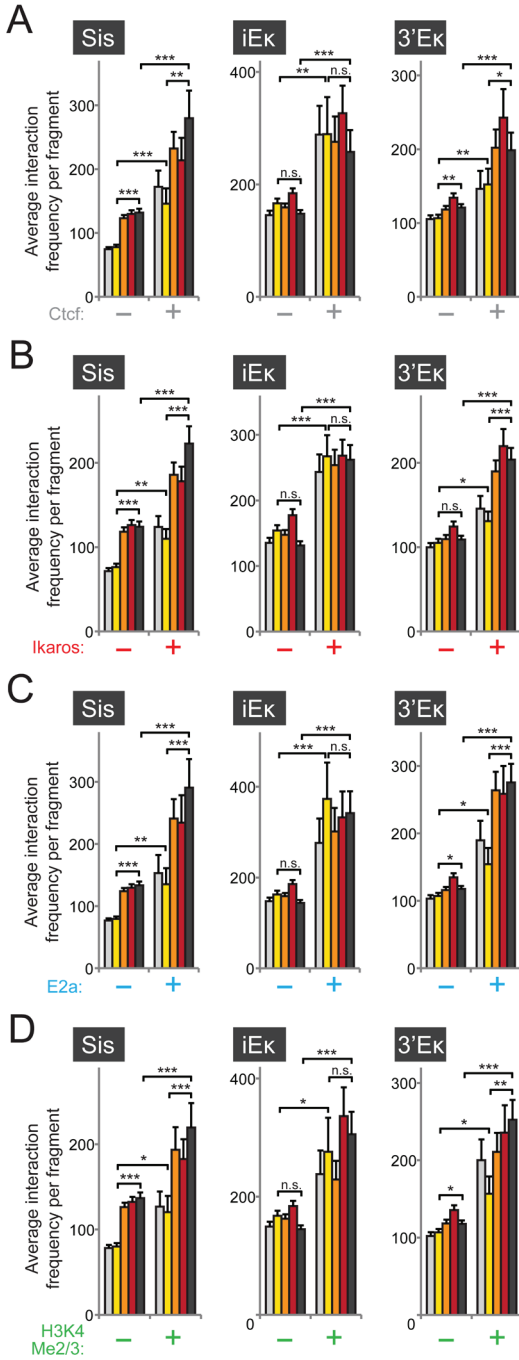


Figure 6. Long-range chromatin interactions of κ regulatory elements correlate with transcription factor binding and histone modifications. (A,D) For fragments within the $V\kappa$ region, average 3C-Seq interaction frequencies were calculated for fragments that did (+) or did not (-) contain binding sites for transcription factors or H3K4 histone modifications (as determined by previous ChIP-Seq studies, see Materials and Methods for references). Data for the three viewpoint and the five B cell precursor fractions representing a pre-BCR signaling gradient are shown for Ctcf (A), Ikaros (B), E2A (C) and H3K4 di- and tri-methylation (Me2/3). Statistical significance was determined using a Mann-Whitney U test (* $p < 0.05$; ** $p < 0.01$; *** $p < 0.001$; n.s. = not significant, $p \geq 0.05$).

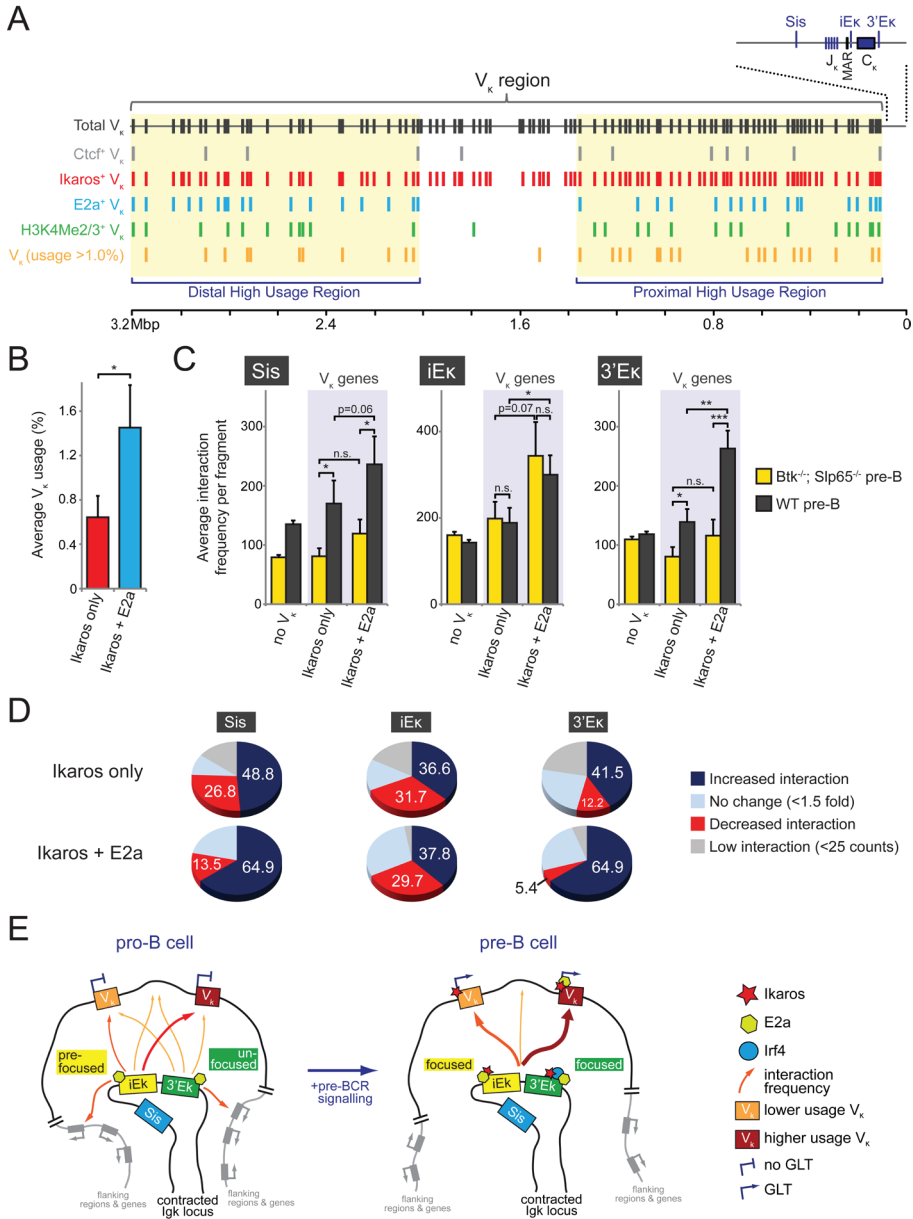


Figure 7. Proximity of V_k genes to E2A-binding sites correlates with frequencies of long-range interactions. (A) Schematic representation of the *Igk* locus, showing the location of all functional V_k (*grey, top*), J_k and C_k gene segments and the κ regulatory elements *Sis*, *iEk* and *3'Ek*. MAR = matrix attachment region. V_k genes within close proximity (as defined by co-localization on the same 3C-Seq restriction fragment) to the indicated transcription factors or H3K4 hypermethylation (as detected by previous ChIP-Seq studies, see

Materials and Methods for references), are shown. At the bottom, highly-used (>1.0% used) V κ gene segments are depicted (*orange*), which cluster within two large high-usage domains (*yellow shading*). Primary V κ gene usage data was taken from.⁵⁴ (B) Average usage of V κ genes marked only by an Ikaros-binding site or those marked by binding sites of both Ikaros and E2A. (C) Comparison of average interaction frequencies (for the three κ regulatory elements indicated) between V κ ⁻ fragments (no V κ), V κ ⁺ fragments containing an Ikaros binding site only and V κ ⁺ fragments containing both an Ikaros and E2A binding site. Bars represent average frequencies for Btk⁻/Slp65⁻ pre-B cells (*yellow*) and WT pre-B cells (*grey*). (D) Classification of V κ ⁺ fragments, containing an Ikaros binding-site only (*top*) or containing both an Ikaros and E2A binding site (*bottom*), based on the effect of pre-BCR signaling on their interactions with the three κ regulatory elements indicated. Increase and decrease were defined as >1.5-fold change of interaction frequencies detected in WT pre-B cells versus Btk⁻/Slp65⁻ pre-B cells. (E) Proposed model of pre-BCR signaling-mediated changes in κ enhancer action, In pro-B cells (*left*) the enhancers show minimal coordination and their interactions are not yet (fully) focused on the V κ genes. Upon pre-BCR signaling and differentiation to pre-B cells (*right*), transcription factors bind the locus to coordinate enhancer action and focus their interactions to the V κ genes, inducing germline transcription (GLT) and accessibility to the V(D)J recombinase. See Discussion for more details. Statistical significance was determined using a Mann-Whitney U test (*p<0.05; **p<0.01; ***p<0.001; n.s. = not significant, p≥0.05).

Long-range interactions with κ regulatory elements correlate with the presence of Ctcf, Ikaros, E2A and H3K4 hypermethylation

Next, we investigated whether long-range interactions between κ regulatory elements and the V κ region correlated with the presence of the transcription factors Ctcf,²¹ Ikaros⁵⁵ and E2A,⁵⁶ which have been implicated in *Igk* locus recombination.^{21, 37, 55, 57, 58} Notably, Ikaros and E2A both strongly bind all three κ regulatory elements, while the Sis element is also occupied by Ctcf (²¹; data not shown).

Remarkably, we found similar striking correlations between the presence of *in vivo* binding sites for each of these transcription factors (as determined by ChIP experiments, see Materials and Methods for the relevant references) and long-range chromatin interactions with the κ regulatory elements (**Figure 6A-C**), even though Ctcf sites are mostly located in between V κ genes²¹ and Ikaros/E2A sites were frequently found close to V κ gene promoter regions (²; **Figure 7A**). Even when pre-BCR signaling was absent (Rag1⁻ pro B cells) or very low (Btk⁻/Slp65⁻ pre-B cells) the average interaction frequencies of the κ regulatory elements with fragments containing Ctcf, Ikaros or E2A bindings sites were higher than those without binding sites. Irrespective of the presence or absence of bindings sites for these transcription factors, we found that upon pre-BCR signaling interaction frequencies with the Sis element increased and those with the iE κ did not change. In contrast, for the 3'E κ we found that pre-BCR signaling specifically increased interaction frequencies with fragments occupied by Ctcf, Ikaros or E2A.

Finally, we found that the presence of di- or trimethylation of histone 3 lysine 4 (H3K4Me2/3), an epigenetic signature associated with locus accessibility⁵⁹ and Rag-binding,^{60, 61} also correlated with increased interaction frequencies with κ regulatory elements, revealing a similar pre-BCR signaling dependency as seen for the transcription factors analyzed (**Figure 6D**).

We conclude that the presence of essential transcription factors or H3K4Me2/3 in the V κ region strongly correlates with the formation of long-range chromatin interactions with the κ regulatory elements, and that for the Sis and 3'E κ elements this interaction preference is further enhanced by pre-BCR signaling.

Proximity of V κ genes to E2A-binding sites correlates with high V κ usage and increased long-range chromatin interactions

Since the long-range interactions with κ regulatory elements correlated with the presence of transcription factors implicated in *Ig κ* recombination, we next asked whether the κ regulatory elements preferentially interacted with V κ genes that are in close proximity to binding sites for Ctfc, Ikaros or E2A.

Strikingly, the majority of functional V κ genes (95/101) was found to have an Ikaros-binding site in close proximity, i.e. located on the same 3C-Seq restriction fragment (average length of ~3kb, data not shown) (**Figure 7A**). Proximity of V κ genes to an E2A-binding site (37%) or H3K4Me2/3 positive region (~28%) is more selective, while only a small fraction of V κ genes are close to Ctfc-binding sites (~12%) (²²; **Figure 7A**). All V κ genes marked by E2A, Ctfc, H3K4Me2/3 or a combination of these also contain an Ikaros-binding site. Frequently used V κ genes (>1.0% usage; 33/101 genes) were located into two separate regions, a proximal and a distal region, which also contained virtually all E2A and H2K4Me2/3-marked V κ genes (**Figure 7A**).

We found that V κ genes marked by both Ikaros and E2A were used substantially more often than those only bound by Ikaros (**Figure 7B**), suggesting that these V κ genes are preferentially targeted for V κ -to-J κ gene rearrangement. Our 3C-Seq analyses showed that in WT pre-B cells interaction frequencies with the three κ regulatory elements were higher for Ikaros/E2A-marked V κ genes compared to genes marked by Ikaros-binding alone (**Figure 7C**). In fact, V κ ⁺ restriction fragments containing an Ikaros-binding site but not an E2A-binding site showed interaction frequencies similar to V κ ⁻ restriction fragments. Under conditions of very low pre-BCR signaling (in *Btk*^{-/-}*Slp65*^{-/-} pre-B cells) we observed strongly reduced interaction frequencies of V κ ⁺ E2A-binding restriction fragments with the Sis and 3'E κ elements. These interaction frequencies were in the same range as those of V κ ⁻ fragments or V κ ⁺ fragments that harbored an Ikaros site only (**Figure 7C**). Interaction frequencies with the iE κ enhancer, however, were independent of pre-BCR signaling. As shown in **Figure 7D**, for the majority of Ikaros/E2A-marked V κ ⁺ fragments (65%) pre-BCR signaling was associated with increased interactions with the Sis and 3'E κ elements (comparing wildtype and *Btk*^{-/-}*Slp65*^{-/-} pre-B cells). In these analyses only ~13.5% and ~5.4% of Ikaros/E2A-marked V κ ⁺ fragments showed a decreased interaction frequency upon pre-BCR signaling. In contrast, almost equal

proportions of Ikaros/E2A-marked $V\kappa^+$ fragments showed increased (~37%) and decreased (~30%) interactions with $iE\kappa$ upon pre-BCR signaling.

Taken together, these data reveal strong positive correlations between the presence of E2A-binding sites, $V\kappa$ usage and long-range chromatin interactions with κ regulatory elements in pre-B cells. Remarkably, for the $iE\kappa$ element these correlations are largely independent of Btk/Slp65-mediated pre-BCR signaling, whereas for the $3'E\kappa$ they are completely dependent on signaling.

DISCUSSION

During B-cell development the pre-BCR checkpoint is known to regulate the expression of many genes, part of which control the increase in $Ig\kappa$ locus accessibility to the V(D)J recombinase complex. However, it remained unknown how pre-BCR signaling events affect accessibility in terms of $Ig\kappa$ locus contraction and topology.

Here we identified numerous genes involved in IgL chain recombination, chromatin modification, signaling and cell survival to be aberrantly expressed in pre-B cells lacking the pre-BCR signaling molecules Btk and/or Slp65. We found that GLT over the $V\kappa$ region, reflecting $V\kappa$ accessibility, is strongly reduced in these cells. We used 3C-Seq to show that in pro-B cells both the intronic and the $3'\kappa$ enhancers frequently interact with the ~3.2 Mb $V\kappa$ region, as well as with $Ig\kappa$ flanking sequences, indicating that the $Ig\kappa$ locus is already contracted at the pro-B cell stage. 3C-Seq analyses in wild-type and Btk/Slp65 single and double-deficient pre-B cells demonstrated that pre-BCR signaling significantly affects $Ig\kappa$ locus topology. First, pre-BCR signaling reduces the interactions of the intronic and $3'\kappa$ enhancers with $Ig\kappa$ flanking regions, effectively focusing enhancer action towards the $V\kappa$ region to facilitate $V\kappa$ -to- $J\kappa$ recombination. Second, pre-BCR signaling strongly increases nuclear proximity of the $3'\kappa$ enhancer to $V\kappa$ genes, whereby this increase is more substantial for more frequently used $V\kappa$ genes and for $V\kappa$ genes close to a binding-site for the basic helix-loop-helix protein E2A. Third, pre-BCR signaling augments interactions between κ regulatory elements and fragments within the $V\kappa$ region bound by the key B-cell transcription factors (TFs) Ikaros and E2A and the architectural protein Ctf. Fourth, pre-BCR signaling has limited effects on interactions of the intronic κ enhancer with fragments within the $Ig\kappa$ locus, as this enhancer already displays interaction specificity for functional $V\kappa$ genes and TF-bound regions in pro-B cells. Fifth, pre-BCR signaling has limited effects on the interactions between the intronic or $3'\kappa$ enhancers and fragments that do not contain a $V\kappa$ gene or an Ikaros, E2A or Ctf binding site, emphasizing the specificity of pre-BCR signaling-induced changes in $Ig\kappa$ locus topology. Sixth, pre-BCR signaling appears to induce mutual regulatory

coordination between the three regulatory elements, since their interaction profiles with individual V κ genes become highly correlated upon signaling. Finally, pre-BCR signaling increases interactions of the Sis element with DNA fragments in the Ig κ locus, irrespective of the presence of a V κ gene or TF. Collectively, our findings demonstrate that pre-BCR signals relayed through Btk and Slp65 are required to create a chromatin environment that facilitates proper Ig κ locus recombination. This multi-step process is initiated by upregulation of key TFs like Aiolos, Ikaros, Irf4 and E2A. These proteins are then recruited to, or further accumulate at the Ig κ locus and its regulatory elements, resulting in a specific fine-tuning of enhancer-mediated locus topology that increases locus accessibility to the Rag recombinase proteins.

Importantly, the presence of strong lineage-specific interaction signals between the C κ /enhancer region and distal V κ genes in pro-B cells indicates that the Ig κ locus is already contracted at this stage. In contrast to a previous microscopy study indicating that Ig κ locus contraction did not occur until the small pre-B cell stage,³⁶ our 3D DNA FISH analysis indeed detected similar nuclear distances between distal V κ and the C κ /enhancer region in cultured pro-B and pre-B cells. Recently Hi-C was employed to study global early B cell genomic organization whereby substantial interaction frequencies were found between the intronic κ enhancer and the V κ region in pro-B cells.⁴⁰ E2A-deficient pre-pro-B cells, which are not yet fully committed to the B cell lineage,⁶² showed very few interactions among the iE κ and the distal part of the V κ region,⁴⁰ resembling the interactions we observed in non-lymphoid cells (Figure 3A). Accordingly, 3D-FISH analysis showed that the Ig κ locus adopted a non-contracted topology in these pre-pro-B cells (Figure 3B). These data indicate that Ig κ locus contraction is already achieved in pro-B cells and depends on the presence of E2A. Supporting this notion, active histone modifications and E2A were already detected at the κ enhancers and V κ genes at the pro-B cell stage,^{56, 63} whereby E2A was frequently found at the base of long-range chromatin interactions together with Ctf and Pu.1, possibly acting as ‘anchors’ to organize genome topology.⁴⁰ The observed correlation between E2A binding, V κ gene usage and iE κ proximity in pro-B cells (Figures 5C, 7C), further strengthens an early critical role for E2A in regulating Ig κ locus topology, V κ gene accessibility and recombination.

Our 3C-Seq experiments revealed that pre-BCR signaling is not required to induce long-range interactions between the κ regulatory elements and distal parts of the V κ locus, indicating that TFs strongly induced by signaling, i.e. Aiolos, Ikaros and Irf4, are not strictly necessary to form a contracted Ig κ locus. Prime candidates for achieving Ig κ locus contraction at the pro-B cell stage are E2A and Ctf, as they have been implicated in regulating Ig locus topology^{21, 40, 64, 65} and E2A already marks frequently used V κ genes at the pro-B cell stage (Figure 7), although we did observe reduced E2A expression and binding to the iE κ enhancer and V κ genes when pre-B cell signaling was low (Figure

1 and Table S3), suggesting that pre-BCR signaling is required for high level E2A occupancy of the V κ genes. We previously reported that Ig κ gene recombination can occur in the absence of Ctf and that Ctf mainly functions to limit interactions of the κ enhancers with proximal V κ regions and to prevent prevents inappropriate interactions between these strong enhancers and elements outside the Ig κ locus.²¹ Because at the pro-to-pre B cell transition Aiolos, Ikaros and Irf4 are recruited to the Ig κ locus and histone acetylation and H3K4 methylation increases,^{17, 38, 63, 66} we hypothesize that pre-BCR induced TFs act upon an E2A/Ctf-mediated topological scaffold to further refine the long-range chromatin interactions of the κ regulatory elements. Hereby, these TFs mainly act to focus and to coordinate the interactions of the two κ enhancers to the V κ gene segments, in particular to frequently used V κ genes, thereby increasing their accessibility for recombination (See Figure 7E for a model for pre-BCR signaling-induced changes in Ig κ locus accessibility).

In this context, our 3C-Seq data show that the two κ enhancer elements have distinct roles. Both 3'E κ and iE κ elements manifest interaction-specificity for highly used, E2A-marked, V κ genes. However, whereas iE κ already shows this specificity in pro-B cells (although pre-BCR signaling does augment this specificity), 3'E κ only does so in pre-B cells upon pre-BCR signaling. These observations indicate that iE κ is already 'pre-focused' at the pro-B cell stage and that pre-BCR signals are required to fully activate and focus the 3'E κ to allow synergistic promotion of Ig κ recombination by both enhancers (See Figure 7E).⁵² In agreement with such distinct sequential roles, iE κ and not the 3'E κ was found to be required for the initial increase in Ig κ locus accessibility, which occurred upon binding of E2A only.^{37, 38, 67} The 3'E κ on the other hand requires binding of pre-BCR signaling-induced Irf4 to promote locus accessibility,^{19, 38} followed by further recruitment of E2A to both κ enhancers and highly-used V κ genes (Table S3 and ^{38, 57}).

The Sis regulatory element was shown to dampen proximal V κ -J κ rearrangements and to specify the targeting of Ig κ transgenes to centromeric heterochromatin in pre-B cells.²⁰ As Sis is extensively occupied by the architectural Ctf protein and deletion of Sis or Ctf both resulted in increased proximal V κ usage,^{21, 23} it was postulated that Sis functions as a barrier element to prevent the κ enhancers from too frequently targeting proximal V κ genes for recombination. In this context, we now provide evidence that interactions between the proximal V κ genes, Sis and iE κ - but not 3' κ - are already coordinated before pre-BCR signaling occurs (Figure S9). Perhaps not surprisingly, Sis-mediated long-range chromatin interactions displayed a pattern and pre-BCR signaling response that was different from the κ enhancers. Unlike for the enhancers, upon pre-BCR signaling Sis-mediated interactions with regions outside the Ig κ locus were maintained and interaction within the V κ region increased, irrespective of the presence of V κ genes or TF binding sites. Because Sis is involved in targeting the non-recombining Ig κ allele to

heterochromatin,²⁰ the observed interaction pattern of the *Sis* element might reflect its action in pre-B cells to sequester the non-recombining *Igκ* locus and target it towards heterochromatin. This might also explain the increased interaction frequencies of *Sis* with highly used *Vκ* genes upon pre-BCR signaling (Figure 5C, 7C), as such highly accessible genes likely require an even tighter association with *Sis* and heterochromatin to prevent undue recombination.

Surprisingly, we observed a striking correlation between *Ikaros* binding and *Vκ* gene location (94% of *Vκ* genes were in close proximity to an *Ikaros* binding site, Figure 7A). Although *Ikaros* and *Aiolos* have a positive role in regulating gene expression during B cell development^{55, 58} and *Ikaros* is required for *IgH* and *IgL* recombination,^{39, 58} *Ikaros* has also been reported to silence gene expression through its association with pericentromeric heterochromatin⁶⁸ or through recruitment of repressive co-factor complexes.^{69, 70} Recruitment of *Ikaros* to the *Igκ* locus was found increased in pre-B cells as compared to pro-B cells,⁶³ in agreement with its upregulation in pre-B cells (Figure 1). Furthermore, *Ikaros* binds the *Sis* element, where it was suggested to mediate heterochromatin-targeting of *Igκ* alleles by the *Sis* region.²⁰ *Aiolos*, although not essential for B cell development like *Ikaros*,^{58, 71} is strongly induced by pre-B cell signaling and has been reported to co-operate with *Ikaros* in regulation gene expression.²⁷ Although their synergistic role during *IgL* chain recombination has not been extensively studied, the *Ikaros/Aiolos* ratio changes upon pre-BCR signaling (Figure 1). Increased recruitment of *Ikaros/Aiolos* to *Vκ* genes and the κ enhancers likely increases *Igκ* locus accessibility and contraction (Figure 6), as *Ikaros* was very recently shown to be essential for *IgL* recombination.⁵⁸ On the other hand, it is conceivable that on the non-recombining allele increased recruitment of *Ikaros/Aiolos* to *Vκ* genes and the *Sis* region could facilitate silencing of this allele. Further investigations using allele-specific approaches⁷² will be required to clarify the allele-specific action of the *Sis* element during *Igκ* recombination.

In summary, by investigating the effects of a pre-BCR signaling gradient - rather than deleting individual transcription factors - we have taken a more integrative approach to study the regulation of *Igκ* locus topology. Our 3C-Seq analyses in wild-type, *Btk* and *Slp65* single and double-deficient pre-B cells show that interaction frequencies between *Sis*, *iEκ* or 3' *Eκ* and the *Vκ* region are already high in pro-B cells and that pre-BCR signaling induces accessibility through a functional redistribution of long-range chromatin interactions within the *Vκ* region, whereby the *iEκ* and 3' *Eκ* enhancer elements play distinct roles.

MATERIALS AND METHODS

Mice

VH81X transgenic mice⁷³ on the Rag-1^{-/-} background⁷⁴ that were either wildtype, Btk^{-/-},⁷⁵ Slp65^{-/-42} or Btk^{-/-}Slp65^{-/-} have been previously described.³⁴ Mice were crossed on the C57BL/6 background for >8 generations, bred and maintained in the Erasmus MC animal care facility under specific pathogen-free conditions and were used at 6-13 wks of age. Experimental procedures were reviewed and approved by the Erasmus University committee of animal experiments.

Flow cytometry

Preparation of single-cell suspensions and incubations with monoclonal antibodies (mAbs) were performed using standard procedures. Bone marrow B-lineage cells were purified using fluorescein isothiocyanate (FITC)-conjugated anti-B220(RA3-6B2) and peridinin chlorophyll protein (PCP)-conjugated anti-CD19, together with biotinylated mAbs specific for lineage markers Gr-1, Ter119, and CD11b and APC-conjugated streptavidin as a second step to further exclude non-B cells. Cells were sorted with a FACSARIA (BD Biosciences). The following mAbs were used for flow cytometry: FITC-, PerCP-anti-B220 (RA3-6B2), phycoerythrin (PE)-anti-CD2 (LFA-2), PCP-, allophycocyanin (APC)- or APC-Cy7-anti-CD19 (ID3), PE- or APC anti-CD43 (S7). All these antibodies were purchased from BD Biosciences or eBiosciences. Samples were acquired on an LSRII flow cytometer (BD Biosciences) and analyzed with FlowJo (Tree Star) and FACSDiva (BD Biosciences) software.

Quantitative RT-PCR and DNA microarray analysis

Extraction of total RNA, reverse-transcription procedures, design of primers and cDNA amplification have been described previously.²¹ Gene expression was analyzed using an ABI Prism 7300 Sequence Detector and ABI Prism Sequence Detection Software version 1.4 (Applied Biosystems). All PCR primers used for quantitative RT-PCR of transcription factors or κ^0 , λ^0 and V_{κ} GLT are described in²¹, except for Obf1 (forward: 5'-CCTGGCCACCTACAGCAC-3', reverse 5'-GTGGAAGCAGAAA CCTCCAT-3', obtained from the Roche Universal Probe Library).

Biotin-labeled cRNA was hybridized to the Mouse Gene 1.0 ST Array according to the manufacturer's instructions (Affymetrix); data were analyzed with BRB-ArrayTools (version 3.7.0, National Cancer Institute) using Affymetrix CEL files obtained from

GCOS (Affymetrix). The RMA approach was used for normalization. The TIGR MultiExperiment Viewer software package (MeV version 4.8.1) was used to perform data analysis and visualize results.⁴⁵ One-way ANOVA analysis of the five experimental groups of B-cells was used to identify genes significantly different from wildtype V μ 81X Tg Rag1^{-/-} pre-B cells (p<0.01).

Chromatin Immunoprecipitation (ChIP)

ChIP experiments were performed as previously described⁷⁶ using FACS sorted bone marrow pre-B cell fractions (0.3-2.0 million cells per ChIP). Antibodies against E2A (sc-349, Santa Cruz Biotechnology) and Ikaros (sc-9861, Santa Cruz Biotechnology) were used for immunoprecipitation. Purified DNA was analyzed by quantitative RT-PCR as described above. Primer sequences are available on request.

Chromosome conformation capture coupled to high-throughput sequencing (3C-Seq)

3C-Seq experiments were essentially carried out as described previously.^{21, 41} For 3C-Seq library preparation BglII was used as the primary restriction enzyme; NlaIII as a secondary restriction enzyme. 3C-Seq template was prepared from WT E13.5 fetal liver erythroid progenitors and FACS-sorted bone marrow pro-B cell or pre-B cell fractions (see above) from pools of 4-6 mice. In total, between 1-8 million cells were used for 3C-Seq analysis. Primers for the Sis, iE κ and 3'E κ viewpoint-specific inverse PCR were described previously.²¹ 3C-Seq libraries were sequenced on an Illumina Hi-Seq 2000 platform. 3C-Seq data processing was performed as described elsewhere.^{41, 77} Two replicate experiments were sequenced for each genotype and viewpoint and normalized interaction frequencies per BglII restriction fragment were averaged between the two experiments.

For quantitative analysis, the *Ig κ* locus and surrounding sequences were divided into three parts (mm9 genome build): a ~2 Mb upstream region (chr6:65,441,978-67,443,029; 759 fragments), a ~3.2 Mb V κ region (chr6:67,443,034-70,801,754; 1290 fragments) and a downstream ~3.2 Mb region (chr6:70,801,759-73,993,074; 1143 fragments). For each cell type (as described above) sequence read counts within individual BglII restriction fragments were normalized for differences in library size (expressed as 'reads per million', see⁷⁸) and averaged between the 2 replicates before further use in the various calculations. Very small BglII fragments (<100 bp) were excluded from the analysis. Fragments in the immediate vicinity of the regulatory elements (chr6:70,659,392-70,693,183; 10 fragments) were also excluded because of high levels of noise around the viewpoint, a characteristic of all 3C-based experiments. V κ gene coordinates (both functional genes

and pseudogenes) were obtained from IMGT¹¹ and NCBI (Gene ID: 243469) databases. V κ gene usage data (C57BL/6 strain, bone marrow) were obtained from ref. ⁵⁴. ChIP-Seq datasets were obtained from (Ctcf),²¹ (Ikaros)⁵⁵ and (E2A, H3K4Me2 and H3K4Me3).⁵⁶ V κ genes were scored positive for transcription factor binding sites or for a histone modification, if they were located on the same BglIII restriction fragment (corresponding to the 3C-Seq analysis).

3D DNA immunofluorescence in situ hybridization (FISH)

Rag-1^{-/-} pro-B and Rag-1^{-/-};VH81X pre-B cells were isolated from femoral bone marrow suspensions by positive enrichment of CD19⁺ cells using magnetic separation (Miltenyi Biotec). Cells were cultured for 2 weeks in Iscove's Modified Dulbecco's medium containing 10% fetal calf serum, 200 U/ml penicillin, 200 mg/ml streptomycin, 4 nM L-glutamine, and 50 μ M β -mercaptoethanol, supplemented with IL-7 and stem cell factor at 2 ng/ml. E2A^{-/-} hematopoietic progenitors were grown as described previously.⁷⁹ Prior to 3D-FISH analysis, cells were characterized by flow cytometric analysis of CD43, CD19 and CD2 surface marker expression to verify their phenotype (Figure S6).

3D DNA FISH was performed as described previously⁸⁰ with BAC clones RP23-234A12 and RP23-435I4 (located at the distal end of the V κ region and at the C κ /enhancer region, respectively, **Figure 3A**) obtained from BACPAC Resources, Oakland, CA. Probes were directly labeled with Chromatide Alexa Fluor 488-5 dUTP and Chromatide Alexa Fluor 568-5 dUTP (Invitrogen) using Nick Translation Mix (Roche Diagnostics GmbH).

Cultured primary cells were fixed in 4% paraformaldehyde, and permeabilized in a PBS/0.1% Triton X-100/0.1% saponin solution and subjected to liquid nitrogen immersion following incubation in PBS with 20% glycerol. The nuclear membranes were permeabilized in PBS/0.5% Triton X-100/0.5% saponin prior to hybridization with the DNA probe cocktail. Coverslips were sealed and incubated for 48hr at 37°C, washed and mounted on slides with 10 μ l of Prolong gold anti-fade reagent (Invitrogen).

Pictures were captured with a Leica SP5 confocal microscope (Leica Microsystems). Using a 63 \times lens (NA 1.4), we acquired images of \sim 70 serial optical sections spaced by 0.15 μ m. The data sets were deconvolved and analyzed with Huygens Professional software (Scientific Volume Imaging, Hilversum, the Netherlands). The 3D coordinates of the center of mass of each probe were transferred to Microsoft Excel, and the distances separating each probe were calculated using the equation: $\sqrt{(X_a - X_b)^2 + (Y_a - Y_b)^2 + (Z_a - Z_b)^2}$, where X, Y, Z are the coordinates of object a or b.

Statistical analysis

Statistical significance was analyzed using a nonparametric Mann-Whitney U test (IBM SPSS Statistics 20). P values <0.05 were considered significant.

Accession Numbers

3C-Seq datasets have been submitted to Sequence Read Archive (SRA, accession number SRP032509).

ACKNOWLEDGEMENTS

We thank H. Jumaa (Ulm, Germany), J. Kearney (Birmingham, AB) and C. Murre (San Diego, CA) for kindly providing Slp65^{-/-}, V_H81X transgenic and E2A^{-/-} mice, respectively. We thank D. Nemazee (La Jolla, CA) for providing detailed V_κ usage data. We also thank Z. Özgür, C.E.M. Kockx, Rutger Brouwer and Mirjam van den Hout (Biomics, Erasmus MC), M. Pescatori (Bioinformatics, Erasmus MC) and P.F. van Loo, I. Bergen and V. Ta (Pulmonary Medicine, Erasmus MC) for their contribution.

REFERENCES

1. Jung, D., C. Giallourakis, R. Mostoslavsky, and F. W. Alt. 2006. Mechanism and control of V(D)J recombination at the immunoglobulin heavy chain locus. *Annu Rev Immunol* 24:541-570.
2. Bossen, C., R. Mansson, and C. Murre. 2012. Chromatin Topology and the Regulation of Antigen Receptor Assembly. *Annu Rev Immunol* 30:337-356.
3. Herzog, S., M. Reth, and H. Jumaa. 2009. Regulation of B-cell proliferation and differentiation by pre-B-cell receptor signalling. *Nat Rev Immunol* 9:195-205.
4. Hendriks, R. W., and S. Middendorp. 2004. The pre-BCR checkpoint as a cell-autonomous proliferation switch. *Trends Immunol* 25:249-256.
5. Jhunjhunwala, S., M. C. van Zelm, M. M. Peak, and C. Murre. 2009. Chromatin architecture and the generation of antigen receptor diversity. *Cell* 138:435-448.
6. Ji, Y., W. Resch, E. Corbett, A. Yamane, R. Casellas, and D. G. Schatz. 2010. The in vivo pattern of binding of RAG1 and RAG2 to antigen receptor loci. *Cell* 141:419-431.
7. Perlot, T., and F. W. Alt. 2008. Cis-regulatory elements and epigenetic changes control genomic rearrangements of the IgH locus. *Adv Immunol* 99:1-32.
8. Cobb, R. M., K. J. Oestreich, O. A. Osipovich, and E. M. Oltz. 2006. Accessibility control of V(D)J recombination. *Adv Immunol* 91:45-109.

9. Oestreich, K. J., R. M. Cobb, S. Pierce, J. Chen, P. Ferrier, and E. M. Oltz. 2006. Regulation of TCRbeta gene assembly by a promoter/enhancer holocomplex. *Immunity* 24:381-391.
10. Seitan, V. C., M. S. Krangel, and M. Merckenschlager. 2012. Cohesin, CTCF and lymphocyte antigen receptor locus rearrangement. *Trends Immunol* 33:153-159.
11. Lefranc, M. P., V. Giudicelli, Q. Kaas, E. Duprat, J. Jabado-Michaloud, D. Scaviner, C. Ginestoux, O. Clement, D. Chaume, and G. Lefranc. 2005. IMGT, the international ImmunoGeneTics information system. *Nucleic Acids Res* 33:D593-597.
12. Yancopoulos, G. D., and F. W. Alt. 1985. Developmentally Controlled and Tissue-Specific Expression of Unrearranged Vh Gene Segments. *Cell* 40:271-281.
13. Abarrategui, I., and M. S. Krangel. 2009. Germline transcription: a key regulator of accessibility and recombination. *Adv Exp Med Biol* 650:93-102.
14. Schlissel, M. S., and D. Baltimore. 1989. Activation of immunoglobulin kappa gene rearrangement correlates with induction of germline kappa gene transcription. *Cell* 58:1001-1007.
15. Murre, C. 2005. Helix-loop-helix proteins and lymphocyte development. *Nat Immunol* 6:1079-1086.
16. Muljo, S. A., and M. S. Schlissel. 2003. A small molecule Abl kinase inhibitor induces differentiation of Abelson virus-transformed pre-B cell lines. *Nat Immunol* 4:31-37.
17. Lu, R., K. L. Medina, D. W. Lancki, and H. Singh. 2003. IRF-4,8 orchestrate the pre-B-to-B transition in lymphocyte development. *Genes Dev* 17:1703-1708.
18. Ma, S., A. Turetsky, L. Trinh, and R. Lu. 2006. IFN regulatory factor 4 and 8 promote Ig light chain kappa locus activation in pre-B cell development. *J Immunol* 177:7898-7904.
19. Johnson, K., T. Hashimshony, C. M. Sawai, J. M. Pongubala, J. A. Skok, I. Aifantis, and H. Singh. 2008. Regulation of immunoglobulin light-chain recombination by the transcription factor IRF-4 and the attenuation of interleukin-7 signaling. *Immunity* 28:335-345.
20. Liu, Z., P. Widlak, Y. Zou, F. Xiao, M. Oh, S. Li, M. Y. Chang, J. W. Shay, and W. T. Garrard. 2006. A recombination silencer that specifies heterochromatin positioning and ikaros association in the immunoglobulin kappa locus. *Immunity* 24:405-415.
21. Ribeiro de Almeida, C., R. Stadhouders, M. J. de Bruijn, I. M. Bergen, S. Thongjuea, B. Lenhard, W. van Ijcken, F. Grosveld, N. Galjart, E. Soler, and R. W. Hendriks. 2011. The DNA-binding protein CTCF limits proximal V kappa recombination and restricts kappa enhancer interactions to the immunoglobulin kappa light chain locus. *Immunity* 35:501-513.
22. Ribeiro de Almeida, C., R. Stadhouders, S. Thongjuea, E. Soler, and R. W. Hendriks. 2012. DNA-binding factor CTCF and long-range gene interactions in V(D)J recombination and oncogene activation. *Blood* 119:6209-6218.
23. Xiang, Y., X. Zhou, S. L. Hewitt, J. A. Skok, and W. T. Garrard. 2011. A multifunctional element in the mouse Igkappa locus that specifies repertoire and Ig loci subnuclear location. *J Immunol* 186:5356-5366.
24. Pan, X., M. Papasani, Y. Hao, M. Calamito, F. Wei, W. J. Quinn Iii, A. Basu, J. Wang, S. Hodawadekar, K. Zaprazna, H. Liu, Y. Shi, D. Allman, M. Cancro, and M. L. Atchison. 2013. YY1 controls Igkappa repertoire and B-cell development, and localizes with condensin on the Igkappa locus. *EMBO J* 32:1168-1182.

25. Melchers, F. 2005. The pre-B-cell receptor: selector of fitting immunoglobulin heavy chains for the B-cell repertoire. *Nat Rev Immunol* 5:578-584.
26. Li, Z., D. I. Dordai, J. Lee, and S. Desiderio. 1996. A conserved degradation signal regulates RAG-2 accumulation during cell division and links V(D)J recombination to the cell cycle. *Immunity* 5:575-589.
27. Thompson, E. C., B. S. Cobb, P. Sabbattini, S. Meixlsperger, V. Parelho, D. Liberg, B. Taylor, N. Dillon, K. Georgopoulos, H. Jumaa, S. T. Smale, A. G. Fisher, and M. Merkenschlager. 2007. Ikaros DNA-binding proteins as integral components of B cell developmental-stage-specific regulatory circuits. *Immunity* 26:335-344.
28. Nakayama, J., M. Yamamoto, K. Hayashi, H. Satoh, K. Bundo, M. Kubo, R. Goitsuka, M. A. Farrar, and D. Kitamura. 2009. BLNK suppresses pre-B-cell leukemogenesis through inhibition of JAK3. *Blood* 113:1483-1492.
29. Herzog, S., E. Hug, S. Meixlsperger, J. H. Paik, R. A. DePinho, M. Reth, and H. Jumaa. 2008. SLP-65 regulates immunoglobulin light chain gene recombination through the PI(3)K-PKB-Foxo pathway. *Nat Immunol* 9:623-631.
30. Amin, R. H., and M. S. Schlissel. 2008. Foxo1 directly regulates the transcription of recombination-activating genes during B cell development. *Nat Immunol* 9:613-622.
31. Novobrantseva, T. I., V. M. Martin, R. Pelanda, W. Muller, K. Rajewsky, and A. Ehlich. 1999. Rearrangement and expression of immunoglobulin light chain genes can precede heavy chain expression during normal B cell development in mice. *J Exp Med* 189:75-88.
32. Melchers, F., E. ten Boekel, T. Seidl, X. C. Kong, T. Yamagami, K. Onishi, T. Shimizu, A. G. Rolink, and J. Andersson. 2000. Repertoire selection by pre-B-cell receptors and B-cell receptors, and genetic control of B-cell development from immature to mature B cells. *Immunol Rev* 175:33-46.
33. Schlissel, M. S. 2004. Regulation of activation and recombination of the murine Igkappa locus. *Immunol Rev* 200:215-223.
34. Kersseboom, R., V. B. Ta, A. J. Zijlstra, S. Middendorp, H. Jumaa, P. F. van Loo, and R. W. Hendriks. 2006. Bruton's tyrosine kinase and SLP-65 regulate pre-B cell differentiation and the induction of Ig light chain gene rearrangement. *J Immunol* 176:4543-4552.
35. Dingjan, G. M., S. Middendorp, K. Dahlenborg, A. Maas, F. Grosveld, and R. W. Hendriks. 2001. Bruton's tyrosine kinase regulates the activation of gene rearrangements at the lambda light chain locus in precursor B cells in the mouse. *J Exp Med* 193:1169-1178.
36. Roldan, E., M. Fuxa, W. Chong, D. Martinez, M. Novatchkova, M. Busslinger, and J. A. Skok. 2005. Locus 'decontraction' and centromeric recruitment contribute to allelic exclusion of the immunoglobulin heavy-chain gene. *Nat Immunol* 6:31-41.
37. Inlay, M. A., H. Tian, T. Lin, and Y. Xu. 2004. Important roles for E protein binding sites within the immunoglobulin kappa chain intronic enhancer in activating V kappa J kappa rearrangement. *J Exp Med* 200:1205-1211.
38. Lazorchak, A. S., M. S. Schlissel, and Y. Zhuang. 2006. E2A and IRF-4/Pip promote chromatin modification and transcription of the immunoglobulin kappa locus in pre-B cells. *Mol Cell Biol* 26:810-821.

39. Reynaud, D., I. A. Demarco, K. L. Reddy, H. Schjerven, E. Bertolino, Z. Chen, S. T. Smale, S. Winandy, and H. Singh. 2008. Regulation of B cell fate commitment and immunoglobulin heavy-chain gene rearrangements by Ikaros. *Nat Immunol* 9:927-936.
40. Lin, Y. C., C. Benner, R. Mansson, S. Heinz, K. Miyazaki, M. Miyazaki, V. Chandra, C. Bossen, C. K. Glass, and C. Murre. 2012. Global changes in the nuclear positioning of genes and intra- and interdomain genomic interactions that orchestrate B cell fate. *Nat Immunol* 13:1196-1204.
41. Stadhouders, R., P. Kolovos, R. Brouwer, J. Zuin, A. van den Heuvel, C. Kockx, R. J. Palstra, K. S. Wendt, F. Grosveld, W. van Ijcken, and E. Soler. 2013. Multiplexed chromosome conformation capture sequencing for rapid genome-scale high-resolution detection of long-range chromatin interactions. *Nat Protoc* 8:509-524.
42. Jumaa, H., B. Wollscheid, M. Mitterer, J. Wienands, M. Reth, and P. J. Nielsen. 1999. Abnormal development and function of B lymphocytes in mice deficient for the signaling adaptor protein SLP-65. *Immunity* 11:547-554.
43. Middendorp, S., G. M. Dingjan, and R. W. Hendriks. 2002. Impaired precursor B cell differentiation in Bruton's tyrosine kinase-deficient mice. *J Immunol* 168:2695-2703.
44. Jumaa, H., M. Mitterer, M. Reth, and P. J. Nielsen. 2001. The absence of SLP65 and Btk blocks B cell development at the preB cell receptor-positive stage. *Eur J Immunol* 31:2164-2169.
45. Saeed, A. I., N. K. Bhagabati, J. C. Braisted, W. Liang, V. Sharov, E. A. Howe, J. Li, M. Thiagarajan, J. A. White, and J. Quackenbush. 2006. TM4 microarray software suite. *Methods Enzymol* 411:134-193.
46. Kersseboom, R., S. Middendorp, G. M. Dingjan, K. Dahlenborg, M. Reth, H. Jumaa, and R. W. Hendriks. 2003. Bruton's tyrosine kinase cooperates with the B cell linker protein SLP-65 as a tumor suppressor in Pre-B cells. *J Exp Med* 198:91-98.
47. Bertocci, B., A. De Smet, C. Berek, J. C. Weill, and C. A. Reynaud. 2003. Immunoglobulin kappa light chain gene rearrangement is impaired in mice deficient for DNA polymerase mu. *Immunity* 19:203-211.
48. Baldwin, A. S., Jr., K. P. LeClair, H. Singh, and P. A. Sharp. 1990. A large protein containing zinc finger domains binds to related sequence elements in the enhancers of the class I major histocompatibility complex and kappa immunoglobulin genes. *Mol Cell Biol* 10:1406-1414.
49. Engel, H., A. Rolink, and S. Weiss. 1999. B cells are programmed to activate kappa and lambda for rearrangement at consecutive developmental stages. *Eur J Immunol* 29:2167-2176.
50. Gorman, J. R., N. van der Stoep, R. Monroe, M. Cogne, L. Davidson, and F. W. Alt. 1996. The Ig(kappa) enhancer influences the ratio of Ig(kappa) versus Ig(lambda) B lymphocytes. *Immunity* 5:241-252.
51. Xu, Y., L. Davidson, F. W. Alt, and D. Baltimore. 1996. Deletion of the Ig kappa light chain intronic enhancer/matrix attachment region impairs but does not abolish V kappa J kappa rearrangement. *Immunity* 4:377-385.
52. Inlay, M., F. W. Alt, D. Baltimore, and Y. Xu. 2002. Essential roles of the kappa light chain intronic enhancer and 3' enhancer in kappa rearrangement and demethylation. *Nat Immunol* 3:463-468.
53. Greenbaum, S., and Y. Zhuang. 2002. Identification of E2A target genes in B lymphocyte development by using a gene tagging-based chromatin immunoprecipitation system. *Proc Natl Acad Sci U S A* 99:15030-15035.

54. Aoki-Ota, M., A. Torkamani, T. Ota, N. Schork, and D. Nemazee. 2012. Skewed primary Igkappa repertoire and V-J joining in C57BL/6 mice: implications for recombination accessibility and receptor editing. *J Immunol* 188:2305-2315.
55. Ferreiros-Vidal, I., T. Carroll, B. Taylor, A. Terry, Z. Liang, L. Bruno, G. Dharmalingam, S. Khadayate, B. S. Cobb, S. T. Smale, M. Spivakov, P. Srivastava, E. Petretto, A. G. Fisher, and M. Merkenschlager. 2013. Genome-wide identification of Ikaros targets elucidates its contribution to mouse B-cell lineage specification and pre-B-cell differentiation. *Blood* 121:1769-1782.
56. Lin, Y. C., S. Jhunjhunwala, C. Benner, S. Heinz, E. Welinder, R. Mansson, M. Sigvardsson, J. Hagman, C. A. Espinoza, J. Dutkowski, T. Ideker, C. K. Glass, and C. Murre. 2010. A global network of transcription factors, involving E2A, EBF1 and Foxo1, that orchestrates B cell fate. *Nat Immunol* 11:635-U109.
57. Sakamoto, S., K. Wakae, Y. Anzai, K. Murai, N. Tamaki, M. Miyazaki, K. Miyazaki, W. J. Romanow, T. Ikawa, D. Kitamura, I. Yanagihara, N. Minato, C. Murre, and Y. Agata. 2012. E2A and CBP/p300 act in synergy to promote chromatin accessibility of the immunoglobulin kappa locus. *J Immunol* 188:5547-5560.
58. Heizmann, B., P. Kastner, and S. Chan. 2013. Ikaros is absolutely required for pre-B cell differentiation by attenuating IL-7 signals. *J Exp Med*.
59. Feeney, A. J. 2011. Epigenetic regulation of antigen receptor gene rearrangement. *Curr Opin Immunol* 23:171-177.
60. Liu, Y., R. Subrahmanyam, T. Chakraborty, R. Sen, and S. Desiderio. 2007. A plant homeodomain in Rag-2 that binds hypermethylated lysine 4 of histone H3 is necessary for efficient antigen-receptor-gene rearrangement. *Immunity* 27:561-571.
61. Matthews, A. G., A. J. Kuo, S. Ramon-Maiques, S. Han, K. S. Champagne, D. Ivanov, M. Gallardo, D. Carney, P. Cheung, D. N. Ciccone, K. L. Walter, P. J. Utz, Y. Shi, T. G. Kutateladze, W. Yang, O. Gozani, and M. A. Oettinger. 2007. RAG2 PHD finger couples histone H3 lysine 4 trimethylation with V(D)J recombination. *Nature* 450:1106-1110.
62. Bain, G., E. C. Robanus Maandag, H. P. te Riele, A. J. Feeney, A. Sheehy, M. Schlissel, S. A. Shinton, R. R. Hardy, and C. Murre. 1997. Both E12 and E47 allow commitment to the B cell lineage. *Immunity* 6:145-154.
63. Goldmit, M., Y. Ji, J. Skok, E. Roldan, S. Jung, H. Cedar, and Y. Bergman. 2005. Epigenetic ontogeny of the Igk locus during B cell development. *Nat Immunol* 6:198-203.
64. Degner, S. C., J. Verma-Gaur, T. P. Wong, C. Bossen, G. M. Iverson, A. Torkamani, C. Vettermann, Y. C. Lin, Z. Ju, D. Schulz, C. S. Murre, B. K. Birshtein, N. J. Schork, M. S. Schlissel, R. Riblet, C. Murre, and A. J. Feeney. 2011. CCCTC-binding factor (CTCF) and cohesin influence the genomic architecture of the Igh locus and antisense transcription in pro-B cells. *Proc Natl Acad Sci U S A* 108:9566-9571.
65. Guo, C., H. S. Yoon, A. Franklin, S. Jain, A. Ebert, H. L. Cheng, E. Hansen, O. Despo, C. Bossen, C. Vettermann, J. G. Bates, N. Richards, D. Myers, H. Patel, M. Gallagher, M. S. Schlissel, C. Murre, M. Busslinger, C. C. Giallourakis, and F. W. Alt. 2011. CTCF-binding elements mediate control of V(D)J recombination. *Nature* 477:424-430.

66. Xu, C. R., and A. J. Feeney. 2009. The epigenetic profile of Ig genes is dynamically regulated during B cell differentiation and is modulated by pre-B cell receptor signaling. *J Immunol* 182:1362-1369.
67. Inlay, M. A., T. Lin, H. H. Gao, and Y. Xu. 2006. Critical roles of the immunoglobulin intronic enhancers in maintaining the sequential rearrangement of IgH and Igk loci. *J Exp Med* 203:1721-1732.
68. Brown, K. E., S. S. Guest, S. T. Smale, K. Hahm, M. Merkenschlager, and A. G. Fisher. 1997. Association of transcriptionally silent genes with Ikaros complexes at centromeric heterochromatin. *Cell* 91:845-854.
69. Kim, J., S. Sif, B. Jones, A. Jackson, J. Koipally, E. Heller, S. Winandy, A. Viel, A. Sawyer, T. Ikeda, R. Kingston, and K. Georgopoulos. 1999. Ikaros DNA-binding proteins direct formation of chromatin remodeling complexes in lymphocytes. *Immunity* 10:345-355.
70. Koipally, J., A. Renold, J. Kim, and K. Georgopoulos. 1999. Repression by Ikaros and Aiolos is mediated through histone deacetylase complexes. *EMBO J* 18:3090-3100.
71. Schmitt, C., C. Tonnelle, A. Dalloul, C. Chabannon, P. Debre, and A. Rebollo. 2002. Aiolos and Ikaros: regulators of lymphocyte development, homeostasis and lymphoproliferation. *Apoptosis* 7:277-284.
72. Holwerda, S. J., H. J. van de Werken, C. Ribeiro de Almeida, I. M. Bergen, M. J. de Bruijn, M. J. Verstegen, M. Simonis, E. Splinter, P. J. Wijchers, R. W. Hendriks, and W. de Laat. 2013. Allelic exclusion of the immunoglobulin heavy chain locus is independent of its nuclear localization in mature B cells. *Nucleic Acids Res* 41:6905-6916.
73. Martin, F., X. Chen, and J. F. Kearney. 1997. Development of VH81X transgene-bearing B cells in fetus and adult: sites for expansion and deletion in conventional and CD5/B1 cells. *Int Immunol* 9:493-505.
74. Mombaerts, P., J. Iacomini, R. S. Johnson, K. Herrup, S. Tonegawa, and V. E. Papaioannou. 1992. RAG-1-deficient mice have no mature B and T lymphocytes. *Cell* 68:869-877.
75. Hendriks, R. W., M. F. de Bruijn, A. Maas, G. M. Dingjan, A. Karis, and F. Grosveld. 1996. Inactivation of Btk by insertion of lacZ reveals defects in B cell development only past the pre-B cell stage. *EMBO J* 15:4862-4872.
76. Stadhouders, R., S. Thongjuea, C. Andrieu-Soler, R. J. Palstra, J. C. Bryne, A. van den Heuvel, M. Stevens, E. de Boer, C. Kockx, A. van der Sloot, M. van den Hout, W. van Ijcken, D. Eick, B. Lenhard, F. Grosveld, and E. Soler. 2012. Dynamic long-range chromatin interactions control Myb proto-oncogene transcription during erythroid development. *EMBO J* 31:986-999.
77. Thongjuea, S., R. Stadhouders, F. G. Grosveld, E. Soler, and B. Lenhard. 2013. r3Cseq: an R/Bioconductor package for the discovery of long-range genomic interactions from chromosome conformation capture and next-generation sequencing data. *Nucleic Acids Res*.
78. Mombaerts, P., J. Iacomini, R. S. Johnson, K. Herrup, S. Tonegawa, and V. E. Papaioannou. 1992. Rag-1-Deficient Mice Have No Mature Lymphocytes-B and Lymphocytes-T. *Cell* 68:869-877.
79. Ikawa, T., H. Kawamoto, L. Y. Wright, and C. Murre. 2004. Long-term cultured E2A-deficient hematopoietic progenitor cells are pluripotent. *Immunity* 20:349-360.
80. Sayegh, C. E., S. Jhunjunwala, R. Riblet, and C. Murre. 2005. Visualization of looping involving the immunoglobulin heavy-chain locus in developing B cells. *Genes Dev* 19:322-327.



Chapter III

Nuclear positioning rather than contraction controls ordered rearrangements of immunoglobulin loci

Magdalena B. Rother¹, Robert-Jan Palstra², Suchit Jhunjhunwala³, Kevin A.M. van Kester¹, Wilfred F.J. van IJcken⁴, Rudi W. Hendriks⁵, Jacques J.M. van Dongen¹, Cornelis Murre³ and Menno C. van Zelm^{1,6}

(1) Department of Immunology, (2) Department of Biochemistry, (4) Center for Biomics, (5) Department of Pulmonary Medicine, Erasmus MC, University Medical Center, Rotterdam, The Netherlands, (3) Department of Molecular Biology, University of California, San Diego, La Jolla, California, USA, (6) present address: Department of Immunology, Central Clinical School, Monash University, Melbourne, Victoria, Australia

Manuscript accepted at *Nucleic Acids Research*

The online version of this article contains the supplemental material.

ABSTRACT

Progenitor-B cells recombine their immunoglobulin (Ig) loci to create unique antigen receptors. Despite a common recombination machinery, the Ig heavy and Ig light chain loci rearrange in a stepwise manner. We studied pre-pro-B cells and Rag^{-/-} progenitor-B cells to determine whether Ig locus contraction or nuclear positioning is decisive for stepwise rearrangements. We found that both Ig loci were contracted in pro-B and pre-B cells. *Igh* relocated from the nuclear lamina to central domains only at the pro-B cell stage, whereas, *Igk* remained sequestered at the lamina, and only at the pre-B cell stage located to central nuclear domains. Finally, in vitro induced re-positioning of Ig alleles away from the nuclear periphery increased germline transcription of Ig loci in pre-pro-B cells. Thus, Ig locus contraction juxtaposes genomically distant elements to mediate efficient recombination, however, sequential positioning of Ig loci away from the nuclear periphery determines stage-specific accessibility of Ig loci.

INTRODUCTION

During differentiation in bone marrow, each progenitor-B cell assembles a unique immunoglobulin molecule (Ig) through genetic recombination of V, D and J genes in their Ig heavy chain (*Igh*) and Ig light chain loci (*Igk* or *Igl*).^{1,2} The lymphoid-specific recombination activating gene proteins 1 and 2 (Rag1 and Rag2) are crucial in this process through induction of double strand DNA breaks at recombination signal sequences (RSS) flanking each V, D and J gene.^{3,4} The V(D)J recombination of Ig is initiated in uncommitted pre-pro-B cells by formation of incomplete D_H-J_H rearrangements followed by rearrangement of V_H to D_HJ_H junction in pro-B cells. Subsequently, V to J gene rearrangements in the Ig light chain loci are induced in pre-B cells with expression of functional Ig μ molecules on the cell surface.^{1,2}

Although the core machinery for V(D)J recombination is identical for the different loci, each locus undergoes recombination in a developmental stage-specific manner. This stage-specific accessibility of the Ig loci for the V(D)J recombination machinery has been extensively addressed and is thought to involve 3 epigenetic processes: DNA and chromatin modifications, nuclear positioning, and locus contraction.^{1,5,6}

It is well-established that non-coding RNA transcription,^{6,7} and epigenetic modifications of histones and/or DNA^{8,9} modulate gene accessibility. Ig genes poised for V(D)J recombination are wrapped around histones that are extensively acetylated and methylated.^{10,11} Importantly, stage-specific trimethylation of lysine 4 in H3 (H3K4me3) in Ig genes can directly recruit Rag2.¹²⁻¹⁴

During cellular maturation, genes can change their nuclear ‘neighborhoods’ by re-positioning from repressive sites to transcriptionally active compartments, and vice versa.^{9, 15-17} Relocation of genes in the nucleus towards transcription factories occurs through extruding of decondensed chromatin loops into interchromosomal space and intermingling with neighboring chromosome territories.^{9, 15, 18} The nuclear periphery represents a repressive region through tethering of chromosomal domains to nuclear lamins, thereby creating lamina associated domains (LADs).^{16, 17} The nuclear positioning of Ig loci also seems tightly regulated, as they are positioned centrally in committed B-cell progenitors, while in non-B cells they are located at the nuclear periphery.^{17, 19, 20}

Committed B-cell progenitors show large-scale Ig locus contraction to provide a diverse antigen receptor repertoire.^{7, 21-27} Initially, Ig locus contraction was thought to only occur at the stage in which the locus undergoes recombination.^{26, 27} However, recent observations indicate that the *Igκ* locus is contracted in both pro-B and pre-B cells^{28, 29} with similar levels of long-range interactions.²⁹⁻³¹ Since *Igκ* gene rearrangements rarely occur prior to the pre-B-cell stage,³² the question arises whether Ig locus contraction is decisive for V(D)J recombination.

Here we have examined how Ig locus contraction and nuclear positioning are associated with the stepwise control of V(D)J recombination. We found that nuclear localization rather than Ig locus topology is closely linked with the developmental regulation of *Igh* and *Igκ* locus assembly.

RESULTS

Igh locus contraction in pro-B and pre-B cells

To study the role of 3D organization of the *Igh* locus in the stepwise *Igh* and *Igκ* gene rearrangement processes, we employed 3D DNA FISH in uncommitted pre-pro-B cells, and in committed pro-B cells and pre-B cells. Each of these subsets was obtained from specific mouse models to enable studies on the *Igh* and *Igκ* loci in their germline configuration. Uncommitted pre-pro-B cells (B220+CD19-CD43+; **Figure 1A**) were cultured from E2A^{-/-} mice and did not contain complete V_H to DJ_H, nor incomplete DJ_H to J_H rearrangements.³³ Pro-B cells were derived from Rag1 or Rag2-deficient mice and expressed CD19 and CD43 in absence of Ig gene rearrangements.³⁴ Pre-B cells were derived from transgenic mice expressing a functional murine (V_H81X) or human Igh μ chain on a Rag-deficient background or from Rag-deficient pro-B cells transduced with human Igh μ chain. These cells express a pre-BCR, while their endogenous Ig loci are preserved in germline configuration and remain non-functional.^{35, 36}

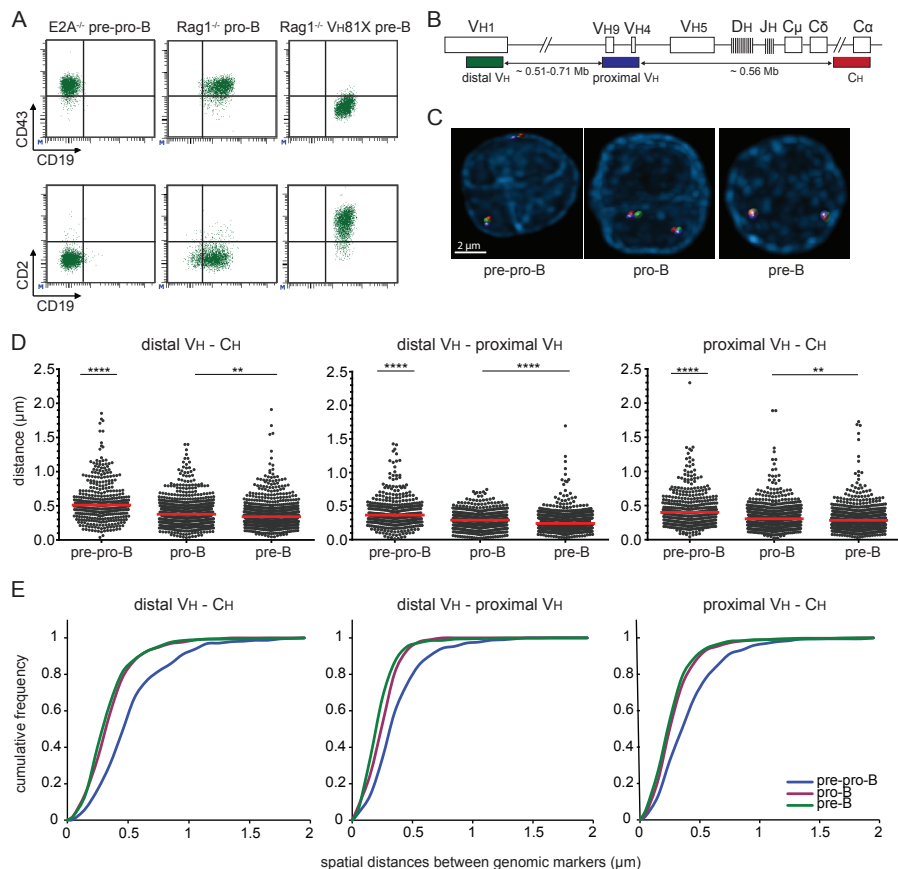


Figure 1. The *Igh* locus is contracted in pro-B and pre-B cells. (A) Flow cytometric analysis of cultured precursor-B cells from E2A⁺, Rag1⁺, and Rag1^{-/-} Vh81X mice confirmed their differentiation block at the pre-pro-B, pro-B and pre-B cells stage, respectively.⁶³ (B) Schematic representation of the murine *Igh* locus. Bacterial artificial chromosome clones used as 3D FISH probes are indicated.²⁷ The distal VH probe was conjugated with Alexa488, the proximal VH probe with Cy5 and the CH probe with Alexa568. The indicated distance separating each of the 3 probes and their positions within the *Igh* locus were determined from the Ensembl mouse genome database. (C) Representative FISH images of *Igh* loci in the different populations. (D) Scatter plots show the spatial distances separating the FISH probes with red lines representing median distances. 2-4 mice were used for each condition and at least 200 alleles were analyzed per population. The non-parametric Mann-Whitney test was used to calculate significance levels: **, P < .01; ****, P < .0001. (E) Cumulative frequency plots showing the distribution of spatial distances between the distal VH, proximal VH, and CH probes in the 3 B-cell subsets.

To determine *Igh* locus contraction during B-cell development, we measured spatial distances between 3 BAC probes hybridized to distal VH, proximal VH and CH regions of the *Igh* locus (Figure 1B-C). Spatial distances between each of these three regions were significantly shorter in pro-B cells than in pre-pro-B cells, in line with previous

findings.²⁵⁻²⁷ More interestingly, we found that the spatial distances measured in pre-B cells were also significantly shorter than in pre-pro-B cells, and were similar to the spatial distances in pro-B cells (**Figure 1D-E**). The contraction was not affected by the choice of model, because the distances were similar between Rag1^{-/-} and Rag2^{-/-} progenitor-B cells, and between V_H81X and hIgM transgenics (Figure S1A-B). Furthermore, transduction of hIgM into cultured Rag2^{-/-} pro-B cells also did not affect contraction (Figure S1C). The *Igh* locus was also contracted in freshly isolated pro-B cells, excluding effects of culture in the spatial organization of *Igh* (Figure S1A).

Thus, in line with previous observations, the *Igh* locus is contracted in pro-B cells, but, contrary to previous observations,²⁶ it was not decontracted in pre-B cells. The 3D chromatin organization might therefore facilitate locus accessibility for recombination, however, it does not seem decisive for closure of *Igh* in pro-B cells.

***Igk* locus contraction in pro-B and pre-B cells is independent of the intronic κ enhancer (iE κ)**

We next evaluated in our model system with germline Ig genes whether the *Igk* locus was contracted in pre-B cells only,²⁶ or already in pro-B cells.^{28, 29} 3D DNA FISH was performed with 3 BAC probes detecting distal V κ , proximal V κ and C κ regions (**Figure 2A-B**). The spatial distances between the *Igk* probes were similar between pro-B cells and pre-B cells as previously published,³⁷ and significantly shorter than in pre-pro-B cells (**Figure 2C-D**). *Igk* contraction was similar between Rag1^{-/-}, Rag2^{-/-}, V_H81X, hIgM transgenic and hIgM transduced progenitor-B cells, and freshly isolated pro-B cells, excluding effects of genetic background or cell culture (Figure S1D-E).

The intron enhancers in *Igh* (iE μ) and *Igk* (iE κ) are known to contribute to stage-specific Ig gene rearrangements. Mice carrying homozygous mutations in E-box motifs in the iE κ element (κ E1/E2^{mut} mice) show reduced efficiencies of *Igk* rearrangements,³⁸ while *Igk* alleles with targeted replacement of iE κ by iE μ (E μ R mice) already rearrange at the pro-B-cell stage.³⁹ To study whether *Igk* locus contraction can take place in the absence of a functional iE κ , we crossed κ E1/E2^{mut} mice on the Rag2^{-/-} Ig μ background, and performed 3D DNA FISH with the three *Igk* BAC probes. The spatial distances measured between *Igk* BAC probes in κ E1/E2^{mut} pre-B cells were similar to pre-B cells with a wildtype iE κ and were significantly shorter than in pre-pro-B cells (**Figure 2C-D**). Additional analysis of κ E1/E2^{mut} pro-B and E μ R pro-B cells also revealed full contraction of these *Igk* loci (Figure S2). These results suggest that contraction of the *Igk* locus in pro-B and pre-B cells does not critically depend on a functional iE κ . Thus, the *Igk* locus undergoes locus contraction in pro-B cells and remained contracted in pre-B cells, independent of iE κ functionality.

III. Nuclear Positioning Rather Than Contraction Controls Ordered Rearrangements of Immunoglobulin Loci

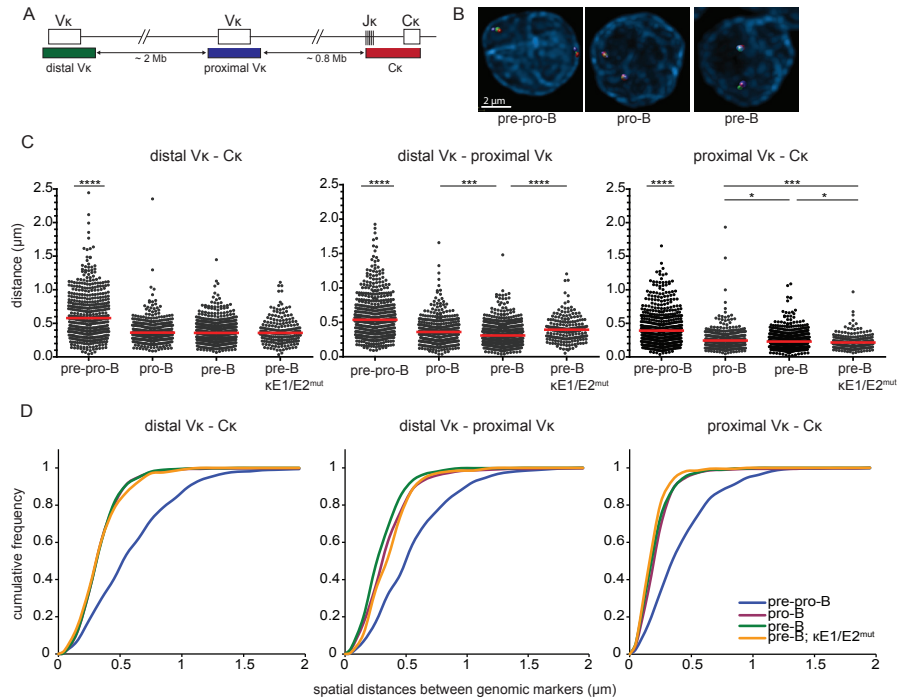


Figure 2. *Igk* locus contraction in pro-B and pre-B cells is independent of iE κ . (A) Schematic representation of the murine *Igk* locus including the bacterial artificial chromosome clones used as 3D FISH probes: distal $V\kappa$ – Alexa488, proximal $V\kappa$ – Cy5, $C\kappa$ – Alexa568. The indicated distances separating each of the 3 probes and their positions within the *Igk* locus were determined from the Ensembl mouse genome database. (B) Representative images of the *Igk* locus in the 3 B-cell subsets. (C) Scatter plots show the distances between distal $V\kappa$, proximal $V\kappa$, and $C\kappa$ regions in cultured E2A^{-/-} pre-pro-B, Rag1^{-/-} pro-B, Rag1^{-/-} Ig μ pre-B and Rag2^{-/-} $\kappa\text{E1/E2}^{\text{mut}}$ pre-B cells. For each condition 2-3 mice were used and at least 200 alleles were analyzed per population. Red horizontal lines represent median distances. The non-parametric Mann-Whitney test was used to calculate significance levels: *, $P < .05$; ***, $P < .001$; ****, $P < .0001$. (D) Cumulative frequency plots showing the distribution of spatial distances between the distal $V\kappa$, proximal $V\kappa$, and $C\kappa$ region probes in the 4 progenitor-B cell subsets.

Long-range interactions within the *Igh* and *Igk* loci

To further study the nature of the contracted *Igh* and *Igk* loci in pro-B and pre-B cells, we analyzed interactions within these Ig loci using Chromosome Conformation Capture and sequencing (3C-Seq). Viewpoints in iE μ and iE κ were selected and their long-range interactions were studied in non-lymphoid erythroid progenitors, E2A^{-/-} pre-pro-B, Rag1^{-/-} pro-B and Rag1^{-/-} VH81X pre-B cells.

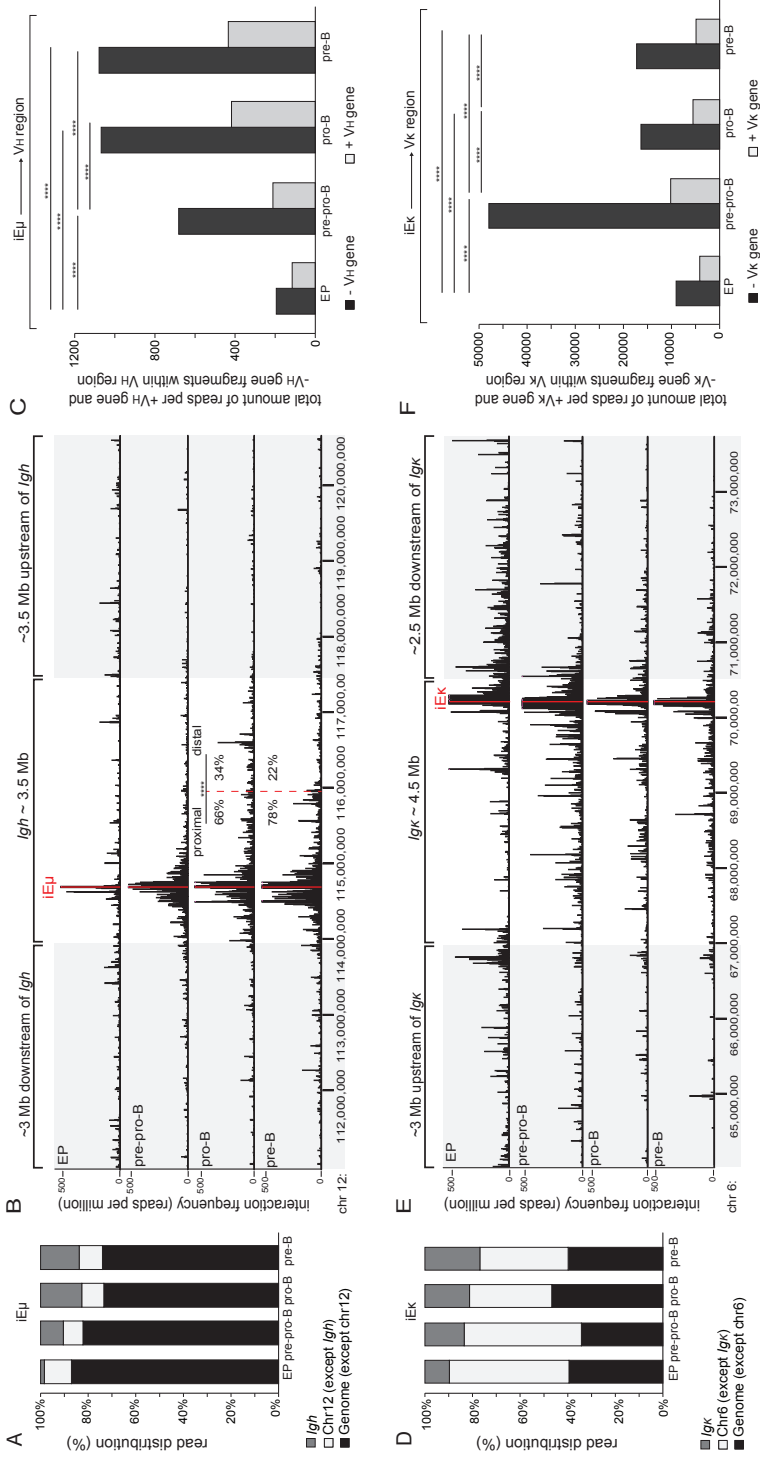


Figure 3. (Legend on the next page)

The bulk of interactions for iE μ were found with sites on other chromosomes or other regions on chromosome 12 outside of *Igh* (**Figure 3A**). Still many interactions were confined to the 3.5 Mb *Igh* locus (**Figure 3B**), creating its own discrete topologically associated domain (TAD).⁴⁰ This confinement of interactions within the *Igh* locus was also found with 3 additional viewpoints located in the distal V_H, proximal V_H and 3'RR regions (Figure S3A-B). Still, pro-B and pre-B cells contained clearly more interactions between iE μ and V_H regions than pre-pro-B cells and erythroid progenitors (**Figure 3A-B**). Moreover, pro-B cells carried specific interactions between iE μ and the distal V_H region (**Figure 3B**), whereas in pre-B cells these were mainly found between iE μ and proximal V_H genes (**Figure 3B**). To study whether these interactions preferentially involved V_H genes, we determined the frequencies of interactions with fragments that contained a V_H gene (+V_H gene) or not (-V_H gene; **Figure 3C**). Of the 869 BglII fragments within the V_H region, only a minority contained one or more of the 110 V_H genes. B-lineage cells showed more interactions between iE μ and the entire V_H region than erythroid progenitors. Erythroid progenitors displayed low amounts of interactions to the V_H region (**Figure 3C**). These numbers were significantly higher in pre-pro-B-cells and the highest numbers were found in pro-B and pre-B cells. Moreover, the committed pro-B and pre-B cells showed relatively more interactions with +V_H fragments than uncommitted pre-pro-B cells. Thus, committed B-cell precursors showed frequent interactions between iE μ and V_H genes, with distal V_H interactions being more frequent in pro-B than in pre-B cells.

Similar to *Igh*, the iE κ viewpoint showed many interactions with sites on other chromosomes or other regions on chromosome 6 outside *Igk* (**Figures 3D** and S3C-D). Interactions within *Igk* increased with more mature subsets and were most frequent in pre-B cells (**Figure 3D**).

Figure 3. Long-range interactions within the *Igh* and *Igk* loci. (A) Bar graphs showing the relative distribution of 3C-Seq reads in the *Igh* locus, the rest of chromosome 12 (chr12 except *Igh*) and rest of the genome (genome except chr12). Read distributions across the genome were analyzed for iE μ enhancer viewpoint in erythroid progenitors (EP), cultured E2A^{-/-} pre-pro-B, Rag1^{-/-} pro-B and Rag1^{-/-} V_H81X pre-B cells. Indicated cell fractions were obtained from 4 mice. Data represent average of 2 biological replicates. (B) 3C-Seq long-range interactions of the iE μ viewpoint along ~10 Mb range of chromosome 12 were plotted as reads per million for erythroid progenitors (EP), E2A^{-/-} pre-pro-B, Rag1^{-/-} pro-B and Rag1^{-/-} V_H81X pre-B cells. The frequency of reads within proximal V_H and distal V_H regions are presented for Rag1^{-/-} pro-B and Rag1^{-/-} V_H81X pre-B cells as % of total interactions within the entire V_H region. The χ^2 test was used to calculate significance level. ****, P < .0001. (C) Bar graphs showing total amount of 3C-Seq interactions within the V_H region of *Igh* analyzed for BglII fragments that contain V_H genes (+V_H gene) or not (-V_H gene). Bars represent sum of interactions. The χ^2 test was used to calculate significance levels between +V_H gene and -V_H gene fragments of two cell types. ****, P < .0001. (D) Bar graphs showing the relative distribution of 3C-Seq reads in the *Igk* locus, the rest of chromosome 6 (chr6 except *Igk*) and rest of the genome (genome except chr6). Read distributions across the genome were analyzed for iE κ enhancer viewpoint in erythroid progenitors (EP), cultured E2A^{-/-} pre-pro-B, Rag1^{-/-} pro-B and Rag1^{-/-} V_H81X pre-B cells. Indicated cell fractions were obtained from 4 mice. Data represent average of 2 biological replicates. (E) 3C-Seq long-range interactions of the iE κ enhancer viewpoint along ~10 Mb range of chromosome 6 were plotted as reads per million for erythroid progenitors (EP), E2A^{-/-} pre-pro-B, Rag1^{-/-} pro-B and Rag1^{-/-} V_H81X pre-B cells. (F) Bar graphs showing total amount of 3C-Seq interactions within the V_K region of *Igk* analyzed for BglII fragments that contain V_K genes (+V_K gene) or not (-V_K gene). Bars represent sum of interactions. The χ^2 test was used to calculate significance levels between +V_K gene and -V_K gene fragments of two cell types. ****, P < .0001

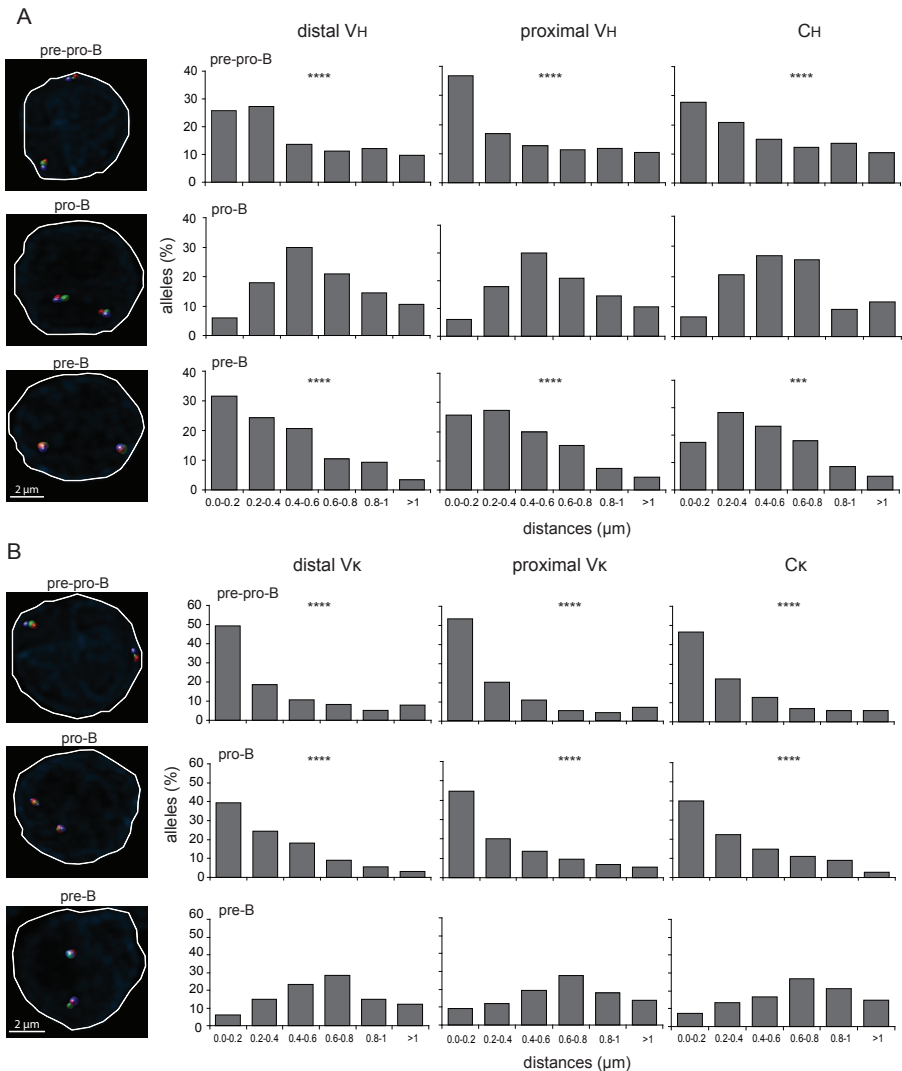


Figure 4. Stage-specific positioning of Ig loci away from the nuclear lamina. (A) Bar graphs showing the frequencies of *Igh* alleles positioned within a distance range from the nuclear lamina in cultured $E2A^{-/-}$ pre-pro-B, $Rag1^{-/-}$ pro-B and $Rag1^{-/-}$ hIgM pre-B cells. (B) Bar graphs depicting frequencies of *Igk* alleles positioned within a distance range from the nuclear lamina in cultured $E2A^{-/-}$ pre-pro-B, $Rag1^{-/-}$ pro-B and $Rag1^{-/-}$ hIgM pre-B cells. In A and B, X-axis represents the distance ranges from the nuclear lamina and y-axis represents the % of alleles positioned within a certain distance range. Distances were measured with 3D DNA FISH of >100 alleles, obtained from 2 mice. Statistical significance was calculated with the χ^2 test between $Rag1^{-/-}$ pro-B and $E2A^{-/-}$ pre-pro-B and $Rag1^{-/-}$ hIgM pre-B cells in A or between $Rag1^{-/-}$ hIgM pre-B and $E2A^{-/-}$ pre-pro-B and $Rag1^{-/-}$ pro-B cells in B based on the sum of alleles located <0.4 μm from the lamina and the sum of alleles located >0.4 μm of the lamina. Significant changes in distribution of distances were calculated with the χ^2 test; ***, $P < .001$; ****, $P < .0001$. Representative microscope images on the left indicate differential nuclear positioning of Ig loci in the 3 precursor-B-cell populations.

Long-range interactions within *Igκ* were found in pre-pro-B, pro-B and pre-B cells. In contrast to pre-pro-B and pro-B cells, these interactions were more dispersed in pre-B cells, showing fewer hotspots with high interaction frequencies (**Figure 3E-F**) Taken together, both *Igh* and *Igκ* loci were associated with locus contraction in committed B-lineage cells indicating that locus contraction as such does not correlate with the developmental regulation of Ig locus assembly.

Nuclear positioning is associated with stage-specific induction of Ig gene rearrangements

To study whether the nuclear positioning of Ig loci orchestrates the stepwise Ig gene rearrangements, we analyzed spatial distances between the *Igh* and *Igκ* loci and the nuclear lamina using 3D DNA FISH. The *Igh* locus was preferentially positioned at the nuclear periphery in uncommitted E2A^{-/-} pre-pro-B cells, and became more centrally positioned in Rag1^{-/-} pro-B cells (**Figure 4A**). Importantly, the *Igh* alleles were positioned back to the nuclear lamina compartments in Rag1^{-/-} Igu pre-B cells. On the other hand, *Igκ* was located at the nuclear periphery in both pre-pro-B and pro-B cells, and only in pre-B cells *Igκ* was located in the center (**Figure 4B**). The re-positioning involved both Ig loci in each cell as shown by independent analysis of the most lamina-proximal and lamina-distal loci (Figure S4A-B). The stage-specific positioning did not appear to involve the iEκ: the *Igκ* allele with the iEμR knock-in was also located at the nuclear lamina in pro-B cells, and the *Igκ* alleles with κE1/E2^{mut} were not fully retained at the nuclear periphery in pre-B cells (Figures S5 and S6). Thus, the Ig locus positioning in the nucleus, rather than the large-scale contractions, is directly associated with the sequential rearrangement of the Ig loci.

Positioning away from the nuclear lamina increases germline Ig loci transcription

To study whether the nuclear re-positioning was related to the changes in transcriptional activity, we investigated the nuclear localization of *Igh* and *Igκ* in E2A^{-/-} pre-pro-B cells treated with histone deacetylase inhibitor trichostatin A (TSA). TSA was previously shown to modulate gene localization at the nuclear periphery by disturbing the interactions of LAD-derived sequences with the nuclear lamina.^{41, 42} As a read out for locus accessibility, germline transcription from the Ig loci was assessed. From previously generated microarray studies^{29, 30} and with RQ-PCR, we analyzed *Igh* and *Igκ* germline transcripts. In line with established concepts, we found high expression of *Igh* germline transcripts in Rag1^{-/-} pro-B cells, while *Igκ* germline transcripts were high in Rag1^{-/-}VH81X pre-B cells (**Figure 5A-C** and Table S2).

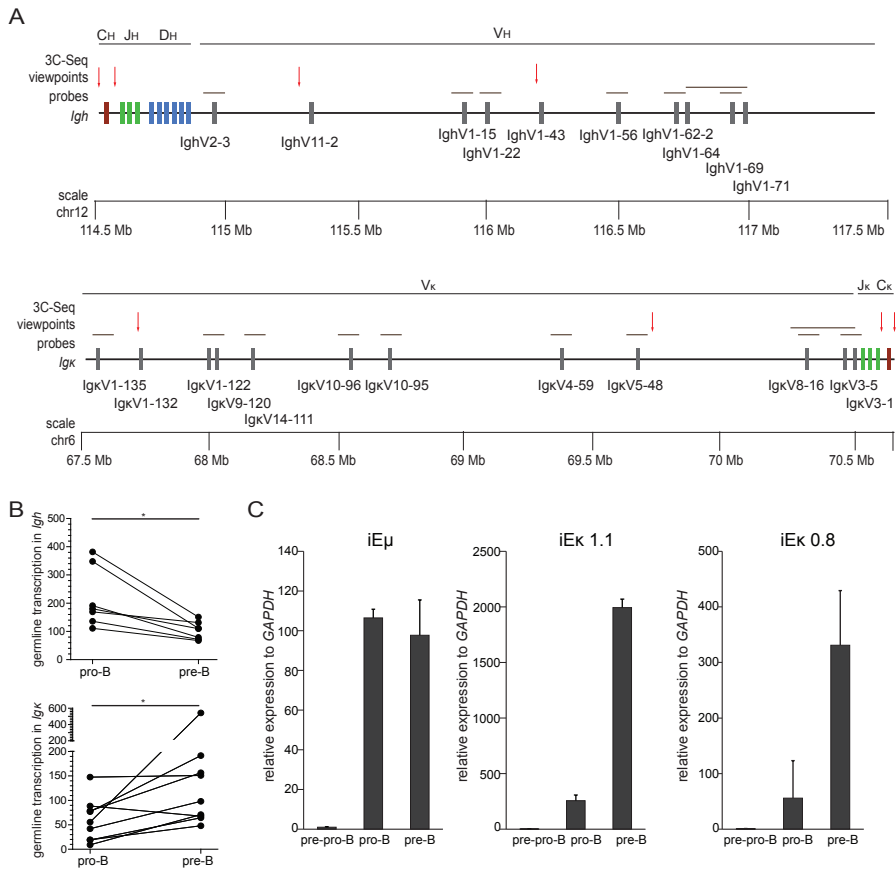


Figure 5. Developmentally regulated germline transcription of Ig loci. (A) Schematic representation of *Igh* (top panel) and *Igk* (bottom panel) loci with indicated positions of certain V (grey rectangles), D (blue rectangles), J (green rectangles) and C genes (purple rectangles). In addition, the positions of microarray probes (grey horizontal lines) for detection of germline transcripts, and 3C-Seq viewpoints (red arrows) are depicted. (B) Graphs represent germline transcripts in *Igh* and *Igk* paired between $Rag1^{-/-}$ pro-B and $Rag1^{-/-}$ VH81X pre-B cells. Data was derived from previously generated expression profiles (Table S2 and ^{29,30}) and significance was calculated with the Mann-Whitney U test; *, $P < 0.05$. (C) Germline transcript levels of *iEμ* and *iEκ* as assessed in $E2A^{-/-}$ pre-pro-B, $Rag1^{-/-}$ pro-B and $Rag1^{-/-}$ VH81X pre-B with RQ-PCR in 2 independent cultures. Bars represent average with SD. Gene expression levels were normalized to the levels of *GAPDH*, and the values in $E2A^{-/-}$ pre-pro-B cells were set to 1.

Following 10hr incubation of $E2A^{-/-}$ pre-pro-B cells with TSA, spatial distances between the C_H and C_K probes, and the nuclear lamina were measured by 3D DNA FISH. Indeed, incubation with TSA resulted in positioning of both *Igh* and *Igk* away from the nuclear lamina in these uncommitted early precursor cells (Figure 6A-C). This movement was associated directly with increased expression of germline transcription of both the *Igh* and *Igk* loci (Figure 6D-E).

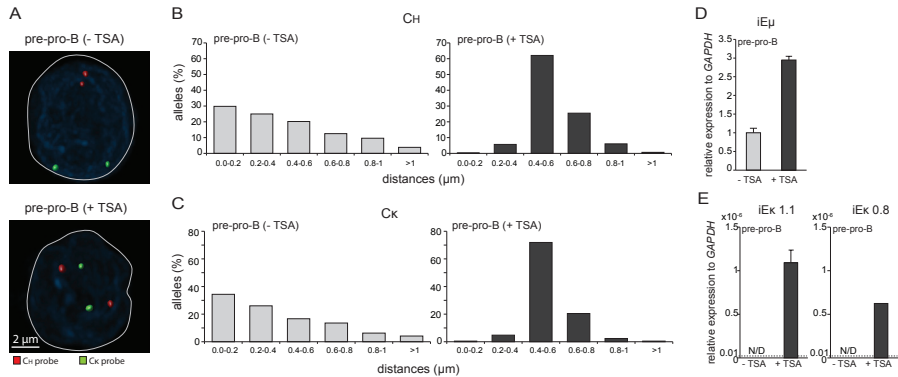


Figure 6. Positioning away from the nuclear lamina increases germline transcription of *Igh* and *Igk*. (A) Representative microscopy images indicate differential nuclear positioning of *Igh* (red) and *Igk* (green) loci in *E2A*^{-/-} pre-pro-B-cells cultured with (+) or without (-) TSA. Bar graphs showing the frequencies of (B) CH regions and (C) *Ck* regions positioned within a distance range from the nuclear lamina in *E2A*^{-/-} pre-pro-B cultured with (+) or without (-) TSA. >100 alleles were acquired for each condition. Germline transcript levels of (D) *iEμ* and (E) *iEκ* as assessed with RQ-PCR in 2 independent cultures. Bars represent average with SD. ND, not detectable. Dashed lines indicate the detection limit at cycle-threshold 40.

Taken together, these data indicate that large-scale contraction of Ig loci facilitates equal utilization of V genes during Ig gene rearrangements. However, it is the spatial positioning in the nucleus that orchestrates the Ig loci accessibility for V(D)J recombination machinery and thereby directs the sequential nature of Ig gene rearrangements in precursor-B cells (**model in Figure 7**).

DISCUSSION

We studied locus contraction, long-range chromatin interactions and nuclear positioning of the germline *Igh* and *Igk* alleles in three consecutive progenitor-B-cell subsets with 3D DNA FISH and 3C-Seq. This integrated approach enabled us to identify that both Ig loci were already contracted in the earliest committed pro-B-cell stage and retained this configuration in pre-B cells. In contrast, positioning away from the nuclear lamina was tightly regulated for *Igh* in pro-B cells and for *Igk* in pre-B cells, and correlated with germline transcription. Thus, nuclear localization rather than Ig locus topology is closely linked with the developmental regulation of *Igh* and *Igk* locus assembly.

In line with previous observations, we observed contraction of *Igh* in pro-B cells as compared to pre-pro-B cells.²⁵⁻²⁷ However, contrasting a previous study using wild type precursor-B-cells,²⁶ our Rag-deficient cells kept the *Igh* locus contracted in pre-B cells. The absence of functional Rag in our system creates an artificial situation, because no DNA

breaks are induced that could affect gene expression programs in the progenitor-B cells.⁴³ Still, the immunophenotypes of our Rag-deficient pro-B and pre-B cells were normal, as was the stage-specific upregulation of *Igh* and *Igk* germline transcripts. Rag-proficient pre-B cells will carry rearranged Ig genes with unknown spans of excised DNA. Moreover, FISH signals could be derived from excision products. Therefore, a model with *Igh* and *Igk* in germline configuration is best-suited to study their 3D structural organization.

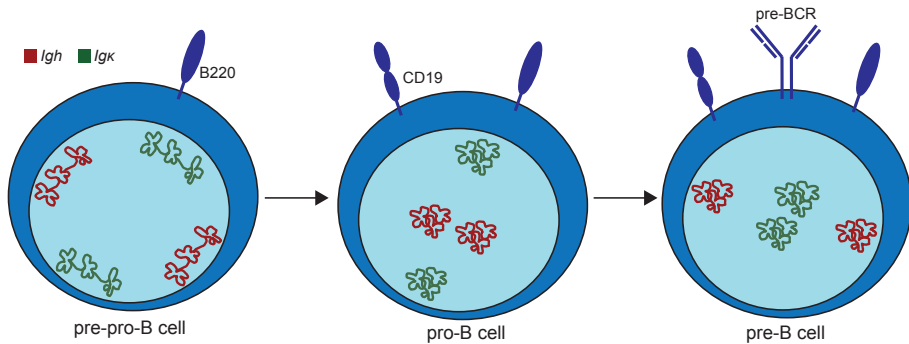


Figure 7. A model for nuclear positioning of *Igh* and *Igk* loci during B-cell development. Nuclei in pre-pro-B, pro-B and pre-B cells are indicated with schematic drawing of differentially positioned *Igh* (red) and *Igk* (green) loci. Both Ig loci were already contracted in the earliest committed pro-B-cell stage and retained this configuration in pre-B cells. In contrast, positioning away from the nuclear lamina was tightly regulated for *Igh* in pro-B cells and for *Igk* in pre-B cells. Thus, nuclear localization rather than Ig locus topology is closely linked with the developmental regulation of *Igh* and *Igk* locus assembly.

Similar to *Igh*, we observed that *Igk* was already contracted in pro-B cells.^{28, 29} This contraction, as well as abundant intra-locus interactions have been described before.^{7, 21-23, 29-31, 44} The germline Ig loci on our studies retained *cis*-regulatory elements that potentially drive locus contraction. These include the intergenic control region 1 (IGCR1) downstream of the V_H region,^{22, 23} and the contracting element for recombination (Cer) located within the V_K - J_K intervening region.⁴⁵ These elements likely function similarly as the newly described regulatory elements between V and DJ region of the $TCR\beta$ locus to mediate locus topology.^{46, 47} Thus, by choosing Rag-deficient models we did not study a heterogeneous pool of cells with and without deletion of these intergenic elements. The main limitation is the retained presence of IGCR1 in *Igh* that might affect *Igh* locus contraction resulting in differences between rearranged and non-rearranged alleles.

The consistent Ig locus contraction is potentially mediated by the ubiquitously expressed CTCF and YY1, which mediate the global DNA folding,^{21, 31, 48-50} and the B-cell specific transcription factors E2A, EBF1, Pax5, Ikaros and PU.1, which likely further facilitate contraction.^{24, 31, 49, 51-53} This is supported by observations in CTCF^{-/-} pro-B cells

where the *Igh* locus was more compacted than in *E2A*^{-/-} pre-pro-B cells and only slightly decontracted as compared to wild type pro-B cells.²¹ Because these factors are highly expressed in both pro-B and pre-B cells (Table S3 and ²⁹), it is well-possible that they function similarly in both developmental stages to maintain the contracted conformation of the chromatin fiber. Importantly, our refined model for Ig locus organization supports a role for Ig locus contraction in efficient V(D)J recombination, but excludes a role in developmental regulation of Ig gene rearrangements.

We found that the *E2A*-binding sites in *iEκ* were unimportant for *Igκ* locus contraction, despite their role in *Igκ* gene rearrangements.^{38, 39} Previously, deletion of the *iEμ* and 3'RR enhancers in *Igh* were found to be redundant for contraction or long-range interactions in *Igh*.^{44, 54} This could imply that the enhancers in Ig loci are not involved in 3D structural organization, and mediate efficient V(D)J recombination through different means. Multiple DNA-binding proteins have been implicated in Ig locus contraction and they can bind to regulatory elements disseminated along the loci, such as PAIR elements within the *V_H* region.⁴⁹ CTCF binding to the *Cer* region within *Igκ* mediated the locus contraction.⁴⁵ Likely CTCF binding to *IGCR1* also established the *Igh* folding. Thus, the enhancers could be involved in contraction of wild type alleles, but the disruption of a single transcription factor binding site would only have a minor impact on large-scale chromatin contraction.

Although the decontracted *Igκ* locus in *E2A*^{-/-} pre-pro-B cells is not yet a target for V(D)J recombination,³¹ we found a large number of intra-locus interactions. Further analysis showed that these mostly involved fragments that did not contain *Vκ* genes. Thus, the extent of spatial decontraction in pre-pro-B cells still allowed physical contacts between chromatin domains within the Ig loci, and in fact enabled freedom for random interactions. Rather, spatial contraction in pro-B and pre-B cells restricted these interactions with a preference for DNA regions containing V genes, specifically for *Igκ* following pre-BCR signaling.²⁹

Stage-specific accessibility of *Igh* and *Igκ*, as measured by increased germline transcription, was associated with positioning of the loci away from the nuclear periphery specifically at the stage of increased germline transcription. Movement of *Igh* away from the nuclear lamina in pro-B cells has been observed before,¹⁹ but we are the first to show re-location towards the nuclear lamina in pre-B cells. Unexpectedly, our finding of *Igκ* positioning at the nuclear lamina in pro-B cells contradicts previous observations.¹⁹ This is potentially due to the fact that in these studies 2D FISH was performed and the nuclear lamina were not stained. Goldmit *et al.* found that of the centrally-located *Igκ* alleles in pre-B cells, one was silenced by association with heterochromatin, forming the basis of allelic exclusion.⁵⁵ In their studies, *Igκ* alleles in pro-B cells hardly associated with heterochromatin, most likely because they are associated with the nuclear lamina as observed

here. Thus, in pro-B cells *Igκ* is inaccessible at the nuclear lamina, and this is a different process from heterochromatic recruitment necessary for allelic exclusion.

The nuclear lamina were previously shown to act as a repository for transcriptionally inactive chromatin domains,^{16, 17} and repositioning of genes can occur at specific stages of cellular differentiation.^{9, 15, 16, 18} Increased acetylation of Ig loci due to histone deacetylase inhibitor TSA resulted in movement of Ig loci towards the nuclear interior in *E2A*^{-/-} pre-pro-B cells and increase of germline Ig transcription. This suggests that locus mobility and gene transcription stay in relation and are controlled by histone modifications. Recently, histone modifications were shown to direct V(D)J recombination.¹⁰ Specifically, Rag2 is recruited through binding to H3K4me3 histone marks.^{13, 14} These histone modifications were detected within the *Igh* locus in pro-B cells, and in *Igκ* in the pre-B cell stage.¹² It is conceivable that nuclear positioning towards the nuclear center enables the induction of H3K4me3 histone modifications. Alternatively, H3K4me3 histone modifications poise the Ig loci to migrate away from the nuclear lamina. A potential signal guiding histone modifications could be induced by IL-7. Recently, Mandal *et al.* showed that IL-7 signaling inhibited *Igκ* rearrangements in pro-B cells by recruiting STAT5 heterodimers to *iEκ*, which further induced Ezh2 methyltransferase and thereby silenced the *Igκ* locus through H3K27me3 modifications.⁵⁶ These modifications could keep *Igκ* positioned at the nuclear lamina, while subsequent attenuation of IL-7R signaling by Ikaros would then induce re-positioning of *Igκ* and enable induction of gene rearrangements.^{57, 58}

It still remains puzzling, however, which mechanisms control allelic exclusion of the second non-rearranged *Igh* locus in pre-B cells. We here used a model system with an Ig heavy chain transgene to study the locus organization and positioning of *Igh* alleles in the germline. As a result, all of our observations in pre-B cells concerned the relocation of non-functional *Igh* alleles towards the nuclear periphery and the down regulation of germline transcripts (Figure 4B, Figure E4A-B). Thus, repositioning of *Igh* towards nuclear lamina and away from transcription factories could be a potential mechanism to decrease the locus accessibility and mediate allelic exclusion. However, the question remains whether a functionally rearranged *Igh* locus with a genomically proximal V_H promoter and *iEμ* will also move towards the nuclear periphery or remain transcriptionally active in the nuclear center.⁵⁹ Addressing this issue would require a more complex model system with a functional *Igh* rearrangement on one allele and sufficient genomic markers to distinguish it from the other germline allele with DNA probes.

Taken together, our studies confirm that murine *Igh* and *Igκ* loci undergo contraction prior to gene rearrangement to allow juxtaposing of genomically distant gene segments in order to create equal opportunities for recombination. However, we here show that nuclear positioning is associated with germline transcription and the developmental regulation of *Igh* and *Igκ* locus assembly. These combined new insights are important for

future studies on the factors that regulate stepwise control of Ig gene rearrangements and indicate that these are likely to be controlled via nuclear positioning of Ig loci.

MATERIALS AND METHODS

Mice

Rag1^{-/-}, Rag2^{-/-}, VH81X transgenic, human IgM transgenic, κE1/E2^{mut} and EμR mice were obtained^{34-36, 38, 39, 60} and kept on a C57BL/6 background under specific pathogen-free conditions. Mice were euthanized at 5-13 weeks of age. The experiments were performed on pooled cells from 2-4 mice. Experimental procedures were reviewed and approved by the Erasmus University committee of animal experiments.

Cell culture and flow cytometry

CD19⁺ B cells were enriched from femoral bone marrow suspensions by magnetic separation (Miltenyi Biotec), and cultured for 2-3 weeks in Iscove's Modified Dulbecco's medium containing 10% fetal calf serum, 200 U/ml penicillin, 200 mg/ml streptomycin, 4nM L-glutamine, 50 μM β-mercaptoethanol, and 2 ng/mL of both IL-7 and SCF. E2A^{-/-} hematopoietic progenitors were grown as described previously.³³

Flow cytometric immunophenotyping of bone marrow suspensions and cultured progenitor cells was performed after staining with B220-PerCP-Cy5.5 (RA3-6B2), CD19-APC-Cy7 (1D3), CD43-APC (S7), CD2-PE (RM2-5; all from BD Biosciences) on an LSRII flow cytometer (BD Biosciences) and analyzed with BD FACSDiva Software.

Probe preparation and 3D DNA fluorescence in situ hybridization (FISH)

BAC clones CT7-526A21, RP23-24I12, CT7-34H6 for detecting regions in the murine *Igh* locus,²⁷ and RP23-234A12, RP24-475M8, RP23-435I4 recognizing regions within murine *Igk* locus (all from BACPAC Resources) were used as FISH probes. Probe labelling and DNA FISH were performed as described previously.^{27, 61, 62} Images were acquired on a Leica SP5 confocal microscope (Leica Microsystems), followed by deconvolution and analysis with Huygens Professional software (Scientific Volume Imaging).^{61,}

⁶² Details of the procedures are available in the supplementary Materials and Methods.

Circular chromosome conformation capture with high-throughput sequencing (3C-Seq)

3C libraries were prepared from cultured E2A^{-/-}, Rag1^{-/-} and Rag1^{-/-}VH81X B-cell progenitors and wild type fetal liver erythroid progenitors,^{29, 30, 37} and interactions were studied with 4 *Igh* and 4 *Igk* viewpoints (primers sequences are available in the Table S1). More details about the 3C-Seq procedure and data analysis can be found in the supplementary Materials and Methods. The high-throughput sequencing datasets have been submitted to the Sequence Read Archive (SRA), accession number: SRP055900.

Gene Expression profiling

The expression profiles of Rag1^{-/-} pro-B and Rag1^{-/-}VH81X pre-B cells were previously generated with Affymetrix Mouse Gene 1.0 ST Arrays,^{29, 30} and obtained from the Gene Expression Omnibus (GEO; accession number GSE53896).

Inhibition of histone deacetylase activity

For inhibition of histone deacetylase activity, E2A^{-/-} pre-pro-B cells were incubated at 37°C for 10hr with trichostatin A (TSA, Sigma-Aldrich) or DMSO at 3ng/ml (*Igh*) or 10ng/ml (*Igk*) concentration.^{41, 42} Next, 3D DNA FISH was performed with the Alexa-568-labeled CT7-34H6 probe (CH), Cy5-labeled RP23-43514 probe (CK) and MarinaBlue-labeled nuclear lamina. Germline transcripts from the iE μ and iE κ enhancers were quantified with a TaqMan-based RQ-PCR. More details are available in the supplementary Materials and Methods.

Statistics

Statistical significance was calculated with the non-parametric Mann-Whitney U test or the χ^2 test. The Mann-Whitney U test was used to analyze statistical significance between two groups of data following unknown (not normal) distribution, whereas χ^2 test was used to compare the distribution of two data sets of two groups. All statistical tests were performed using GraphPad Prism version 5.0. P values <0.05 were considered as significant.

ACKNOWLEDGEMENTS

We thank Gert van Cappellen and Gert-Jan Kremers (Optical Imaging Center, Erasmus MC) for support with confocal microscopy, Ralph Stadhouders (Cell Biology, Erasmus MC) for his help with 3C-Seq experiments and data analysis, Rutger Brouwer (Biomics, Erasmus MC) and Harmen van der Werken (Cell Biology, Erasmus MC) for their computational contribution, and Y. Xu for providing the $\kappa E1/E2^{mut}$ and E μ R mice. This study was performed in the department of Immunology as part of the Molecular Medicine Postgraduate School of the Erasmus MC. This work was supported by The Netherlands Organization for Health Research and Development ZonMW, Veni grant 916.116.090 to Menno C. van Zelm.

REFERENCES

1. Bossen, C., R. Mansson, and C. Murre. 2012. Chromatin Topology and the Regulation of Antigen Receptor Assembly. *Annu Rev Immunol* 30:337-356.
2. Jung, D., C. Giallourakis, R. Mostoslavsky, and F. W. Alt. 2006. Mechanism and control of V(D)J recombination at the immunoglobulin heavy chain locus. *Annu Rev Immunol* 24:541-570.
3. Curry, J. D., J. K. Geier, and M. S. Schlissel. 2005. Single-strand recombination signal sequence nicks in vivo: evidence for a capture model of synapsis. *Nat Immunol* 6:1272-1279.
4. Gellert, M. 2002. V(D)J recombination: RAG proteins, repair factors, and regulation. *Annu Rev Biochem* 71:101-132.
5. Cobb, R. M., K. J. Oestreich, O. A. Osipovich, and E. M. Oltz. 2006. Accessibility control of V(D)J recombination. *Adv Immunol* 91:45-109.
6. Yancopoulos, G. D., and F. W. Alt. 1985. Developmentally Controlled and Tissue-Specific Expression of Unrearranged Vh Gene Segments. *Cell* 40:271-281.
7. Verma-Gaur, J., A. Torkamani, L. Schaffer, S. R. Head, N. J. Schork, and A. J. Feeney. 2012. Noncoding transcription within the Igh distal V-H region at PAIR elements affects the 3D structure of the Igh locus in pro-B cells. *P Natl Acad Sci USA* 109:17004-17009.
8. Gilbert, N., S. Boyle, H. Fiegler, K. Woodfine, N. P. Carter, and W. A. Bickmore. 2004. Chromatin architecture of the human genome: Gene-rich domains are enriched in open chromatin fibers. *Cell* 118:555-566.
9. Schneider, R., and R. Grosschedl. 2007. Dynamics and interplay of nuclear architecture, genome organization, and gene expression. *Gene Dev* 21:3027-3043.
10. Xu, C. R., and A. J. Feeney. 2009. The Epigenetic Profile of Ig Genes Is Dynamically Regulated during B Cell Differentiation and Is Modulated by Pre-B Cell Receptor Signaling. *Journal of Immunology* 182:1362-1369.

11. Choi, N. M., S. Loguercio, J. Verma-Gaur, S. C. Degner, A. Torkamani, A. I. Su, E. M. Oltz, M. Artyomov, and A. J. Feeney. 2013. Deep Sequencing of the Murine Igh Repertoire Reveals Complex Regulation of Nonrandom V Gene Rearrangement Frequencies. *Journal of Immunology* 191:2393-2402.
12. Ji, Y., W. Resch, E. Corbett, A. Yamane, R. Casellas, and D. G. Schatz. 2010. The in vivo pattern of binding of RAG1 and RAG2 to antigen receptor loci. *Cell* 141:419-431.
13. Liu, Y., R. Subrahmanyam, T. Chakraborty, R. Sen, and S. Desiderio. 2007. A plant homeodomain in Rag-2 that binds hypermethylated lysine 4 of histone H3 is necessary for efficient antigen-receptor-gene rearrangement. *Immunity* 27:561-571.
14. Matthews, A. G. W., A. J. Kuo, S. Ramon-Maiques, S. M. Han, K. S. Champagne, D. Ivanov, M. Gallardo, D. Carney, P. Cheung, D. N. Ciccone, K. L. Walter, P. J. Utz, Y. Shi, T. G. Kutateladze, W. Yang, O. Gozani, and M. A. Oettinger. 2007. RAG2 PHD finger couples histone H3 lysine 4 trimethylation with V(D)J recombination. *Nature* 450:1106-U1118.
15. Osborne, C. S., L. Chakalova, K. E. Brown, D. Carter, A. Horton, E. Debrand, B. Goyenechea, J. A. Mitchell, S. Lopes, W. Reik, and P. Fraser. 2004. Active genes dynamically colocalize to shared sites of ongoing transcription. *Nature Genetics* 36:1065-1071.
16. Peric-Hupkes, D., W. Meuleman, L. Pagie, S. W. Bruggeman, I. Solovei, W. Brugman, S. Graf, P. Flicek, R. M. Kerkhoven, M. van Lohuizen, M. Reinders, L. Wessels, and B. van Steensel. 2010. Molecular maps of the reorganization of genome-nuclear lamina interactions during differentiation. *Mol Cell* 38:603-613.
17. Reddy, K. L., J. M. Zullo, E. Bertolino, and H. Singh. 2008. Transcriptional repression mediated by repositioning of genes to the nuclear lamina. *Nature* 452:243-247.
18. Simonis, M., P. Klous, E. Splinter, Y. Moshkin, R. Willemsen, E. de Wit, B. van Steensel, and W. de Laat. 2006. Nuclear organization of active and inactive chromatin domains uncovered by chromosome conformation capture-on-chip (4C). *Nature Genetics* 38:1348-1354.
19. Kosak, S. T., J. A. Skok, K. L. Medina, R. Riblet, M. M. Le Beau, A. G. Fisher, and H. Singh. 2002. Subnuclear compartmentalization of immunoglobulin loci during lymphocyte development. *Science* 296:158-162.
20. Skok, J. A., K. E. Brown, V. Azuara, M. L. Caparros, J. Baxter, K. Takacs, N. Dillon, D. Gray, R. P. Perry, M. Merckenschlager, and A. G. Fisher. 2001. Nonequivalent nuclear location of immunoglobulin alleles in B lymphocytes. *Nat Immunol* 2:848-854.
21. Degner, S. C., J. Verma-Gaur, T. P. Wong, C. Bossen, G. M. Iverson, A. Torkamani, C. Vettermann, Y. C. Lin, Z. Ju, D. Schulz, C. S. Murre, B. K. Birshstein, N. J. Schork, M. S. Schlissel, R. Riblet, C. Murre, and A. J. Feeney. 2011. CCCTC-binding factor (CTCF) and cohesin influence the genomic architecture of the Igh locus and antisense transcription in pro-B cells. *Proc Natl Acad Sci U S A* 108:9566-9571.
22. Guo, C., T. Gerasimova, H. Hao, I. Ivanova, T. Chakraborty, R. Selimyan, E. M. Oltz, and R. Sen. 2011. Two forms of loops generate the chromatin conformation of the immunoglobulin heavy-chain gene locus. *Cell* 147:332-343.
23. Guo, C., H. S. Yoon, A. Franklin, S. Jain, A. Ebert, H. L. Cheng, E. Hansen, O. Despo, C. Bossen, C. Vettermann, J. G. Bates, N. Richards, D. Myers, H. Patel, M. Gallagher, M. S. Schlissel, C. Murre, M.

- Busslinger, C. C. Giallourakis, and F. W. Alt. 2011. CTCF-binding elements mediate control of V(D)J recombination. *Nature* 477:424-430.
24. Fuxa, M., J. Skok, A. Souabni, G. Salvagiotto, E. Roldan, and M. Busslinger. 2004. Pax5 induces V-to-DJ rearrangements and locus contraction of the immunoglobulin heavy-chain gene. *Genes Dev* 18:411-422.
25. Jhunjhunwala, S., M. C. van Zelm, M. M. Peak, S. Cutchin, R. Riblet, J. J. van Dongen, F. G. Grosveld, T. A. Knoch, and C. Murre. 2008. The 3D structure of the immunoglobulin heavy-chain locus: implications for long-range genomic interactions. *Cell* 133:265-279.
26. Roldan, E., M. Fuxa, W. Chong, D. Martinez, M. Novatchkova, M. Busslinger, and J. A. Skok. 2005. Locus 'decontraction' and centromeric recruitment contribute to allelic exclusion of the immunoglobulin heavy-chain gene. *Nat Immunol* 6:31-41.
27. Sayegh, C. E., S. Jhunjhunwala, R. Riblet, and C. Murre. 2005. Visualization of looping involving the immunoglobulin heavy-chain locus in developing B cells. *Genes Dev* 19:322-327.
28. Fitzsimmons, S. P., R. M. Bernstein, E. E. Max, J. A. Skok, and M. A. Shapiro. 2007. Dynamic changes in accessibility, nuclear positioning, recombination, and transcription at the Ig kappa locus. *Journal of Immunology* 179:5264-5273.
29. Stadhouders, R., M. J. de Bruijn, M. B. Rother, S. Yuvaraj, C. Ribeiro de Almeida, P. Kolovos, M. C. Van Zelm, W. van Ijcken, F. Grosveld, E. Soler, and R. W. Hendriks. 2014. Pre-B Cell Receptor Signaling Induces Immunoglobulin kappa Locus Accessibility by Functional Redistribution of Enhancer-Mediated Chromatin Interactions. *PLoS Biol* 12:e1001791.
30. Ribeiro de Almeida, C., R. Stadhouders, M. J. de Bruijn, I. M. Bergen, S. Thongiuca, B. Lenhard, W. van Ijcken, F. Grosveld, N. Galjart, E. Soler, and R. W. Hendriks. 2011. The DNA-binding protein CTCF limits proximal V kappa recombination and restricts kappa enhancer interactions to the immunoglobulin kappa light chain locus. *Immunity* 35:501-513.
31. Lin, Y. C., C. Benner, R. Mansson, S. Heinz, K. Miyazaki, M. Miyazaki, V. Chandra, C. Bossen, C. K. Glass, and C. Murre. 2012. Global changes in the nuclear positioning of genes and intra- and interdomain genomic interactions that orchestrate B cell fate. *Nat Immunol* 13:1196-1204.
32. Novobrantseva, T. I., V. M. Martin, R. Pelanda, W. Muller, K. Rajewsky, and A. Ehlich. 1999. Rearrangement and expression of immunoglobulin light chain genes can precede heavy chain expression during normal B cell development in mice (vol 189, pg 75, 1999). *Journal of Experimental Medicine* 189:1361-1361.
33. Ikawa, T., H. Kawamoto, L. Y. Wright, and C. Murre. 2004. Long-term cultured E2A-deficient hematopoietic progenitor cells are pluripotent. *Immunity* 20:349-360.
34. Mombaerts, P., J. Iacomini, R. S. Johnson, K. Herrup, S. Tonegawa, and V. E. Papaioannou. 1992. Rag-1-Deficient Mice Have No Mature Lymphocytes-B and Lymphocytes-T. *Cell* 68:869-877.
35. Martin, F., X. Chen, and J. F. Kearney. 1997. Development of VH81X transgene-bearing B cells in fetus and adult: sites for expansion and deletion in conventional and CD5/B1 cells. *Int Immunol* 9:493-505.

36. Nussenzweig, M. C., A. C. Shaw, E. Sinn, D. B. Danner, K. L. Holmes, H. C. Morse, 3rd, and P. Leder. 1987. Allelic exclusion in transgenic mice that express the membrane form of immunoglobulin mu. *Science* 236:816-819.
37. Stadhouders, R., P. Kolovos, R. Brouwer, J. Zuin, A. van den Heuvel, C. Kockx, R. J. Palstra, K. S. Wendt, F. Grosveld, W. van Ijcken, and E. Soler. 2013. Multiplexed chromosome conformation capture sequencing for rapid genome-scale high-resolution detection of long-range chromatin interactions. *Nat Protoc* 8:509-524.
38. Inlay, M. A., H. Tian, T. X. Lin, and Y. Xu. 2004. Important roles for E protein binding sites within the immunoglobulin kappa chain intronic enhancer in activating V(kappa)J(kappa) rearrangement. *Journal of Experimental Medicine* 200:1205-1211.
39. Inlay, M. A., T. X. Lin, H. H. Gao, and Y. Xu. 2006. Critical roles of the immunoglobulin intronic enhancers in maintaining the sequential rearrangement of IgH and Igk loci. *Journal of Experimental Medicine* 203:1721-1732.
40. Dixon, J. R., S. Selvaraj, F. Yue, A. Kim, Y. Li, Y. Shen, M. Hu, J. S. Liu, and B. Ren. 2012. Topological domains in mammalian genomes identified by analysis of chromatin interactions. *Nature* 485:376-380.
41. Zink, D., M. D. Amaral, A. Englmann, S. Lang, L. A. Clarke, C. Rudolph, F. Alt, K. Luther, C. Braz, N. Sadoni, J. Rosenecker, and D. Schindelbauer. 2004. Transcription-dependent spatial arrangements of CFTR and adjacent genes in human cell nuclei. *J Cell Biol* 166:815-825.
42. Zullo, J. M., I. A. Demarco, R. Pique-Regi, D. J. Gaffney, C. B. Epstein, C. J. Spooner, T. R. Luperchio, B. E. Bernstein, J. K. Pritchard, K. L. Reddy, and H. Singh. 2012. DNA sequence-dependent compartmentalization and silencing of chromatin at the nuclear lamina. *Cell* 149:1474-1487.
43. Bredemeyer, A. L., B. A. Helmink, C. L. Innes, B. Calderon, L. M. McGinnis, G. K. Mahowald, E. J. Gapud, L. M. Walker, J. B. Collins, B. K. Weaver, L. Mandik-Nayak, R. D. Schreiber, P. M. Allen, M. J. May, R. S. Paules, C. H. Bassing, and B. P. Sleckman. 2008. DNA double-strand breaks activate a multi-functional genetic program in developing lymphocytes. *Nature* 456:819-823.
44. Medvedovic, J., A. Ebert, H. Tagoh, I. M. Tamir, T. A. Schwickert, M. Novatchkova, Q. Sun, P. J. Huis In 't Veld, C. Guo, H. S. Yoon, Y. Denizot, S. J. Holwerda, W. de Laat, M. Cogne, Y. Shi, F. W. Alt, and M. Busslinger. 2013. Flexible long-range loops in the VH gene region of the Igh locus facilitate the generation of a diverse antibody repertoire. *Immunity* 39:229-244.
45. Xiang, Y., S. K. Park, and W. T. Garrard. 2013. V kappa gene repertoire and locus contraction are specified by critical DNase I hypersensitive sites within the V kappa-J kappa intervening region. *J Immunol* 190:1819-1826.
46. Majumder, K., O. I. Koues, E. A. Chan, K. E. Kyle, J. E. Horowitz, K. Yang-Iott, C. H. Bassing, I. Taniuchi, M. S. Krangel, and E. M. Oltz. 2015. Lineage-specific compaction of Tcrb requires a chromatin barrier to protect the function of a long-range tethering element. *J Exp Med* 212:107-120.
47. Murre, C. 2015. Ensuring an equal playing field for antigen receptor loci variable regions. *J Exp Med* 212:2.

48. Degner, S. C., T. P. Wong, G. Jankevicius, and A. J. Feeney. 2009. Cutting edge: developmental stage-specific recruitment of cohesin to CTCF sites throughout immunoglobulin loci during B lymphocyte development. *J Immunol* 182:44-48.
49. Ebert, A., S. McManus, H. Tagoh, J. Medvedovic, G. Salvaggio, M. Novatchkova, I. Tamir, A. Sommer, M. Jaritz, and M. Busslinger. 2011. The distal V(H) gene cluster of the Igh locus contains distinct regulatory elements with Pax5 transcription factor-dependent activity in pro-B cells. *Immunity* 34:175-187.
50. Liu, H., M. Schmidt-Suppran, Y. Shi, E. Hobeika, N. Barteneva, H. Jumaa, R. Pelanda, M. Reth, J. Skok, and K. Rajewsky. 2007. Yin Yang 1 is a critical regulator of B-cell development. *Genes Dev* 21:1179-1189.
51. Bain, G., E. C. Maandag, D. J. Izon, D. Amsen, A. M. Kruisbeek, B. C. Weintraub, I. Krop, M. S. Schlissel, A. J. Feeney, M. van Roon, and et al. 1994. E2A proteins are required for proper B cell development and initiation of immunoglobulin gene rearrangements. *Cell* 79:885-892.
52. Lin, H., and R. Grosschedl. 1995. Failure of B-cell differentiation in mice lacking the transcription factor EBF. *Nature* 376:263-267.
53. Reynaud, D., I. A. Demarco, K. L. Reddy, H. Schjerven, E. Bertolino, Z. S. Chen, S. T. Smale, S. Winandy, and H. Singh. 2008. Regulation of B cell fate commitment and immunoglobulin heavy-chain gene rearrangements by Ikaros. *Nature Immunology* 9:927-936.
54. Perlot, T., F. W. Alt, C. H. Bassing, H. Suh, and E. Pinaud. 2005. Elucidation of IgH intronic enhancer functions via germ-line deletion. *Proc Natl Acad Sci U S A* 102:14362-14367.
55. Goldmit, M., Y. Ji, J. Skok, E. Roldan, S. Jung, H. Cedar, and Y. Bergman. 2005. Epigenetic ontogeny of the Igh locus during B cell development. *Nat Immunol* 6:198-203.
56. Mandal, M., S. E. Powers, M. Maienschein-Cline, E. T. Bartom, K. M. Hamel, B. L. Kee, A. R. Dinner, and M. R. Clark. 2011. Epigenetic repression of the Igh locus by STAT5-mediated recruitment of the histone methyltransferase Ezh2. *Nat Immunol* 12:1212-1220.
57. Heizmann, B., P. Kastner, and S. Chan. 2013. Ikaros is absolutely required for pre-B cell differentiation by attenuating IL-7 signals. *Journal of Experimental Medicine* 210:2823-2832.
58. Schwickert, T. A., H. Tagoh, S. Gultekin, A. Dakic, E. Axelsson, M. Minnich, A. Ebert, B. Werner, M. Roth, L. Cimmino, R. A. Dickins, J. Zuber, M. Jaritz, and M. Busslinger. 2014. Stage-specific control of early B cell development by the transcription factor Ikaros. *Nat Immunol* 15:283-293.
59. Holwerda, S. J., H. J. van de Werken, C. Ribeiro de Almeida, I. M. Bergen, M. J. de Bruijn, M. J. Verstegen, M. Simonis, E. Splinter, P. J. Wijchers, R. W. Hendriks, and W. de Laat. 2013. Allelic exclusion of the immunoglobulin heavy chain locus is independent of its nuclear localization in mature B cells. *Nucleic Acids Res* 41:6905-6916.
60. Hao, Z. Y., and K. Rajewsky. 2001. Homeostasis of peripheral B cells in the absence of B cell influx from the bone marrow. *Journal of Experimental Medicine* 194:1151-1163.
61. Jensen, K., M. B. Rother, B. S. Brusletto, O. K. Olstad, H. C. D. Aass, M. C. van Zelm, P. Kierulf, and K. M. Gautvik. 2013. Increased ID2 Levels in Adult Precursor B Cells as Compared with Children Is Associated with Impaired Ig Locus Contraction and Decreased Bone Marrow Output. *J Immunol* 191:1210-1219.

62. Nodland, S. E., M. A. Berkowska, A. A. Bajer, N. Shah, D. de Ridder, J. J. van Dongen, T. W. LeBien, and M. C. van Zelm. 2011. IL-7R expression and IL-7 signaling confer a distinct phenotype on developing human B-lineage cells. *Blood* 118:2116-2127.
63. Hardy, R. R., and K. Hayakawa. 2001. B cell development pathways. *Annu Rev Immunol* 19:595-621.



Chapter IV

Increased ID2 levels in adult precursor-B cells as compared with children is associated with impaired Ig locus contraction and decreased bone marrow output

Kristin Jensen^{1,2}, Magdalena B. Rother³, Berit Sletbakk Brusletto¹, Ole K. Olstad¹, Hans Christian Dalsbotten Aass¹, Menno C. van Zelm³, Peter Kierulf¹, and Kaare M. Gautvik^{1,4}

(1) Department of Medical Biochemistry, (2) Department of Pediatrics, Oslo University Hospital, 0407 Oslo, Norway (3) Department of Immunology, Erasmus MC, University Medical Center, Rotterdam, The Netherlands, and (4) Institute of Basic Medical Sciences, University of Oslo, 0407 Oslo, Norway

Manuscript published in *J Immunol* 2013; 191:1210-1219

The online version of this article contains the supplemental material.

ABSTRACT

Precursor-B-cell production from bone marrow (BM) in mice and humans declines with age. Because the mechanisms behind are still unknown, we studied 5 precursor-B-cell subsets (pro-B, pre-BI, pre-BII large, pre-BII small, immature-B) and their differentiation-stage characteristic gene expression profiles in healthy individual toddlers and middle-aged adults. Notably, the composition of the precursor-B-cell compartment did not change with age. The expression levels of several transcripts encoding V(D)J recombination factors were decreased in adults as compared to children: RAG1 expression was significantly reduced in pro-B cells, and DNA-PKcs, Ku80 and XRCC4 were decreased in pre-BI cells. In contrast, TdT was 3-fold up-regulated in immature-B cells of adults. Still, N-nucleotides, P-nucleotides and deletions were similar for *IGH* and *IGK* junctions between children and adults. Pre-BII large cells in adults, but not in children, showed highly up-regulated expression of the differentiation inhibitor ID2, in absence of changes in expression of the ID2-binding partner E2A. We here identified impaired Ig locus contraction in adult precursor-B cells as a likely mechanism by which ID2-mediated blocking of E2A function results in reduced BM B-cell output in adults. The reduced B-cell production was not compensated by increased proliferation in adult immature-B cells, despite increased Ki67 expression. These findings demonstrate distinct regulatory mechanisms in B-cell differentiation between adults and children with a central role for transcriptional regulation of ID2.

INTRODUCTION

Commitment and differentiation of early precursor-B cells to immunoglobulin (Ig) producing B lymphocytes is a key requirement for a competent adaptive immune system. Each differentiation step is tightly controlled by integrated activities of multiple transcription factors in a complex gene regulatory network.¹ In fact, a handful of key transcription factors is used in multiple contexts and distinct combinations to initiate and maintain the commitment process throughout the lifespan of the B cell.²

Production of B lymphocytes from bone marrow (BM) continues throughout life. Similar to T lymphocytes,³ the precursor-B cell pool is decreasing with age in both man^{4,5} and mice,⁶⁻⁸ whereas the production of other hematopoietic lineages seems to continue unchanged.⁹ With advancing age, the capacity to induce protective antibody responses decreases, leading to reduced ability to deal with new and previously encountered pathogens.¹⁰ Some studies in mice suggest that the impact of aging on lymphoid progenitors is first manifested in hematopoietic stem cells (HSCs).^{11,12} Other studies link the waning B-cell production in mice to the inability of immature-B cells to replenish the peripheral

compartments,⁶ to decreased transition of pro-B cells into pre-B cells^{6,13} and/or to micro-environmental changes causing altered Ig gene rearrangements.^{14,15} The question has also been raised whether specific transcriptionally regulated mechanisms obstruct B-cell generation with age, such as changes in expression of ID2 (inhibitor of DNA binding 2)¹⁶⁻²⁰ – a physiological regulator of the essential transcription factor E2A. E2A protein levels in mice have been reported to decrease with age,¹⁷ but thus far, no age-related changes were found for ID2 protein using *in vitro* expanded pro-B/early pre-B cells from aged and young mice.¹⁶

In contrast to mouse studies, the effects of aging on human precursor-B-cell development have been scarcely studied so far. Global gene expression has only been studied in successive maturation stages of precursor-B cells in children²¹ and adults,²² separately. We have previously reported that the total pool of precursor-B cells in human BM decreased rapidly during the first two years of life concomitantly with reduced expression of RAG1.⁵ Still, these studies were unable to address the issue of decreased BM output of B cells. Therefore, we analyzed precursor B cell subsets and their gene expression profiles in BM from healthy young children and adults. Through differentiation-stage dependent analysis of 5 precursor-B-cell subsets and pair wise comparisons between children and adults, we identified several mechanisms that suggest tighter checkpoint control in adult precursor-B cells.

RESULTS

The relative distribution of precursor-B cells in BM does not change with age

Within the total leukocyte populations in BM from children and adults, we found considerable variations in lymphocyte frequencies, but no age-related differences (mean \pm 2SD): adults 49.7% \pm 8.9, and children 41.3% \pm 16.6, respectively. In contrast, the absolute number of isolated BM restricted CD10⁺ cells (mean \pm 2SD) was significantly higher ($p < 10^{-5}$) in children ($8.2 \times 10^6/\text{ml} \pm 1.2 \times 10^6/\text{ml}$) than in adults ($2.7 \times 10^6/\text{ml} \pm 2.2 \times 10^6/\text{ml}$).

To study whether the decrease in adults was due to impaired B-cell differentiation, we analyzed progenitor-B-cell subsets using a panel of 7 membrane markers (**Figure 1A-B**). The relative sizes of the five major subsets, pro-B, pre-BI, pre-BII large, pre-BII small and immature-B cells, varied individually, but was not related to age (**Figure 1C**). About 20% of the compartment consisted of the early CD34⁺ pro-B and pre-BI progenitor cells, whereas pre-BII large and small cells were dominating (~70%). Immature-B cells

constituted about 12%. This indicates a seemingly similar profile of precursor-B-cell differentiation with age.

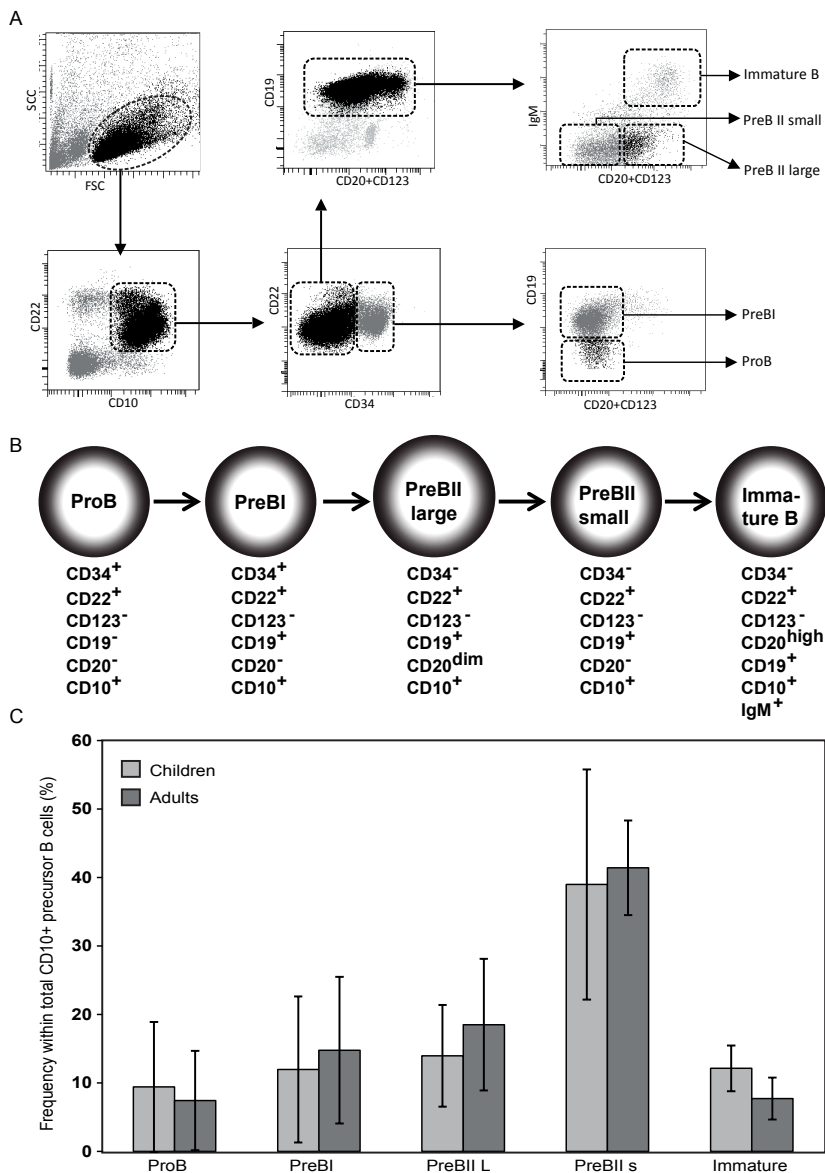


Figure 1. Precursor-B-cell subset definition and distribution in childhood and adult bone marrow. (A) Sort strategy to define five precursor-B-cell subsets from CD10⁺-enriched BM cells according to van Zelm *et al.* 2005.²¹ (B) Nomenclature and membrane marker definition of the five precursor-B-cell subsets. (C) Distribution of precursor-B-cell subsets in bone marrow. Shown are frequencies within the total CD10⁺ precursor-B-cell compartment (mean ± SD) obtained from 4 children and 4 adults.

Stage-dependent global mRNA expression in precursor-B cells from children and adults

To study whether transcriptional regulation of precursor-B-cell differentiation was affected by age, we analyzed the gene expression profiles of all 5 precursor-B-cell stages in 4 children and 4 adults. First, differences in gene expression levels were determined per cell stage in children and adults separately using cut off p-value < 0.05 and fold change > ± 2 (Table S2). Between pro-B and pre-BI, pre-BI and pre-BII large, pre-BII large and pre-BII small, and pre-BII small and immature-B, respectively, a total of 141, 279, 31, 697 transcripts had an ANOVA p-value less than 0.05 in children (**Figure 2**). These 0.2–4.4 % of the transcripts describe the differentiation processes from one stage to the next. Corresponding numbers in adults were 294, 683, 174, and 525, representing 1.9 %, 4.3 %, 1.1 % and 3.3 %, of all transcripts present on the array, respectively. Therefore, the total number of transcripts changing expression during differentiation from pro-B to pre-BI, pre-BI to pre-BII large and further to pre-BII small were about 2–5 fold higher in adults than in children. Only in the last passage from pre-BII small to immature-B, about 25% more transcripts were differentially expressed in children than in adults.

A striking difference was up-regulation of 529 transcripts in the pre-BI to pre-BII large transition in adults versus 111 transcripts in children. Of these, about 1/6 of the transcripts in adults and 2/3 of the transcripts in children were shared. The other cell transitions involved a more equal number of up-regulated transcripts with age (**Figure 2A**). The number of down-regulated transcripts also showed marked age-related differences (**Figure 2B**). Notably, in the last differentiation step, 36% more transcripts were down-regulated in children (**Figure 2B**). Common transcripts in this step represented about 1/2 of the transcripts in children and 3/4 in the adult group.

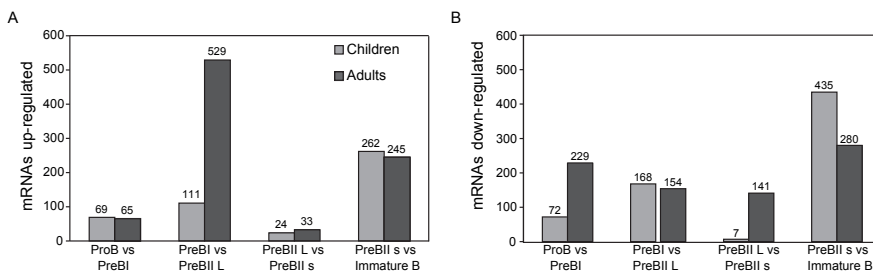


Figure 2. Differentially expressed genes in each of the four stage transits. Number of mRNAs (A) up-regulated and (B) down-regulated in each differentiation step in children (black) and adults (grey), respectively.

Differences in transcripts essential in V(D)J recombination and their effects on Ig gene rearrangements

We first examined if transcripts reported to be involved in precursor-B-cell commitment and differentiation showed similar expression in children and adults, here allowing fold change values less than |2|. Of 164 transcripts previously described to be precursor-B cell associated,²¹⁻²³ 23 transcripts were differentially expressed between children and adults (**Table 1**) (mean fold change 2.14, range 1.22 – 5.81; mean p-value 0.02, range 7×10^{-6} – 0.04).

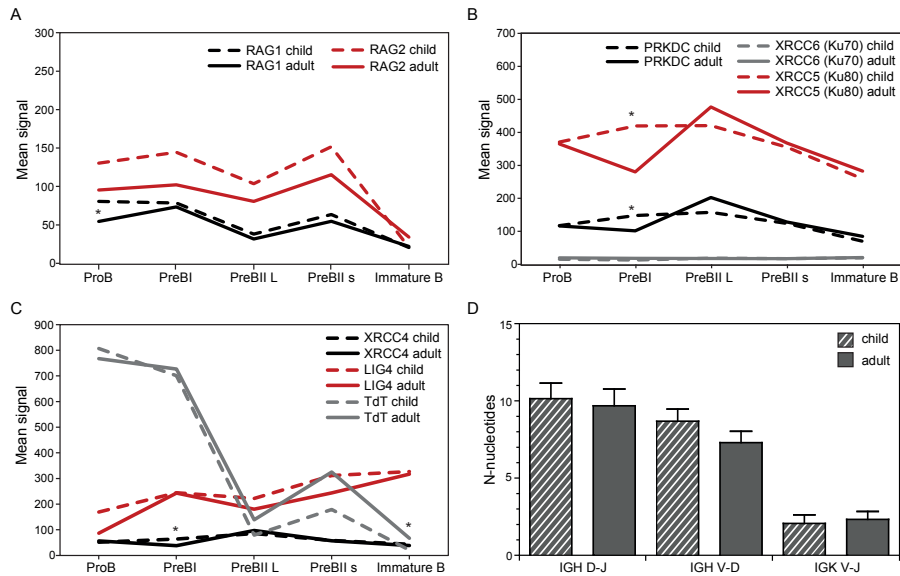


Figure 3. V(D)J gene rearrangement processes in precursor-B cells of children and adults. Expression levels of (A) RAG1 and RAG2, causing DNA double strand breaks, (B) the DNA-PKcs/Ku70/Ku80 complex signaling the "DNA damage", and (C) the DNA repair machinery DNA ligase4/ XRCC4 and the DNA polymerase TdT. Dotted lines represent children, solid lines adults. Significant differences in expression for a specific stage are indicated with an asterisk. (D) N-nucleotide additions in *IGH* gene rearrangements from purified pre-BI cells and *IGK* gene rearrangements from pre-BII small cells of 2 healthy children and 2 healthy adults. Data from children are reproduced from Nodland *et al.* 2011,²⁴ adult *IGH* (n =70) and *IGK* (n=82) gene rearrangement data were newly generated.

Among genes higher expressed in children were multiple genes involved in V(D) J recombination. The recombination activating gene *RAG1* was 1.5 higher expressed ($p = 0.03$) in pediatric pro-B cells, while for the other subsets, we found no age-related differences. RAG1 and RAG2 mRNA were specifically up-regulated in pre-BI and small pre-BII cells of both children and adults, fitting with their involvement in Ig heavy and light chain gene rearrangements (**Figure 3A**). The non-homologous end-joining factors Ku80 and DNA-PKcs²⁸ were both 1.5 fold higher ($p = 0.01$ and 0.02 , respectively) in

pediatric pre-BI cells than in adults (**Figure 3B**). Of transcripts encoding DNA ligation components, XRCC4 showed a 1.7 fold higher expression ($p = 0.03$) in pre-BI cells in children while LIG4 (encoding DNA ligase IV) was similarly expressed in all subsets in children and adults (**Figure 3C**). IGKC, representing the Ig kappa constant region, was significantly higher expressed in adult pro-B (3.6 fold up, $p = 7 \times 10^{-6}$) and pre-BI (4.2 fold up, $p = 4 \times 10^{-6}$) cells. The template-independent DNA polymerase TdT, inserting random nucleotides during V(D)J recombination, was over 3.2 fold higher expressed ($p = 0.02$) in adult immature-B cells than in children (**Figure 3C**).

To study whether the reduced RAG expression and increased TdT and IGKC levels affected V(D)J recombination, we analyzed *IGH* and *IGK* gene rearrangements. To avoid the impact of selection, we analyzed *IGH* gene rearrangements in pre-BI cells and *IGK* gene rearrangements in small pre-BII cells (**Figure 3D**).²¹ Since IGH D-J junctions are formed in pro-B cells,²¹ this analysis allowed us to study the Ig gene rearrangement process in three differentiation stages: pro-B, pre-BI and pre-BII small. The analyzed rearrangements did not show differences for deletions and P-nucleotides between children and adults (not shown). Both D-J and V-D rearrangements showed high numbers of N-nucleotides, reflecting the high TdT levels in pro-B and pre-BI stages. N-nucleotide additions in *IGK* gene rearrangements were much lower and did not differ significantly between children and adults. Thus, the low levels of TdT in pre-BII small as compared to pro-B and pre-BI cells result in fewer TdT insertions, but the difference in TdT levels between children and adults in pre-BII small does not affect N-nucleotide insertions in pre-BII small.

Transcripts encoding pre-BCR components and downstream signaling molecules

Several component of the (pre-)BCR were significantly differentially expressed between children and adults. CD79A expression was significantly higher in childhood pre-BI and pre-BII small cells than in adults (**Table 1**). Furthermore, IGLL1 (immunoglobulin lambda-like polypeptide 1) was slightly higher expressed (fold change 1.3, $p < 0.05$) in pro-B cells in children than in adults, but similar during further differentiation. VPREB1, however, was 1.7 fold higher expressed ($p < 0.002$) in adult immature-B cells than in children, but otherwise showed no age differences. We also analyzed key transcripts in the pre-BCR-signaling pathway²⁹ and found no age-related differences in the proliferation inhibiting transcripts BLNK (B-cell linker) and BTK (Bruton's tyrosine kinase) or other components, except for a sole 1.3 fold higher expression ($p < 0.05$) of SYK (spleen tyrosine kinase) in pre-BII large cells in children. These results strongly suggest that pre-BCR-signaling in humans as evaluated through these pathways, are predominantly unchanged with age.

Table 1. Genes encoding B-cell commitment and differentiation factors that are differentially expressed between children and adults.

ID	Gene	pro-B		pre-BI		pre-BII L		pre-BII S		immature-B	
		p-value	Fold change	p-value	Fold change	p-value	Fold change	p-value	Fold change	p-value	Fold change
2597867	IKZF2	0.01	1.99	0.01	2.23	0.48	1.20	0.07	1.62	0.83	-1.06
3327143	RAG1	0.03	1.48	0.72	1.07	0.29	1.20	0.40	1.16	0.69	-1.07
2468622	ID2	0.03	-2.45	0.54	-1.29	9×10^{-5}	-5.81	0.06	-2.16	0.16	-1.75
2563785	IGKC	7×10^{-6}	-3.58	4×10^{-6}	-4.16	0.43	1.21	0.61	-1.13	0.99	-1.00
2597867	IKZF2	0.01	1.99	0.01	2.23	0.48	1.20	0.07	1.62	0.83	-1.06
3755862	IKZF3	0.40	1.17	1×10^{-3}	2.08	0.21	1.27	0.14	1.33	0.17	1.30
2818454	XRCC4	0.69	-1.09	0.03	1.68	0.54	-1.14	0.94	1.02	0.60	1.12
2526980	XRCC5 (Ku 80)	0.90	1.02	0.01	1.50	0.33	-1.13	0.79	-1.03	0.49	-1.09
3134034	DNA-PKcs	0.94	1.01	0.02	1.46	0.08	-1.29	0.80	-1.04	0.19	-1.21
3820921	SMARCA4	0.26	-1.13	0.03	-1.29	0.33	-1.11	0.09	-1.20	0.02	-1.30
3834502	CD79A	0.24	-1.24	0.01	-1.79	0.36	-1.18	0.04	-1.47	0.75	1.06
2563785	IGKC	7×10^{-6}	-3.58	4×10^{-6}	-4.16	0.43	1.21	0.61	-1.13	0.99	-1.00
3178952	SYK	0.98	-1.00	0.85	-1.02	0.01	1.30	0.06	1.22	0.68	1.04
4011844	IL2RG	0.13	-1.30	0.70	-1.07	0.02	-1.55	0.21	-1.24	0.22	1.24
2468622	ID2	0.03	-2.45	0.54	-1.29	9×10^{-5}	-5.81	0.06	-2.16	0.16	-1.75
3655109	CD19	0.58	1.05	0.17	-1.15	0.26	1.11	0.04	1.22	0.93	1.01
3834502	CD79A	0.24	-1.24	0.01	-1.79	0.36	-1.18	0.04	-1.47	0.75	1.06
3820921	SMARCA4	0.26	-1.13	0.03	-1.29	0.33	-1.11	0.09	-1.20	0.02	-1.30
3078348	EZH2	0.95	1.01	0.37	1.19	0.60	-1.10	0.93	-1.02	0.03	-1.51
3938792	VPREB1	0.53	1.11	0.44	-1.15	0.24	-1.22	0.38	-1.16	0.00	-1.77
2793951	HMG2	1.00	-1.00	0.36	1.25	0.87	1.04	1.00	1.00	0.01	-1.83
3312490	Ki67	0.70	1.09	0.47	1.20	0.65	-1.11	0.97	-1.01	3×10^{-4}	-2.57
3259503	TdT	0.91	1.05	0.94	-1.04	0.23	-1.76	0.20	-1.82	0.02	-3.22

Differentially expressed genes involved in precursor-B-cell commitment and differentiation are shown. A positive fold change indicates higher expression in children and vice versa.

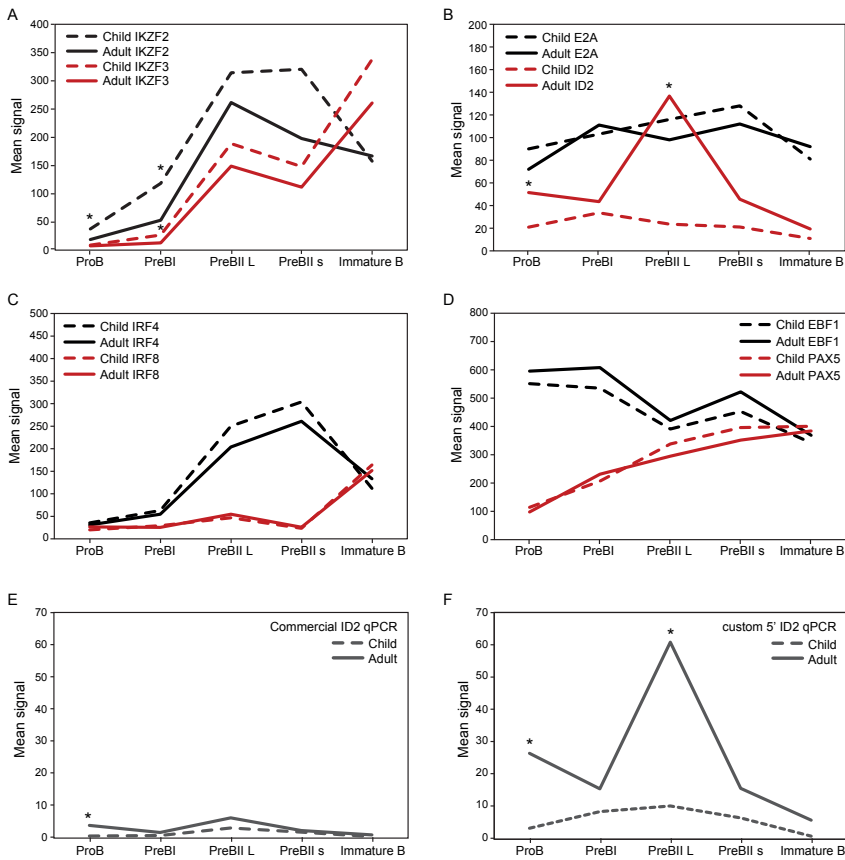


Figure 4. (A-D) Expression levels of transcription factors essential in B-cell commitment and differentiation. Dotted lines represent children, solid lines adults. Relative levels of ID2 mRNA were confirmed with RT-qPCR using (E) a commercial ID2 assay, and (F) a custom-designed primer/probe set targeted to the 5' end of the transcript. Significant differences in expression between children and adults for a specific stage are indicated with an asterisk.

Differences in transcripts essential in B-cell commitment and differentiation and the effects on IGH locus contraction

Multiple transcription factors involved in B-cell commitment and differentiation were differentially expressed between children and adults. These included transcription factors Helios (IKZF2),³⁰ which was 2 fold up in pro-B ($p = 0.01$) and 2.2 fold up in pre-BI ($p = 0.01$), and Aiolos (IKZF3), which was 2.1 fold up in pre-BI cells ($p = 0.0001$; **Figure 4A**). Furthermore, the differentiation inhibitor ID2 was up-regulated in adult pro-B (2.5 fold, $p = 0.028$) and pre-BII large cells (5.8 fold, $p < 9 \times 10^{-5}$). In children, ID2 was expressed at relatively low levels with no significant change from one stage to another

(Figure 4B). In adults, a 3.1-fold increase ($p = 0.01$) in ID2 expression was seen in the transition from pre-BI to pre-BII large and a corresponding 3.0-fold decrease ($p = 0.008$) in the subsequent transition to pre-BII small, followed by a further 2.4 fold decrease ($p = 0.03$) differentiating into immature-B cells (Figure 4B). The ID2 expressional pattern was confirmed with RT-qPCR (Figures 4E-F and Table S3). The target of ID2, E2A, was similarly expressed during differentiation in children and adults (Figure 4B), although with a slightly higher expression, 20% ($p = 0.02$) in pediatric pro-B cells and a similar, but not significant ($p = 0.06$) increase in large pre-BII cells. Furthermore, other transcription factors involved in B cell differentiation showed strikingly similar expression in children and adult in all differentiation stages (Figures 4C-D). These included: EBF1 (Early B cell factor 1), PAX5 (Paired box 5), IRF4 (Interferon regulatory factor 4), IRF8, and POU2AF1 (POU class 2 associating factor 1).

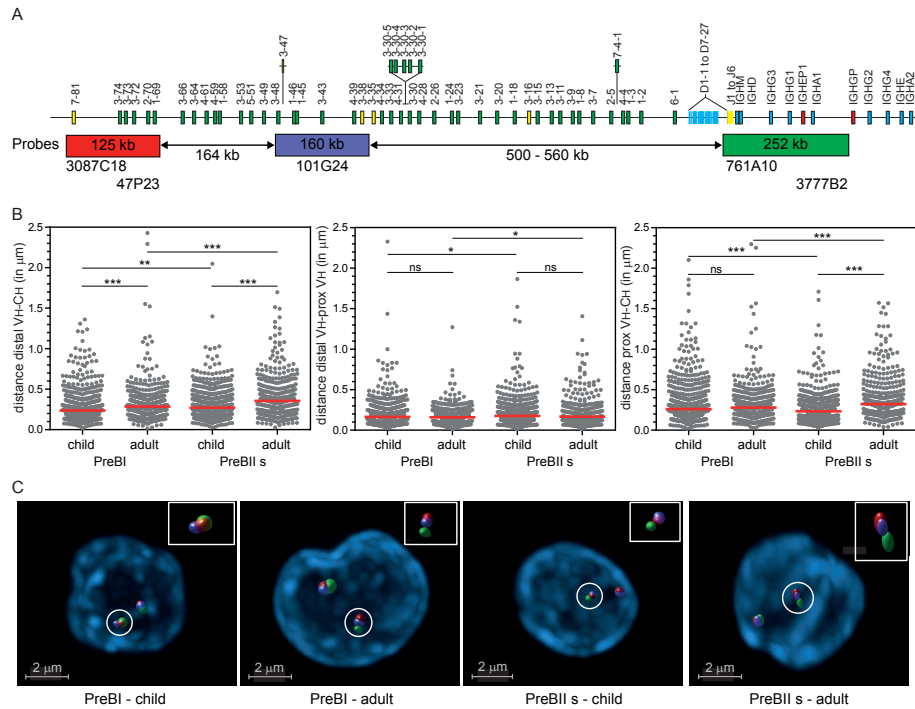


Figure 5. 3D Spatial organization of the *IGH* locus in precursor-B cells of children and adults. (A) Schematic representation of the human *IGH* locus and the combinations of bacterial artificial chromosome clones used as 3D FISH probes are shown. The distance separating each of the 3 probes and their positions within the *IGH* locus were determined from the IMGT database.²⁶ Numbers in the rectangles represent the size of the regions recognized by the probes and the numbers below the arrows represent genomic distances between probe sets. (B) Scatter plots showing the distances in micrometers (y-axis) separating distal V_H , proximal V_H , and CH regions in sorted pediatric and adult pre-BI and pre-BII small cells. For each condition, 2 independent

sorts were performed on material from 1-3 donors each and at least 900 alleles were analyzed per population. Red horizontal lines represent median distances between indicated probes in each population. The nonparametric Mann-Whitney test was used to calculate significance levels between paired populations (horizontal bars). *, $P < .05$; **, $P < .01$; *** $P < .001$. (C) Representative images of *IGH* loci in the different populations.

The up-regulation of ID2 in adults, without differences in E2A, PAX5 and EBF1 expression levels, suggests that of these critical factors, only E2A function is potentially reduced. E2A is implicated in regulating Ig gene rearrangements [reviewed in ³¹]. The *IGH* locus was previously found to contract prior to the initiation of complete V to DJ rearrangements in mouse and human pre-BI cells.^{23,24,32-34} To study whether reduced E2A function might be contributing to reduced B-cell production in adults as compared to children, we measured the spatial distances between 3 probe sets recognizing distal V_H, proximal V_H, and C_H regions (**Figure 5A**). Spatial distances between distal V_H and C_H regions, distal V_H and proximal V_H regions, and proximal V_H and C_H regions were short in childhood pre-BI cells and significantly larger in small pre-BII cells (**Figures 5B-C**), confirming previous observations.²⁴ The *IGH* locus of adult pre-BI cells was also more contracted than in adult pre-BII cells. Importantly, in both stages the distances between distal V_H and C_H regions were larger than in their childhood counterpart (**Figures 5B-C**). The distances between distal V_H and proximal V_H between childhood and adult cells were not different, but the distance between proximal V_H and C_H regions in adult pre-BII cells was significantly larger than in children. Thus, the *IGH* locus was more contracted in childhood than in adult precursor-B cells.

ID2 interacting molecules are involved in DNA replication, recombination and repair, cell cycle progression and checkpoint control

We further analyzed functional annotations of other transcripts changing with ID2 in the pre-BI to pre-BII large transition in adults by building a network starting with ID2 and E2A using Ingenuity Pathway Analysis. The resulting network consisted of 36 transcripts involved in DNA replication, recombination, repair and cell cycle progression (**Figure 6**). Of these transcripts, 28 were up-regulated concomitantly with ID2 and 6 down-regulated. Eleven of the up-regulated molecules were transcription factors, and 6 were kinases. The cell cycle regulators CDK1 (cyclin-dependent kinase 1) and CDK2 were located centrally in the interacting hub. Together with cyclin E (CCNE1), these kinases regulate the G1/S phase transition, in collaboration with cyclin A the S/G2 phase traverse, and with cyclin B (CCNB1 and CCNB2) the G2/M (mitosis) transition. Both CDK1 and CDK2 complexes are able to phosphorylate ID2, assumed to relieve its inhibitory effects on E2A. Notably, it has been suggested that the E2A protein level is modulated by both the abundance and phosphorylation status of ID2.³⁵ The network also includes the important regulator CHEK1, which is involved in several check points

of the cell cycle (**Figure 6**). Other transcripts up-regulated in the network are key factors in DNA replication, such as DNA polymerase α (POLA1) and δ (POLD3) and the primases PRIM1 and PRIM2, which add RNA primers to Okazaki fragments on the lagging strand during DNA synthesis.³⁶ Down-regulated transcripts included the cell cycle regulator cyclin D (CCND2) – possibly caused by ID2 as previously documented.³⁷ Altogether, it seems that with increased ID2 expression in adult pre-BII large cells, a network of transcripts involved in DNA replication and cell cycle regulation is concomitantly activated or repressed. This is in contrast to children, where only 5 transcripts in this network were significantly up-regulated (LYN, IRF4, TFDP2, PTPN6, HDAC9) and 4 significantly down-regulated (SLC22A16, ITPR1, ELK3, DNNTT) (Table S2). Thus, the differential up-regulation of ID2 in adult pre-BII large cells ties in with an ensemble of other known cell cycle checkpoint regulators, supporting the hypothesis of the pre-BII large stage as an important restriction step in adults.

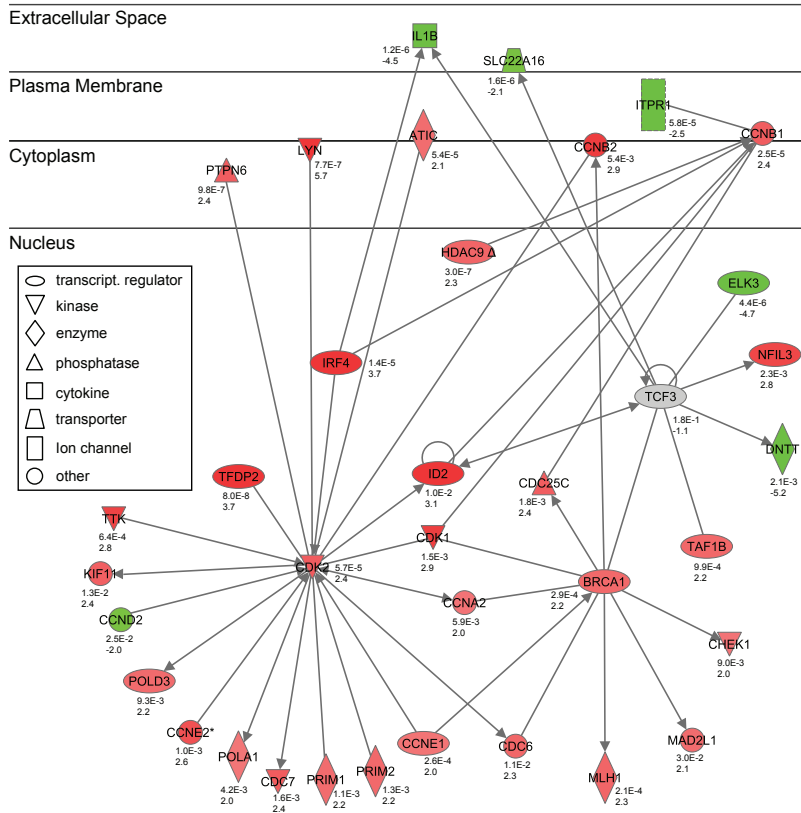


Figure 6. Functional network of ID2 interacting molecules. Red denotes up-regulated and green down-regulated transcripts in the differentiation step pre-BI to pre-BII large stage in adults. Nodes are displayed using various shapes that represent the functional class of gene products.

Adult immature-B cells do not show signs of compensatory proliferation

In addition to the up-regulation of cell cycle regulators CDK1 and CDK2 in adult pre-BII large cells, Ki67 was up-regulated in adult immature-B cells (**Figure 7A**). Adults and children both showed strong up-regulation in their pre-BII cells of this marker for cells that are in cycle.³⁸ However, immature-B cells of adults showed significantly higher expression of Ki67 than children (2.6 fold up, $p = 3 \times 10^{-4}$).³⁹ The up-regulation of proliferation markers could suggest that adult precursor-B cell undergo proliferation to compensate for reduced B-cell production. To study this, we determined the replication history of small pre-BII and immature-B cells of children and adults using the KREC assay.²⁷ In line with previous observations,²⁷ we did not observe any cell divisions in precursor-B cells of children (**Figure 7B**). Furthermore, pre-BII small and immature-B cells of adults did not show signs of proliferation either. Thus, despite the differences in gene expression levels of Ki67, adult immature-B cells do not undergo proliferation to compensate for the reduced production of B-cell progenitors.

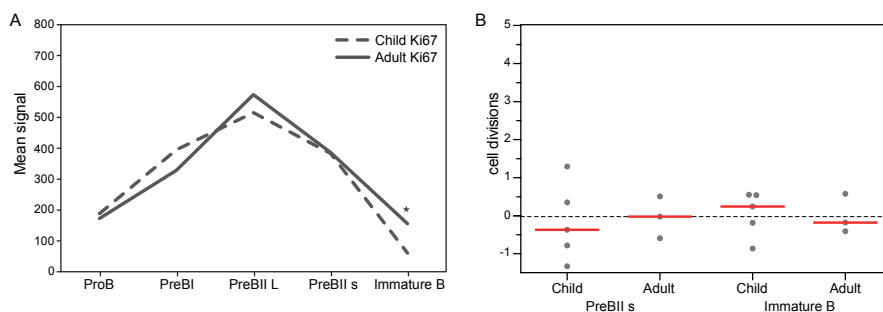


Figure 7. Proliferation in precursor-B cells from children and adults. (A) Expression levels of Ki67 mRNA in the 5 precursor-B-cell subsets. Significant differences in expression between children and adults for a specific stage are indicated with an asterisk. (B) The replication history of pre-BII and immature-B cells from children and adults determined with the KREC assay. Each grey dot represents the replication history in a sorted subset from a single donor. Red horizontal lines represent median distances.

DISCUSSION

B-cell precursors are committed to differentiation or apoptosis. Here, we characterized the differences in transcriptional activity of precursor-B cells in adults and children, and identified differences in V(D)J recombination factors, ID2, and cell cycle genes that could underlie the marked reduction in the human precursor-B-cell compartment occurring with age.^{4,5} Functional analysis of potentially involved mechanisms indicated that up-regulation of ID2 in adults inhibited E2A-mediated Ig locus contraction to reduce efficient V(D)J recombination and precursor-B-cell differentiation.

Our cellular analysis of precursor-B cells in BM revealed a 67% decrease in their absolute number in adults as compared to 2-year-old children. This decrease in BM precursor-B-cell numbers corresponded to the decline in the absolute size of the B-cell population in peripheral blood of adults.⁴⁰ Importantly, the relative composition of the various subsets was unchanged with age and in accordance with previous reports from both humans and mice.^{5,40,41} Thus, the reduced output from BM seemed the result of lower numbers of all B-cell progenitors and not restricted to a specific differentiation stage.

The issue whether RAG1 and RAG2 expression decrease with age in precursor-B-cell subsets has been explored in several studies in mice,^{15,41-43} but very few reports exist from humans. To our knowledge only one human study⁴⁴ has reported, based on RT-PCR and agarose gel electrophoresis, that there was no change in transcription of RAG1 and RAG2 in precursor-B cells from fetal and adult BM. This contrasts more recent experimental studies in mice,^{15,42} adopting transgenic and knock-in RAG2 reporter animals showing that the frequency of pro-B cells expressing RAG2 was significantly lower in aged mice as compared to young. We found a 50% higher ($p = 0.03$) RAG1 expression in pediatric pro-B cells as compared to adults; a result which should be confirmed due to the present small cohort size. Of other transcripts involved in the V(D)J rearrangement process: DNA-PKcs, Ku80 and XRCC4 showed a 50-70% higher expression ($p = 0.01 - 0.03$) in pre-BI cells in children as compared to adults. TdT, on the other hand, was 3.2-fold up-regulated ($p = 0.02$) in adult immature-B cells. Despite these differences in gene expression levels, we did not observe differences in *IGH* and *IGK* gene rearrangements regarding N-nucleotides, P-nucleotides and deletions between children and adults. These suggest that processing and repair of RAG-induced dsDNA breaks is not affected by age. Still, the reduced RAG1 expression levels in adults could negatively affect the efficiency of Ig gene rearrangements. Because reduced RAG function is not apparent from junction analysis [reviewed in ⁴⁵], this may contribute to the lower output of precursor-B cells from normal BM with age.

We then analyzed transcriptional activity of genes required for commitment and differentiation of precursor-B cells. The most striking finding was the temporal increase in ID2 mRNA levels restricted to pre-BII large cells in adults, and only once reported previously in mice.⁴⁶ As an E2A inhibitory protein, ID2 is assumed to have a central role in modulating the E2A dependent transcriptional regulatory networks, and hence inhibit B-cell lineage commitment and differentiation.^{47,48} ID2 has been shown to negatively regulate B-cell differentiation in mice spleen,^{49,50} and knock-down by shRNA in hematopoietic progenitor cells promoted B-cell differentiation and induction of B-cell lineage specific genes.⁵¹ In aged, but not in young murine B-cell precursors, reduced E2A protein expression was seen in the presence of maintained E2A mRNA levels.⁵²⁻⁵⁴ The reduced

E2A protein levels in aged murine precursor-B cells seemed to be due to accelerated degradation, since it was effectively blocked by proteasome inhibitors indicating involvement of the ubiquitin/proteasome pathway.⁵⁵ Frasca *et al.*¹⁶ were unable to detect ID2 protein using *in vitro* expanded aged and young precursor-B cells, but found E2A protein levels decreased in adults. We found no age-related decrease in E2A mRNA expression in any precursor-B subsets in agreement with the situation in mice.¹⁶ Notably, the above referred study¹⁶ analyzed only pro-B/early pre-B cells for ID2 expression and no further maturation stages. In our study, a striking age-related difference in ID2 expression was seen first in pre-BII large cells – a subpopulation more mature than the subsets analyzed in mice. We also found a smaller, but significantly higher expression in adult pro-B cells – a difference that probably would have been blurred if pro-B and pre-BI subsets had been analyzed together.¹⁶ Another difference between the studies by Frasca *et al.*¹⁶ and our study was that they analyzed ID2 protein levels in cultured precursor-B cells while we analyzed ID2 mRNA expression in freshly isolated precursor-B cells. Bordon *et al.*¹⁶ in contrast, demonstrated fluctuations in ID2 mRNA expression during precursor-B-cell differentiation in adult wild type and transgenic mice overexpressing POU2AF1 (OBF1), concordant with our findings in humans.

To study whether the high ID2 gene expression levels indeed negatively affected E2A function, we analyzed one of the processes in which E2A is involved: Ig locus contraction. Indeed, we observed decreased contraction of *IGH* in pre-BI and small pre-BII cells in adults. These subsets were analyzed, because they are poised to undergo complete Ig gene rearrangements.²¹ ID2 transcripts were significantly higher in adults in pro-B and large pre-BII cells, the stages that directly precede the subsets analyzed for Ig locus contraction. Still, high ID2 transcript levels are likely to affect the subsequent differentiation stage, because the resulting protein products function to decrease E2A activity. Because E2A transcript levels are not up-regulated with age, the effect of high ID2 transcripts is not compensated for. Thus, in addition to reduced RAG activity, the efficiency of V(D)J recombination in adult precursor-B cells is further reduced by ID2 inhibition of Ig locus contraction.

With increased ID2 mRNA expression in adult pre-BII large cells, we identified a concomitant up-regulation of transcripts involved in cell cycle progression and control as previously reported.^{56,57} As pre-BII large cells are characterized by a transient proliferative burst,²¹ we observed a similar transcriptional activity in this subset in children and adults by using Ki67 as a proliferation marker. On the other hand, there was a clear up-regulation of cell cycle and checkpoint associated genes in the adult subset, concordant with a more stringent cell cycle regulation and control.

Only at the immature-B cell stage we found differential expression of the mitotic marker Ki67 with a 2.6-fold ($p = 3.4 \times 10^{-4}$) higher expression in adults indicating a

higher fraction of cycling cells. In 2005, Cancro⁸ suggested a decreased turnover rate in the immature-B-cell subset in adult mice as a homeostatic mechanism counteracting the reduced production rate. Our expression data, however, rather suggest an expansion with age of the immature-B-cell subset, possibly to compensate for reduced production rate. This was not supported by our studies on the relative composition of the immature-B-cell subset and of the replication history of pre-BII small and immature-B cells. Thus, the increased levels of Ki67 indicate that more cells are in cell cycle, but these cells do not show signs of (extensive) proliferation to compensate for the reduced production of B cells in adults.

In conclusion, the human precursor-B-cell pool, although smaller, does not show major compositional variations with age, and comprises dynamic subpopulations held at steady state to support a lifelong production of B lymphocytes. Elevated mRNA levels of the differentiation inhibitory molecule ID2 along with a network of transcripts related to cell cycle checkpoint control in adult pre-BII large cells, indicate restriction in precursor-B-cell differentiation. Moreover, the increased ID2 levels are a likely cause for the observed impaired Ig locus contraction due to limited E2A function. These findings demonstrate distinct regulatory mechanisms in B-cell differentiation between adults and children with a central role for transcriptional regulation of ID2.

MATERIALS AND METHODS

Bone marrow samples

We obtained BM samples from healthy children aged 18 ± 2 months (mean \pm range) and healthy adults aged 50 ± 5 years (mean \pm range). The children were eligible for minor surgery, the adults for elective orthopaedic surgery. Both groups were haematologically healthy, and none of the middle-aged adults had active inflammatory disease requiring regular anti-inflammatory medication. Written informed consent was obtained using protocols approved by the Regional Medical Research Ethics Committee of Eastern Norway (REK Øst, Accession no. 473-02132) (<https://helseforskning.etikkom.no/>). The study was performed according to the Norwegian Health Regulations.

Isolation of CD10 positive cells

BM aspirates (~ 20 ml from children and 120 ml from adults) were subjected to Ficoll density gradient centrifugation (Ficoll-Paque PLUS). CD10⁺ precursor-B cells were positively selected using streptavidin coated Dynabeads FlowComp Flexi (Invitrogen Dynal

AS, Oslo, Norway) and biotin-labeled CD10 antibody (SN5c, Abcam Inc. Cambridge, MA, USA). Subsequently, five precursor-B-cell subsets were purified from single individuals on a FACSAria cell sorter (BD Biosciences) (**Figure 1A**) after staining with the following antibodies: IgM-FITC (G20-127), CD19-APC (HIB19), CD20-PE (2H7), CD22-APC (IS7), CD123-PE (6H6), CD10-PE-Cy7 (HI10a) and CD34-PerCP (8G12). The membrane marker CD123 was used in combination with CD22 to distinguish precursor-B cells from basophilic progenitor cells (CD123⁺), which also appear in the lymphogate.

RNA isolation

Total RNA was extracted and purified from each precursor-B-cell subset using the miRNeasy Mini Kit (Qiagen) and Phase Lock Gel Heavy (5 PRIME GmbH, Hamburg, Germany). RNA was quantified with a NanoDrop ND-1000 Spectrophotometer (Saveen Werner, Malmö, Sweden), and in case of concentrations using the RiboGreen method (Invitrogen, Eugene, OR, USA). Quality was assessed with Agilent 2100 Bioanalyzer using either the Agilent RNA 6000 Nano or Pico Kit (Agilent Technologies, Palo Alto, CA, USA) depending on sample concentration. The samples concentrations ranged from 3.9 to 149.5 ng/μl and from 6.4 to 9.9 (mean 8.4, n = 39) for Bioanalyzer RIN indicating high RNA purity and integrity.

Microarray analyses and statistical analysis of data

Microarray analyses were performed on subsets from single individuals using the GeneChip Human Exon 1.0 (Affymetrix, Santa Clara, CA, USA). 5 ng total RNA was used to generate cDNA with the Ovation Pico WTA System protocol (NuGEN). MinElute Spin Columns (Qiagen) were used for purification of amplified cDNA. Sense strand cDNA was generated from 3 μg cDNA with the WT-Ovation Exon Module Version 1.0 (NuGEN) according to the manufacturers' protocols for whole genome gene expression analysis. The resulting sense strand cDNA was fragmented and biotinylated using the Encore Biotin Module (NuGEN). The labeled cDNA was hybridized on the array, washed, and stained. The arrays were scanned using the Affymetrix Gene Chip Scanner 3000 7G. The scanned images were processed using the AGCC (Affymetrix GeneChip Command Console) Software and the CEL files were imported into Partek Genomics Suite software (Partek, Inc. MO, USA). The Robust Multichip Analysis (RMA) algorithm was applied for generation of signal values and normalization. On each array, 21,989 transcripts could be detected. Transcripts were analyzed in core mode (see www.affymetrix.com) using signal values of less than 22.6 across arrays as threshold to filter

for low and non-expressed genes yielding 15,830 expressed genes. For expression comparisons of different groups, profiles were compared using a one-way ANOVA model. The results were expressed as fold change. Gene lists were generated with the criteria of fold change ≥ 2 and p-values < 0.05 . For analysis of genes involved in the V(D)J process and in B-cell commitment and differentiation, fold change less than $|2|$ was shown. The complete gene expression material is available online at ArrayExpress (<http://www.ebi.ac.uk/arrayexpress/>) with accession number E-MTAB-1422.

Ingenuity Pathway Analysis (IPA)

Gene networks and canonical pathways representing key genes were identified using Ingenuity Pathways Analysis (IPA) (www.ingenuity.com). Briefly, the data set containing gene identifiers and corresponding fold changes and p-values was uploaded into the web-delivered application and each gene identifier was mapped to its corresponding gene object in The Ingenuity Pathway Analysis (IPA) software (www.ingenuity.com). The functional analysis identified the biological functions and/or diseases that were most significant to the data sets. Fisher's exact test was performed to calculate a p-value assigning probability to each biological function.

DNA probe preparation and 3D immunofluorescence in situ hybridization (FISH)

3D DNA FISH was performed as described previously^{23,24} with fosmid clones 761A10 and 3777B2 (BACPAC Resources, Oakland, CA), BAC clones 47P23, 101G24 (BACPAC Resources) and 3087C18 (Open Biosystems, Huntsville, AL) recognizing regions within the human *IGH* locus. Probes were either directly labeled with Chromatide Alexa Fluor 488-5 dUTP or Chromatide Alexa Fluor 568-5 dUTP (Invitrogen) using Nick Translation Mix (Roche Diagnostics GmbH); or they were indirectly labeled using DIG-Nick Translation Mix (Roche Diagnostics GmbH). Just prior to use, the probes were precipitated and a hybridization cocktail was prepared containing 600 ng of each labeled probe, 4 μg of human Cot-1 DNA (Invitrogen), 5 μg of salmon sperm DNA dissolved in 2 \times SSC, 50% formamide, 10% dextran sulfate. The probes were denatured at 75°C for 5 min prior to hybridization.

Approximately 100 μl of a 1×10^6 cells/ml suspension of freshly sorted cells was directly attached to poly-L-lysine-coated coverslips. The cells were fixed in 4% paraformaldehyde, and permeabilized in a PBS, 0.1% Triton X-100, 0.1% saponin solutions and subjected to liquid nitrogen immersion following incubation in PBS with 20% glycerol. The nuclear membranes were permeabilized in PBS, 0.5% Triton X-100, 0.5% saponin

prior to hybridization with the DNA probe cocktail for 5 min in a HYBrite machine at 75°C. The coverslips were sealed with nail polish and incubated for 48hr at 37°C. Subsequently, the coverslips were washed and incubated with Cy5-conjugated mouse anti-DIG antibodies (Jackson ImmunoResearch) to detect dig-labeled probes. Finally, the coverslips were washed and mounted on slides with 10 µl of Prolong gold anti-fade reagent (Invitrogen) and sealed with nail polish.

Image acquisition, distance calculations and statistics

Pictures were captured with a Leica SP5 confocal microscope (Leica Microsystems). Using a 63× lens (NA 1.4), we acquired images of ~70 serial optical sections spaced by 0.15 µm. The data sets were deconvolved and analyzed with Huygens Professional software (Scientific Volume Imaging, Hilversum, the Netherlands). The 3D coordinates of the center of mass of each probe were input into Microsoft Excel, and the distances separating each probe were calculated using the equation: $\sqrt{(X_a - X_b)^2 + (Y_a - Y_b)^2 + (Z_a - Z_b)^2}$, where X, Y, Z are the coordinates of object a or b. Differences in distances between each two groups of cells were performed with the non-parametric Mann-Whitney test using Graphpad Prism version 5.0.

Quantitative RT-PCR for key differentially expressed transcripts

TaqMan Gene Expression Assays (384-well plates) (Applied Biosystems) were used for quantitative PCR for selected differentially expressed genes. The arrays were run on the ViiA 7 Real-time PCR System (Applied Biosystems). The relative mRNA expression was calculated with the Comparative Ct method (fold change = $2^{-\Delta\Delta C_t}$) using B2M (Beta 2 microglobulin) as endogenous control.²⁵ Additional primer/probe sets were used for ID2 that covered the 5' end of the transcript (Table S1); two sets for exon I, and one set for exon II, because the custom ID2 assay covered only the exon II and III boundary, which was partially outside the protein coding area.

***IGH* and *IGK* junctional region analysis**

DNA was isolated from sorted pre-BI and small pre-BII cells of healthy children or healthy adults using a GenElute genomic DNA extraction kit (Sigma Aldrich, St. Louis, MO). Multiplex PCR was performed to amplify complete *IGH* gene rearrangements from pre-BI cells and *IGK* gene rearrangements from small pre-BII cells with V subgroup-specific forward primers and a consensus J primer, and cloned into the pGEM-T Easy vector (Promega Benelux BV, Leiden, The Netherlands).²¹ Individual clones were

sequenced on an ABI Prism 3031 XL fluorescent sequencer (Applied Biosystems, Carlsbad, CA). The size and composition of the junctional region with regards to deletions, P- and N-nucleotides were analyzed using the international ImMunoGeneTics (IMGT) information system (<http://imgt.cines.fr/>).²⁶ Statistical analyses were performed using the Mann-Whitney test.

Replication history analysis using the KREC assay

The replication history of sorted precursor-B-cell subsets was determined with the Kappa-deleting Recombination Excision Circles (KREC) assay as described previously.²⁷ Briefly, the amounts of coding and signal joints of the *IGK*-deleting rearrangement were measured by RQ-PCR in DNA from sorted precursor-B-cell populations on an ABI Prism 7000 (Applied Biosystems). Signal joints, but not coding joints are diluted two-fold with every cell division.²⁷ To measure the number of cell divisions undergone by each population, we calculated the ratio between the number of coding joints and signal joints. The previously established control cell line U698 DB01 (InVivoScribe) contains one coding and one signal joint per genome and was used to correct for minor differences in efficiency of both RQ-PCR assays.

ACKNOWLEDGEMENTS

We thank all participating adults, children and their parents for their trust and generous help, and Mr. S.J.W. Bartol and Ms. F.S. van de Bovenkamp for technical support. This work was supported by grants from Torsteds legat, Raket og Otto Kr. Bruuns legat, and Olav Raagholt og Gerd Meidel Raagholt's stiftelse for forskning. Menno C. van Zelm is supported by Veni Grant 916.110.90 from ZonMW/NWO.

REFERENCES

1. Matthias, P., and A. G. Rolink. 2005. Transcriptional networks in developing and mature B cells. *Nat. Rev. Immunol.* 5: 497-508.
2. Nutt, S. L., and B. L. Kee. 2007. The transcriptional regulation of B cell lineage commitment. *Immunity.* 26: 715-725.
3. Dorshkind, K., E. Montecino-Rodriguez, and R. A. Signer. 2009. The ageing immune system: is it ever too old to become young again? *Nat. Rev. Immunol.* 9: 57-62.

4. Rossi, M. I., T. Yokota, K. L. Medina, K. P. Garrett, P. C. Comp, A. H. Schipul, Jr., and P. W. Kincade. 2003. B lymphopoiesis is active throughout human life, but there are developmental age-related changes. *Blood* 101: 576-584.
5. Jensen, K., L. Schaffer, O. K. Olstad, A. G. Bechensteen, M. Hellebostad, G. E. Tjonnfjord, P. Kierulf, K. M. Gautvik, and L. T. Osnes. 2010. Striking decrease in the total precursor B-cell compartment during early childhood as evidenced by flow cytometry and gene expression changes. *Pediatr. Hematol. Oncol.* 27: 31-45.
6. Johnson, K. M., K. Owen, and P. L. Witte. 2002. Aging and developmental transitions in the B cell lineage. *Int. Immunol.* 14: 1313-1323.
7. Allman, D., and J. P. Miller. 2005. The aging of early B-cell precursors. *Immunol. Rev.* 205: 18-29.
8. Cancro, M. P. 2005. B cells and aging: gauging the interplay of generative, selective, and homeostatic events. *Immunol. Rev.* 205: 48-59.
9. Henry, C. J., A. Marusyk, and J. DeGregori. 2011. Aging-associated changes in hematopoiesis and leukemogenesis: what's the connection? *Aging (Albany, NY)* 3: 643-656.
10. Siegrist, C. A., and R. Aspinall. 2009. B-cell responses to vaccination at the extremes of age. *Nat. Rev. Immunol.* 9: 185-194.
11. Rossi, D. J., D. Bryder, J. M. Zahn, H. Ahlenius, R. Sonu, A. J. Wagers, and I. L. Weissman. 2005. Cell intrinsic alterations underlie hematopoietic stem cell aging. *Proc. Natl. Acad. Sci. U. S. A* 102: 9194-9199.
12. Cho, R. H., H. B. Sieburg, and C. E. Muller-Sieburg. 2008. A new mechanism for the aging of hematopoietic stem cells: aging changes the clonal composition of the stem cell compartment but not individual stem cells. *Blood* 111: 5553-5561.
13. Kline, G. H., T. A. Hayden, and N. R. Klinman. 1999. B cell maintenance in aged mice reflects both increased B cell longevity and decreased B cell generation. *J. Immunol.* 162: 3342-3349.
14. Labrie, J. E., III, A. P. Sah, D. M. Allman, M. P. Cancro, and R. M. Gerstein. 2004. Bone marrow microenvironmental changes underlie reduced RAG-mediated recombination and B cell generation in aged mice. *J. Exp. Med.* 200: 411-423.
15. Labrie, J. E., III, L. Borghesi, and R. M. Gerstein. 2005. Bone marrow microenvironmental changes in aged mice compromise V(D)J recombinase activity and B cell generation. *Semin. Immunol.* 17: 347-355.
16. Frasca, D., D. Nguyen, E. Van der Put, R. L. Riley, and B. B. Blomberg. 2003. The age-related decrease in E47 DNA-binding does not depend on increased Id inhibitory proteins in bone marrow-derived B cell precursors. *Front Biosci.* 8: a110-a116.
17. Frasca, D., D. Nguyen, R. L. Riley, and B. B. Blomberg. 2003. Decreased E12 and/or E47 transcription factor activity in the bone marrow as well as in the spleen of aged mice. *J. Immunol* 170: 719-726.
18. Van der Put, E., D. Frasca, A. M. King, B. B. Blomberg, and R. L. Riley. 2004. Decreased E47 in senescent B cell precursors is stage specific and regulated posttranslationally by protein turnover. *J. Immunol.* 173: 818-827.

19. Frasca, D., A. M. Landin, S. C. Lechner, J. G. Ryan, R. Schwartz, R. L. Riley, and B. B. Blomberg. 2008. Aging down-regulates the transcription factor E2A, activation-induced cytidine deaminase, and Ig class switch in human B cells. *J. Immunol* 180: 5283-5290.
20. Frasca, D., and B. B. Blomberg. 2011. Aging impairs murine B cell differentiation and function in primary and secondary lymphoid tissues. *Aging Dis.* 2: 361-373.
21. van Zelm, M. C., M. van der Burg, D. de Ridder, B. H. Barendregt, E. F. de Haas, M. J. Reinders, A. C. Lankester, T. Revesz, F. J. Staal, and J. J. van Dongen. 2005. Ig gene rearrangement steps are initiated in early human precursor B cell subsets and correlate with specific transcription factor expression. *J. Immunol.* 175: 5912-5922.
22. Hystad, M. E., J. H. Myklebust, T. H. Bo, E. A. Sivertsen, E. Rian, L. Forfang, E. Munthe, A. Rosenwald, M. Chiorazzi, I. Jonassen, L. M. Staudt, and E. B. Smeland. 2007. Characterization of early stages of human B cell development by gene expression profiling. *J. Immunol.* 179: 3662-3671.
23. Sayegh, C. E., S. Jhunjhunwala, R. Riblet, and C. Murre. 2005. Visualization of looping involving the immunoglobulin heavy-chain locus in developing B cells. *Genes Dev.* 19: 322-327.
24. Nodland, S. E., M. A. Berkowska, A. A. Bajer, N. Shah, R. D. de, J. J. van Dongen, T. W. LeBien, and M. C. van Zelm. 2011. IL-7R expression and IL-7 signaling confer a distinct phenotype on developing human B-lineage cells. *Blood* 118: 2116-2127.
25. Livak, K. J., and T. D. Schmittgen. 2001. Analysis of relative gene expression data using real-time quantitative PCR and the 2(-Delta Delta C(T)) Method. *Methods* 25: 402-408.
26. Alamyar, E., P. Duroux, M. P. Lefranc, and V. Giudicelli. 2012. IMGT((R)) tools for the nucleotide analysis of immunoglobulin (IG) and T cell receptor (TR) V-(D)-J repertoires, polymorphisms, and IG mutations: IMGT/V-QUEST and IMGT/HighV-QUEST for NGS. *Methods Mol. Biol.* 882: 569-604.
27. van Zelm, M. C., T. Szczepanski, M. van der Burg, and J. J. van Dongen. 2007. Replication history of B lymphocytes reveals homeostatic proliferation and extensive antigen-induced B cell expansion. *J. Exp. Med.* 204: 645-655.
28. Ochi, T., B. L. Sibanda, Q. Wu, D. Y. Chirgadze, V. M. Bolanos-Garcia, and T. L. Blundell. 2010. Structural biology of DNA repair: spatial organisation of the multicomponent complexes of nonhomologous end joining. *J. Nucleic Acids* 2010.
29. Hendriks, R. W., and S. Middendorp. 2004. The pre-BCR checkpoint as a cell-autonomous proliferation switch. *Trends Immunol.* 25: 249-256.
30. John, L. B., and A. C. Ward. 2011. The Ikaros gene family: transcriptional regulators of hematopoiesis and immunity. *Mol. Immunol.* 48: 1272-1278.
31. Bossen, C., R. Mansson, and C. Murre. 2012. Chromatin topology and the regulation of antigen receptor assembly. *Annu. Rev. Immunol.* 30: 337-356.
32. Jhunjhunwala, S., M. C. van Zelm, M. M. Peak, S. Cutchin, R. Riblet, J. J. van Dongen, F. G. Grosveld, T. A. Knoch, and C. Murre. 2008. The 3D structure of the immunoglobulin heavy-chain locus: implications for long-range genomic interactions. *Cell* 133: 265-279.

33. Kosak, S. T., J. A. Skok, K. L. Medina, R. Riblet, M. M. Le Beau, A. G. Fisher, and H. Singh. 2002. Subnuclear compartmentalization of immunoglobulin loci during lymphocyte development. *Science* 296: 158-162.
34. Roldan, E., M. Fuxa, W. Chong, D. Martinez, M. Novatchkova, M. Busslinger, and J. A. Skok. 2005. Locus 'decontraction' and centromeric recruitment contribute to allelic exclusion of the immunoglobulin heavy-chain gene. *Nat. Immunol.* 6: 31-41.
35. Hara, E., M. Hall, and G. Peters. 1997. Cdk2-dependent phosphorylation of Id2 modulates activity of E2A-related transcription factors. *EMBO J.* 16: 332-342.
36. Bae, S. H., K. H. Bae, J. A. Kim, and Y. S. Seo. 2001. RPA governs endonuclease switching during processing of Okazaki fragments in eukaryotes. *Nature* 412: 456-461.
37. Lasorella, A., A. Iavarone, and M. A. Israel. 1996. Id2 specifically alters regulation of the cell cycle by tumor suppressor proteins. *Mol. Cell Biol.* 16: 2570-2578.
38. Hoffmann, R., T. Seidl, M. Neeb, A. Rolink, and F. Melchers. 2002. Changes in gene expression profiles in developing B cells of murine bone marrow. *Genome Res.* 12: 98-111.
39. Bendall, S. C., E. F. Simonds, P. Qiu, e. Amir, P. O. Krutzik, R. Finck, R. V. Bruggner, R. Melamed, A. Trejo, O. I. Ornatsky, R. S. Balderas, S. K. Plevritis, K. Sachs, D. Pe'er, S. D. Tanner, and G. P. Nolan. 2011. Single-cell mass cytometry of differential immune and drug responses across a human hematopoietic continuum. *Science* 332: 687-696.
40. Comans-Bitter, W. M., R. de Groot, R. van den Beemd, H. J. Neijens, W. C. Hop, K. Groeneveld, H. Hooijkaas, and J. J. van Dongen. 1997. Immunophenotyping of blood lymphocytes in childhood. Reference values for lymphocyte subpopulations. *J. Pediatr.* 130: 388-393.
41. Rossi, M. I., T. Yokota, K. L. Medina, K. P. Garrett, P. C. Comp, A. H. Schipul, Jr., and P. W. Kincade. 2003. B lymphopoiesis is active throughout human life, but there are developmental age-related changes. *Blood* 101: 576-584.
42. Labrie, J. E., III, A. P. Sah, D. M. Allman, M. P. Cancro, and R. M. Gerstein. 2004. Bone marrow microenvironmental changes underlie reduced RAG-mediated recombination and B cell generation in aged mice. *J. Exp. Med.* 200: 411-423.
43. Linton, P. J., and K. Dorshkind. 2004. Age-related changes in lymphocyte development and function. *Nat. Immunol.* 5: 133-139.
44. Nunez, C., N. Nishimoto, G. L. Gartland, L. G. Billips, P. D. Burrows, H. Kubagawa, and M. D. Cooper. 1996. B cells are generated throughout life in humans. *Journal of Immunology. Vol. 156(2)(pp 866-872), 1996.* 866-872.
45. Berkowska, M. A., M. van der Burg, J. J. van Dongen, and M. C. van Zelm. 2011. Checkpoints of B cell differentiation: visualizing Ig-centric processes. *Ann. N. Y. Acad. Sci.* 1246: 11-25.
46. Bordon, A., N. Bosco, R. C. Du, B. Bartholdy, H. Kohler, G. Matthias, A. G. Rolink, and P. Matthias. 2008. Enforced expression of the transcriptional coactivator OBF1 impairs B cell differentiation at the earliest stage of development. *PLoS. One.* 3: e4007.
47. Kee, B. L. 2009. E and ID proteins branch out. *Nat. Rev. Immunol.* 9: 175-184.

48. Greenbaum, S., and Y. Zhuang. 2002. Regulation of early lymphocyte development by E2A family proteins. *Semin. Immunol.* 14: 405-414.
49. Becker-Herman, S., F. Lantner, and I. Shachar. 2002. Id2 negatively regulates B cell differentiation in the spleen. *J. Immunol.* 168: 5507-5513.
50. Gore, Y., F. Lantner, G. Hart, and I. Shachar. 2010. Mad3 negatively regulates B cell differentiation in the spleen by inducing Id2 expression. *Mol. Biol. Cell* 21: 1864-1871.
51. Ji, M., H. Li, H. C. Suh, K. D. Klarmann, Y. Yokota, and J. R. Keller. 2008. Id2 intrinsically regulates lymphoid and erythroid development via interaction with different target proteins. *Blood* 112: 1068-1077.
52. Van der Put, E., D. Frasca, A. M. King, B. B. Blomberg, and R. L. Riley. 2004. Decreased E47 in senescent B cell precursors is stage specific and regulated posttranslationally by protein turnover. *J. Immunol.* 173: 818-827.
53. Frasca, D., D. Nguyen, R. L. Riley, and B. B. Blomberg. 2003. Decreased E12 and/or E47 transcription factor activity in the bone marrow as well as in the spleen of aged mice. *J. Immunol.* 170: 719-726.
54. Riley, R. L., B. B. Blomberg, and D. Frasca. 2005. B cells, E2A, and aging. *Immunol. Rev.* 205: 30-47.
55. Van der Put, E., D. Frasca, A. M. King, B. B. Blomberg, and R. L. Riley. 2004. Decreased E47 in senescent B cell precursors is stage specific and regulated posttranslationally by protein turnover. *J. Immunol.* 173: 818-827.
56. Iavarone, A., P. Garg, A. Lasorella, J. Hsu, and M. A. Israel. 1994. The helix-loop-helix protein Id-2 enhances cell proliferation and binds to the retinoblastoma protein. *Genes Dev.* 8: 1270-1284.
57. Zebedee, Z., and E. Hara. 2001. Id proteins in cell cycle control and cellular senescence. *Oncogene* 20: 8317-8325.



Chapter V

Altered V(D)J recombination underlies the skewed immunoglobulin repertoires in normal and malignant B-cell precursors from fetal origin

Magdalena B. Rother¹, Kristin Jensen^{2,3}, Mirjam van der Burg¹, Fleur S. van de Bovenkamp¹, Roel Kroek¹, Wilfred F.J. van IJcken⁴, Vincent H.J. van der Velden¹, Tom Cupedo⁵, Ole K. Olstad^{2,3}, Jacques J.M. van Dongen¹ and Menno C. van Zelm^{1,6}

(1) Department of Immunology, (4) Center for Biomics, (5) Department of Hematology, Erasmus MC, University Medical Center Rotterdam, The Netherlands, (2) Department of Medical Biochemistry, Oslo University Hospital, Norway, (3) Volvat Medical Center, Oslo, Norway, (6) present address: Department of Immunology, Central Clinical School, Monash University, Melbourne, Victoria, Australia

Manuscript submitted

ABSTRACT

B cells with rearranged immunoglobulin (Ig) genes appear already during fetal development. Still, newborns are unable to mount antibody responses towards certain antigens, potentially caused by a restricted Ig gene repertoire. To study the nature of this restricted repertoire, we analyzed precursor-B cells and Ig gene rearrangements in fetal liver, fetal bone marrow (BM), and pediatric BM. Fetal liver and BM contained precursor-B cells with a relative increase of the early pro-B and pre-BI stages and normal contraction of the *IGH* locus. Complete *IGH* gene rearrangements showed diverse V, D and J gene usage, but the junctional regions were short due to fewer N-nucleotides; this was also observed in *IGH* rearrangements of precursor-B-cell leukemia cells of presumed prenatal origin. Fetal pro-B and pre-BI cells expressed less TdT, XRCC4, ATM, IL-7R α and FLT3, which might contribute to the different Ig repertoire. Indeed, progenitor-B cells from IL7R α -deficient patients had low TdT expression and fewer N-nucleotides in D_H-J_H junctions than controls. Our data indicate that fetal precursor-B cells form a diverse but skewed Ig repertoire, likely due to decreased IL-7R signaling and subsequent altered *IGH* junction processing. These new insights provide a better understanding of the build-up of adaptive immunity in the developing fetus.

INTRODUCTION

During the second trimester of human fetal development, B cells are generated in the liver and bone marrow (BM), providing the neonate with a diverse immunoglobulin (Ig) repertoire. Still, antibody responses towards certain antigens (e.g. tetanus or diphtheria toxoid) are impaired in neonates, and the ability to respond is only acquired with age.¹⁻³ Various processes can underlie this initial inability to mount such responses, including a “pre-mature” diversity of the Ig repertoire.

B-cell development has been extensively studied in human postnatal BM, where 5 distinct stages can be identified. In the early pro-B and pre-BI cell stages, D to J gene rearrangements and V to DJ gene rearrangements are induced in the Ig heavy chain (*IGH*) locus.^{4,5} Functional IgH proteins are expressed on the membrane together with surrogate light chain molecules VpreB and λ 14.1 to induce proliferation and further differentiation into pre-BII large cells.⁶⁻⁸ Subsequently, the cells induce V to J gene rearrangements in their Ig light chain loci (*IGK* or *IGL*) as pre-B-II small cells and the complete Ig molecule is selected for functionality at the immature-B cell stage prior to migration out of the BM.^{6,8} The lymphoid-specific recombination activating gene proteins 1 and 2 (Rag1 and Rag2) are crucial for V(D)J recombination of both *IGH* and Ig light chain genes through induction of double stranded DNA breaks.^{9,10} The Rag-induced double stranded DNA

breaks activate cell cycle checkpoint protein ATM and the non-homologous end joining (NHEJ) pathway,¹¹⁻¹³ which enhances diversity in the junctional region that encodes the antigen-binding complementary determining region (CDR)3. A central player is the lymphoid-specific deoxynucleotidyl transferase protein (TdT) that randomly adds N-nucleotides to the junction.¹⁴⁻¹⁶

Several studies have addressed the Ig gene repertoire in human fetuses, and reported restricted repertoires due to shorter CDR3 regions in *IGH*. This restriction was the result of limited N-nucleotides in the junctions and more frequent usage of the relatively short DH7-27, JH3 and JH4 genes.^{1, 2, 17-24} Furthermore, mouse embryos only used DH-proximal VH genes, which dramatically narrowed the Ig combinatorial repertoire.^{17, 18, 21, 22} Such restricted use was not observed in human fetuses, although the DH-proximal VH6-1 and VH1-2 genes seemed more frequently used than in cord blood.^{1, 25-28} Still, studies in human fetuses have been based on limited sequences and mostly in functional and thus positively selected rearrangements. Paucity in N-nucleotide additions has also been found in incomplete and thus unselected D-J gene junctions,¹⁹ suggestive of altered junction formation. These observations are supported by analysis of a restricted set of B-cell precursor acute lymphoblastic leukemia (BCP-ALL) in children ≤ 3 year old. These ALL from presumed fetal origin showed fewer N-nucleotide additions in *IGH* gene rearrangements than those in older children.²⁹ Nowadays, BCP-ALL are classified based on chromosomal abnormalities. Subgroups with *MLL*-rearrangements or with *TEL-AML1* fusion genes have been reported to originate from fetal B-cell progenitors. *MLL*-rearranged BCP-ALL is generally associated with a poor outcome and typically is diagnosed early in infancy, whereas *TEL-AML1* positive BCP-ALL is associated with good prognosis and has a peak incidence around 4 years of age. Both BCP-ALL subtypes have been proven to originate *in utero* based on studies in identical twins and analysis of Guthrie cards.²⁹⁻³² Previous studies have shown typical Ig rearrangement patterns in both BCP-ALL subtype,^{33, 34} but it is currently not known how the *IGH* gene repertoires of these subgroups relate to others and to their normal counterparts. Thus, the real extent of a restricted Ig gene repertoire in normal and malignant fetal B-cell progenitors, and the underlying mechanisms for the reported differences with postnatal B cells remains unclear.

We here studied the differences in formation of the Ig repertoire between fetal and pediatric B-cell precursors at 4 levels, i.e. cellular composition of the precursor-B-cell compartment in BM, epigenetic organization of the *IGH* locus, genetic composition of Ig gene rearrangements, and expression of factors involved in V(D)J recombination. With this approach, we could demonstrate in both normal and malignant fetal B-cell progenitors that the skewed V, D, and J gene usage and the paucity of N-nucleotide additions in *IGH* gene rearrangements resulted from altered V(D)J recombination rather than Ig

V. Altered V(D)J Recombination Underlies The Skewed Immunoglobulin Repertoires In Normal And Malignant B-Cell Precursors From Fetal Origin

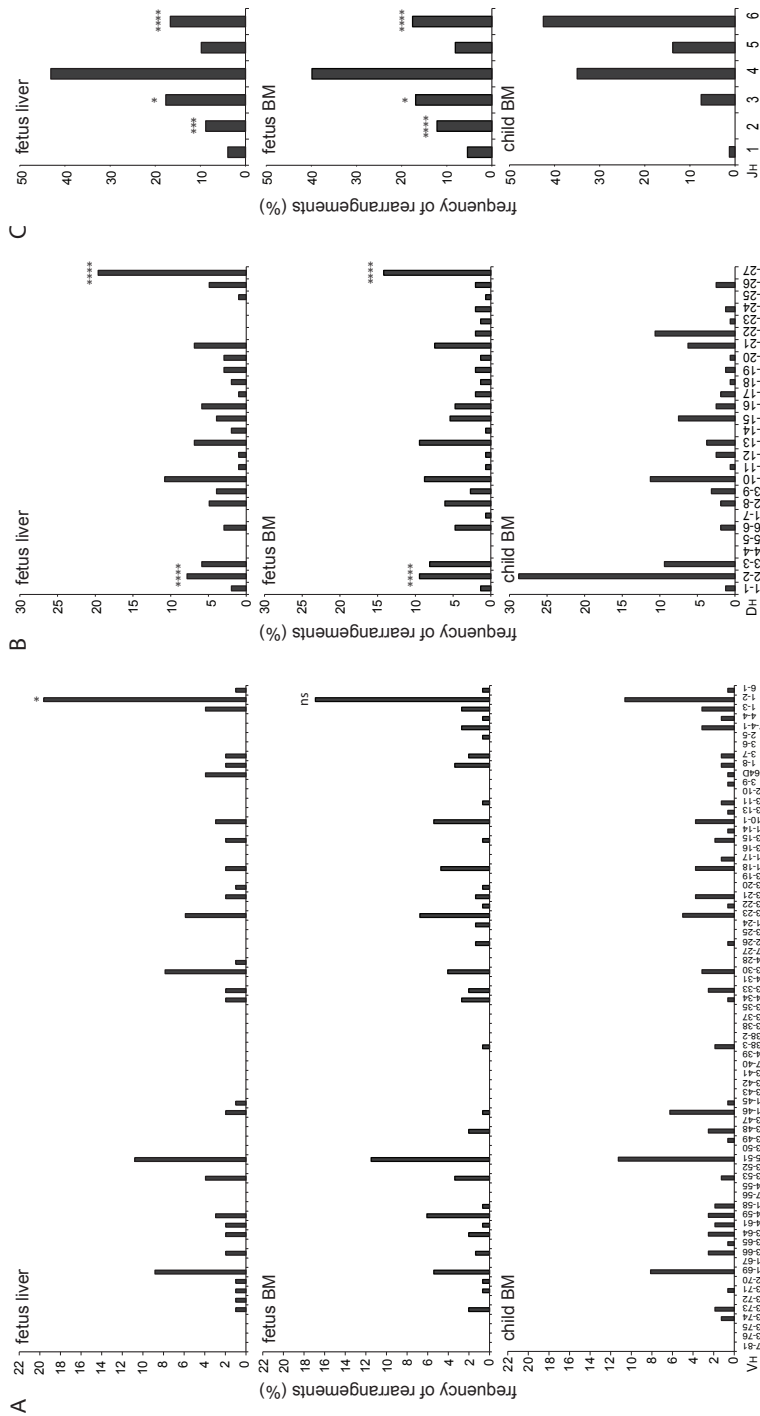


Figure 1. Skewed Ig repertoire generation in fetal B cell precursors. (A) *IGHV*, (B) *IGH* and (C) *IGHD* gene usage in bulk sorted pre-B1 cells from fetal liver, fetal bone marrow (BM) and pediatric BM. *IGH* gene rearrangements were amplified from DNA, and both in-frame and out-of-frame rearrangements were included in the analysis. The genes are ordered according to their genomic positions in the locus (IMGT).³⁷ In total, 102 sequences were derived from 3 fetal liver samples, 148 sequences from 4 fetal BM samples and 160 from 5 pediatric BM donors. Data from individual samples showed similar patterns of gene usage. Statistical significance in gene usage between fetal liver and pediatric BM, and fetal BM and pediatric BM was determined with the χ^2 test. *, $p < 0.05$; **, $p < 0.01$; ***, $p < 0.001$; ****, $p < 0.0001$; ns, not significant.

repertoire selection. These rearrangements were formed in a different molecular environment with reduced expression of XRCC4, TdT and ATM, as well as IL7R α and FLT3.

RESULTS

Skewed Ig repertoire generation in fetal B-cell precursors

To study the Ig repertoire formation in fetal development, we purified B-cell subsets from 2nd trimester fetal BM and fetal liver, as well as from neonatal cord blood and pediatric BM. In line with previous observations,^{1, 19, 20, 23-26, 28, 35} mature B cells (CD19⁺CD20⁺CD10⁺IgM⁺IgD⁺) in fetal BM showed more frequent usage of V_H1-2, D_H7-27, J_H2 and J_H3 genes than pediatric B cells (**Figure S1**). This was typical for early development, because the *IGH* repertoire in B cells from neonatal cord blood was more similar to pediatric than to fetal B cells. Moreover, CD19⁺CD34⁺CD10⁺ pre-BI cells derived from either fetal liver or fetal BM already contained the same skewed *IGH* repertoire (**Figure 1A-C**). These pre-BI cells initiate V_H to D_{JH} gene rearrangements, but do not yet express cytoplasmic IgM and are not selected for functional *IGH* genes.³⁶ This was supported by analysis of only the out-of-frame and thus unproductive *IGH* gene rearrangements (**Figure S2A-C**). Approximately 1/3rd of the pre-BI cells carried in-frame and thereby potentially productive *IGH* gene rearrangements (31% in fetal liver, 29% in fetal BM and 33% in pediatric BM). Thus, fetal B-cell progenitors are generated with a skewed *IGH* gene repertoire, which is similar between fetal liver and fetal BM, and does not seem to be affected by selection processes.

In contrast to *IGH*, the *IGK* gene repertoire was not different between fetal and pediatric mature B cells nor small pre-B-II cells (**Figures S3, S4**). Because the vast majority of *IGK* gene rearrangements are formed in small pre-B-II cells, the formation and selection processes for the *IGK* repertoire do not seem to differ between pediatric and fetal B-cell development.

Short D_H genes and fewer N-nucleotides in fetal B cells

In addition to the skewed V, D and J gene usage, *IGH* gene rearrangements in fetal naïve mature B cells carried shorter IgH-CDR3 than pediatric B cells (**Figure 2A-B**).^{1, 2, 19, 20, 24, 38} This was mostly the result of fewer N-nucleotide additions in both the D_H-J_H and V_H-D_{JH} junctions. The IgH-CDR3 of B cells from neonatal cord blood were intermediate in size between fetal and pediatric B cells with slightly more N-nucleotides in the V_H-D_{JH} junction than fetal B cells. Both in fetal and in pediatric tissue, the IgH-CDR3

regions in pre-BI cells were larger than in naive mature B cells. Still, fetal pre-BI carried shorter IgH-CDR3 with fewer N-nucleotides than their pediatric counterparts (**Figure 2B**).

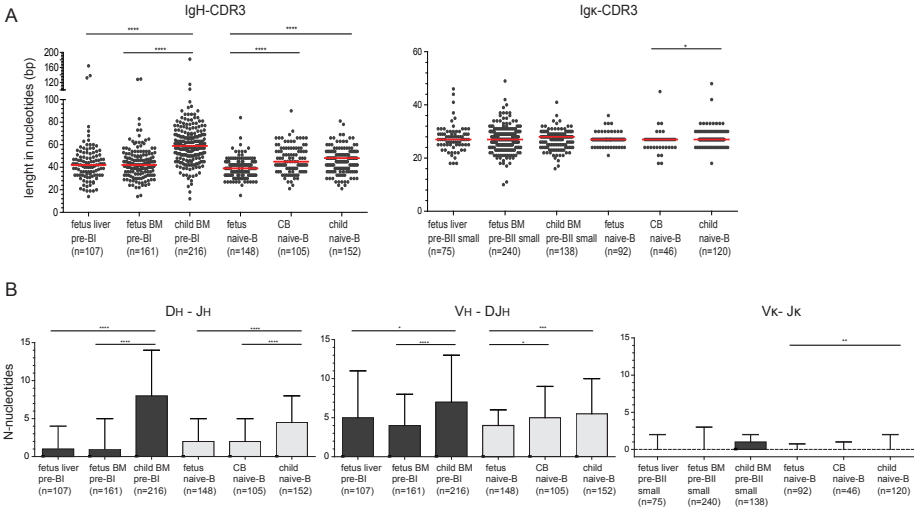


Figure 2. Fetal B cells have short IgH-CDR3 regions and few N-nucleotides. (A) Scatter plots showing the CDR3 length in nucleotides of *IGH* and *IGK*. Red horizontal lines represent median values. (B) Bar graphs showing the median numbers of N-nucleotides in DH-JH, VH-DJH and Vκ-Jκ junctions with inter-quartile range. Numbers in brackets indicate the amount of analyzed sequences. Both in-frame and out-of-frame rearrangements were included in the analysis of precursor-B cells, whereas only in-frame functional rearrangements were included for the analysis of naive mature-B cells. The nonparametric Mann-Whitney U test was used to calculate significance levels. *, p<.05; **, p<.01; ***, p<.001; ****, p<.0001.

On top of junctional region processing, the choice of DH affects the IgH-CDR3 size, because DH genes differ greatly in size. Indeed, the DH7-27 gene that was abundantly found in fetal B cells is the shortest of all D genes. In addition, the large DH genes were less frequently used in fetal than in pediatric B cells (**Figure S5A-B**). Still, as previously suggested,¹⁹ N-nucleotide additions seem dependent on DH gene usage. The incomplete DH-JH rearrangements involving the short DH7-27 carried more N-nucleotides than rearrangements involving any other DH gene families (**Figure S5C**). Finally, the shorter IgH-CDR3 in naive mature B cells than in pre-BI cells (**Figure 2**) was associated with selection against long DH genes. Thus, the IgH-CDR3 size seems tightly regulated through N-nucleotide additions and DH gene usage, which differ between fetal and pediatric B-cell progenitors.

In contrast to *IGH*, the *IGK* locus does not contain D genes, and Vκ-Jκ gene rearrangements hardly contain any N-nucleotide, thus rendering small CDR3 regions. Indeed, the Igκ-CDR3 regions of the fetal, neonatal and pediatric B-cell subsets were

much smaller than IgH-CDR3 and did not show overt differences between any of the subsets (**Figure 2A**). Although the pediatric naive mature B cells tended to have more N-nucleotide additions (**Figure 2B**), there was no indication of a different Igκ-CDR3 repertoire in fetus.

B cells in BCP-ALL of presumed fetal origin show fetal Ig repertoire characteristics

Our data indicate that normal B-cell precursors from fetal tissue differ from children. To study whether these cellular and molecular differences were retained in a disease model, we analyzed the *IGH* gene repertoire in BCP-ALL patients. BCP-ALL can be classified based on chromosomal aberrations. Of these subgroups, BCP-ALL with *MLL* rearrangements or with *TEL-AML1* fusion genes can originate *in utero*.²⁹⁻³² We therefore studied the *IGH* gene repertoire of these presumed fetal BCP-ALL subgroups and compared with the rest, i.e., subgroups containing *E2A-PBX* translocations, *BCR-ABL* translocations, hyperdiploidy or none of these abnormalities. The average age in years at diagnosis was 0.65 ± 0.68 for *MLL* rearranged BCP-ALL and 4.85 ± 2.95 for *TEL-AML1*-positive BCP-ALL, while the non-fetal origin group aged 6.39 ± 4.18 .

The BCP-ALL of presumed fetal origin indeed showed increased usage of the D_H-proximal VH6-1 gene, similar to fetal B cells (**Figure 3A**). In contrast, the usage of D_H and J_H genes did not differ between the BCP-ALL patients (**Figure 3B-C**). Still, BCP-ALL of presumed fetal origin showed a trend to less frequently use long D_H genes than the other BCP-ALL (**Figures S5A, S6A**), and the IgH-CDR3 length was shorter in BCP-ALL of presumed fetal origin. The latter was mostly due to significantly fewer N-nucleotides in D_H-J_H junctions (**Figure 3D-E**), and equally apparent in BCP-ALL with *MLL*-rearrangements and with *TEL-AML1* translocations (**Figure S6B-C**).

Concluding, these observations in BCP-ALL confirm and extend our results that the *IGH* gene repertoire differences between fetus and child are the result of altered V(D)J recombination processes in early progenitors rather than Ig repertoire selection processes in mature B cells.

Enrichment of early B-cell precursors in fetal liver and BM

To study the nature of the skewed *IGH* gene repertoire generation in prenatal development, we first analyzed the precursor-B cells in fetal liver and BM in more detail by flow cytometry. The relative distributions of the five major precursor-B-cell subsets in these fetal tissues were determined using a panel of membrane and intracellular markers and compared with pediatric BM (**Figure 4A**).^{39, 40} The frequencies of the pro-B, pre-BII

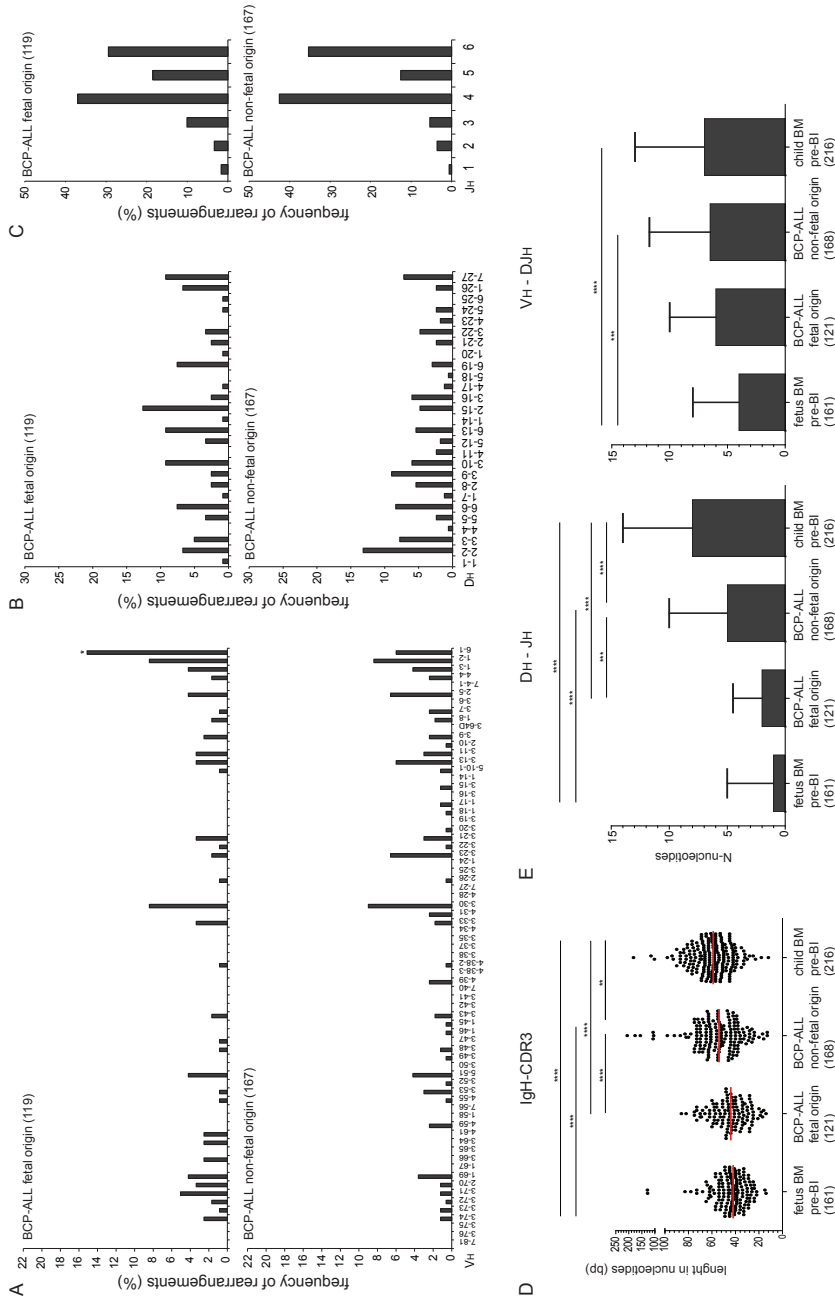


Fig. 3. BCP-ALL of presumed fetal origin show fetal Ig repertoire characteristics. (A) *IGHV*, (B) *IGHD* and (C) *IGHJ* gene usage in *IGH* gene rearrangements. (D) Scatter plots showing the IgH-CDR3 length in nucleotides with inter-quartile range. Data include in-frame and out-of-frame *IGH* gene rearrangements from BCP-ALL samples. BCP-ALL of fetal origin and VH-DJH junctions with inter-quartile range. Data include in-frame and out-of-frame *IGH* gene rearrangements from BCP-ALL samples. BCP-ALL of fetal origin included MLL-rearranged (n=19) and TEL-AML1 positive (n=102) cases, whereas the E2A-PBX positive (n=8), BCR-ABL positive (n=7), hyperdiploid (n=74) and other cases (n=79) constituted group of BCP-ALL from non-fetal origin. Healthy fetal and pediatric BM data are reproduced from the Fig. 2. The numbers of sequences are indicated between brackets. Genes coordinates within the *IGH* locus were retrieved from IMGT.³⁷ Statistical significance was determined with the χ^2 test (panels A-C) or the Mann-Whitney U test (panels D and E); ***, p<.001; ****, p<.0001.

large and pre-BII small within the total CD22⁺ B-cell precursors were similar between fetal liver and fetal BM. Fetal livers contained on average less pre-BI and more immature-B cells, but these differences were not significant. Both fetal tissues contained more CD34⁺ precursors than pediatric BM (**Figure 4B**). This was mostly the result of increased pro-B cell frequencies (~12% vs 4%), and was to the expense of reduced pre-BII large frequencies (~10% vs 20%).

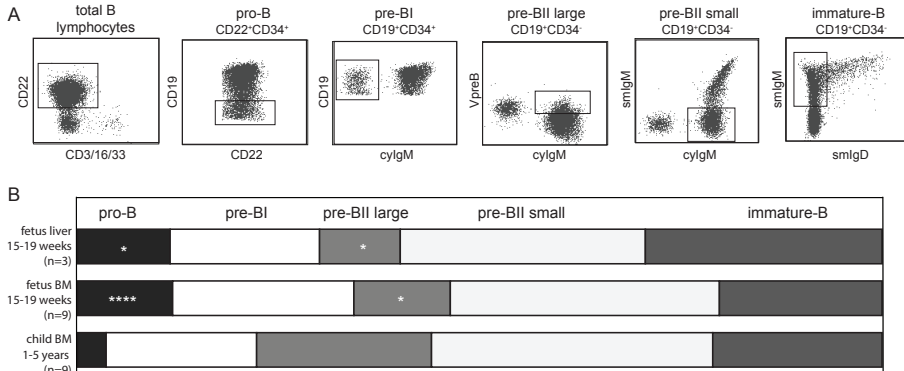


Figure 4. Relative increase of early precursor-B cells in fetus. (A) Gating strategy to define 5 precursor B-cell subsets according to previous studies.^{36, 39, 40} (B) Relative distributions of the 5 precursor-B-cell subsets in fetal liver, fetal BM and pediatric BM. The nonparametric Mann-Whitney U test was used to calculate significance levels between fetal and pediatric paired populations. *, $p < 0.05$; ****, $p < 0.0001$

***IGH* locus contraction in fetal precursor-B cells**

The skewed Ig repertoire formation and developmental block observed in fetus at pro-B/pre-BI stage could potentially result from inefficiently formed *IGH* gene rearrangements. To study whether the *IGH* topology provided optimal conditions for V(D)J recombination, we measured spatial distances between distal V_H, proximal V_H, and C_H regions with 3D DNA FISH in precursor-B cells of fetal and pediatric BM (**Figure 5A**). In line with our previous studies,^{41, 42} spatial distances between all three DNA regions were short in pediatric pre-BI cells and slightly, yet significantly, larger in pediatric pre-BII small cells (**Figure 5B-C**). *IGH* locus contraction did not seem defective in fetal pre-BI cells, as all spatial distances between C_H and both V_H regions were similarly small and between both V_H regions even smaller than in pediatric pre-BI cells. *IGH* locus contraction is therefore likely to facilitate rearrangement of both proximal and distal V_H gene rearrangements similarly between fetal and pediatric B-cell precursors. Still, it does not provide further insight into the relative abundance of V_H1-2 in the fetal *IGH* gene repertoire.

V. Altered V(D)J Recombination Underlies The Skewed Immunoglobulin Repertoires In Normal And Malignant B-Cell Precursors From Fetal Origin

Table 1. Gene expression profiling of fetal and pediatric precursor-B cells.

	Pro-B				Pre-BI			
	mean fetus	mean child	fold change	p-value	mean fetus	mean child	fold change	p-value
E2A (TCF3)	226.09	154.98	1.5	0.02	259.49	209.27	1.2	0.02
ID2	121.79	43.51	2.8	0.23	195.40	80.31	2.4	0.03
EBF1	389.42	876.11	-2.3	0.33	1182.40	1090.52	1.1	0.12
PAX5	257.97	189.37	1.4	0.52	618.04	456.95	1.4	0.02
HEB (TCF12)	87.07	224.12	-2.6	0.07	204.00	279.67	-1.4	0.01
PU.1 (Sp1)	90.22	57.57	1.6	<0.01	91.75	72.83	1.3	0.06
Foxo1	182.02	167.64	1.1	0.56	231.92	224.62	1	0.58
IRF4	99.81	81.96	1.2	0.45	140.36	135.16	1	0.87
IRF8	106.55	48.62	2.2	0.03	113.48	74.69	1.5	0.02
IKZF1 (Ikaros)	86.01	151.17	-1.8	0.05	201.46	172.66	1.2	0.25
IKZF2 (Helios)	59.77	65.55	-1.1	0.77	248.02	277.30	-1.1	0.66
IKZF3 (Aiolos)	21.92	17.95	1.2	0.43	58.31	76.44	-1.3	0.32
RAG1	103.62	121.84	-1.2	0.47	165.91	150.29	1.1	0.39
RAG2	113.90	209.38	-1.8	0.43	227.32	309.86	-1.4	0.05
XRCC5 (Ku80)	186.08	554.95	-2	0.15	606.18	725.66	-1.2	0.04
XRCC6 (Ku70)	44.06	39.20	1.1	0.50	48.62	31.89	1.5	0.09
DNA-PKcs (PRKDC)	60.68	196.41	-3.2	0.01	149.73	290.76	-1.9	0.02
Artemis (DCLRE1C)	41.31	71.56	-1.7	0.02	87.42	121.32	-1.4	0.03
XRCC4	31.30	80.04	-2.6	0.049	79.37	124.96	-1.6	0.049
XLF (NHEJ1)	51.80	49.12	-1.1	0.26	54.44	49.08	1.1	0.14
LIG4	243.02	300.93	-1.2	0.84	746.53	472.78	1.6	0.14
TdT (DNNTT)	399.84	1693.51	-4.2	0.17	1111.20	1656.59	-1.5	0.02
pol λ	47.36	31.85	1.5	0.15	33.68	31.84	1.1	0.52
pol μ	85.47	55.48	1.5	0.02	74.14	58.40	1.3	0.05
ATM	48.57	166.38	-3.4	0.04	106.49	199.37	-1.9	0.01
MRE11A	41.67	169.07	-4.1	0.02	96.98	212.86	-2.2	<0.01
NBS (NBN)	43.04	174.16	-4.1	0.02	85.99	178.98	-2.1	0.02
Rad50	96.36	290.60	-3	0.15	264.57	326.31	-1.2	0.049

	CD22	83.09	64.89	1.3	0.18	545.90	295.23	1.9	<0.01
	CD19	117.52	68.81	1.7	0.01	138.91	82.83	1.7	<0.01
	CD34	210.88	295.12	-1.4	0.42	329.68	268.36	1.2	0.48
	CD10	217.69	969.99	-4.5	0.15	880.24	1275.02	-1.5	0.03
	CD79A	150.68	139.54	1.1	0.86	268.79	143.01	1.9	<0.01
	CD79B	183.05	103.54	1.8	0.27	228.40	158.76	1.4	0.05
	VPREB1	297.75	501.40	-1.7	0.49	778.90	644.68	1.2	0.18
	IL14.1 (IGLL5)	38.86	29.63	1.3	0.10	36.88	35.34	1	0.24
	BTK	106.92	142.97	-1.3	0.50	193.35	183.15	1.1	0.64
	SYK	106.83	170.55	-1.6	0.23	208.60	219.74	-1.1	0.14
	BLNK	284.80	812.93	-2.9	0.20	696.87	672.31	1	0.68
	IGHG1	89.03	65.57	1.4	<0.01	110.02	82.20	1.3	0.01
	IGKC	137.41	54.08	2.5	0.09	313.73	192.59	1.6	0.10
	IL2RG	100.12	238.93	-2.4	0.05	174.79	155.79	1.1	0.28
	Ki-67 (MKI67)	182.64	305.69	-1.7	0.39	689.30	833.39	-1.2	0.24
	IL7R α	44.38	171.98	-3.9	0.04	169.35	150.13	1.1	0.75
	LEF1	258.38	355.16	-1.4	0.7	893.34	1002.85	-1.1	0.03
	STAT5A	80.84	67.61	1.2	0.23	89.54	77.34	1.2	0.06
	STAT5B	66.58	92.58	-1.4	0.09	85.84	90.19	-1.1	0.43
	JAK1	170.76	303.35	-1.8	0.35	419.79	366.42	1.2	0.01
	JAK2	38.05	81.16	-2.1	<0.01	39.67	76.44	-1.9	0.07
	JAK3	61.46	42.30	1.5	0.06	60.12	48.21	1.3	0.02
	TYK2	77.17	56.01	1.4	0.049	75.25	64.44	1.2	0.64
	FLT3	34.20	279.61	-8.2	0.01	64.21	157.15	-2.5	0.30
	c-KIT	35.86	73.68	-2.1	0.03	31.01	32.66	-1.1	0.02

Differences in gene expression levels between fetus and child which showed $p < 0.05$ and fold change > 1.5 are marked in bold. Statistical significance was calculated with one-way ANOVA test. Gene expression profiling was performed on pro-B and pre-B1 cells purified from 3 fetal BM and 4 pediatric BM donors.

V. Altered V(D)J Recombination Underlies The Skewed Immunoglobulin Repertoires In Normal And Malignant B-Cell Precursors From Fetal Origin

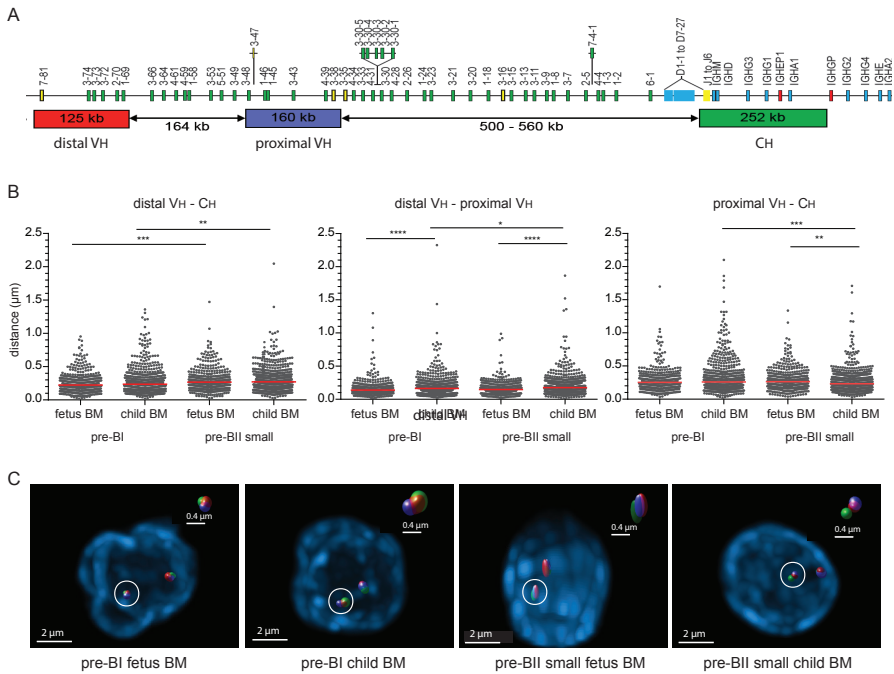


Figure 5. IGH locus contraction in fetal and pediatric B-cell precursors. (A) Schematic representation of the human *IGH* locus including the combinations of bacterial artificial chromosome clones that were used as three-dimensional immunofluorescence in situ hybridization (3D FISH) probes.^{41, 42} (B) Scatter plots of distances separating distal V_H, proximal V_H, and C_H regions in pre-BI and pre-BII small cells purified from fetal and pediatric BM. For each condition, at least 200 alleles from 2 donors were analyzed. Red horizontal lines represent median distances. The nonparametric Mann–Whitney U test was used to calculate significance levels. *, p<0.05; **, p<0.01; ***, p<0.001. (C) Representative fluorescence microscopy images of *IGH* loci in precursor B cell subsets

Mechanisms causing formation of skewed Ig repertoire in fetuses

To delve deeper into the mechanism responsible for generation of the different Ig repertoires between fetal and pediatric early B-cell progenitors, we performed genome-wide gene expression profiling of fetal and childhood B-cell progenitors (Figure S7A). The analysis was performed in fetal pro-B and pre-BI cells, which were compared to previously published childhood subsets,⁴¹ and was focused on genes important for B-cell

Figure 6. (A) TdT, (B) IL-7Rα, (C) Ki-67, and (D) FLT3 protein expression levels in B-cell progenitors. Graphs represent merged data from 3 fetal BM and 3 pediatric BM samples as determined by flow cytometry analysis. Immature-B cells of pediatric BM were included as a negative control. The median fluorescence intensities (MFI) for each subset are indicated in each plot.

Formation of the Immunoglobulin Repertoire in Precursor-B-cell Development

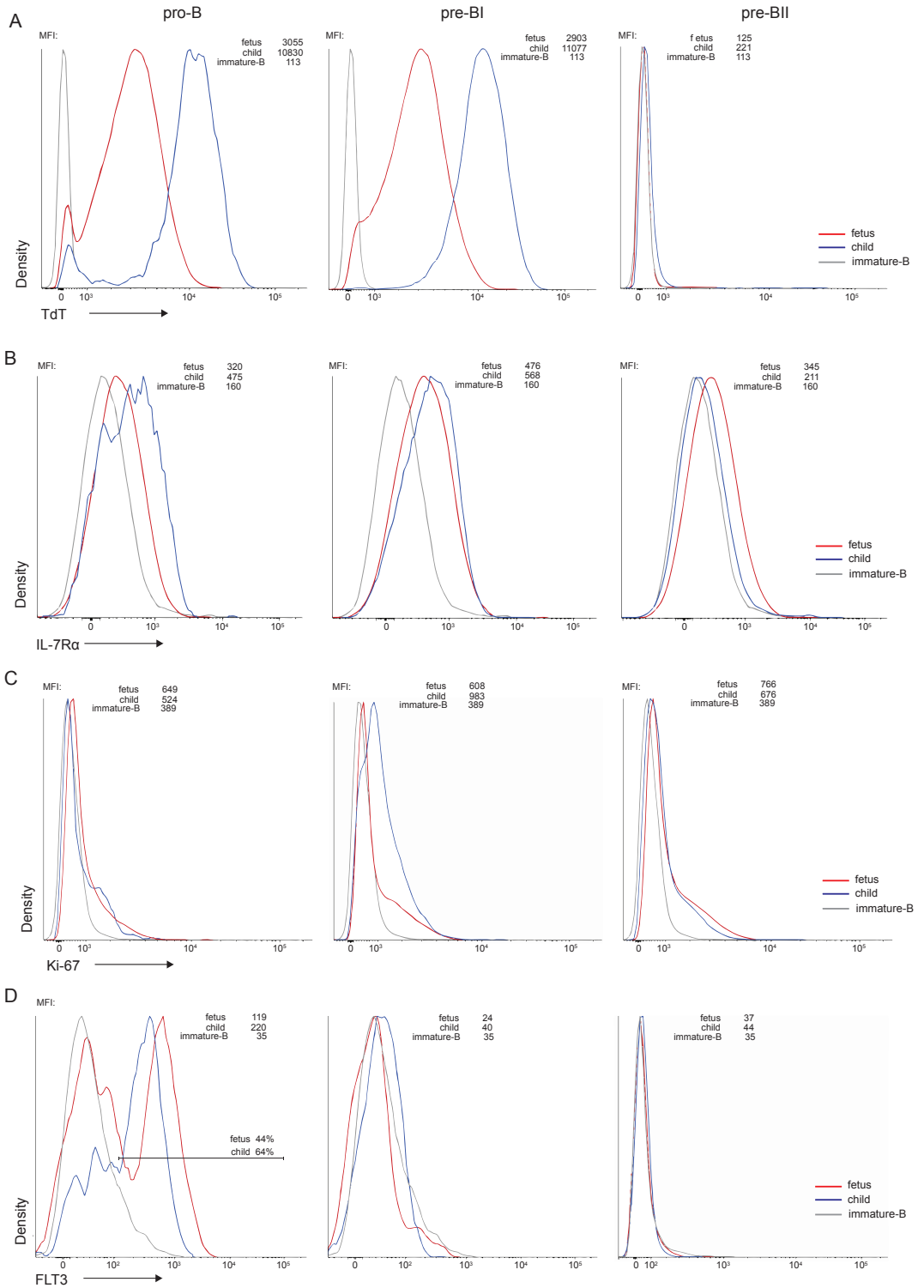


Figure 6. (Legend at the bottom of the previous page)

development and V(D)J recombination to provide insights into the molecular environment in which Ig gene rearrangements are formed.

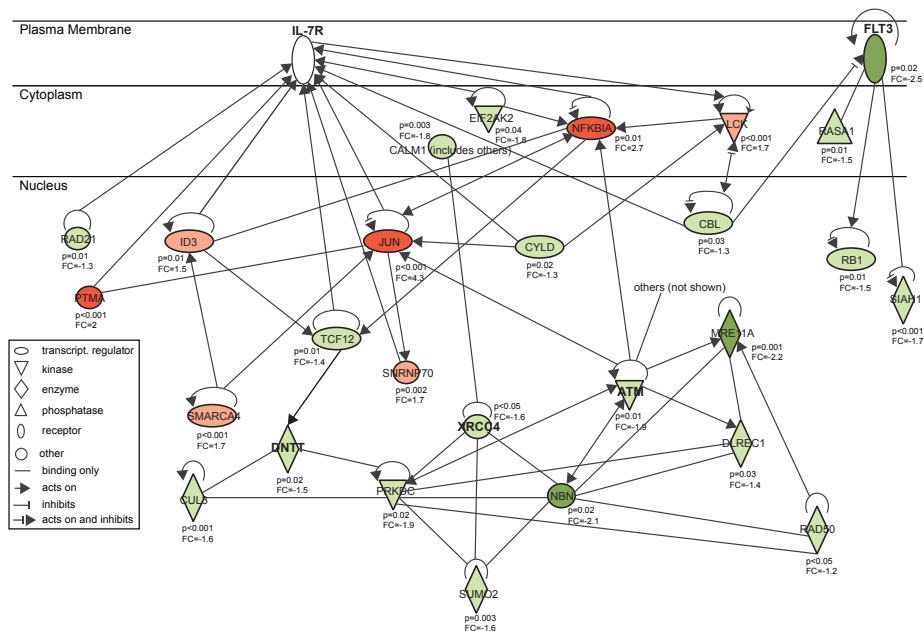
The expression of RAG1 and RAG2 was similar between fetus and child for both pro-B and pre-BI cells. However, gene encoding XRCC4 that is part of the NHEJ pathway,¹³ was downregulated in fetus (**Table 1** and **Figure S7B**). XRCC4 forms a protein complex with TdT, the enzyme responsible for N-nucleotide additions, and it was shown that XRCC4 promotes N-nucleotides addition by TdT.⁴³ Importantly, we also observed decreased expression of DNTP1, which encodes TdT (**Table 1**). Additional intracellular TdT staining by flow cytometry revealed that these decreased transcripts resulted in decreased protein levels in both pro-B and pre-BI in fetuses (**Figure 6A**). Thus, fetal B-cell precursors differ from their pediatric counterparts in the repair of Rag-induced DNA breaks, and especially in the levels of XRCC4 and TdT expression.

The genes encoding key B-cell transcription factors E2A and PAX5 were highly expressed in fetal progenitors, as was FOXO1, which regulates RAG gene expression.⁴⁴ ⁴⁵ This is in line with the diverse IGH gene repertoire and normal RAG transcripts in fetus. Furthermore, the genes encoding pre-BCR signaling components were normally expressed and do not seem rate-limiting for differentiation into pre-BII cells. ATM transcripts were downregulated in fetuses (**Table 1** and **Figure S7B**). Because ATM is important for cell cycle arrest and recruitment of NHEJ factors to DNA breaks,^{11, 12, 46, 47} this could affect Rag-induced break repair and a relative increase of early precursor-B cells due to delayed formation of a functional IgH (**Figure 4B**).

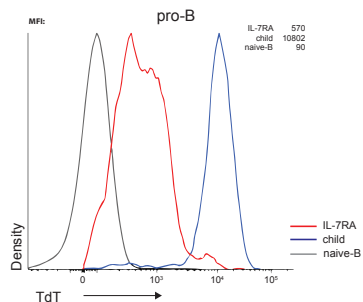
IL-7R signaling affects IGH gene rearrangements and inhibits IGK gene rearrangements.^{42, 48, 49} Fetal pro-B cells showed low expression of IL7R α transcripts and membrane protein (**Table 1** and **Figure 6B**). In addition, transcripts encoding the IL-7R signaling molecule JAK2 were reduced. Furthermore, transcripts of ID2 and germline IGK, which are suppressed by IL-7R signaling,⁵⁰⁻⁵² were upregulated (**Table 1**). The decreased IL-7R α expression did not seem to affect proliferation as transcripts for nuclear Ki-67 levels were not different between fetuses and children (**Table 1** and **Figure 6C**). FLT3, the hematopoietic progenitor cell receptor, was also downregulated in fetal pro-B cells likely affecting the signals received by the cells at early stages of development (**Table 1** and **Figure 6D**).

Together, the differences in the IGH gene repertoire and precursor-B-cell subset composition between fetal and pediatric BM seem to result from reduced expression of transcripts encoding NHEJ, TdT and signaling proteins IL-7R and FLT3 in fetus.

A



B



C

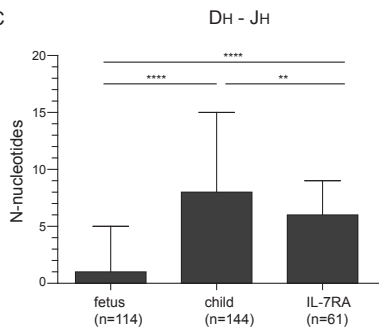


Figure 7. IL7R α -regulated expression of TdT and IGH junctional processing. (A) Functional network of molecules interacting with IL-7R, FLT3, ATM, XRCC4 and TdT (*DNTT*) in pro-B cells. Upregulated (red) and downregulated (green) transcripts in fetus vs child as determined by genome-wide expression profiling ($p < 0.05$). Dark shades indicate fold change > 2 in transcript expression, and light shades fold change between 1.5 and 2. The 5 transcripts of interest are depicted in bold font. Nodes are displayed using various shapes that represent the functional class of gene products. The interactions were identified with Ingenuity Pathways Analysis (www.ingenuity.com) starting with IL-7R, FLT3, ATM, XRCC4 and TdT (indicated in bold font). FC, fold change. (B) TdT protein expression in pro-B cells of IL7R α -deficient patients and pediatric controls. Graphs represent merged data of cyCD79A⁺CD19⁺ pro-B cells from 3 patients and 3 controls. Naive-B cells of pediatric BM were included as a negative control. The median fluorescence intensities (MFI) for each subset are indicated. (C) Bar graphs showing the median numbers of N-nucleotides in DH-JH and VH-DJH junctions with inter-quartile range. Numbers in brackets indicate the amount of analyzed sequences. Data were obtained from out-of-frame rearrangements from pre-BI cells of 3 fetal and 3 pediatric donors, and from naive-B cells of 2 IL7R α -deficient patients. The nonparametric Mann-Whitney U test was used to calculate significance levels. **, $p < 0.01$; ****, $p < 0.0001$.

TdT expression and N-nucleotide additions in *IL7R α* -deficient patients

Ingenuity pathway analysis revealed that IL-7R and FLT3 signaling interact with the NHEJ pathway (**Figures 7A and S8**), indicating that these proteins form a functional network in precursor-B cells that determine the molecular environment in which *IGH* gene rearrangements take place. To study whether the altered junction processing in fetal B cells resulted from decreased IL-7R signaling, we analyzed TdT protein expression and *IGH* junctions in B cells of *IL7R α* -deficient patients. CD79A⁺CD19⁻ pro-B cells of *IL7R α* -deficient patients showed lower nuclear TdT protein than healthy children (**Figure 7B**). Out-of-frame *IGH* gene rearrangements in B cells of these patients contained fewer N-nucleotides in the DH-JH junctions (**Figure 7C**). Since these DH-JH junctions were generated in pro-B cells,³⁶ and were not subjected to selection processes, this confirms that IL-7R signaling affects *IGH* junction processing.

DISCUSSION

In the present study, we showed that already during fetal development a diverse Ig repertoire is formed. Still, this repertoire is skewed with regards to combinatorial diversity but more importantly to junctional diversity as compared to pediatric-B cells. These changes were the result of an altered balance in V(D)J recombination components, as they were evident in unselected B-cell progenitors and fetal-derived BCP-ALL. Fetal B-cell progenitors showed decreased expression of several NHEJ factors and cytokine receptors and analysis of *IL7R α* -deficient patients revealed that IL-7R signaling affects TdT protein-dependent N-nucleotide additions in the *IGH* junctions.

The fetal Ig repertoire has been a subject of study for the past 3 decades.^{1, 2, 19, 20, 23-28, 35} Differences with postnatal B cells have been reported regarding V, D, and J gene usage, as well as N-nucleotide additions,^{1, 19, 20, 23, 35} but unfortunately the results were ambiguous and included evident differences between studies.^{1, 25, 35} We acknowledged the apparent difficulties in the assessment of the fetal Ig repertoire, and took a two-step approach to tackle these. First, we assessed the repertoire in single-sorted naive mature B cells, thereby avoiding potentially preferential PCR-based amplification of V genes. Consequently, we obtained an unbiased view of the naive B cell-repertoire. Secondly, we amplified *IGH* and *IGK* gene rearrangements from early precursors that have not yet been selected for in-frame rearrangements.³⁶ This approach allowed us to study which of the characteristics in the mature repertoire were the result of altered V(D)J recombination processes rather than selection. Thus, we confirmed that the fetal naive mature Ig repertoire contained more VH1-2, DH7-27, JH2 and JH3 genes than pediatric B cells.^{1, 19, 20, 23} Despite the high VH1-2 usage, the DH-proximal VH genes were in general not more frequently used in

the human fetal repertoire,²⁵⁻²⁷ in contrast to the mouse.^{17, 18, 21, 22} Importantly, we now established that these changes in the *IGH* gene repertoire were the result of altered V(D)J recombination, and not due to changes in Ig repertoire selection.

The skewed *IGH* gene repertoire in fetus did not seem to result from changes in chromatin organization as the *IGH* locus in fetal B-cell precursors was highly contracted. Moreover, critical transcription factors for this process, such as E2A and Pax5 were highly expressed. The 3D spatial organization would thus normally support the utilization of diverse V_H genes in fetal B-cell precursors independent of genomic proximity to the D_H-J_H-C_H region.^{17, 18, 21, 22} It is possible that the V_H1-2, D_H7-27, J_H3 and J_H4 genes were more efficiently recombined due to their optimal RSS sequences (www.imgt.org). However, *RAG* gene expression was equally high in both fetal and pediatric B-cell progenitors, making it difficult to understand how these were rate-limiting in fetus. Alternatively, the V_H1-2 gene promoter activity could be affected by B-cell intrinsic or extrinsic factors. A likely candidate pathway would be IL-7R signaling that is known to affect *IGH* locus activity.^{42, 53} We were unable to study the production of IL-7 in fetal or pediatric BM, but we did find evidence for reduced IL-7R α expression and lower IL-7R signaling in fetal B-cell progenitors, indicating that specific changes in V_H gene usage could be the result of altered susceptibility for IL-7.

We found additional evidence for differences in the generation of *IGH* gene rearrangements in fetal precursors through analysis of BCP-ALL. ALL cases with *MLL* rearrangements or *TEL-AML1* translocations can arise already during fetal development. Although not all cases will actually have a prenatal origin, our comparison of these cases with other BCP-ALL subsets confirmed previously observed paucity of N and P nucleotides in *IGH* junctions in ALL cells in neonatal blood spots⁵⁴ and low TdT transcript levels in *MLL*-rearranged BCP-ALL.⁵⁵ Furthermore, we report similar changes in the V_H, D_H and J_H gene usage as in normal fetal B-cell precursors. Considering the distinct gene expression repertoires between fetal and postnatal B-cell precursors, our observations in BCP-ALL indicate that those of *in utero* origin will be derived from distinct precursors than other ALL. Thus, it is possible that the differences between BCP-ALL subsets will not only be determined by their genetic abnormalities, but also by their origin from fetal or postnatal precursor-B cells.

The fetal mature *IGH* gene repertoire has been consistently shown to contain only few N-nucleotides.^{1, 20, 35, 56} We here extended these findings to unselected B-cell precursors, thereby showing that these were the result of altered TdT activity. In addition, transcripts encoding NHEJ factor XRCC4 were reduced in fetal B-cell precursors. Because TdT acts during DNA repair via NHEJ, XRCC4 affects TdT function as well.⁴³ Moreover, our analysis of IL7R α -deficient patients provided the first evidence of cytokine-receptor mediated expression of TdT and consequent *IGH* junction processing. Despite complete

absence of a functional IL-7R, IL7R α -deficient patients showed more N-nucleotide additions in *IGH* than fetal progenitor-B cells that still expressed low levels of IL-7R α . Thus, TdT expression and function do not completely depend on IL-7R signaling. In contrast to IL7R α -deficient patients, who only have a defect in *IL-7R α* , fetal B-cell progenitors had downregulated FLT3 and XRCC4. The combined effects of two cytokine signaling pathways might have a stronger impact on TdT and XRCC4 function as it was previously shown that the IL-7R acts in synergy with Flt-3 signaling to expand the hematopoietic progenitors.⁵⁷

What would be advantage of having low TdT activity in fetal B-cell precursors? A potential explanation can be derived from studies in TdT deficient mice.⁵⁸ In a competitive setting with TdT-proficient B-cell precursors, TdT-deficient B cells developed quicker and demonstrated an advantage in populating peripheral lymphoid tissues. Through low TdT expression, the developing fetus would thus be able to provide a fast wave of B cells. Decreased ATM expression likely further enhanced expansion of early progenitor-B cells in fetus with less strict processing of *IGH* junctions. Considering the low levels of TdT in fetal thymus,⁵⁹⁻⁶² and the low numbers of N-nucleotides in *TRB* junctions,⁵⁶ it is likely that similar mechanisms apply for T cells. Importantly, we did not find differences in *IGK* between fetus and child. This is partly due to the already low TdT activity in junctional processing and was obvious from the low TdT expression levels in pre-BII cells. Considering the absence of differences in V κ and J κ gene usage, it appears that, in contrast to pre-BI cells that rearrange *IGH*, pre-BII cells from fetus are more similar to pediatric pre-BII cells regarding V(D)J recombination processes. In addition to fast formation of *IGH* gene rearrangements, selection processes could be affected. The naive B cell repertoire contains fewer long IgH-CDR3 regions than B-cell precursors, indicating that these would be negatively selected. By reducing the number of B cells with long IgH-CDR3, more precursors might be included in the mature compartment resulting in more efficient B-cell generation during fetal life.

Taken together, we here showed that the skewed fetal *IGH* gene repertoire that has been postulated to contribute to the poor ability of neonates to mount humoral responses, was the result of altered V(D)J recombination, rather than repertoire selection. Specifically, fetal pro-B and pre-BI cells expressed reduced levels of a network of components that included receptors IL-7R α and FLT3, as well as DNA repair factors ATM, XRCC4 and TdT, thereby containing an altered molecular environment in which the skewed *IGH* gene repertoire is formed. These new insights into precursor-B cell development could contribute to a better understanding of the build-up of adaptive immunity in the developing fetus.

MATERIALS AND METHODS

Fetal and postnatal tissue

The use of human fetal and pediatric tissue, and cord blood was approved by the Medical Ethical Committees of the Erasmus MC and Eastern Norway, and was contingent on informed consent in accordance with the Declaration of Helsinki. Fetal liver (3 donors) and fetal BM (9 donors) were obtained from elective abortions. Gestational age was determined by ultrasonic measurement of the diameter of the skull and ranged from 15 to 19 weeks. Four blood samples were obtained from the umbilical cord vein after birth, and 12 pediatric BM samples from children aged 2-11 years.^{36, 41} PBMC and BM B cells from IL-7R α -deficient patients were obtained from left-over material of the diagnostic work-up. The IL-7RA mutations all resulted in premature stop codons. Anonymized data from routine diagnostics of children (aged 1-18 years) diagnosed in the Erasmus MC between 2004-2014 with B-cell precursor acute lymphoblastic leukemia (BCP-ALL) were retrospectively analysed.

Flow cytometric immunophenotyping and cell sorting

Flow cytometric immunophenotyping for B-cell subsets analysis in pediatric BM aspirates, fetal limb BM suspensions and fetal liver homogenates was performed as described previously.^{39, 40} Additional stainings were performed for expression analysis using: CD20-PB (2H7), IgM-BV510 (MHM-88), IgD-PerCP-Cy5.5 (IA6-2), CD127-APC (A019D5; all from BioLegend), CD34-FITC (8G12), CD22-PE (S-HCL-1), CD19-PE-Cy7 (SJ25C1), CD34-APC (8G12, all from BD Biosciences) and CD10-APC-C750 (HI10A, Cytognos). TdT-FITC (HT-6) and Ki-67-FITC (KI-67; both from Zebra Biosciences) were used following fixation and permeabilization (AnDerGrub). Cells were acquired on a LSRII flow cytometer (BD Biosciences) and analyzed with FACSDiva (BD Biosciences) and Infinicyt software (Cytognos).

B cell subsets were purified from pediatric BM aspirates, fetal limb BM suspensions and fetal liver homogenates as described previously.^{36, 41} Following Ficoll density gradient centrifugation (Ficoll-Paque PLUS), mononuclear cells were directly stained with monoclonal antibodies: CD20-PB (2H7), IgM-BV510 (MHM-88), IgD-PerCP-Cy5.5 (IA6-2, all from BioLegend), CD34-FITC (8G12), CD123-PE (9F45), CD19-PE-Cy7 (SJ25C1), CD22-APC (S-HCL-1; all from BD Biosciences), and CD10-APC-C750 (HI10A, Cytognos). Five precursor-B-cell subsets (pro-B, pre-BI, pre-BII large, pre-BII small and immature-B) were bulk sorted.³⁶ Naive mature-B cells can be detected in BM samples likely due to blood contamination and these were single-cell sorted on a FACSAria cell sorter with FACSDiva software (BD Biosciences).

PCR-amplification and sequence analysis of complete *IGH* and *IGK* gene rearrangements

Complete *IGH* and *IGK* gene rearrangements were amplified in multiplex PCR reactions using V subgroup-specific forward primers and a consensus J primer^{36, 63} on DNA from bulk-sorted pediatric and fetal pre-BI and pre-BII small cells, from umbilical cord blood mononuclear cells and PBMC of IL7R α -deficient patients (**Table S1**). PCR products from bulk sorted precursor-B cells were subsequently cloned into the pGEM-T Easy vector (Promega Benelux BV, Leiden, The Netherlands). From RNA of single-cell sorted naive mature-B cells, cDNA was prepared and gene rearrangements were amplified in nested PCR reactions.⁶⁴ Single-cell PCR products and individual bacterial clones were sequenced on an ABI Prism 3031 XL fluorescent sequencer (Applied Biosystems, Carlsbad, CA). *IGH* gene rearrangements in BCP-ALL samples were determined as part of the diagnostic work-up.⁶⁵ The usage of V, (D), J genes as well as size and composition of the junctional region with regards to N-nucleotides were analyzed using the international ImMunoGeneTics (IMGT) information system (<http://imgt.cines.fr/>).³⁷ All sequence data have been deposited in GenBank (accession numbers KP771015 - KP771662).

3D immunofluorescence in situ hybridization (FISH)

3D DNA FISH of *IGH* was performed as described previously^{41, 42, 66} with fosmid clones 761A10 and 3777B2 (BACPAC Resources, Oakland, CA), BAC clones 47P23, 101G24 (BACPAC Resources) and 3087C18 (Open Biosystems, Huntsville, AL). Probes were either directly labeled with Chromatide Alexa Fluor 488-5 dUTP or Chromatide Alexa Fluor 568-5 dUTP (Invitrogen) using Nick Translation Mix (Roche Diagnostics GmbH); or they were indirectly labeled using DIG-Nick Translation Mix (Roche Diagnostics GmbH). Freshly sorted pre-BI and pre-BII small cells were fixed in 4% paraformaldehyde, and permeabilized in a PBS/0.1% Triton X-100/0.1% saponin solution and subjected to liquid nitrogen immersion following incubation in PBS with 20% glycerol. The nuclear membranes were permeabilized in PBS/0.5% Triton X-100/0.5% saponin prior to hybridization with the DNA probe cocktail. Coverslips were sealed and incubated for 48hr at 37°C, washed and mounted on slides with 10 μ l of Prolong gold anti-fade reagent (Invitrogen). Pictures were captured with a Leica SP5 confocal microscope (Leica Microsystems). Using a 63 \times lens (NA 1.4), we acquired images of \sim 70 serial optical sections spaced by 0.15 μ m. The data sets were deconvolved and analyzed with Huygens Professional software (Scientific Volume Imaging, Hilversum, the Netherlands). The 3D coordinates of the center of mass of each probe were transferred to Microsoft Excel, and the distances separating each probe were calculated using the equation: $\sqrt{((X_a - X_b)^2 + (Y_a - Y_b)^2 + (Z_a - Z_b)^2)}$, where X, Y, Z are the coordinates of object a or b.

Microarray analyses

The microarray analysis was performed as described previously.⁴¹ Briefly, total RNA was extracted from bulk sorted pro-B and pre-BI subsets using the miRNeasy Mini Kit (Qiagen) and used to synthesize cDNA with the Ovation Pico WTA System protocol (NuGEN). Sense strand cDNA was generated with the WT-Ovation Exon Module Version 1.0 (NuGEN), fragmented and biotinylated using the Encore Biotin Module (NuGEN). The labeled cDNA was hybridized on the GeneChip Human Exon 1.0 (Affymetrix, Santa Clara, CA, USA) for whole genome gene expression analysis. The arrays were scanned using the Affymetrix Gene Chip Scanner 3000 7G and images were processed using the AGCC (Affymetrix GeneChip Command Console Software) and the CEL files were imported into Partek Genomics Suite software (Partek, Inc. MO, USA). The Robust Multichip Analysis (RMA) algorithm was applied for generation of signal values and normalization. Transcripts were analyzed in core mode (see www.affymetrix.com) using signal values of less than 22.6 across arrays as threshold to filter for low and non-expressed genes. The results were expressed as fold change. One-way ANOVA test was calculated on all arrays grouped into 4 categories, i.e. fetus pro-B, fetus pre-BI, child pro-B and child pre-BI in Partek Genomics Suite to select transcripts for clustering. Non-supervised cluster analysis was then performed on 1,257 transcripts which showed a false discovery rate (FDR) <0.05% using the euclidean/average linkage algorithm. Gene networks and canonical pathways representing key genes were identified using Ingenuity Pathways Analysis (www.ingenuity.com) following criteria of fold change >1.5 and $p < 0.5$ in differences in gene expression. All microarray data have been deposited in ArrayExpress (accession number E-MTAB-1422).

Quantitative RT-PCR Analysis

A TaqMan-based RQ-PCR was used to confirm the expression levels of 5 NHEJ genes: *ATM*, *DCLRE1C* (Artemis), *NBN* (NBS), *PRKDC* (DNA-PKcs) and *XRCC4*. Total RNA was extracted from bulk sorted pre-BI cells using the miRNeasy Mini Kit (Qiagen) and reverse-transcribed with SuperScript II reverse transcriptase (Invitrogen). For cDNA amplification, 15 μ l reaction mix was used with Taq-Man Universal MasterMix (Applied Biosystems), 670 nM of each primer and 100 nM of FAM-TAMRA-labeled probe.⁶⁷ Primers were designed with the ProbeFinder software (Roche Applied Science) and probes were from the Universal ProbeLibrary (Roche Applied Science) (**Table S2**). Duplicate reactions were performed for each cDNA sample. Gene expression was analyzed with a StepOnePlus Real-Time PCR system and StepOne Software version 2.3

(Applied Biosystems). Cycle-threshold levels were calculated for each gene and normalized to values obtained for the endogenous reference gene *ABL*.

Statistics

Statistical significance was calculated by a non-parametric Mann-Whitney U test, χ^2 test or one-way ANOVA as indicated in the Figure legends. P values <0.05 were considered as significant.

ACKNOWLEDGEMENTS

We thank Drs. W.A. van Cappellen and G. Kremers (Optical Imaging Center, Erasmus MC) for support with confocal microscopy, Mr. E. Oole (Biomics, Erasmus MC) for support with gene expression profiling, Mr. S.J.W. Bartol and Mrs. H. Bouallouch-Charif for their help with high-speed cell sorting, Dr. E. van Roon (Dept. Pediatrics, Erasmus MC) for help with processing fetal tissue, and Ms. P. Hoogeveen for support with retrospective *IGH* gene rearrangement analysis in BCP-ALL. This study was performed in the department of Immunology as part of the Molecular Medicine Postgraduate School of the Erasmus MC, and was supported by ZonMW Veni grant 916.116.090 to MCvZ and ZonMW Vidi grant 91712323 to Mvdb.

REFERENCES

1. Schroeder, H. W., Jr., F. Mortari, S. Shiokawa, P. M. Kirkham, R. A. Elgavish, and F. E. Bertrand, 3rd. 1995. Developmental regulation of the human antibody repertoire. *Ann NY Acad Sci* 764:242-260.
2. Schroeder, H. W., Jr., L. Zhang, and J. B. Philips, 3rd. 2001. Slow, programmed maturation of the immunoglobulin HCDR3 repertoire during the third trimester of fetal life. *Blood* 98:2745-2751.
3. Stein, K. E. 1992. Thymus-independent and thymus-dependent responses to polysaccharide antigens. *J Infect Dis* 165 Suppl 1:S49-52.
4. Alt, F. W., G. D. Yancopoulos, T. K. Blackwell, C. Wood, E. Thomas, M. Boss, R. Coffman, N. Rosenberg, S. Tonegawa, and D. Baltimore. 1984. Ordered rearrangement of immunoglobulin heavy chain variable region segments. *EMBO J* 3:1209-1219.
5. Ghia, P., E. tenBoekel, E. Sanz, A. delaHera, A. Rolink, and F. Melchers. 1996. Ordering of human bone marrow B lymphocyte precursors by single-cell polymerase chain reaction analyses of the rearrangement status of the immunoglobulin H and L chain gene loci. *J Exp Med* 184:2217-2229.

6. Bossen, C., R. Mansson, and C. Murre. 2012. Chromatin Topology and the Regulation of Antigen Receptor Assembly. *Annu Rev Immunol* 30:337-356.
7. Jung, D., C. Giallourakis, R. Mostoslavsky, and F. W. Alt. 2006. Mechanism and control of V(D)J recombination at the immunoglobulin heavy chain locus. *Annu Rev Immunol* 24:541-570.
8. Hendriks, R. W., and S. Middendorp. 2004. The pre-BCR checkpoint as a cell-autonomous proliferation switch. *Trends Immunol* 25:249-256.
9. Curry, J. D., J. K. Geier, and M. S. Schlissel. 2005. Single-strand recombination signal sequence nicks in vivo: evidence for a capture model of synapsis. *Nat Immunol* 6:1272-1279.
10. Gellert, M. 2002. V(D)J recombination: RAG proteins, repair factors, and regulation. *Annu Rev Biochem* 71:101-132.
11. Matsuoka, S., B. A. Ballif, A. Smogorzewska, E. R. McDonald, 3rd, K. E. Hurov, J. Luo, C. E. Bakalarski, Z. Zhao, N. Solimini, Y. Lerenthal, Y. Shiloh, S. P. Gygi, and S. J. Elledge. 2007. ATM and ATR substrate analysis reveals extensive protein networks responsive to DNA damage. *Science* 316:1160-1166.
12. Shiloh, Y. 2003. ATM and related protein kinases: safeguarding genome integrity. *Nat Rev Cancer* 3:155-168.
13. van Gent, D. C., and M. van der Burg. 2007. Non-homologous end-joining, a sticky affair. *Oncogene* 26:7731-7740.
14. Alt, F. W., and D. Baltimore. 1982. Joining of immunoglobulin heavy chain gene segments: implications from a chromosome with evidence of three D-JH fusions. *Proc Natl Acad Sci USA* 79:4118-4122.
15. Benedict, C. L., S. Gilfillan, T. H. Thai, and J. F. Kearney. 2000. Terminal deoxynucleotidyl transferase and repertoire development. *Immunol Rev* 175:150-157.
16. Desiderio, S. V., G. D. Yancopoulos, M. Paskind, E. Thomas, M. A. Boss, N. Landau, F. W. Alt, and D. Baltimore. 1984. Insertion of N Regions into Heavy-Chain Genes Is Correlated with Expression of Terminal Deoxytransferase in B-Cells. *Nature* 311:752-755.
17. Jeong, H. D., and J. M. Teale. 1988. Comparison of the Fetal and Adult Functional B-Cell Repertoires by Analysis of Vh Gene Family Expression. *J Exp Med* 168:589-603.
18. Perlmutter, R. M., J. F. Kearney, S. P. Chang, and L. E. Hood. 1985. Developmentally Controlled Expression of Immunoglobulin-Vh Genes. *Science* 227:1597-1601.
19. Shiokawa, S., F. Mortari, J. O. Lima, C. Nunez, F. E. Bertrand, P. M. Kirkham, S. G. Zhu, A. P. Dasanayake, and H. W. Schroeder. 1999. IgM heavy chain complementarity-determining region 3 diversity is constrained by genetic and somatic mechanisms until two months after birth. *J Immunol* 162:6060-6070.
20. Souto-Carneiro, M. M., G. P. Sims, H. Girschik, J. Lee, and P. E. Lipsky. 2005. Developmental changes in the human heavy chain CDR3. *J Immunol* 175:7425-7436.
21. Yancopoulos, G. D., S. V. Desiderio, M. Paskind, J. F. Kearney, D. Baltimore, and F. W. Alt. 1984. Preferential Utilization of the Most Jh-Proximal Vh Gene Segments in Pre-B-Cell Lines. *Nature* 311:727-733.

22. Yancopoulos, G. D., B. A. Malynn, and F. W. Alt. 1988. Developmentally Regulated and Strain-Specific Expression of Murine Vh Gene Families. *J Exp Med* 168:417-435.
23. Zemlin, M., R. L. Schelonka, K. Bauer, and H. W. Schroeder, Jr. 2002. Regulation and chance in the ontogeny of B and T cell antigen receptor repertoires. *Immunol Res* 26:265-278.
24. Schroeder, H. W., G. C. Ippolito, and S. Shiokawa. 1998. Regulation of the antibody repertoire through control of HCDR3 diversity. *Vaccine* 16:1383-1390.
25. Pascual, V., L. Verkruyse, M. L. Casey, and J. D. Capra. 1993. Analysis of Ig H chain gene segment utilization in human fetal liver. Revisiting the "proximal utilization hypothesis". *J Immunol* 151:4164-4172.
26. Raaphorst, F. M., R. Langlois van den Bergh, J. L. Waaijer, J. M. Vossen, and M. J. van Tol. 1997. Expression of the human immunoglobulin heavy chain VH6 gene element by fetal B lymphocytes. *Scand J Immunol* 46:292-297.
27. Schroeder, H. W., and J. Y. Wang. 1990. Preferential Utilization of Conserved Immunoglobulin Heavy-Chain Variable Gene Segments during Human Fetal Life. *Proc Natl Acad Sci USA* 87:6146-6150.
28. Schroeder, H. W., Jr., J. L. Hillson, and R. M. Perlmutter. 1987. Early restriction of the human antibody repertoire. *Science* 238:791-793.
29. Wasserman, R., N. Galili, Y. Ito, B. A. Reichard, S. Shane, and G. Rovera. 1992. Predominance of Fetal Type-Dj(H) Joining in Young-Children with B-Precursor Lymphoblastic-Leukemia as Evidence for an Inutero Transforming Event. *J Exp Med* 176:1577-1581.
30. Bueno, C., R. Montes, P. Catalina, R. Rodriguez, and P. Menendez. 2011. Insights into the cellular origin and etiology of the infant pro-B acute lymphoblastic leukemia with MLL-AF4 rearrangement. *Leukemia* 25:400-410.
31. Ford, A. M., C. A. Bennett, C. M. Price, M. C. A. Bruin, E. R. Van Wering, and M. Greaves. 1998. Fetal origins of the TEL-AML1 fusion gene in identical twins with leukemia. *Proc Natl Acad Sci U S A* 95:4584-4588.
32. Wiemels, J. L., G. Cazzaniga, M. Daniotti, O. B. Eden, G. M. Addison, G. Masera, V. Saha, A. Biondi, and M. F. Greaves. 1999. Prenatal origin of acute lymphoblastic leukaemia in children. *Lancet* 354:1499-1503.
33. Hubner, S., G. Cazzaniga, T. Flohr, V. H. van der Velden, M. Konrad, U. Potschger, G. Basso, M. Schrappe, J. J. van Dongen, C. R. Bartram, A. Biondi, and E. R. Panzer-Grumayer. 2004. High incidence and unique features of antigen receptor gene rearrangements in TEL-AML1-positive leukemias. *Leukemia* 18:84-91.
34. Jansen, M. W., L. Corral, V. H. van der Velden, R. Panzer-Grumayer, M. Schrappe, A. Schrauder, R. Marschalek, C. Meyer, M. L. den Boer, W. J. Hop, M. G. Valsecchi, G. Basso, A. Biondi, R. Pieters, and J. J. van Dongen. 2007. Immunobiological diversity in infant acute lymphoblastic leukemia is related to the occurrence and type of MLL gene rearrangement. *Leukemia* 21:633-641.
35. Kolar, G. R., T. Yokota, M. I. Rossi, S. K. Nath, and J. D. Capra. 2004. Human fetal, cord blood, and adult lymphocyte progenitors have similar potential for generating B cells with a diverse immunoglobulin repertoire. *Blood* 104:2981-2987.

36. van Zelm, M. C., M. van der Burg, D. de Ridder, B. H. Barendregt, E. F. de Haas, M. J. Reinders, A. C. Lankester, T. Revesz, F. J. Staal, and J. J. van Dongen. 2005. Ig gene rearrangement steps are initiated in early human precursor B cell subsets and correlate with specific transcription factor expression. *J Immunol* 175:5912-5922.
37. Alamyar, E., P. Duroux, M. P. Lefranc, and V. Giudicelli. 2012. IMGT((R)) tools for the nucleotide analysis of immunoglobulin (IG) and T cell receptor (TR) V-(D)-J repertoires, polymorphisms, and IG mutations: IMGT/V-QUEST and IMGT/HighV-QUEST for NGS. *Methods Mol Biol* 882:569-604.
38. Meffre, E., and J. E. Salmon. 2007. Autoantibody selection and production in early human life. *J Clin Invest* 117:598-601.
39. Noordzij, J. G., S. de Bruin-Versteeg, W. M. Comans-Bitter, N. G. Hartwig, R. W. Hendriks, R. de Groot, and J. J. van Dongen. 2002. Composition of precursor B-cell compartment in bone marrow from patients with X-linked agammaglobulinemia compared with healthy children. *Pediatr Res* 51:159-168.
40. Noordzij, J. G., S. de Bruin-Versteeg, N. S. Verkaik, J. M. Vossen, R. de Groot, E. Bernatowska, A. W. Langerak, D. C. van Gent, and J. J. van Dongen. 2002. The immunophenotypic and immunogenotypic B-cell differentiation arrest in bone marrow of RAG-deficient SCID patients corresponds to residual recombination activities of mutated RAG proteins. *Blood* 100:2145-2152.
41. Jensen, K., M. B. Rother, B. S. Brusletto, O. K. Olstad, H. C. D. Aass, M. C. van Zelm, P. Kierulf, and K. M. Gautvik. 2013. Increased ID2 Levels in Adult Precursor B Cells as Compared with Children Is Associated with Impaired Ig Locus Contraction and Decreased Bone Marrow Output. *J Immunol* 191:1210-1219.
42. Nodland, S. E., M. A. Berkowska, A. A. Bajer, N. Shah, D. de Ridder, J. J. van Dongen, T. W. LeBien, and M. C. van Zelm. 2011. IL-7R expression and IL-7 signaling confer a distinct phenotype on developing human B-lineage cells. *Blood* 118:2116-2127.
43. Boubakour-Azzouz, I., P. Bertrand, A. Claes, B. S. Lopez, and F. Rougeon. 2012. Terminal deoxynucleotidyl transferase requires KU80 and XRCC4 to promote N-addition at non-V(D)J chromosomal breaks in non-lymphoid cells. *Nucleic Acids Res* 40:8381-8391.
44. Dengler, H. S., G. V. Baracho, S. A. Omori, S. Bruckner, K. C. Arden, D. H. Castrillon, R. A. DePinho, and R. C. Rickert. 2008. Distinct functions for the transcription factor Foxo1 at various stages of B cell differentiation. *Nat Immunol* 9:1388-1398.
45. Lin, Y. C., S. Jhunjunwala, C. Benner, S. Heinz, E. Welinder, R. Mansson, M. Sigvardsson, J. Hagman, C. A. Espinoza, J. Dutkowski, T. Ideker, C. K. Glass, and C. Murre. 2010. A global network of transcription factors, involving E2A, EBF1 and Foxo1, that orchestrates B cell fate. *Nat Immunol* 11:635-U109.
46. Rouse, J., and S. P. Jackson. 2002. Interfaces between the detection, signaling, and repair of DNA damage. *Science* 297:547-551.
47. Zhou, B. B., and S. J. Elledge. 2000. The DNA damage response: putting checkpoints in perspective. *Nature* 408:433-439.

48. Mandal, M., S. E. Powers, M. Maienschein-Cline, E. T. Bartom, K. M. Hamel, B. L. Kee, A. R. Dinner, and M. R. Clark. 2011. Epigenetic repression of the I μ gk locus by STAT5-mediated recruitment of the histone methyltransferase Ezh2. *Nat Immunol* 12:1212-1220.
49. Corfe, S. A., and C. J. Paige. 2012. The many roles of IL-7 in B cell development; mediator of survival, proliferation and differentiation. *Semin Immunol* 24:198-208.
50. Kee, B. L. 2009. E and ID proteins branch out. *Nat Rev Immunol* 9:175-184.
51. Murre, C. 2005. Helix-loop-helix proteins and lymphocyte development. *Nat Immunol* 6:1079-1086.
52. Bain, G., E. C. R. Maandag, H. P. J. T. Riele, A. J. Feeney, A. Sheehy, M. Schlissel, S. A. Shinton, R. R. Hardy, and C. Murre. 1997. Both E12 and E47 allow commitment to the B cell lineage. *Immunity* 6:145-154.
53. Chowdhury, D., and R. Sen. 2001. Stepwise activation of the immunoglobulin mu heavy chain gene locus. *EMBO J* 20:6394-6403.
54. Yagi, T., S. Hibi, Y. Tabata, K. Kuriyama, T. Teramura, T. Hashida, Y. Shimizu, T. Takimoto, S. Todo, T. Sawada, and S. Imashuku. 2000. Detection of clonotypic IGH and TCR rearrangements in the neonatal blood spots of infants and children with B-cell precursor acute lymphoblastic leukemia. *Blood* 96:264-268.
55. Armstrong, S. A., J. E. Staunton, L. B. Silverman, R. Pieters, M. L. de Boer, M. D. Minden, S. E. Sallan, E. S. Lander, T. R. Golub, and S. J. Korsmeyer. 2002. MLL translocations specify a distinct gene expression profile that distinguishes a unique leukemia. *Nat Genet* 30:41-47.
56. Rechavi, E., A. Lev, Y. N. Lee, A. J. Simon, Y. Yinon, S. Lipitz, N. Amariglio, B. Weisz, L. D. Notarangelo, and R. Somech. 2015. Timely and spatially regulated maturation of B and T cell repertoire during human fetal development. *Sci Transl Med* 7:276ra225.
57. Ahsberg, J., P. Tsapogas, H. Qian, J. Zetterblad, S. Zandi, R. Mansson, J. I. Jonsson, and M. Sigvardsson. 2010. Interleukin-7-induced Stat-5 acts in synergy with Flt-3 signaling to stimulate expansion of hematopoietic progenitor cells. *J Biol Chem* 285:36275-36284.
58. Schelonka, R. L., I. I. Ivanov, A. M. Vale, R. A. Dimmitt, M. Khaled, and H. W. Schroeder. 2011. Absence of N addition facilitates B cell development, but impairs immune responses. *Immunogenetics* 63:599-609.
59. George, J. E., and H. W. Schroeder. 1992. Developmental Regulation of D-Beta Reading Frame and Junctional Diversity in T-Cell Receptor-Beta Transcripts from Human Thymus. *J Immunol* 148:1230-1239.
60. Bodger, M. P., G. Janossy, F. J. Bollum, G. D. Burford, and A. V. Hoffbrand. 1983. The Ontogeny of Terminal Deoxynucleotidyl Transferase Positive Cells in the Human-Fetus. *Blood* 61:1125-1131.
61. Bonati, A., C. Casoli, B. Starcich, and M. Buscaglia. 1983. Terminal deoxynucleotidyl transferase (TdT) in human fetuses. An immunofluorescent and biochemical study. *Scand J Haematol* 31:447-453.
62. Deibel, M. R., Jr., L. K. Riley, M. S. Coleman, M. L. Cibull, S. A. Fuller, and E. Todd. 1983. Expression of terminal deoxynucleotidyl transferase in human thymus during ontogeny and development. *J Immunol* 131:195-200.
63. van Dongen, J. J., A. W. Langerak, M. Bruggemann, P. A. Evans, M. Hummel, F. L. Lavender, E. Delabesse, F. Davi, E. Schuurink, R. Garcia-Sanz, J. H. van Krieken, J. Droese, D. Gonzalez, C. Bastard,

- H. E. White, M. Spaargaren, M. Gonzalez, A. Parreira, J. L. Smith, G. J. Morgan, M. Kneba, and E. A. Macintyre. 2003. Design and standardization of PCR primers and protocols for detection of clonal immunoglobulin and T-cell receptor gene recombinations in suspect lymphoproliferations: report of the BIOMED-2 Concerted Action BMH4-CT98-3936. *Leukemia* 17:2257-2317.
64. Tiller, T., E. Meffre, S. Yurasov, M. Tsuiji, M. C. Nussenzweig, and H. Wardemann. 2008. Efficient generation of monoclonal antibodies from single human B cells by single cell RT-PCR and expression vector cloning. *J Immunol Methods* 329:112-124.
65. van der Velden, V. H., and J. J. van Dongen. 2009. MRD detection in acute lymphoblastic leukemia patients using Ig/TCR gene rearrangements as targets for real-time quantitative PCR. *Methods Mol Biol* 538:115-150.
66. Sayegh, C. E., S. Jhunjunwala, R. Riblet, and C. Murre. 2005. Visualization of looping involving the immunoglobulin heavy-chain locus in developing B cells. *Genes Dev* 19:322-327.
67. van Zelm, M. C., S. J. Bartol, G. J. Driessen, F. Mascart, I. Reisli, J. L. Franco, B. Wolska-Kusnierz, H. Kanegane, L. Boon, J. J. van Dongen, and M. van der Burg. 2014. Human CD19 and CD40L deficiencies impair antibody selection and differentially affect somatic hypermutation. *J Allergy Clin Immunol* 134:135-144.

SUPPLEMENTAL MATERIAL

Table S1. Primer sequences used for analysis of complete *IGH* and *IGK* gene rearrangements.

PCR type	Locus	Target	Primer	Type	Sequence (5'-3')
Ig gene rearrangements in precursor B-cells	<i>IGH</i>	V _H - DJ _H	V _H 1-FR2 ⁶³	Forward	CTGGGTGCGACAGGCCCTGGACAA
			V _H 2-FR2 ³⁶	Forward	GATCCGTCAGCCCCAGGAAGG
			V _H 3-FR2 ⁶³	Forward	GGTCCGCCAGGCTCCAGGGAA
			V _H 4-FR2 ³⁶	Forward	GATCCGCCAGCCCCAGGAAGG
			V _H 5-FR2 ³⁶	Forward	GGTGCGCCAGATGCCCGGAAAGG
			V _H 6-FR2 ³⁶	Forward	GATCAGGCAGTCCCCATCGAGAG
			V _H 7-FR2 ³⁶	Forward	TTGGGTGCGACAGGCCCTGGACAA
			J _H cons ³⁶	Reverse	CTTACCTGAGGAGACGGTGACC
Ig gene rearrangements in naive-B cells	<i>IGH</i>	V _H - DJ _H	L-V _H 1 ⁶⁴	Forward	ACAGGTGCCCACTCCAGGTGCAG
			L-V _H 3 ⁶⁴	Forward	AAGGTGTCCAGTGTGARGTGCAG
			L-V _H 4/6 ⁶⁴	Forward	CCCAGATGGGTCTCTGCCAGGTGCAG
			L-V _H 5 ⁶⁴	Forward	CAAGGAGTCTGTTCCGAGGTGCAG
			C _μ CH1 ⁶⁴	Reverse	GGGAATTCTCACAGGAGACGA
Ig gene rearrangements in BCP-ALL	<i>IGH</i>	V _H - DJ _H	V _H 1/7-F1-CLB ⁶⁵	Forward	TCTGGGGCTGAGGTGAAGAA
			V _H 2-F1-CLB ⁶⁵	Forward	ACCTTGAAGGAGTCTGGTCTT
			V _H 3-F1-CLB ⁶⁵	Forward	GGGGTCCCTGAGACTCTC
			V _H 4/6-F1-CLB ⁶⁵	Forward	GCCCAGGACTGGTGAAGC
			V _H 5-F1-CLB ⁶⁵	Forward	CTGGTGCAGTCTGGAGCAG
			J _H -R1-CLB ⁶⁵	Reverse	ACCTGAGGAGACGGTGACC
Ig gene rearrangements in precursor B-cells	<i>IGK</i>	V _κ - J _κ	V _κ 1 ³⁶	Forward	AGGAGACAGAGTCAACATCACT
			V _κ 2 ³⁶	Forward	CTCCATCTCCTGCAGGTCTAGTC
			V _κ 3 ³⁶	Forward	GGAAAGAGCCACCCTCTCCTG
			V _κ 4 ³⁶	Forward	CAACTGCAAGTCCAGCCAGAGTGTTTT
			J _κ 1-4 ⁶³	Reverse	CTTACGTTTGATCTCCACCTTGGTCCC
			J _κ 5 ⁶³	Reverse	CTTACGTTTAATCTCCAGTCGTGTCCC
			Ig gene rearrangements in naive-B cells	<i>IGK</i>	V _κ - J _κ
L-V _κ 3 ⁶⁴	Forward	CTCTTCTCTGCTACTCTGGCTCCCAG			
L-V _κ 4 ⁶⁴	Forward	ATTCTCTGTTGCTCTGGATCTCTG			
C _κ 1 ⁶⁴	Reverse	CCAGATTTCAACTGCTCATCAGA			

Table S2. PCR primers and UPL FAM-labeled hydrolysis probes for expression analysis of NHEJ factor transcripts.

Target	Forward primer (5'-3')	Exon	reverse primer (5'-3')	Exon	UPL Probe #
ABL	GAGAAGGACTACCGCATGGA	8	GGGATTCACACTGCCAACA	9	44
ATM	TTTCTTACAGTAATTTGGAGCAITTTTG	20	GGCAATTTACTAGGGCCCAITC	21	55
DCLRE1C (Artemis)	ACGGCAACACTCAGATCCAT	9	CAGGGTAATTTGCTCCACTGA	10	6
NBN (NBS)	CCTGAAAGCAGTTGAGTCCA	5	GGTTCAATCAAGAGGTGGGTAAA	6	75
PRKDC (DNA-PKcs)	CTGGGAAGTGTCAAGCTCTTTC	22	TCITCTAAAGGAFATTTGCTTGGTTTG	22/23	44
XRCC4	TGAAACCAGTATACTCAITTTCTTACA	2	TGAAACCAGTATACTCAITTTCTTACA	3	47

Table S3. IGH junction characteristics.

	sequence no	CDR3 length (nt)	del, V _H	P ₁ V _H	N, V _H -D _H	P ₁ 5'D _H	del, 5'D _H	del, 3'D _H	P ₁ 3'D _H	N, D _H -J _H	P ₁ J _H	del, J _H
fetus liver pre-BI out-of-frame	74	45.23	1.72	0.30	8.32	0.15	4.84	4.41	0.00	5.19	0.08	4.15
fetus BM pre-BI out-of-frame	114	45.29	1.81	0.25	6.32	0.04	5.49	4.70	0.00	4.26	0.11	3.76
child BM pre-BI out-of-frame	144	60.56	1.84	0.32	8.98	0.22	4.99	4.29	0.03	11.19	0.15	5.49
fetus liver pre-BI total	107	44.57	1.62	0.27	7.61	0.11	5.73	5.13	0.00	4.21	0.07	4.23
fetus BM pre-BI total	161	43.99	1.75	0.23	5.87	0.04	5.65	4.91	0.00	3.73	0.13	3.60
child BM pre-BI total	216	59.86	1.84	0.35	8.62	0.20	4.94	4.89	0.05	10.55	0.15	5.42
BCP-ALL fetal origin	120	44.63	2.83	0.22	7.46	0.12	5.94	4.85	0.08	3.55	0.05	5.98
BCP-ALL non-fetal origin	168	55.74	2.32	0.34	9.29	0.07	5.31	4.05	0.13	7.97	0.17	4.70
fetus BM naive-B	148	39.14	1.15	0.28	4.57	0.11	5.68	4.97	0.13	3.16	0.13	3.23
CB naive-B	105	46.77	1.39	0.19	6.12	0.02	5.24	5.03	0.10	3.25	0.12	3.76
child BM naive-B	152	46.22	1.13	0.40	6.42	0.07	5.07	5.10	0.05	5.78	0.11	4.86

Significant differences in fetal IGH junctions as compared to childhood are indicated in bold font; Mann-Whitney U test; p<0.05

V. Altered V(D)J Recombination Underlies The Skewed Immunoglobulin Repertoires In Normal And Malignant B-Cell Precursors From Fetal Origin

Table S4. *IGK* junction characteristics.

	sequence no	CDR3 length (nt)	del, V κ	P, V κ	N, V κ -J κ	P, J κ	del, J κ
fetus liver pre-BII small out-of-frame	61	28.15	3.13	0.16	3.02	0.10	2.33
fetus BM pre-BII small out-of-frame	182	26.87	3.07	0.13	2.28	0.13	2.63
child BM pre-BII small out-of-frame	105	27.05	3.82	0.11	2.23	0.31	2.01
fetus liver pre-BII small total	75	27.53	3.11	0.13	2.64	0.08	2.47
fetus BM pre-BII small total	240	27.15	2.98	0.12	2.18	0.13	2.41
child BM pre-BII small total	138	27.06	3.75	0.09	2.26	0.30	2.06
fetus BM naive-B	92	27.10	2.48	0.07	0.61	0.09	1.37
CB naive-B	46	26.48	2.63	0.07	0.83	0.09	2.13
child BM naive-B	120	27.63	2.88	0.08	1.44	0.08	1.31

Significant differences in fetal IGH junctions as compared to childhood are indicated in bold font; Mann-Whitney U test; $p < 0.05$

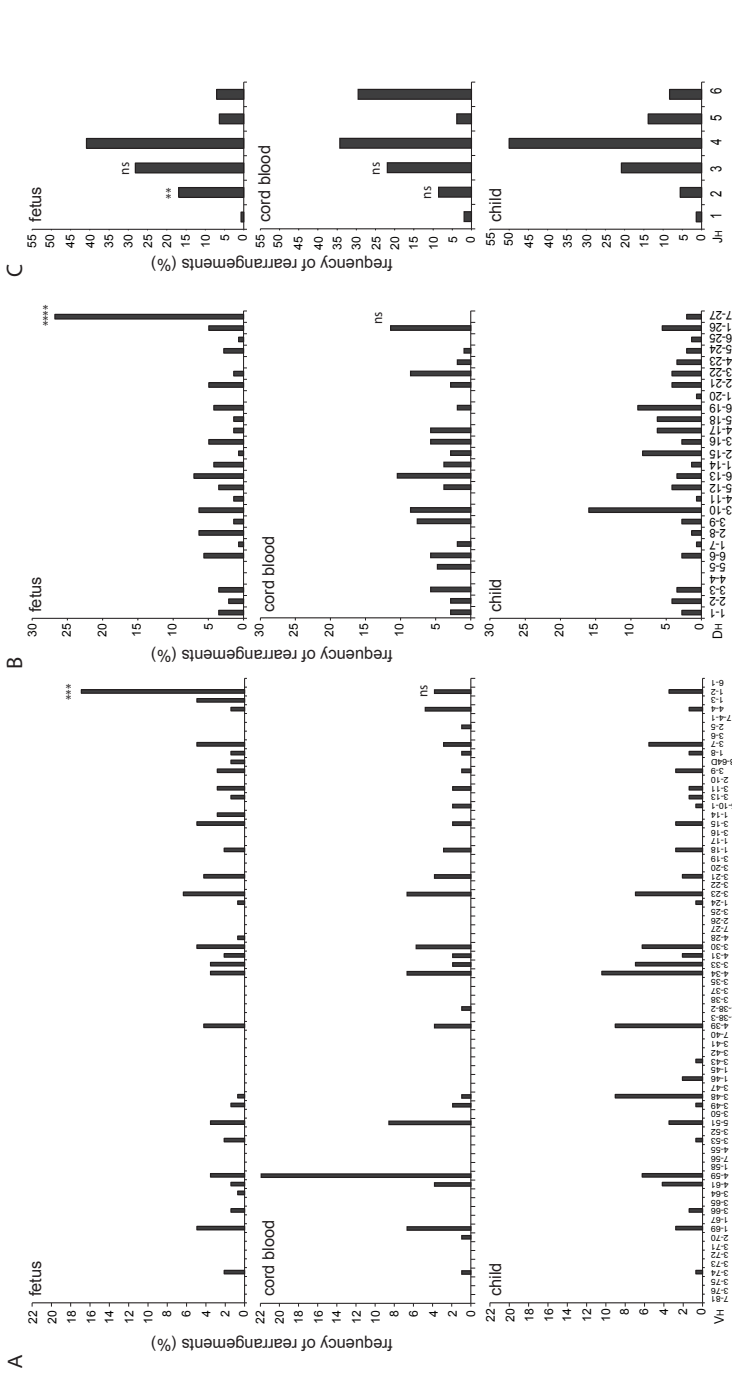
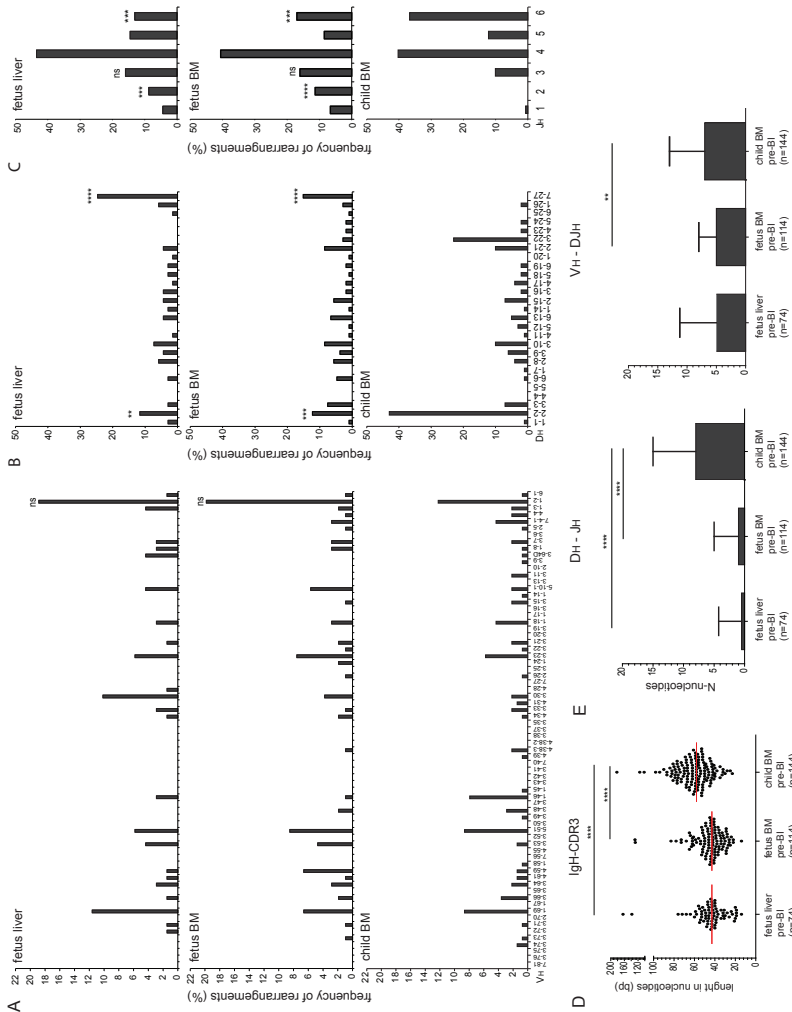


Figure S1. Skewed IGH gene repertoire in fetal naive B cells. *IGHV* (A), *IGHD* (B) and *IGHJ* (C) gene usage in transcripts from single-cell sorted naive mature-B cells from fetal and pediatric bone marrow (BM) and in mononuclear cells from cord blood. The genes are ordered according to their genomic positions in the locus (IMGT).³⁷ In total, 142 sequences were derived from 3 fetal BM samples, 105 from 4 cord blood samples and 144 from 3 pediatric BM donors. Data from individual samples showed similar patterns of gene usage. Statistical significance in gene usage between fetal and pediatric BM or cord blood and pediatric BM was determined with the χ^2 test. **, $p < 0.01$; ***, $p < 0.001$; ****, $p < 0.0001$; ns, not significant.

V. Altered V(D)J Recombination Underlies The Skewed Immunoglobulin Repertoires In Normal And Malignant B-Cell Precursors From Fetal Origin

Figure S2. IGHV (A), IGH D (B) and IGH J (C) gene usage in out-of-frame IGH gene rearrangements amplified from bulk sorted pre-BI cells from fetal liver, fetal BM and pediatric BM. The genes are ordered according to their genomic positions in the locus (IMGT).³⁷ Panels A-C include 69 sequences derived from 3 fetal liver samples, 106 sequences from 4 fetal BM samples and 139 sequences from 5 pediatric BM donors. (D) Scatter plots showing the IgH-CDR3 length in nucleotides with the red horizontal lines representing median values. (E) Bar graphs showing the median numbers of N-nucleotides in D_H-J_H and V_H-D_H junctions with inter-quartile range. Numbers of sequences are depicted between brackets. Statistical significance was determined with the χ^2 test (panels A-C) or the Mann-Whitney U test (panels D-E); **, p<0.01; *, p<.001; ****, p<.0001; ns, not significant.**



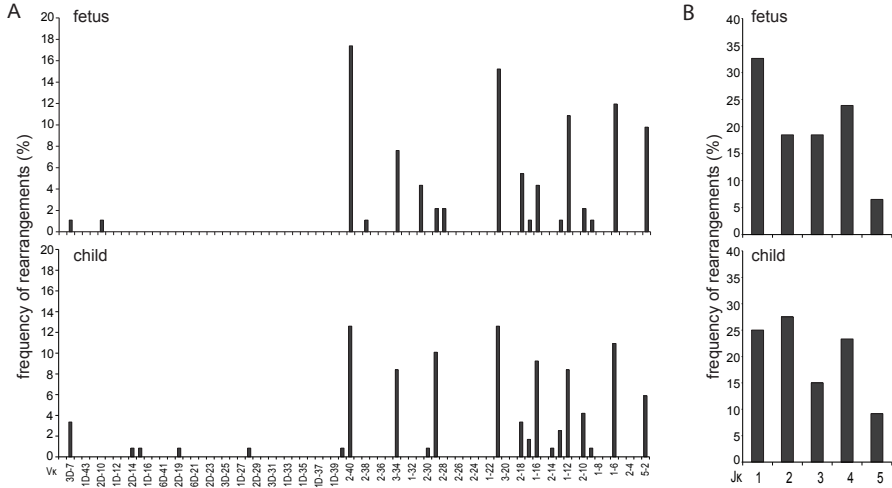


Figure S3. *IGKV* (A) and *IGKJ* (B) gene usage in transcripts from single-cell naive mature-B cells from fetal and pediatric bone marrow (BM). The genes are ordered according to their genomic positions in the locus (IMGT).³⁷ The panels include 92 sequences derived from 3 fetal BM samples and 120 sequences from 3 pediatric BM donors. Data from individual samples showed similar patterns of gene usage.

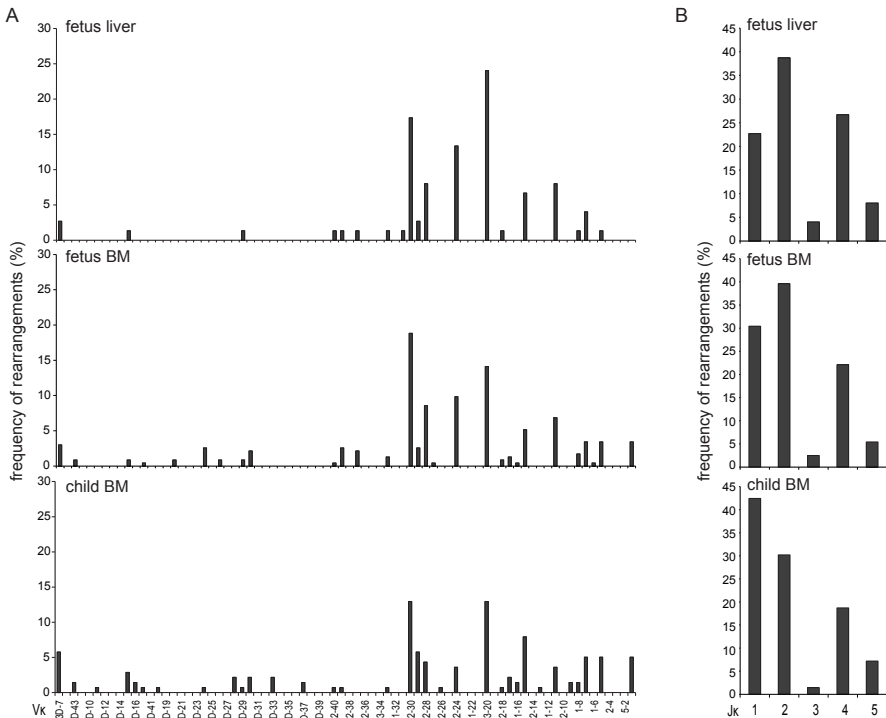


Figure S4. *IGKV* (A) and *IGKJ* (B) gene usage in bulk sorted pre-BII small cells from fetal liver, fetal bone marrow (BM) and pediatric BM. *IGK* gene rearrangements were amplified from DNA, and both in-frame and out-of-frame rearrangements were included in the analysis. The genes are ordered according to their genomic

V. Altered V(D)J Recombination Underlies The Skewed Immunoglobulin Repertoires In Normal And Malignant B-Cell Precursors From Fetal Origin

positions in the locus (IMGT).³⁷ The panels include 75 sequences derived from 3 fetal liver samples, 240 sequences from 4 fetal BM samples and 138 sequences from 5 pediatric BM donors. Data from individual samples showed similar patterns of gene usage.

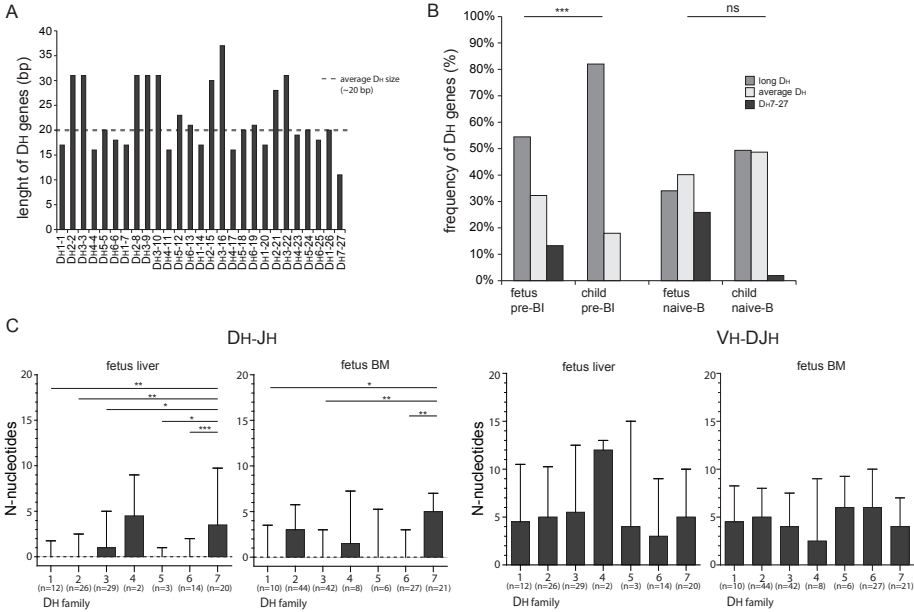


Figure S5. *IGHD* gene sizes. (A) The length of germline *IGHD* genes. The majority of *IGHD* genes is ~20 nucleotides in size. DH2-2, DH3-3, DH2-8, DH3-9, DH3-10, DH2-15, DH3-16, DH2-21, DH3-22 genes are ~30 nucleotides and defined as long, whereas DH7-27 was short, being smaller than 15 nucleotides. (B) Relative usage of long, average and short *IGHD* genes in fetal and pediatric pre-BI and naive mature-B cells. Data include 161 sequences from 4 fetal pre-BI samples, 216 sequences from 5 pediatric pre-BI samples, 148 sequences from 3 fetal naive mature B-cell samples and 152 sequences from 3 pediatric naive mature B-cell samples. (C) N-nucleotides additions in DH-JH and VH-DJH junctions in pre-BI cells from fetal liver and fetal BM separated based on DH gene family usage. Bars represent medians with inter-quartile range, and include data from 3 fetal liver and 4 fetal BM donors. Numbers of analyzed sequences are indicated between brackets. Statistical significance was determined with the χ^2 test (panel B) or the Mann-Whitney U test (panel C). *, $p < .05$; **, $p < .01$; ***, $p < .001$; ns, not significant.

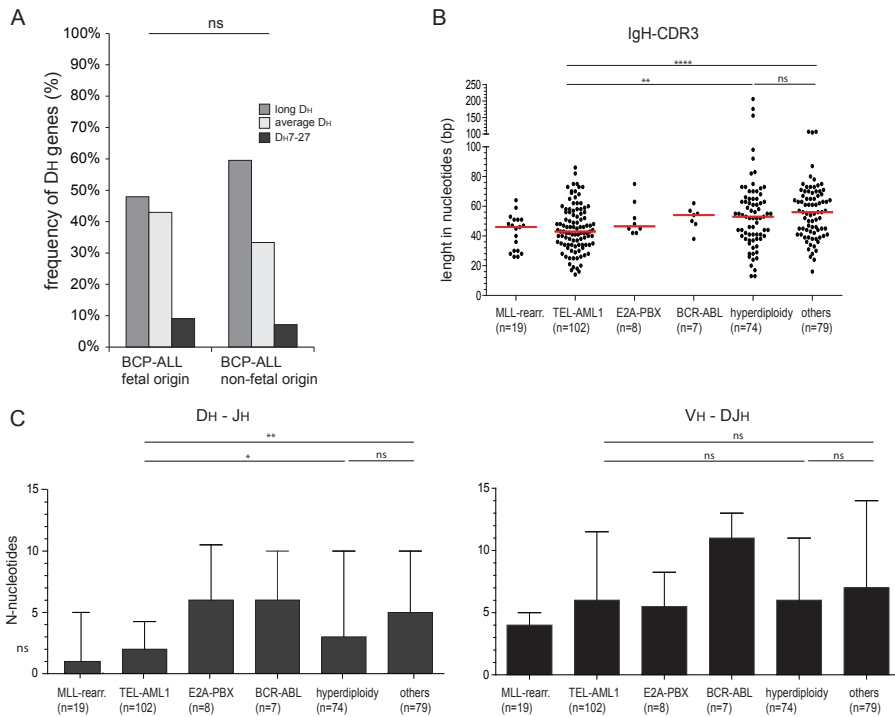


Figure S6. *IGH* junction characteristics in BCP-ALL. (A) Relative usage of long, average and short *IGHD* genes in BCP-ALL subsets. BCP-ALL of fetal origin included MLL-rearranged (n=19) and TEL-AML1 positive (n=102) cases, whereas the E2A-PBX positive (n=8), BCR-ABL positive (n=7), hyperdiploid (n=74) and other cases (n=79) constituted group of BCP-ALL from non-fetal origin. (B) Scatter plots showing the IgH-CDR3 length in nucleotides with red horizontal lines representing median values. (C) Bar graphs showing the number of N-nucleotides in DH-JH and VH-DJH junctions. Values represent the medians with inter-quartile range and the numbers of sequences are indicated between brackets. Data in all panels include in-frame and out-of-frame complete *IGH* gene rearrangements. Statistical significance was calculated with the χ^2 test (panel A) or the Mann-Whitney U test; *, p<0.05; **, p<0.01; ****, p<0.0001, ns-not significant.

V. Altered V(D)J Recombination Underlies The Skewed Immunoglobulin Repertoires In Normal And Malignant B-Cell Precursors From Fetal Origin

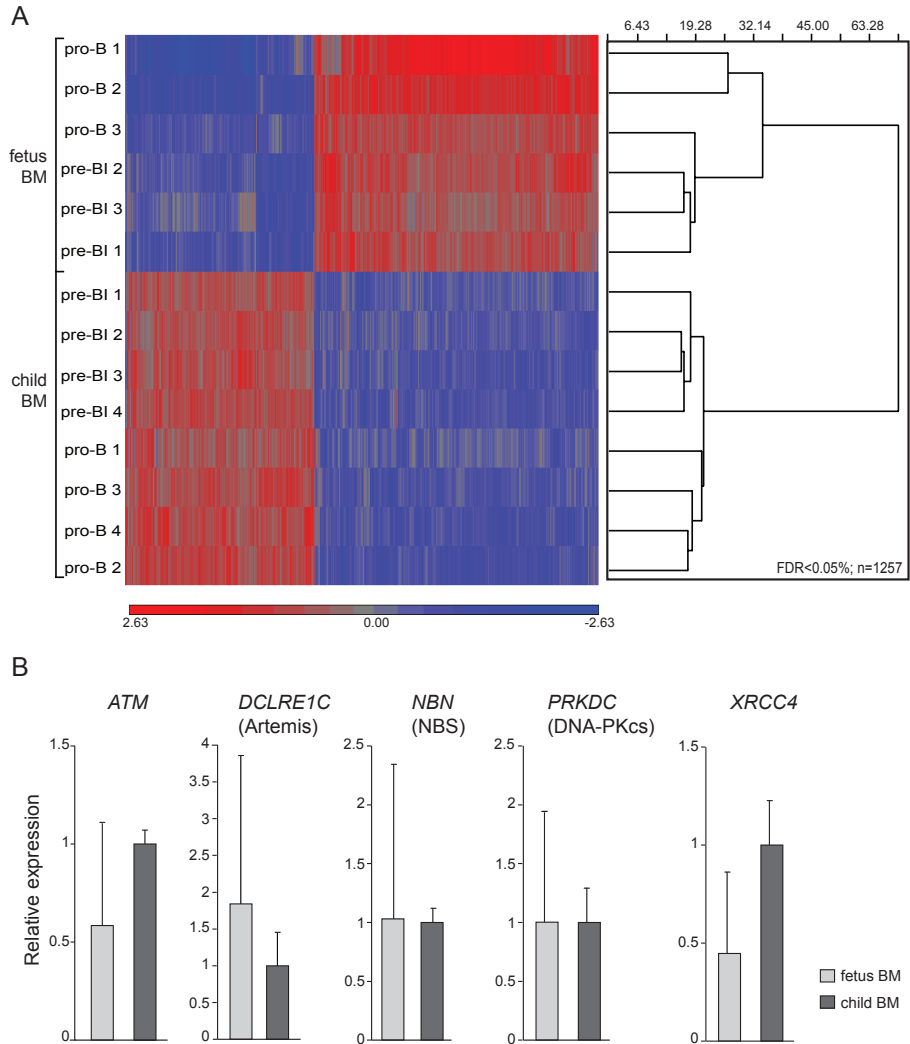


Figure S7. Gene expression profiling of fetal and pediatric precursor-B-cells. (A) Non-supervised cluster analysis of the gene expression profiles from purified fetal (3 donors) and pediatric (4 donors) pro-B and pre-BI cells after one-way ANOVA test. Clustering included 1257 transcripts with a false discovery rate (FDR)<0.05% using the euclidean/average linkage algorithm. (B) Confirmation of gene expression levels of 5 transcripts encoding factors involved in NHEJ by real-time quantitative RT-PCR. Data was generated from bulk-sorted pre-BI cells from 2 fetal BM and 3 pediatric BM samples. Gene expression levels were normalized to the levels of *ABL*, and the values in pediatric pre-BI cells were set to 1.

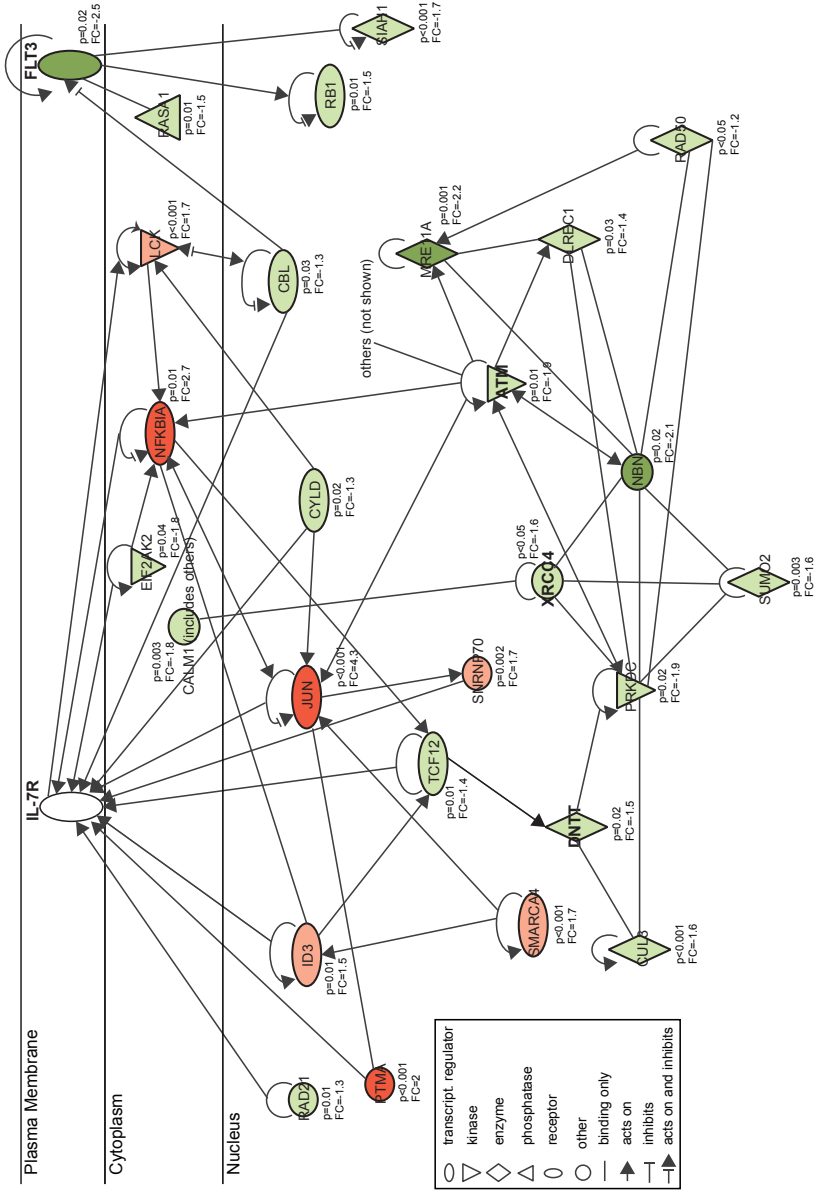


Figure S8. Functional network of molecules interacting with IL-7R, FLT3, ATM, XRCC4 and TdT (*DNTT*) in pre-B1 cells. Upregulated (red) and downregulated (green) transcripts in fetus vs child as determined by genome-wide expression profiling ($p < 0.05$). Dark shades indicates fold change > 2 in transcript expression, and lighter shaded fold change between 1.5 and 2. The interactions were identified with Ingenuity Pathway Analysis (www.ingenuity.com) starting with IL-7R, FLT3, ATM, XRCC4 and TdT (indicated in bold font).



Chapter VI

The human thymus is enriched for autoreactive B cells

Magdalena B. Rother¹, Marco W.J. Schreurs¹, Roel Kroek¹, Sophinus J.W. Bartol¹,
Jacques J.M. van Dongen¹ and Menno C. van Zelm^{1,2}

(1) Department of Immunology, Erasmus MC, University Medical Center Rotterdam,
The Netherlands, (2) present address: Department of Immunology, Central Clinical
School, Monash University, Melbourne, Victoria, Australia

Manuscript submitted

ABSTRACT

The human thymus has been shown to host B cells, which have been implicated in presentation of autoantigens for negative selection of T-cell progenitors. Although these antigens are thought to be taken up through their surface immunoglobulins (Ig), data on thymic Ig gene repertoires are limited and reactivity to autoantigens has not been demonstrated. We therefore studied the Ig gene repertoires and reactivity to autoantigens of single-sorted B cells from pediatric thymus, and compared these with mature B cells from fetal and pediatric bone marrow (BM). Nearly all B cells in thymus were mature and displayed an Ig gene repertoire that was similar to pediatric BM. Fetal mature B cells predominantly used proximal V, D, and J genes, and their antibodies were highly reactive to dsDNA. In contrast, thymic B cells were enriched for autoreactive clones that showed increased specificity to peptide autoantigens. Thus, the majority of B cells in the thymus are resident rather than developing, and are enriched for autoantigen-binding. These features support current models for a role of thymic B cells in presentation of autoantigens to developing T-cells during negative selection.

INTRODUCTION

The thymus is a primary lymphoid organ where T cells differentiate from bone marrow (BM) derived progenitors.^{1, 2} Progenitor-T cells enter the thymus at the cortico-medullary junction and migrate into the cortex where they rearrange their T-cell receptor (TCR) loci.³ TCR expressing progenitors subsequently undergo two important selection events. First, TCRs are selected for capability of binding to the major histocompatibility complex (MHC) molecules through positive selection. This selection is mediated by cortical thymic epithelial cells (cTECs) that express MHC class I (MHCI) and class II (MHCII) molecules. Following positive selection, the remaining thymocytes undergo negative selection for recognition of self-antigens. Self-antigens are presented to T cells by dendritic cells via MHCII and medullary thymic epithelial cells (mTECs) via MHCI and MHCII.⁴ Expression of tissue-specific self-antigens by mTECs is regulated by the transcription factor AIRE.^{5, 6} High affinity interactions of T cells with MHC-self antigen complexes result in apoptosis of the T cell, thereby ensuring proper central immune tolerance.⁷⁻⁹

Despite being a specific site for T-cell development, the human thymus also hosts B cells. These are located in the medulla and created rosette-like structures surrounded by T cells.^{10, 11} It has been suggested that these B cells are involved in autoantigen presentation to T cells.¹²⁻¹⁵ B cells express high levels of MHCII and can efficiently present antigens that they recognize with their surface immunoglobulins.¹⁶

The major site of human B-cell differentiation is the BM. The majority of developing B cells generates autoreactive immunoglobulins (Ig), which are selectively removed, resulting in only 20% autoreactivity in circulating naive mature B cells.¹⁷ Early thymic progenitors have been shown to sustain B-cell potential,^{18, 19} and in some studies progenitor B cells have been detected in human thymus.^{10, 11} Moreover, the Ig gene repertoire of thymic B cells was found to be distinct from pediatric B cells from BM, and more similar to fetal B cells with regards to usage of V_H1-2 and V_H6-1 genes, although thymic B cells contained longer IgH-CDR3 regions than fetal B cells.^{12, 13} Still, data on the thymic Ig gene repertoire is limited, and to date, it remains unclear whether these immunoglobulins indeed bind to self-antigens.

Here, we studied the Ig gene repertoires of single-sorted B cells from fetal BM, pediatric BM and pediatric thymus, and cloned these genes to assess their ability to bind self-antigens. Fetal B cells showed a distinctive *IGH* gene repertoire and many were reactive to dsDNA. While the Ig gene repertoires of pediatric BM and thymus were very similar, thymic B cells showed increased reactivity towards protein autoantigens.

RESULTS

Detection of B cells in human thymus

To confirm the previously reported presence of B cells in human thymus,^{10, 11} we depleted CD8⁺ and CD4⁺ cells by magnetic separation from single cell suspensions prior to multi-color flow cytometric analysis. Within these remaining cells, the CD19⁺ subset hardly contained any IgM-negative progenitor B cells, which predominate in fetal or pediatric BM (**Figure 1**). In contrast, the vast majority of B cells in human thymus were naive mature, being positive for IgM and IgD, and negative for CD34, CD10 and CD27 (**Figure 1**). While this does not exclude the potential of the thymus to support B-cell differentiation, it appears that the majority of B cells in the human thymus are resident mature cells rather than developing progenitors.

Thymic B cells do not express a fetal Ig gene repertoire

To study the nature of these thymic B cells, we first analyzed their Ig gene repertoire. Ig heavy (*IGH*) and Ig light chain (*IGK* and *IGL*) gene rearrangements were amplified and sequenced from single-sorted CD19⁺IgM⁺IgD⁺ naive mature B cells from human thymus, and compared to previously generated rearrangements from naive mature B cells of fetal and pediatric BM (Rother *et al.*, submitted).

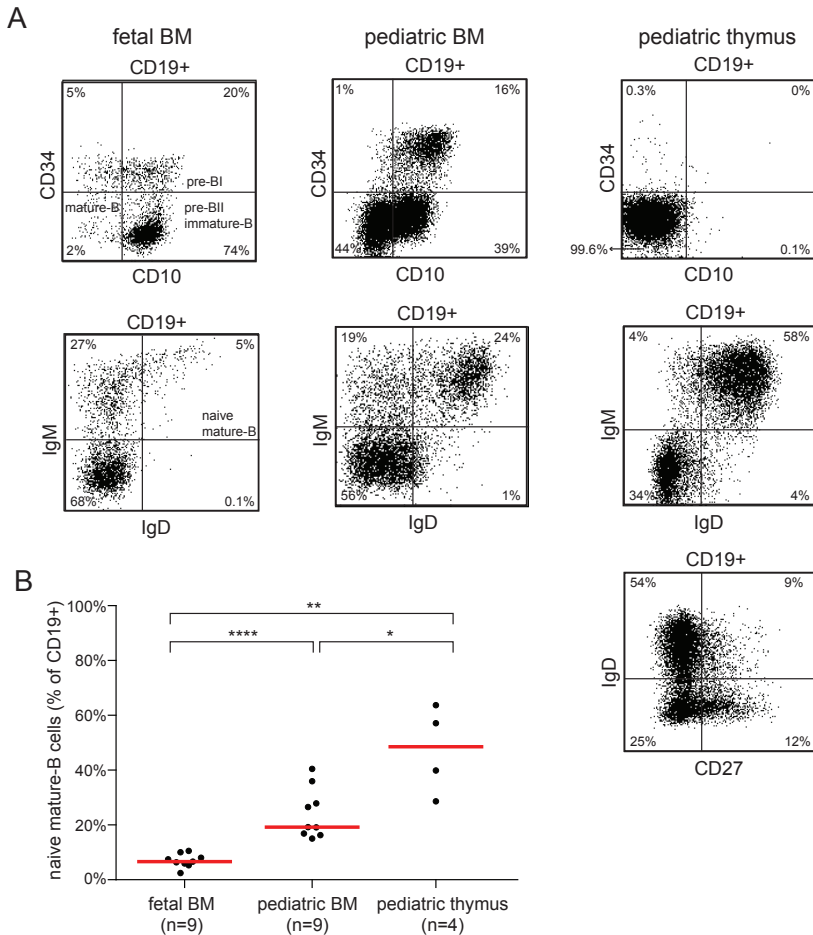


Figure 1. The majority of B cells in the human thymus has a naive mature phenotype. (A) Flow cytometric analysis of CD19⁺ precursor-B and naive-B cells in fetal bone marrow (BM), pediatric BM and pediatric thymus. Representative dot plot images were derived from one donor. (B) Frequencies of naive-B cells within CD19⁺ cells determined by flow cytometric analysis in fetal BM (9 donors), pediatric BM (9 donors) and pediatric thymus (4 donors). Red lines represent median values. The nonparametric Mann-Whitney U test was used to calculate significance levels: *, $p < .05$; **, $p < .01$; ****, $p < .0001$.

The *IGH* and Ig light chain gene rearrangements of thymic B cells were highly diverse regarding V, D and J gene usage (Figures 2, S1A-B, S2A-B). In contrast to fetal BM B cells, the thymic B cells did not show skewed usage of V_{H1-2} , D_{H7-27} , J_{H2} and J_{H3} . In fact, the *IGH* and Ig light chain gene repertoires of pediatric thymus and BM B cells were remarkably similar with the only exception being significantly increased usage of V_{H1-69} in thymic B cells (Figure 2A-C).

In addition to gene usage, the rearranged *IGH* and Ig light chain genes in thymic B cells encoded highly diverse CDR3 regions (Figure 3, S1C-D, S2C-D). The size

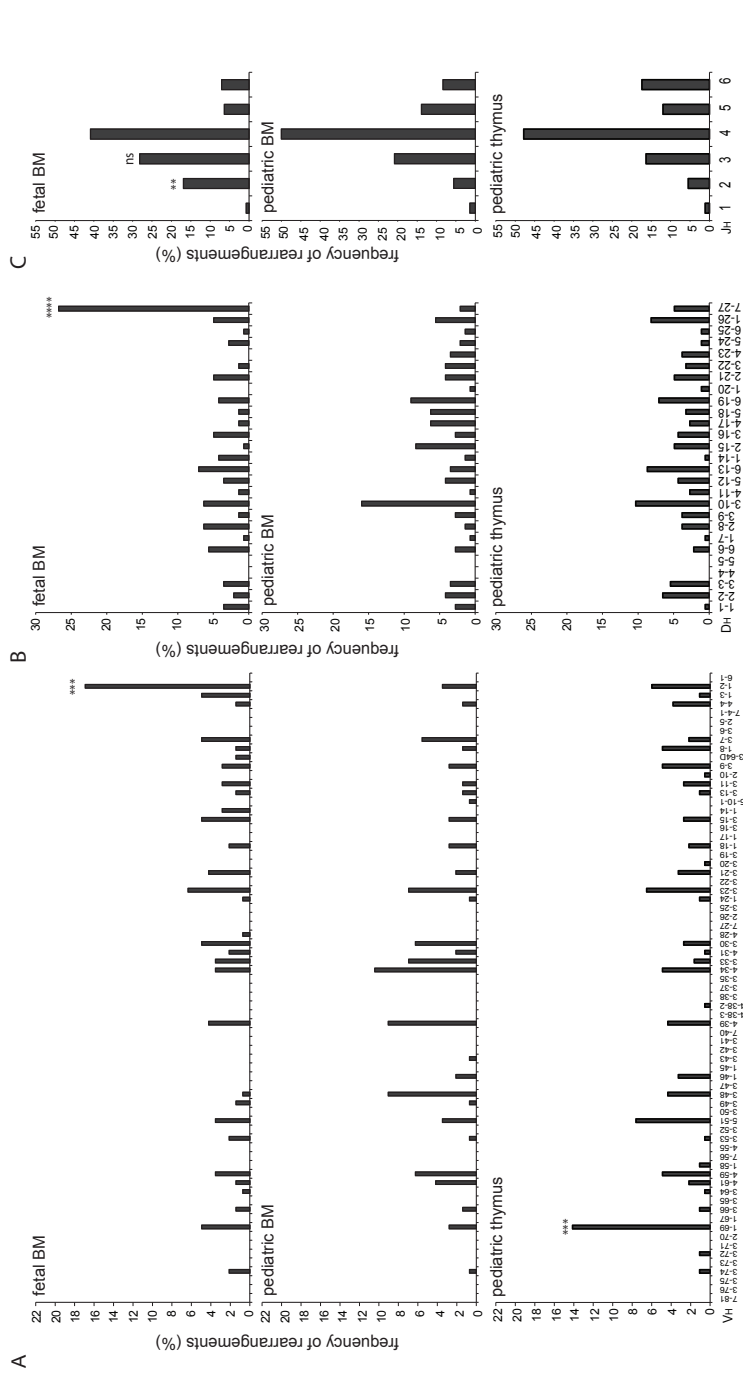


Figure 2. The Ig gene repertoire of thymic B cells does not resemble that of fetal B cells. (A) IGHV (B) IGHD and (C) IGHJ gene usage in transcripts from single-cell sorted naive mature-B cells from fetal BM, pediatric BM and pediatric thymus. The genes are ordered according to their 5' to 3' genomic positions in the IGH locus. In total, 142 sequences were derived from 3 fetal BM samples, 144 from 3 pediatric BM donors and 184 from 3 thymuses. Data from individual samples showed similar patterns of gene usage. Statistical significance in gene usage between fetal and pediatric BM and thymus was determined with the χ^2 test. **, p < 0.01; ***, p < 0.001; ****, p < 0.0001; ns, not significant.

distributions did not significantly differ from B cells of pediatric BM. However, fetal BM B cells carried significantly smaller IgH-CDR3 regions than B cells from pediatric BM or thymus due to smaller numbers of N-nucleotide additions (**Figure 3**). Thymic IgH-CDR3 regions were slightly, but not significantly, smaller than pediatric BM B cells (**Figure 3A**). This was mostly due to significantly fewer N-nucleotides in their DH-JH junctions (**Figure 3B**).

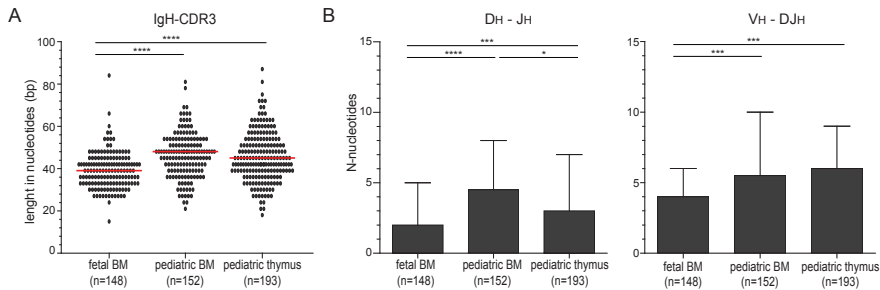


Figure 3. IgH-CDR3 regions and N-nucleotides are similar in B cells from pediatric thymus and pediatric bone marrow (BM), and are distinct from B cells of fetal BM. (A) Scatter plots showing the CDR3 length in nucleotides of *IGH* in single-sorted naive mature-B cells sorted from 3 fetal BM, 3 pediatric BM and 3 thymic donors. Red horizontal lines represent median values. Numbers in brackets indicate the amount of analyzed sequences. In-frame rearrangements were included in the analysis. (B) Bar graphs showing the median numbers of N-nucleotides in DH-JH and VH-DJH junctions with inter-quartile range. The nonparametric Mann-Whitney U test was used to calculate significance levels: *, $p < .05$; ***, $p < .001$; ****, $p < .0001$.

Thus, contrary to previously published data,^{12, 13} we showed that single-cell sorted naive mature B cells from human thymus have a diverse Ig gene repertoire, which does not show the typical skewing of V, D and J gene usage nor short IgH-CDR3 regions that are typically found in fetal BM.

Autoreactivity of thymic B cells

Previous studies suggested that the thymic B cells are enriched for autoreactive clones that are capable to take up auto-antigens and present these to developing T-cells during negative selection.^{10, 12, 13, 15} To test this hypothesis, we generated recombinant antibodies from the Ig genes of single-cell sorted naive mature B cells and tested their reactivity by ELISA to various types of autoantigens and compared these with antibodies derived from naive mature B cells of fetal and pediatric BM.

We were able to successfully clone and express antibodies from 2 donors of fetal BM (26 antibodies), pediatric BM (36 antibodies) and pediatric thymus (31 antibodies). These antibodies showed similar VH, DH and JH gene usage as the overall repertoire of all amplified rearrangements (**Figure S3A-C**). To test reactivity to nuclear antigens,

we first performed an ELISA with Hep-2 cell lysate, a procedure to detect the presence of anti-nuclear antibodies (ANA) in patients with autoimmune disease.²¹ Significantly more antibodies derived from thymic B cells showed reactivity to Hep-2 cell lysate (45%) than those from pediatric BM (17%; **Figure 4A**). Furthermore, the OD levels of thymic antibodies were significantly higher than for pediatric BM. Antibodies derived from fetal BM showed intermediate levels of Hep-2 cell lysate reactivity (39%) and were not significantly different from pediatric BM or thymus.

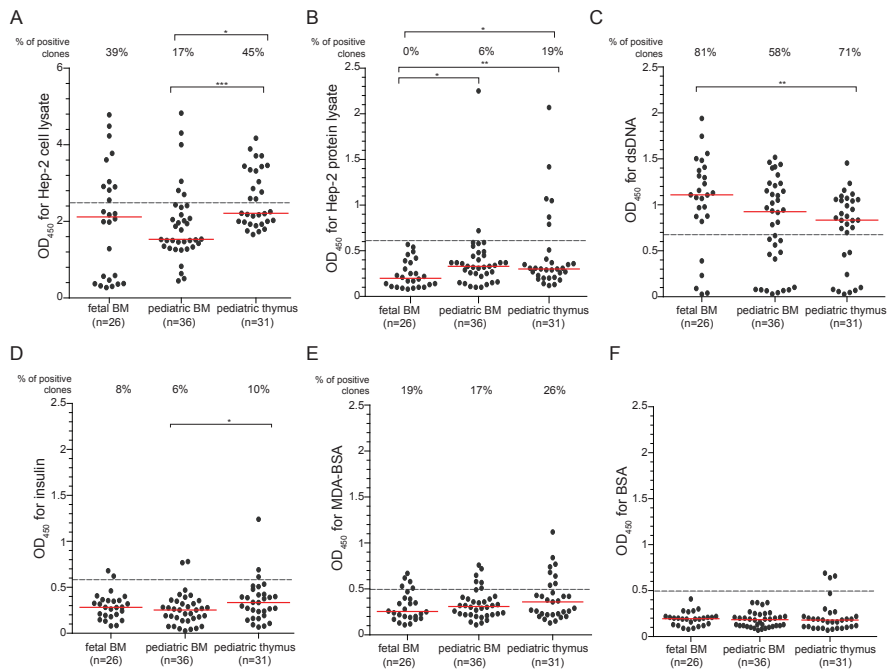


Figure 4. Thymus contains autoreactive B cells. Reactivity of fetal BM, pediatric BM and pediatric thymic recombinant antibodies expressed from single-sorted naive mature-B cells. Reactivity was measured by ELISA for Hep-2 cell lysate (A), Hep-2 protein lysate (B), dsDNA (C), insulin (D), MDA-BSA (E) and BSA (F). In total, 26 fetal BM, 36 pediatric BM and 31 pediatric thymic recombinant antibodies were analyzed, all derived from 2 donors. Each ELISA graph shows OD₄₅₀ values measured for the antibodies and percentage of positive clones. Red lines represent median value. Dashed line depicts cut-off value set at 2.5 (Hep-2 cell lysate), 0.6 (Hep-2 protein lysate), 0.67 (dsDNA), 0.59 (insulin) or 0.5 (MDA-BSA and BSA), above which antibodies were determined as positive. The nonparametric Mann-Whitney U test was used to calculate significance levels between the OD values of antibodies, and the χ^2 test to analyze significance levels of the fractions of positive clones between subsets: *, $p < .05$; **, $p < .0001$; ***, $p < .001$.

Subsequently, we analyzed which cellular components, i.e. Hep-2 cell proteins or dsDNA, were recognized more frequently by the recombinant antibodies from fetal BM, pediatric BM and pediatric thymus. Despite the low numbers of positive clones, significantly more thymus-derived antibodies were reactive to Hep-2 proteins than fetal or

pediatric BM (**Figure 4B**). The frequencies of antibodies reacting to dsDNA were much higher: fetus BM, 81%; child BM, 58%; thymus, 71% (**Figure 4C**), but did not differ between the three tissues. However, the OD value for dsDNA-reactive fetal BM-derived antibodies was significantly higher than for thymus-derived antibodies. Furthermore, 70% of fetal Hep-2 reactive antibodies recognized dsDNA, while this was only 50% for thymus-derived Hep-2 reactive antibodies (**Table S2**).

In contrast to dsDNA, only few of the antibodies showed binding to the insulin peptide, and to malondialdehyde (MDA) groups, which are products of stress-related enhanced lipid peroxidation and are present on apoptotic cells.²² Although the fractions of insulin-binding clones did not differ between fetal BM (8%), pediatric BM (6%) and thymus (10%), thymus-derived antibodies showed significantly higher levels of interaction than pediatric BM-derived antibodies (**Figure 4D**). MDA-binding was measured with an ELISA to an MDA-bovine serum albumin (BSA) conjugate, and the frequency of reactive clones did not differ significantly between fetal BM, pediatric BM and thymus (19%, 17% and 26% respectively; **Figure 4E**). This reactivity was specific for the MDA-BSA conjugate, as nearly all antibodies were negative for binding to BSA only (**Figure 4F**).

Taken together, we showed that B cells from pediatric thymus had increased reactivity to protein autoantigens, while autoreactivity of fetal BM derived clones was mostly directed towards dsDNA.

Polyreactivity of thymic B cells

Subsequently, we analyzed binding of the recombinant antibodies to combinations of molecules with distinct chemical properties, i.e. dsDNA, insulin, MDA-BSA and LPS (**Figures 4C-E and 5A**). We considered polyreactivity as recognition of 3 or 4 out of 4 antigens. While fetal BM and pediatric BM clones showed increased simultaneous recognition of 2 antigens (double-reactivity: fetus BM, 12%; pediatric BM, 11%; pediatric thymus, 3%), thymic antibodies reacted more frequently with 3 or even 4 antigens at the same time (triple-reactivity: fetus BM, 4%; pediatric BM, 8%; pediatric thymus, 13%, quadruple-reactivity: fetus BM, 0%; pediatric BM, 0%; pediatric thymus, 6%) (**Figure 5B**). Thus, thymic B cells showed tendency of increased polyreactivity and binding to multiple different antigenic structures.

Ig repertoire properties of autoreactive B cells

To study whether specific DNA properties underlined autoreactivity, we compared the rearrangements of ANA positive vs negative and dsDNA positive vs negative antibodies

of fetal and pediatric BM and pediatric thymus. HEp-2 cell lysate reactive antibodies from pediatric BM and thymus showed slightly longer IgH-CDR3 and Ig light chain CDR3 regions (IgL-CDR3), of which only the latter were significant (**Figure 6A-B**). Furthermore, Ig λ chain usage was significantly higher in ANA from pediatric BM and thymus (**Figure 6C**).

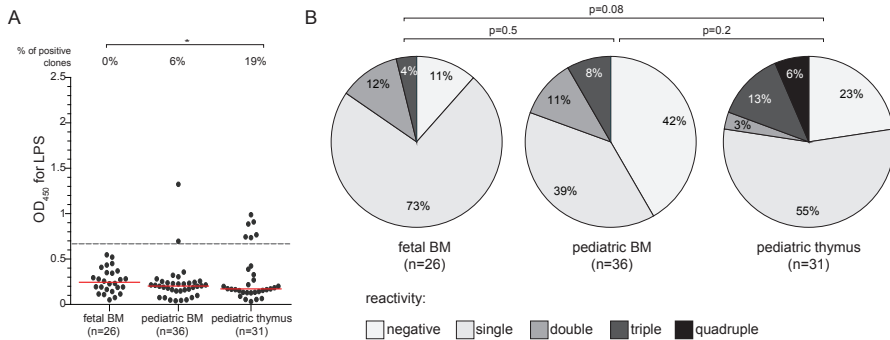


Figure 5. Thymic B cells display increased polyreactivity. (A) Reactivity of fetal BM, pediatric BM and pediatric thymic recombinant antibodies expressed from single-sorted naive mature-B cells towards LPS. Red lines represent median value. Dashed line depicts cut-off value set at 0.67, above which antibodies were determined as positive. The χ^2 test was used to calculate significance levels of the fractions of positive clones between subsets: *, $p < .05$. (B) Frequencies of polyreactive clones within fetal BM, pediatric BM and pediatric thymic recombinant antibodies. Polyreactivity was defined as recognition of 3 or 4 out of 4 antigens with different properties: dsDNA, insulin, MDA-BSA and LPS. Antibodies were grouped into 5 categories, i.e. negative, single-reactive, double-reactive, triple-reactive and quadruple-reactive when recognizing 0, 1, 2, 3 or 4 antigens respectively. The numbers of analyzed clones are indicated in-between brackets. The χ^2 test was used to calculate significance levels of the polyreactive vs non-polyreactive clones between subsets.

dsDNA-binding antibodies had a trend for shorter IgH-CDR3 and IgL-CDR3 lengths (**Figure 6D-E**), of which only the IgL-CDR3 for pediatric thymus was significant. In contrast to ANA, the dsDNA-binding antibodies carried significantly more often an Ig κ light chain (**Figure 6F**).

Taken together, we showed that the reactivity of B cells in fetal BM and pediatric thymus differs from that in pediatric BM. Fetal B cells carried a skewed Ig gene repertoire and their antibodies showed increased reactivity towards dsDNA. In contrast, the thymic B-cell repertoire was not different from pediatric BM, while the antibodies were more reactive to protein autoantigens.

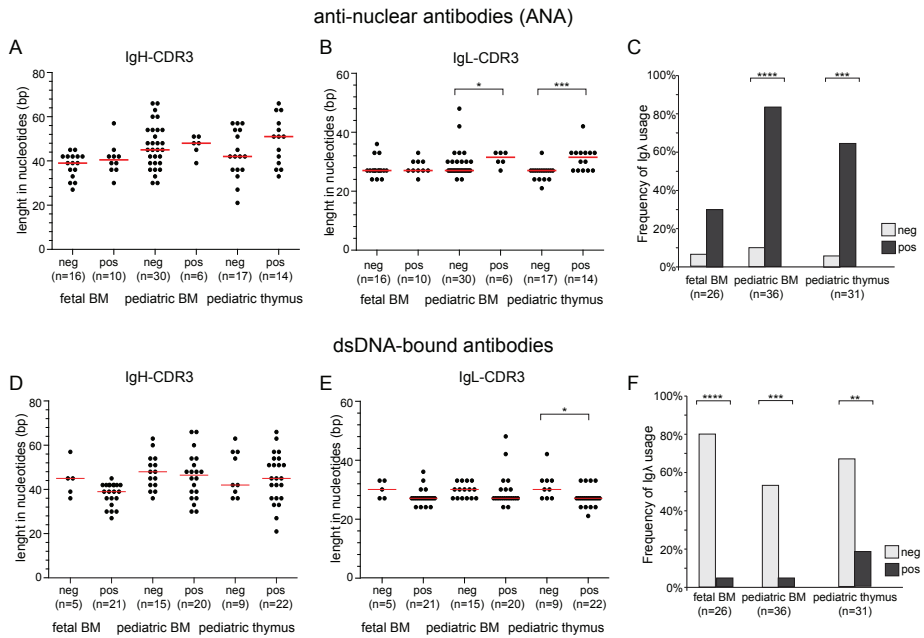


Figure 6. Ig gene repertoire of recombinant antibodies reactive to HEp-2 cell lysate and to dsDNA. IgH-CDR3 length, Ig λ usage, and IgL-CDR3 length analyzed for recombinant antibodies expressed from single-cell sorted naive mature-B cells from fetal BM, pediatric BM and pediatric thymus which were negatively (neg) and positively (pos) reactive to HEp-2 lysate (A, B, C) and to dsDNA (D, E, F). In total, 26 clones were obtained from 2 fetal BM, 36 clones from 2 pediatric BM and 31 clones from 2 pediatric thymic samples. The numbers of analyzed clones are indicated in-between brackets. Red horizontal lines represent median values. The non-parametric Mann-Whitney U test (panels A,B,D,E,) and the χ^2 test (panels C,F) were used to calculate significance levels: *, $p < .05$; **, $p < 0.01$; ***, $p < 0.001$; ****, $p < 0.0001$.

DISCUSSION

Our study shows that B cells from human thymus display an Ig gene repertoire that is similar to pediatric BM and does not show typical skewing in V_H, D_H and J_H gene usage, nor short IgH-CDR3 regions that are typical for fetal BM B cells. Still, thymic B cells appeared enriched for autoreactive clones that showed increased specificity to peptide autoantigens, and not towards dsDNA as seen for fetal B cells.

We here detected B cells in the human thymus. The presence of B cells in human thymus has been postulated almost 30 years ago, and these cells were mainly found in the medulla concentrated around Hassall's corpuscles.^{10, 11, 23} These were all mature Ig-expressing B cells, and in contrast to Weerkamp *et al.*, we and others did not detect IgM-negative B-cell precursors.^{15, 24-26} Furthermore, the Ig gene repertoire of the naive mature thymic B cells was diverse and did not differ from that of pediatric BM-derived B

cells. Importantly, it did not resemble the skewed fetal Ig gene repertoire, which is characterized by shorter IgH-CDR3 regions and more frequent usage of the VH1-2, DH7-27, JH2 and JH3 genes (Rother *et al.*, submitted).²⁷ Our observations do not exclude that the resident mature B cells in human thymus are derived from local precursors. Still, the difficulty in detecting progenitor-B cells and the similarities with the pediatric BM Ig gene repertoire, are more in line with migration into the thymus of BM-derived mature B cells rather than local B-cell development.

In the 1990s, several studies reported that Ig gene rearrangements in human thymus were distinct from peripheral blood B cells, and involved more frequent usage of VH4-34 and the presence of VH1, VH3, VH6 and JH2 families restricted to the fetal Ig repertoire.^{12, 13} Our observations contrast these earlier findings, most likely due to recent advances in Ig repertoire analyses. We and others have more extensively studied the fetal Ig gene repertoire in single-sorted B cells or with next generation sequencing (Rother *et al.*, submitted).²⁷ Thus, the differences between the fetal and pediatric Ig gene repertoires are now better defined. Furthermore, our data set from thymic Ig gene rearrangements is much larger than those of previous studies and was derived from single-sorted B cells. Although in our hands the thymus B-cell repertoire differs greatly from fetal B-cells and was highly similar to BM-derived B cells, we do not exclude that subtle differences exist in V, D or J gene usage that will only be detectable with high throughput sequencing analysis.

We here for the first time were able to study the reactivity of thymic B cells. Interestingly, thymic B cells were enriched for binding to insulin and to HEP-2 protein antigens. Human thymic B cells were previously suggested to be more autoreactive based on the more frequent usage of the inherently autoreactive VH4-34 gene,¹² and other VH4 subgroup genes that were commonly found in autoimmune diseases.¹³ The distinct Ig gene rearrangements in thymic B cells were postulated to display another reactivity and thereby play distinct functions.^{10, 12, 13} Indeed, studies using mouse models have shown that B cells in the thymus are involved in negative selection of T cells.^{14, 15, 28-30} Detection of ANA is a common diagnostic tool in autoimmune diseases.²¹ Therefore, the presence of ANA in thymus fits with the current hypothesis of thymic B cells being involved in auto-antigen presentation to T cells and their role in maintenance of the central tolerance. We here did not find evidence of skewed V, D and J gene usage in ANA. More importantly, both pediatric BM and thymus-derived ANA carried longer IgH-CDR3 and IgL-CDR3. Thus, the autoreactivity of B cells in the human thymus does not seem to be based on a unique Ig gene repertoire, but rather on enrichment for autoreactive B cells with similar sequence properties as BM-derived autoreactive B cells.

In addition to thymic B cells, we here also report for the first time on the reactivity of fetal BM-derived B cells. Although the repertoire of fetal B cells has been documented extensively,^{27, 31-35} the suggestion that these genes would encode autoreactive antibodies

has not been addressed before.³⁶⁻³⁸ We here showed that fetal B-cell derived antibodies bind stronger to dsDNA than pediatric BM-derived B-cells. These results suggest that fetal B cells indeed are more frequently autoreactive, and that their reactivity differs from that of thymic B cells. This would fit with a different function of fetal B cells, as opposed to thymic B cells, in the clearance of cell debris during extensive tissue formation and breakdown in the developing fetus. However, more extensive panels of autoantigens would need to be studied to elucidate the role of such autoreactive B cells in tissue (re) modelling.

Taken together, we here show that B cells present in distinct niches, i.e. fetal BM, pediatric BM and pediatric thymus display different reactivity which underlies their apparent functions. Fetal antibodies were more reactive to dsDNA, whereas thymic antibodies were highly reactive to protein autoantigens. B cells from thymus displayed an Ig gene repertoire that was similar to pediatric BM; thus the majority of B cells in the thymus are resident rather than developing and present auto-antigens to developing T-cells during negative selection.

MATERIALS AND METHODS

Fetal and postnatal tissue

The use of human pediatric and fetal tissue was approved by the Medical Ethical Committees of the Erasmus MC and was contingent on informed consent in accordance with the Declaration of Helsinki and the Dutch Fetal tissue act. Thymus material was obtained from 3 children requiring surgery for congenital heart disease. These children were between 2 months and 1.5 year of age and did not have hematologic or immunologic diseases. Fetal BM (3 donors) were obtained from elective abortions, and informed consent was obtained after the decision to abort was finalized. Inclusion in the study did not affect the treatment regime in any way, and did not involve any form of payment. Gestational age was determined by ultrasonic measurement of the diameter of the skull and ranged from 15 to 18 weeks. 3 pediatric BM samples were obtained previously from children aged 2-6 years.^{39, 40}

Single-cell sorting

B cell subsets were purified from homogenized pediatric thymuses, fetal limb BM suspensions and pediatric BM aspirates as described previously.^{11, 19, 39-41} Following Ficoll density gradient centrifugation (Ficoll-Paque PLUS), mononuclear cells from thymuses

were depleted for CD8 and CD4 positive cells by magnetic separation (Miltenyi Biotec). The obtained cells from thymus, fetal BM and pediatric BM samples were stained with the following monoclonal antibodies: CD20-PB (2H7), CD27-BV421 (O323), IgM-BV510 (MHM-88), IgD-FITC (IA6-2), IgM-PerCP-Cy5.5 (MHM-88), IgD-PerCP-Cy5.5 (IA6-2, all from BioLegend), CD34-FITC (8G12), CD20-PE (L27), CD123-PE (9F45), CD19-PE-Cy7 (SJ25C1), CD22-APC (S-HCL-1), CD34-APC (8G12; all from BD Biosciences), CD45-PO (HI30, Invitrogen) and CD10-APC-C750 (HI10A, Cytognos). Naive mature B cells defined as CD19+CD20+CD10-IgM+IgD+CD27- were single-cell sorted on a FACSAria cell sorter with FACSDiva software (BD Biosciences) into 96-well PCR plates containing 4 μ l lysis solution (0.5 \times PBS containing 10mM DTT, 8 U RNAsin (Promega), and 0.4 U 5'-3' RNase Inhibitor (Eppendorf)) and immediately frozen on dry ice.

cDNA synthesis, Ig genes amplification and antibody production

RNA from single cells was reverse-transcribed in the original 96-well plate in 12.5 μ l reactions containing 100 U Superscript III RT (Life Technologies) for 45 minutes at 42°C. PCR reactions and primer sequences (**Table S1**).^{15, 17, 42, 43} Ig cloning and antibody expression procedures were performed as described previously.^{15, 17, 42, 43} The usage of V, D, J genes as well as the junctional regions were analyzed using the international ImMunoGeneTics (IMGT) information system (<http://imgt.cines.fr/>).²⁰

ELISAs

Antibody reactivity analysis was performed as described previously, and the highly polyreactive ED38 antibody was used as positive control.^{15, 17, 42, 43} Briefly, ELISA assays were performed to determine Ig reactivity to HEp-2 cell lysate (Inova Diagnostic), Hep-2 cell protein lysate (Novus Biologicals), dsDNA, insulin, LPS, BSA (all from Sigma-Aldrich) and MDA-BSA (Academy Bio-medical) using antibodies concentrations of 10 μ g/ml (Hep-2 cell lysate and Hep-2 cell protein lysate) or 1 μ g/ml (dsDNA, insulin, LPS, BSA and MDA-BSA). Anti-human Ig κ and Ig λ horse radish peroxidase (HRP) conjugates were used for detection (both from Sigma). ELISAs were visualized with 3,3',5,5'-Tetramethylbenzidine (TMB) and the reaction was stopped with 1M H₂SO₄ prior to optical density (OD) measurements at 450 nm wavelength. Cut-off values were determined independently for each ELISA assay based on the total measurements, with values above normal Gaussian distribution defined as being positive.

Statistics

Statistical significance was calculated by with the non-parametric Mann-Whitney U test, or the χ^2 test as indicated in the Figure legends. P values <0.05 were considered as significant.

ACKNOWLEDGEMENTS

We thank the technicians of the Autoimmune Diagnostic group for their technical assistance, and Dr. M.A. Berkowska for advice on recombinant antibody production from single cells. This study was performed in the department of Immunology as part of the Molecular Medicine Postgraduate School of the Erasmus MC, and was supported by ZonMW Veni grant 916.116.090 to MCvZ.

REFERENCES

1. Miller, J. F. 2002. The discovery of thymus function and of thymus-derived lymphocytes. *Immunol Rev* 185:7-14.
2. Mitchell, G. F., and J. F. Miller. 1968. Cell to cell interaction in the immune response. II. The source of hemolysin-forming cells in irradiated mice given bone marrow and thymus or thoracic duct lymphocytes. *J Exp Med* 128:821-837.
3. Lind, E. F., S. E. Prockop, H. E. Porritt, and H. T. Petrie. 2001. Mapping precursor movement through the postnatal thymus reveals specific microenvironments supporting defined stages of early lymphoid development. *J Exp Med* 194:127-134.
4. Yang, S. J., S. Ahn, C. S. Park, K. L. Holmes, J. Westrup, C. H. Chang, and M. G. Kim. 2006. The quantitative assessment of MHC II on thymic epithelium: implications in cortical thymocyte development. *Int Immunol* 18:729-739.
5. Mathis, D., and C. Benoist. 2009. Aire. *Annu Rev Immunol* 27:287-312.
6. Metzger, T. C., and M. S. Anderson. 2011. Control of central and peripheral tolerance by Aire. *Immunol Rev* 241:89-103.
7. Anderson, G., and E. J. Jenkinson. 2001. Lymphostromal interactions in thymic development and function. *Nat Rev Immunol* 1:31-40.
8. Hinterberger, M., M. Aichinger, O. Prazeres da Costa, D. Voehringer, R. Hoffmann, and L. Klein. 2010. Autonomous role of medullary thymic epithelial cells in central CD4(+) T cell tolerance. *Nat Immunol* 11:512-519.
9. Klein, L., B. Kyewski, P. M. Allen, and K. A. Hogquist. 2014. Positive and negative selection of the T cell repertoire: what thymocytes see (and don't see). *Nat Rev Immunol* 14:377-391.

10. Spencer, J., M. Choy, T. Hussell, L. Papadaki, J. P. Kington, and P. G. Isaacson. 1992. Properties of human thymic B cells. *Immunology* 75:596-600.
11. Weerkamp, F., E. F. de Haas, B. A. Naber, W. M. Comans-Bitter, A. J. Bogers, J. J. van Dongen, and F. J. Staal. 2005. Age-related changes in the cellular composition of the thymus in children. *J Allergy Clin Immunol* 115:834-840.
12. Dunn-Walters, D. K., C. J. Howe, P. G. Isaacson, and J. Spencer. 1995. Location and sequence of rearranged immunoglobulin genes in human thymus. *Eur J Immunol* 25:513-519.
13. Tonnelle, C., C. D'Ercole, V. Depraetere, D. Metras, L. Boubli, and M. Fougereau. 1997. Human thymic B cells largely overexpress the VH4 Ig gene family. A possible role in the control of tolerance in situ? *Int Immunol* 9:407-414.
14. Frommer, F., and A. Waisman. 2010. B cells participate in thymic negative selection of murine auto-reactive CD4+ T cells. *PLoS One* 5:e15372.
15. Yamano, T., J. Nedjic, M. Hinterberger, M. Steinert, S. Koser, S. Pinto, N. Gerdes, E. Lutgens, N. Ishimaru, M. Busslinger, B. Brors, B. Kyewski, and L. Klein. 2015. Thymic B Cells Are Licensed to Present Self Antigens for Central T Cell Tolerance Induction. *Immunity* 42:1048-1061.
16. Roche, P. A., and K. Furuta. 2015. The ins and outs of MHC class II-mediated antigen processing and presentation. *Nat Rev Immunol* 15:203-216.
17. Wardemann, H., S. Yurasov, A. Schaefer, J. W. Young, E. Meffre, and M. C. Nussenzweig. 2003. Predominant autoantibody production by early human B cell precursors. *Science* 301:1374-1377.
18. Luc, S., T. C. Luis, H. Boukarabila, I. C. Macaulay, N. Buza-Vidas, T. Bouriez-Jones, M. Lutteropp, P. S. Woll, S. J. Loughran, A. J. Mead, A. Hultquist, J. Brown, T. Mizukami, S. Matsuoka, H. Ferry, K. Anderson, S. Duarte, D. Atkinson, S. Soneji, A. Domanski, A. Farley, A. Sanjuan-Pla, C. Carella, R. Patient, M. de Bruijn, T. Enver, C. Nerlov, C. Blackburn, I. Godin, and S. E. Jacobsen. 2012. The earliest thymic T cell progenitors sustain B cell and myeloid lineage potential. *Nat Immunol* 13:412-419.
19. Weerkamp, F., M. R. Baert, M. H. Brugman, W. A. Dik, E. F. de Haas, T. P. Visser, C. J. de Groot, G. Wagemaker, J. J. van Dongen, and F. J. Staal. 2006. Human thymus contains multipotent progenitors with T/B lymphoid, myeloid, and erythroid lineage potential. *Blood* 107:3131-3137.
20. Alamyar, E., P. Duroux, M. P. Lefranc, and V. Giudicelli. 2012. IMGT((R)) tools for the nucleotide analysis of immunoglobulin (IG) and T cell receptor (TR) V-(D)-J repertoires, polymorphisms, and IG mutations: IMGT/V-QUEST and IMGT/HighV-QUEST for NGS. *Methods Mol Biol* 882:569-604.
21. Rehman, H. U. 2015. Antinuclear antibodies: when to test and how to interpret findings. *J Fam Pract* 64:E5-8.
22. Horkko, S., C. J. Binder, P. X. Shaw, M. K. Chang, G. Silverman, W. Palinski, and J. L. Witztum. 2000. Immunological responses to oxidized LDL. *Free Radic Biol Med* 28:1771-1779.
23. Isaacson, P. G., A. J. Norton, and B. J. Addis. 1987. The human thymus contains a novel population of B lymphocytes. *Lancet* 2:1488-1491.

24. Balciunaite, G., R. Ceredig, and A. G. Rolink. 2005. The earliest subpopulation of mouse thymocytes contains potent T, significant macrophage, and natural killer cell but no B-lymphocyte potential. *Blood* 105:1930-1936.
25. Harman, B. C., W. E. Jenkinson, S. M. Parnell, S. W. Rossi, E. J. Jenkinson, and G. Anderson. 2005. T/B lineage choice occurs prior to intrathymic Notch signaling. *Blood* 106:886-892.
26. Porritt, H. E., L. L. Rumfelt, S. Tabrizifard, T. M. Schmitt, J. C. Zuniga-Pflucker, and H. T. Petrie. 2004. Heterogeneity among DN1 prothymocytes reveals multiple progenitors with different capacities to generate T cell and non-T cell lineages. *Immunity* 20:735-745.
27. Rechavi, E., A. Lev, Y. N. Lee, A. J. Simon, Y. Yinon, S. Lipitz, N. Amariglio, B. Weisz, L. D. Notarangelo, and R. Somech. 2015. Timely and spatially regulated maturation of B and T cell repertoire during human fetal development. *Sci Transl Med* 7:276ra225.
28. Mazda, O., Y. Watanabe, J. Gyotoku, and Y. Katsura. 1991. Requirement of dendritic cells and B cells in the clonal deletion of Mls-reactive T cells in the thymus. *J Exp Med* 173:539-547.
29. Zoller, M. 1990. Intrathymic presentation of nominal antigen by B cells. *Int Immunol* 2:427-434.
30. Perera, J., L. Meng, F. Meng, and H. Huang. 2013. Autoreactive thymic B cells are efficient antigen-presenting cells of cognate self-antigens for T cell negative selection. *Proc Natl Acad Sci U S A* 110:17011-17016.
31. Schroeder, H. W., Jr., L. Zhang, and J. B. Phillips, 3rd. 2001. Slow, programmed maturation of the immunoglobulin HCDR3 repertoire during the third trimester of fetal life. *Blood* 98:2745-2751.
32. Shiokawa, S., F. Mortari, J. O. Lima, C. Nunez, F. E. Bertrand, P. M. Kirkham, S. G. Zhu, A. P. Dasanayake, and H. W. Schroeder. 1999. IgM heavy chain complementarity-determining region 3 diversity is constrained by genetic and somatic mechanisms until two months after birth. *J Immunol* 162:6060-6070.
33. Souto-Carneiro, M. M., G. P. Sims, H. Girschik, J. Lee, and P. E. Lipsky. 2005. Developmental changes in the human heavy chain CDR3. *J Immunol* 175:7425-7436.
34. Zemlin, M., R. L. Schelonka, K. Bauer, and H. W. Schroeder, Jr. 2002. Regulation and chance in the ontogeny of B and T cell antigen receptor repertoires. *Immunol Res* 26:265-278.
35. Stein, K. E. 1992. Thymus-independent and thymus-dependent responses to polysaccharide antigens. *J Infect Dis* 165 Suppl 1:S49-52.
36. Meffre, E., and J. E. Salmon. 2007. Autoantibody selection and production in early human life. *J Clin Invest* 117:598-601.
37. Merbl, Y., M. Zucker-Toledano, F. J. Quintana, and I. R. Cohen. 2007. Newborn humans manifest autoantibodies to defined self molecules detected by antigen microarray informatics. *J Clin Invest* 117:712-718.
38. Wang, C., S. P. Turunen, O. Kumm, M. Veneskoski, J. Lehtimäki, A. E. Nissinen, and S. Horkko. 2013. Natural antibodies of newborns recognize oxidative stress-related malondialdehyde acetaldehyde adducts on apoptotic cells and atherosclerotic plaques. *Int Immunol* 25:575-587.
39. Jensen, K., M. B. Rother, B. S. Brusletto, O. K. Olstad, H. C. D. Aass, M. C. van Zelm, P. Kierulf, and K. M. Gautvik. 2013. Increased ID2 Levels in Adult Precursor B Cells as Compared with Children

- Is Associated with Impaired Ig Locus Contraction and Decreased Bone Marrow Output. *J Immunol* 191:1210-1219.
40. van Zelm, M. C., M. van der Burg, D. de Ridder, B. H. Barendregt, E. F. de Haas, M. J. Reinders, A. C. Lankester, T. Revesz, F. J. Staal, and J. J. van Dongen. 2005. Ig gene rearrangement steps are initiated in early human precursor B cell subsets and correlate with specific transcription factor expression. *J Immunol* 175:5912-5922.
 41. Cao, H., B. Williams, and S. K. Nilsson. 2014. Investigating the interaction between hematopoietic stem cells and their niche during embryonic development: optimizing the isolation of fetal and newborn stem cells from liver, spleen, and bone marrow. *Methods Mol Biol* 1185:9-20.
 42. Meffre, E., A. Schaefer, H. Wardemann, P. Wilson, E. Davis, and M. C. Nussenzweig. 2004. Surrogate light chain expressing human peripheral B cells produce self-reactive antibodies. *J Exp Med* 199:145-150.
 43. Tiller, T., E. Meffre, S. Yurasov, M. Tsuiji, M. C. Nussenzweig, and H. Wardemann. 2008. Efficient generation of monoclonal antibodies from single human B cells by single cell RT-PCR and expression vector cloning. *J Immunol Methods* 329:112-124.

SUPPLEMENTAL MATERIAL

Table S1. Primer sequences used for analysis of complete Ig gene rearrangements and cloning.⁴⁵

PCR type	Locus	Target	Primer	Type	Sequence (5'-3')
Ig gene rearrangements in naive-B cells 1st PCR	<i>IGH</i>	V _H - DJ _H	L-V _H 1	Forward	ACAGGTGCCACTCCAGGTGCAG
			L-V _H 3	Forward	AAGGTGTCCAGTGTGARGTGCAG
			L-V _H 4/6	Forward	CCCAGATGGGTCTCTGCCAGGTGCAG
			L-V _H 5	Forward	CAAGGAGTCTGTTCCGAGGTGCAG
			C _H 1	Reverse	GGGAATTCACAGGAGACGA
Ig gene rearrangements in naive-B cells 2nd PCR	<i>IGH</i>	V _H - DJ _H	Age1-V _H 1/5	Forward	CTGCAACCGGTGTACATTCGGAGGTGCAGCTGGTGCAG
			Age1-V _H 3	Forward	CTGCAACCGGTGTACATTCGAGGTGCAGCTGGTGCAG
			Age1-V _H 3-2/3	Forward	CTGCAACCGGTGTACATTCGAGGTGCAGCTGGTGCAG
			Age1-V _H 4	Forward	CTGCAACCGGTGTACATTCGAGGTGCAGCTGGTGCAG
			Age1-V _H 4-3/4	Forward	CTGCAACCGGTGTACATTCGAGGTGCAGCTGGTGCAG
			Sall-J _H 1/2/4/5	Reverse	TCCGAAAGTCGAGCGCTCAGGAGACGGGTGACCCAG
			Sall-J _H 3	Reverse	TCCGAAAGTCGAGCGCTCAGGAGACGGGTGACCCATTG
			Sall-J _H 6	Reverse	TCCGAAAGTCGAGCGCTCAGGAGACGGGTGACCCGTG
			Ig gene rearrangements in naive-B cells 1st PCR	<i>IGK</i>	V _K - J _K
L-V _K 3	Forward	CTCTTCTCTCTGCTACTCTGGCTCCAG			
L-V _K 4	Forward	ATTTCTCTGTTGCTCTGGATCTCTG			
C _K 1	Reverse	CCAGATTTCAACTGCTCATCAGA			
Ig gene rearrangements in naive-B cells 2nd PCR	<i>IGK</i>	V _K - J _K	Age1-V _K 1-5	Forward	CTGCAACCGGTGTACATTCGATCCAGATGACCCAGTGC
			Age1-V _K 1-9	Forward	TTGTGCTGCAACCGGTGTACATTCAGACATCCAGTTGACCCAGTCT
			Age1-V _K 1D-4/3	Forward	CTGCAACCGGTGTACATTCGCCATCCGATGACCCAGTGC
			Age1-V _K 2-2/4	Forward	CTGCAACCGGTGTACATGGGGATATTTGTGATGACCCAGAC
			Age1-V _K 2-2/8	Forward	CTGCAACCGGTGTACATGGGGATATTTGTGATGACTCAGTGC

Age1-Vk3-11	Forward	TTGTGCTGCAACCGGTGTACATTCAGAAATTGTGTGACACAGTC
Age1-Vk3-15	Forward	CTGCAACCGGTGTACATTCAGAAATAGTATGACGCCAGTC
Age1-Vk3-20	Forward	TTGTGCTGCAACCGGTGTACATTCAGAAATTGTGTGACGCCAGTC
Age1-Vk4-1	Forward	CTGCAACCGGTGTACATTCGGACATCGTATGACCCAGTC
Bs1W1-Jk1/4	Reverse	GCCACCGTAGCTTTGATYTCCACCTTGGTC
Bs1W1-Jk2	Reverse	GCCACCGTAGCTTTGATCTCCAGCTTGGTC
Bs1W1-Jk3	Reverse	GCCACCGTAGCTTTGATATCCACTTTGGTC
Bs1W1-Jk5	Reverse	GCCACCGTAGCTTTAAICTCCAGTCGGTGC
<i>IgL</i>		
L-Vλ1	Forward	GGTCTGGGGCCCAGTCTGTGCTG
L-Vλ2	Forward	GGTCTGGGGCCCAGTCTGGCCCTG
L-Vλ3	Forward	GCTCTGTGACCTCCATGAGCTG
L-Vλ4/5	Forward	GGTCTCTCTCSCAGCYTGTGCTG
L-Vλ6	Forward	GTTCTTGGGGCCAAITTTATGCTG
L-Vλ7	Forward	GGTCCAAITTCYCAGGCTGTGGTG
L-Vλ8	Forward	GAGTGGATTCTCAGACTGTGGTG
Cλ	Reverse	CACCAGTGTGGCCITGTTGGCTTG
<i>IgH</i>		
Age1-Vλ1	Forward	CTGTACCCGGTTCCTGGGCCAGTCTGTGCTGACKCAG
Age1-Vλ2	Forward	CTGTACCCGGTTCCTGGGCCAGTCTGCCCTGACTCAG
Age1-Vλ3	Forward	CTGTACCCGGTTCCTGTGACCTCCTATGAGCTGACWCAG
Age1-Vλ4/5	Forward	CTGTACCCGGTTCCTCTCSCAGCYTGTGCTGACTCA
Age1-Vλ6	Forward	CTGTACCCGGTTCCTGGGGCCAAITTTATGCTGACTCAG
Age1-Vλ7/8	Forward	CTGTACCCGGTTCCAAITTCYCAGRCTGTGCTGACYCAG
Xho1-Cλ	Reverse	CTCCTCACTCGAGGGYGGGAACAGAGTG

Ig gene rearrangements in naive-B cells 1st PCR

Ig gene rearrangements in naive-B cells 2nd PCR

Table S2. Reactivities of fetal BM-, pediatric BM- and thymus-derived antibodies towards Hep-2 cell lysate, Hep-2 protein lysate, dsDNA, insulin, MDA-BSA and LPS.

Sample	Hep-2 cell lysate	Hep-2 protein lysate	dsDNA	insulin	MDA-BSA	LPS
fetal BM_1	-	-	+	-	-	-
fetal BM_2	-	-	+	-	-	-
fetal BM_3	-	-	+	-	-	-
fetal BM_4	-	-	+	-	-	-
fetal BM_5	-	-	+	-	-	-
fetal BM_6	-	-	+	-	-	-
fetal BM_7	-	-	-	-	-	-
fetal BM_8	-	-	+	-	-	-
fetal BM_9	-	-	+	-	-	-
fetal BM_10	+	-	+	-	-	-
fetal BM_11	+	-	+	-	-	-
fetal BM_12	-	-	-	-	-	-
fetal BM_13	-	-	+	-	-	-
fetal BM_14	-	-	+	+	-	-
fetal BM_15	-	-	+	-	-	-
fetal BM_16	+	-	-	-	+	-
fetal BM_17	-	-	+	-	-	-
fetal BM_18	-	-	+	-	-	-
fetal BM_19	+	-	-	-	+	-
fetal BM_20	+	-	+	-	-	-
fetal BM_21	-	-	+	+	+	-
fetal BM_22	+	-	+	-	+	-
fetal BM_23	+	-	+	-	-	-
fetal BM_24	+	-	-	-	-	-
fetal BM_25	+	-	+	-	-	-
fetal BM_26	+	-	+	-	+	-
child BM_1	-	-	+	-	-	-
child BM_2	-	-	-	-	-	-
child BM_3	-	-	+	-	-	-
child BM_4	-	-	-	-	-	-
child BM_5	-	-	-	-	-	-
child BM_6	-	-	+	-	-	-
child BM_7	-	-	+	-	-	-
child BM_8	-	-	+	-	+	+

child BM_9	-	-	+	-	+	-
child BM_10	-	-	+	-	-	-
child BM_11	-	-	+	-	+	-
child BM_12	-	-	+	+	-	+
child BM_13	-	-	+	-	+	-
child BM_14	-	-	+	-	-	-
child BM_15	-	-	+	-	-	-
child BM_16	-	-	+	-	-	-
child BM_17	-	-	-	-	-	-
child BM_18	-	+	+	-	-	-
child BM_19	+	-	-	-	-	-
child BM_20	+	-	-	-	-	-
child BM_21	+	-	+	-	-	-
child BM_22	-	-	-	-	-	-
child BM_23	-	-	+	-	-	-
child BM_24	-	-	+	-	-	-
child BM_25	-	-	-	-	-	-
child BM_26	-	-	+	-	+	-
child BM_27	+	-	-	-	-	-
child BM_28	-	+	+	-	-	-
child BM_29	-	-	+	-	-	-
child BM_30	+	-	-	-	-	-
child BM_31	-	-	-	-	-	-
child BM_32	+	-	-	-	-	-
child BM_33	-	-	-	-	-	-
child BM_34	-	-	-	-	-	-
child BM_35	-	-	-	-	-	-
child BM_36	-	-	+	+	+	-
thymus_1	-	-	+	-	-	-
thymus_2	-	-	+	-	-	-
thymus_3	-	-	+	-	-	-
thymus_4	-	-	+	-	-	-
thymus_5	-	-	+	-	-	-
thymus_6	+	-	-	-	-	-
thymus_7	+	-	-	-	-	-
thymus_8	-	+	+	-	-	-
thymus_9	-	+	+	-	-	-
thymus_10	+	-	+	-	-	-

VI. The Human Thymus Is Enriched For Autoreactive B Cells

thymus_11	+	+	-	-	-	-
thymus_12	-	-	+	-	-	-
thymus_13	-	+	+	-	-	-
thymus_14	-	-	+	-	-	-
thymus_15	-	-	+	-	-	-
thymus_16	-	+	+	-	-	-
thymus_17	+	-	+	-	-	-
thymus_18	+	-	+	-	+	-
thymus_19	+	-	-	-	-	-
thymus_20	+	-	-	-	-	-
thymus_21	-	-	+	-	-	-
thymus_22	+	-	-	-	-	-
thymus_23	-	-	-	-	-	-
thymus_24	-	-	+	-	-	-
thymus_25	-	+	-	+	+	+
thymus_26	+	-	-	-	+	-
thymus_27	-	-	+	-	+	+
thymus_28	+	-	+	-	+	+
thymus_29	+	-	+	+	+	+
thymus_30	+	-	+	+	+	+
thymus_31	+	-	+	-	+	+

“+”, positive; “-“, negative

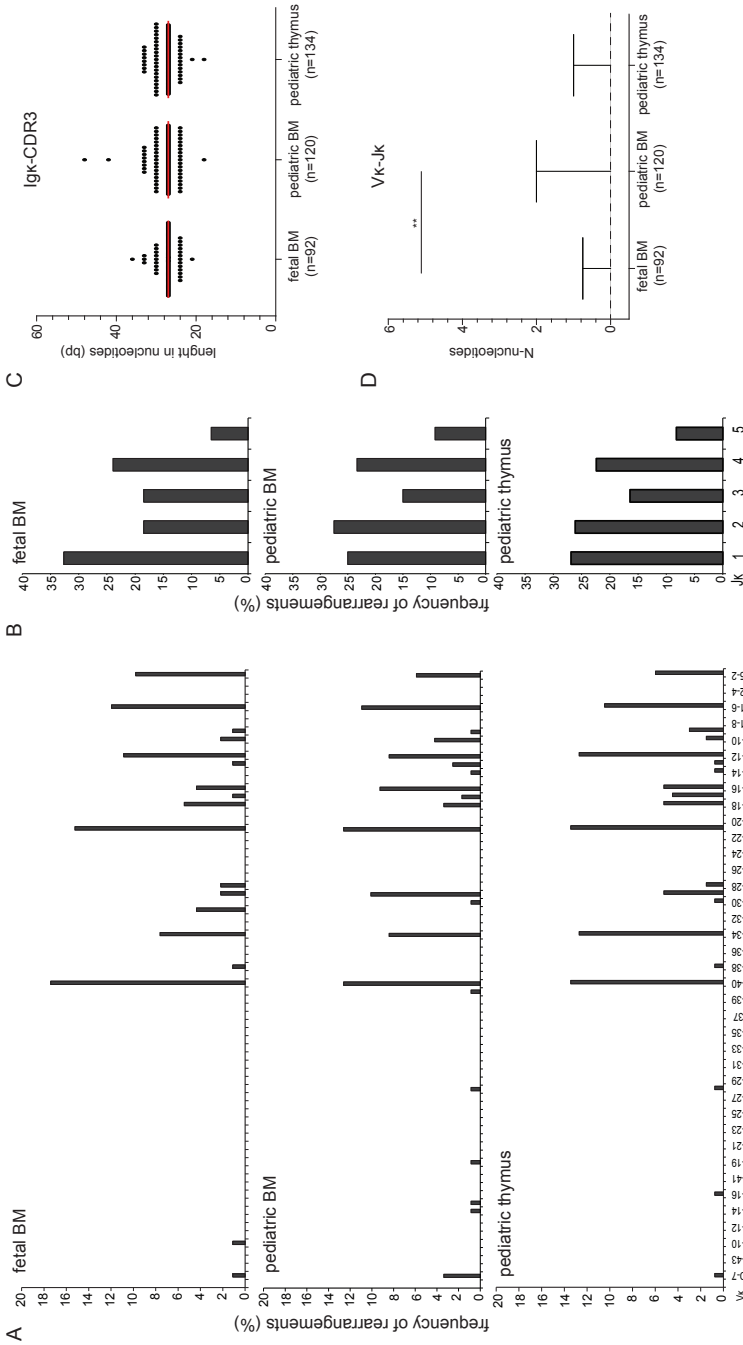


Figure S1. (A) *IGKV* and (B) *IGKJ* gene usage in transcripts from single-cell naive mature-B cells from fetus, pediatric BM and thymus. The genes are ordered according to their genomic positions in the locus (IMGT).²⁰ Panels A-B include 92 sequences derived from 3 fetal BM samples, 120 sequences from 3 pediatric BM samples and 134 sequences from 3 pediatric thymus samples. (C) Scatter plots showing the Igk-CDR3 length in nucleotides with the red horizontal lines representing median values. (D) Bar graphs showing the median numbers of N-nucleotides in Vκ-Jκ junctions with inter-quartile range. Numbers of sequences are depicted between brackets. Statistical significance was determined with the Mann-Whitney U test (panels C-D); **, p<.01.

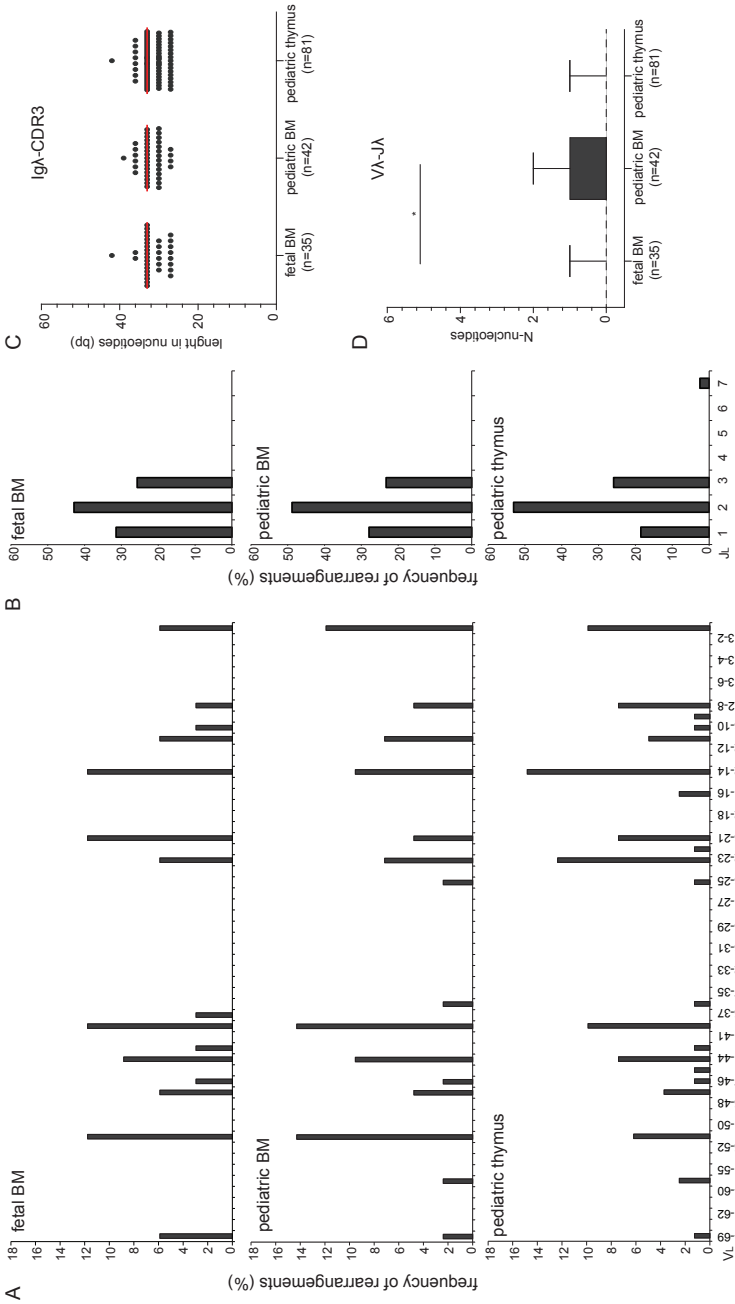


Figure S2. (A) *IGLJ* and (B) *IGLJ* gene usage in transcripts from single-cell naive mature-B cells from fetus, pediatric BM and thymus. The genes are ordered according to their genomic positions in the locus (IMGT).²⁰ Panels A-B include 35 sequences derived from 3 fetal BM samples, 42 sequences from 3 pediatric BM samples and 81 sequences from 3 pediatric thymus samples. (C) Scatter plots showing the Igλ-CDR3 length in nucleotides with the red horizontal lines representing median values. (D) Bar graphs showing the median numbers of N-nucleotides in Vλ-Jλ junctions with inter-quartile range. Numbers of sequences are depicted between brackets. Statistical significance was determined with the Mann-Whitney U test (panels C-D); *, p<.05.

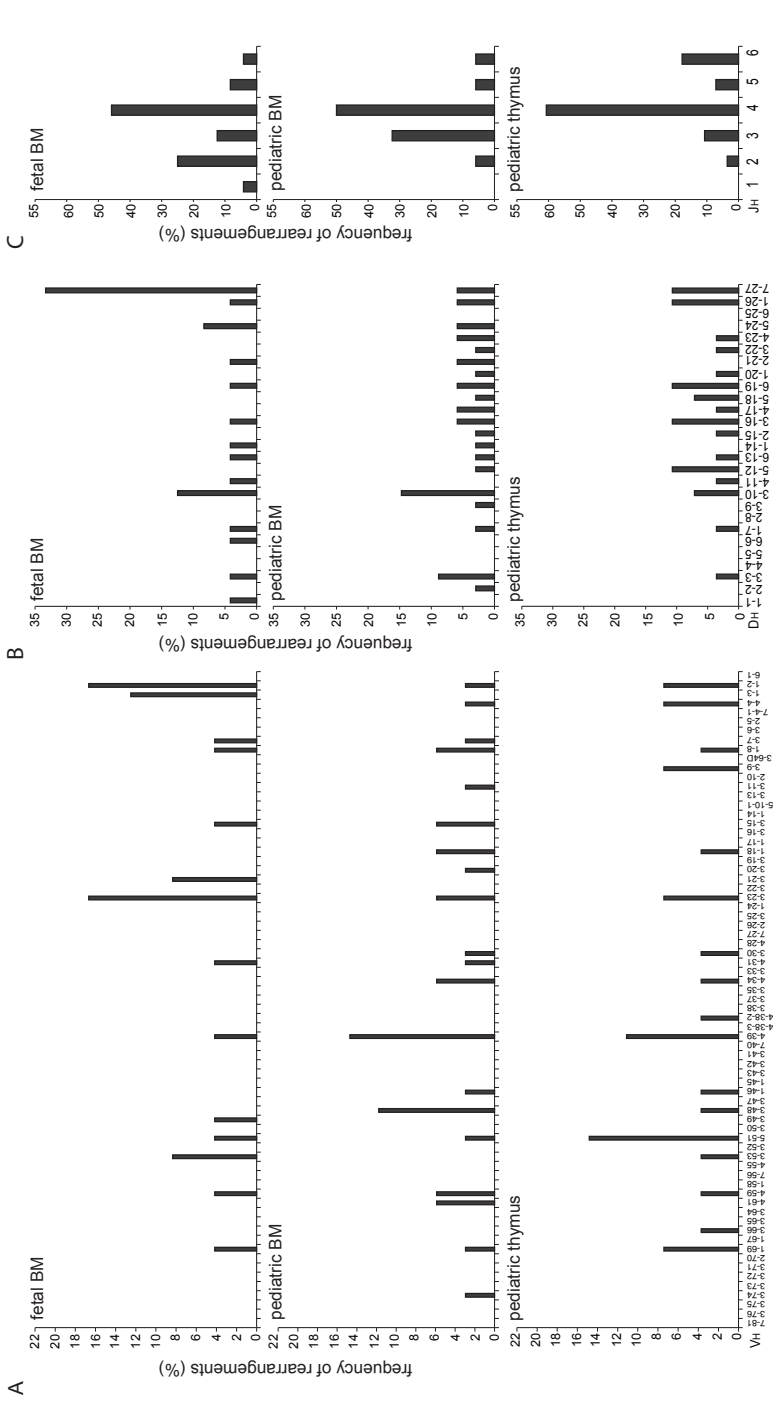


Figure S3. IGH gene repertoire of recombinant antibodies from fetal BM, pediatric BM and pediatric thymus. (A) *IGHV* (B) *IGHD* and (C) *IGHJ* gene usage in recombinant antibodies expressed from single-cell sorted naive mature-B cells from fetal BM, pediatric BM and pediatric thymus. The genes are ordered according to their 5' to 3' genomic positions in the *IGH* locus.²⁰ In total, 26 sequences were derived from 2 fetal BM samples, 36 from 2 pediatric BM donors and 31 from 2 thymuses.



Chapter VII

General Discussion

The total pool of B cells and T cells in every vertebrate provides an enormous antigen receptor repertoire, which enables the host to cope daily with the invading pathogens. Formation of the antigen receptor repertoire occurs through somatic V(D)J recombination of the antigen receptor loci during early stages of lymphocyte development. Still, not all mechanisms underlying the formation of this broad repertoire are fully understood. Studies described in this thesis aimed to investigate how the stage-specific recombination of Ig loci and the generation of a diverse Ig repertoire is controlled during precursor-B-cell development.

The research described in this thesis focused on two main issues. Firstly, it showed in mouse models how spatial organization and long-range interactions within Ig loci and positioning of these loci within the nucleus regulate the stepwise V(D)J recombination process (**Chapters II and III**). Analysis of the murine *IGK* locus showed unexpectedly that the locus underwent contraction already in committed precursor-B cells before the rearrangement-specific stage of development. Still, despite the locus contraction, only pre-B cell receptor signaling induced *IGK* locus accessibility for recombination through a functional redistribution of enhancer-mediated long-range chromatin interactions within the $V\kappa$ region (**Chapter II**). In **Chapter III**, the *IGH* and *IGK* were shown to be both consistently contracted in pro-B and pre-B cells. While Ig locus contraction mediated efficient recombination by juxtaposing genomically distant elements, sequential positioning of the *IGH* and *IGK* loci away from the nuclear periphery determined their stage-specific accessibility for recombination.

In **Chapters IV and V** of this thesis, the diversity of Ig molecules generated at different stages of human life, i.e. in fetal, childhood and aging bone marrow (BM) was analyzed. Furthermore, the diversity and reactivity of Ig molecules was analyzed for B cells residing in the human postnatal thymus (**Chapter VI**). Aging BM produced fewer B cells with a seemingly normal and diverse Ig gene repertoire. The decline in B-cell production was associated with transcriptional upregulation of *ID2* and impaired *IGH* locus contraction (**Chapter IV**). Developing B cells in the human fetus produced a diverse Ig gene repertoire with skewed V, D and J gene use and short IgH-CDR3 regions related to decreased IL-7R signaling and altered *IGH* junction processing (**Chapter V**). The skewed fetal Ig gene repertoire was reactive to dsDNA. Although, the Ig gene repertoires of pediatric BM and thymic B cells were very similar, thymic B cells showed increased reactivity towards auto-antigens (**Chapter VI**).

Putative factors mediating the 3D structural organization of Ig loci

The *IGH* and *IGK* loci were contracted in pro-B cells and both loci remained contracted in pre-B cells (**Chapters II and III**). The consistent contraction of Ig loci in

committed precursor-B cells raises the question how the topology of Ig loci changes during B-cell development and which factors organize the loci into specific spatial structures.

Thus far, the topology of Ig loci was extensively studied for the murine *IGH*, which is organized into three multi-loop domains of rosette-like shapes in E2A-deficient pre-pro-B cells.¹ Based on genetic distance measurements, it was computed that this *IGH* locus structure fits best with the multi-loop subcompartment (MLS) model of chromatin organization.^{1,2} The chromatin folding into MLS structures is mediated by general chromatin architecture proteins. Important candidates are CCCTC-binding factor (CTCF), cohesins and Yin-Yang 1 (YY1).³⁻⁶ CTCF and YY1 recognize specific binding sites across the mammalian genomes and through long-range interactions establish the chromatin loops, whereas cohesins interact with CTCF and form a ring-like structure around the chromatin loops to maintain them.⁵ CTCF and YY binding sites have been found within the murine *IGH* locus at regulatory elements such as Pax5-activated intergenic elements (PAIRs), intergenic control region (IGCR1), iE μ and 3'RR.⁷⁻⁹ Recent analysis of the pro-B cell genome indeed indicates that the interactions between CTCF, cohesins and YY1 form the long-range contacts between chromatin loops which belong to one multi-loop domain of the *IGH* locus.^{7, 10-13} Thus, the organization of the *IGH* locus into MLS structures is established by CTCF, cohesins and YY1 and this specific chromatin topology is already present in uncommitted precursor-B cells (**Figure 1A**).

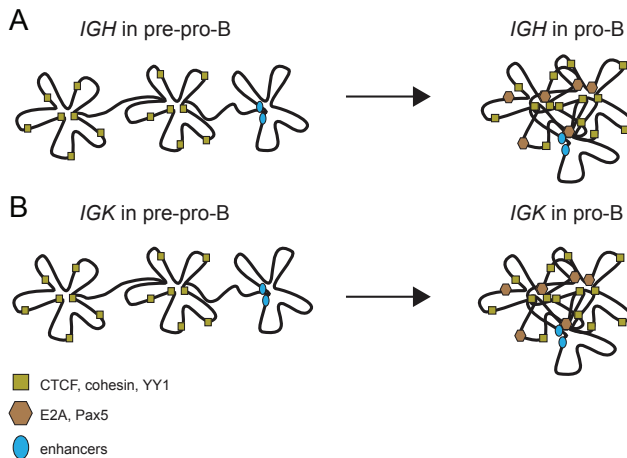


Figure 1. 3D structure of Ig loci. To form a diverse Ig gene repertoire, precursor-B cells rearrange Ig loci in developmentally ordered manner. The stepwise V(D)J recombination is regulated by changes in the 3D structure of Ig loci during B-cell development. **(A)** In uncommitted precursor-B cells, Ig loci are organized into multi-loop subcompartments (MLS) by general chromatin architecture proteins, i.e. CTCF, cohesins and YY1. **(B)** Upon B-cell commitment, both Ig loci are further contracted by B-cell specific factors, such as E2A and Pax5, to bring all Ig coding elements into spatial proximity and facilitate efficient recombination.

The *IGK* locus topology has not been studied yet in such a precise way as it was done for the *IGH* locus. However, we can hypothesize that the *IGK* topology in uncommitted precursor-B cells also fits with the MLS model as CTCF binding sites are present along the *IGK* locus^{11, 14} and CTCF is ubiquitously expressed (**Figure 1B**). Moreover, the *IGH* and *IGK* loci showed the same order of magnitude for spatial distances measured by fluorescence in situ hybridization (FISH) in *E2A*^{-/-} pre-pro-B cells (**Chapter III**) which further suggests that the *IGK* locus is organized into MLS structures in early progenitor-B cells. Still, to prove this assumption, detailed FISH studies of the *IGK* locus in B-lineage and non-B lineage cells are needed.

The 3D structural organization of *IGH* into MLS structures is in line with the current conviction of the mammalian genome organization into clusters of loops.^{12, 15, 16} Still, the general chromatin folding is insufficient to provide high interaction frequencies between V and DJ genes to efficiently mediate V(D)J recombination.¹⁷ We and others indeed observed contraction of *IGH* in pro-B cells as compared to pre-pro-B cells (**Chapter III**).^{1, 18, 19} Because the *IGH* locus is decontracted in *E2A*^{-/-} uncommitted B-cells, T-cells and erythroid progenitors (**Chapter III**),^{19, 20} this contraction is likely established by B-cell specific factors. Thus far, *E2A* and *Pax5* have been shown to be involved in *IGH* locus contraction. These proteins recognize multiple binding sites within the *IGH* regulatory elements⁷ and mice deficient for *E2A* and *Pax5* were unable to contract the *IGH* locus.^{19, 21} Other candidate factors are *EBF1*, *Ikaros* and *PU.1*. Although their role in *IGH* locus contraction has not been proven yet, the long-range interactions between multi-loop chromatin domains of the *IGH* locus were attributed to *EBF1*, *Ikaros* and *PU.1* in addition to *E2A* and *Pax5*.^{7-13, 21-25} To precisely address the role of *EBF1*, *Ikaros* and *PU.1* in locus contraction, B cells deficient for these factors should be subjected to FISH-based microscopic analysis of the *IGH* topology. Selective deficiencies for each factor can be achieved through generation of knockout mice or silencing of gene expression via shRNA. Additional evidence for the role of B-cell specific factors in locus contraction was shown in FISH studies of the *IGH* in *CTCF*^{-/-} pro-B cells.¹⁰ Spatial distances measured between genetic markers aligned across the *IGH* locus were only marginally larger in *CTCF*^{-/-} pro-B cells than in wild type pro-B cells.¹⁰ This suggests that disruption of contacts maintained by CTCF between chromatin loops within multi-loop domain had a minor effect on the total *IGH* contraction established through interactions between chromatin loops belonging to distinct multi-loop domains. Thus, *IGH* locus contraction is most likely maintained by B-cell specific transcription factors, such as *E2A* and *Pax5* (**Figure 1A**).

The *IGK* locus was already contracted in pro-B cells (**Chapters II and III**). Since B-cell specific transcription factors such as *E2A*, *Pax5*, *EBF1*, *Ikaros* and *PU.1* are widely expressed from the earliest stages of B-cell development (**Chapter III**), it is tempting to

speculate that upon B-cell commitment, these B-cell specific factors also mediate *IGK* locus contraction. *IGK* locus contraction in pro-B and pre-B cells was dependent on the presence of E2A (**Chapters II and III**). E2A was already detected at the κ enhancers and $V\kappa$ genes in pro-B cells,^{26, 27} where E2A was frequently found at the base of long-range chromatin interactions together with CTCF and PU.1, possibly acting as ‘anchors’ to organize genome topology.¹² The correlation between E2A binding, $V\kappa$ gene usage and iE κ proximity in pro-B cells (**Chapter II**) further strengthens an early critical role for E2A in regulating *IGK* locus topology (**Figure 1B**). Still, to better chart the *IGK* topology during B-cell development and define the locus remodeling mediators, more extensive FISH microscopy and chromatin immunoprecipitation (ChIP-Seq) studies of the *IGK* locus in pro-B and pre-B cells are needed.

Due to their large genomic sizes, Ig loci need to undergo contraction to bring all Ig genes in spatial proximity to provide their equal usage during recombination. Still, the current model of Ig loci accessibility for recombination postulates that the loci contract only at the stage of rearrangement and they decontract after successful rearrangement to ensure allelic exclusion.^{1, 18-20, 28} Our consistent finding of locus contraction of both *IGH* and *IGK* in pro-B and pre-B cells contrasts with the current model (**Chapters II and III**). In previous studies, purified wild type precursor-B-cell subsets were used,¹⁸ whereas the studies described in this thesis were performed in cells derived from RAG-deficient mice. These precursor-B cells retain the *IGH* and *IGK* loci in germline configuration, excluding any effects of Ig gene rearrangements on the 3D structural organization. The absence of RAG creates a slightly artificial situation, because no DNA breaks are induced that could affect gene expression programs in the progenitor-B cells.²⁹ Still, the immunophenotypes of the pro-B and pre-B cells were normal, as was the specific upregulation of *IGH* and *IGK* germline transcripts (**Chapters II and III**). Thus, the limitations of using RAG-deficient models were marginal and did not outweigh the advantage of having the Ig genes in germline configuration to establish contraction of both *IGH* and *IGK* loci in committed precursor-B cells. By contrast, the wild type pro-B cells and pre-B cells can have already rearranged Ig genes that affect the spatial distance measurements and mislead the analysis of locus structure. Thus, the current model of Ig loci contraction only at the stage of rearrangement was established based on observations in a limited model system.¹⁸

Similarly to murine Ig loci, the human *IGH* locus undergoes topological changes during B-cell differentiation²⁰ which are essential for efficient Ig gene rearrangements (**Chapters IV and V**). Impaired *IGH* locus contraction in B-cell progenitors developing in aging BM decreased the V(D)J recombination efficiency and consequently resulted in decline of B-cell output from BM (**Chapter IV**). Our knowledge about human Ig loci organization and factors mediating their 3D structure is still limited. The spatial distances measured within the human and murine *IGH* loci in pro-B cells were very similar and

smaller than in uncommitted precursor-B cells or T-cells (**Chapter III**).^{19, 20} Thus, the human *IGH* locus is likely also organized into MLS structures by general folding factors, and in committed B-cell precursors it is further contracted by B-cell specific proteins. This assumption, however, requires further investigation. Future chromosome conformation capture and microscopy studies of the human Ig loci could extend our knowledge about the locus topology and establish the presence of long-range interactions. ChIP-Seq studies could provide information about factors involved in the 3D organization of the loci. Still, wild type precursor-B cells potentially sorted from human BM constitute heterogeneous populations containing partially rearranged Ig genes. Therefore, it is important to establish a human system with germline Ig loci, which would allow for unbiased studies of 3D locus organization. A possible solution can be the use of precursor-B cells from RAG-deficient patients. During the diagnostic work-up BM aspirates are obtained from these patients, which could be a source for precursor-B cell. The rate-limiting factor is the low number of precursor-B cells in these patients, however, this could be overcome by expansion of these cells via *in vitro* culture or transplantation of hematopoietic stem cells into RAG^{-/-}γC^{-/-} mice.²⁰

Repressing genes by tethering to the lamins

The consistent contraction of both Ig loci (*IGH* and *IGK*) in pro-B cells and pre-B cells (**Chapter III**) raises an important question about the mechanisms that mediate the developmentally ordered recombination. We here showed induction of changes in chromatin mobility during B-cell development. Ig loci changed their nuclear localization within chromosome territories in interphase nucleus from the transcriptionally repressive nuclear periphery to central active domains only at the developmental stage at which these loci would normally undergo V(D)J recombination (**Figure 2A-B**) (**Chapter III**).^{30, 31} The exact mechanisms by which the loci re-localize are currently not known.

Repression of genes positioned at the nuclear periphery occurs through locus binding to the lamina (**Figure 2B**).³²⁻³⁴ The *IGH* locus was repressed in fibroblasts by association to lamina through specific lamina associated sequences (LASs) which were enriched for a GAGA motif.³⁵ This repeated motif was bound by the transcriptional repressor cKrox in a complex with histone deacetylase HDAC3 and the nuclear envelope protein and transcriptional repressor LAP2beta.^{35, 36} Blockage of HDAC3 in pre-pro-B cells resulted in disruption of the repressive complex and consequently reduced the Ig loci localization at the nuclear periphery and induced transcriptional activation (**Chapter III**). Interestingly, another histone mark, i.e. H3K9 redirects genes back to the nuclear lamina.³⁷ Perhaps the repressive H3K27me3 histone mark common within the *IGK* locus in pro-B cells, could also mediate interactions of the *IGK* with the lamina. This could be determined with

experiments in which lamina associated domains (LADs) are determined in the three consecutive B-cell developmental stages, i.e. pre-pro-B, pro-B and pre-B cells and these data are correlated with the ChIP-Seq results of the H3K27me3 histone mark.

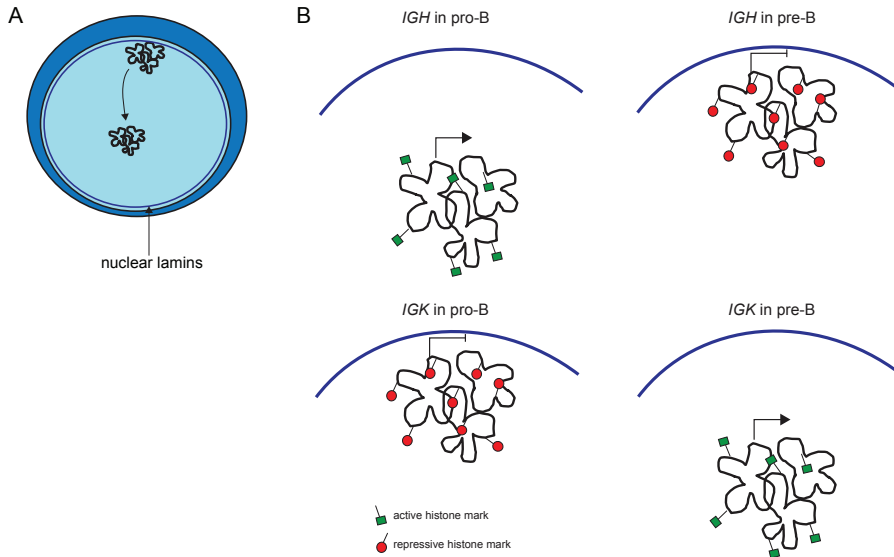


Figure 2. Nuclear re-positioning of Ig loci. Both the *IGH* and *IGK* loci are contacted in committed precursor-B cells, although *IGH* is rearranged in pro-B cells, and *IGK* in pre-B cells (A) During progenitor B-cell development, the stepwise accessibility of consistently contracted Ig loci is established through repositioning of the loci at the stage of rearrangement from repressive nuclear periphery (nuclear lamina) closer to transcriptional hubs localized in the nuclear center. (B) In pro-B cells, the *IGH* locus is specifically repositioned from the nuclear periphery to the central nuclear domains, while for the *IGK* locus this movement occurs only in pre-B cells.

Another issue that remains unsolved is whether movement of Ig loci away from the nuclear lamina is an active process, or occurs passively once the direct interaction is disrupted. Recent evidence indicates that the Ig loci are rather stably positioned within the nucleus of pro-B cells.³⁸ Thus, it is more likely that the loci are moved in an active manner, for instance by chromatin remodelers. These large ATP-dependent complexes can shift nucleosomes or in some cases remove or replace them to create space within DNA for transcription factors.³⁹⁻⁴¹ Recently, the chromatin remodeler INO80-complex was shown to enhance the long-range chromatin mobility which consequently correlated with increased recombination.⁴² Remodeling complexes can read specific histone marks, which allows them to carry out their remodeling tasks.⁴¹ Thus, the ordered pattern of histone modifications within Ig loci during early B-cell development could act as a trigger for deposition of chromatin remodelers, thereby changing the nuclear position of the loci

and consequently providing the ordered rearrangement. Future studies on factors mediating the Ig locus mobility within the nucleus during B-cell development could provide milestone knowledge in our understanding how the stepwise rearrangement process is controlled.

Ig enhancers facilitate the stepwise rearrangements

The iE μ and iE κ enhancers are important for induction of Ig gene rearrangements,⁴³⁻⁴⁶ and E2A-mediated locus contraction increases the interaction levels between IgV genes and iE μ and iE κ in pro-B cells and pre-B cells (**Chapter II and III**). Still, the *IGK* locus was not accessible for rearrangement until the pre-B cells stage (**Chapter II**). Thus, it remains puzzling how the enhancers control induction of the rearrangement event in a developmentally ordered manner.

The histones within Ig regulatory elements undergo modifications during B-cell development to increase the locus accessibility for RAG proteins.⁴⁷ RAG2 is recruited to Ig loci through binding to H3K4me3 histone marks,^{48, 49} and these modifications were detected within the *IGH* locus in pro-B cells, but within the *IGK* locus only in pre-B cells.⁵⁰ Additionally in pro-B cells, *IGK* was localized at the nuclear periphery, which correlates with transcriptional repression (**Chapter III**). IL-7R recruited STAT5 tetramers to iE κ in pro-B cells, which induced Ezh2 methyltransferase and repressive H3K27me3 marks within the iE κ enhancer (**Figure 3**).⁵¹ Perhaps the H3K27me3 mark mediates attachment of the *IGK* locus in pro-B cells to the nuclear lamina and thereby makes the locus inaccessible for the V(D)J recombinase. Still, incorporation of iE μ into the *IGK* locus and deletion of E-boxes from iE κ did not reposition the *IGK* locus from the nuclear periphery to more centrally located domains (**Chapter III**). Because E-boxes within iE μ and iE κ contain binding sites for E2A, this suggest that E2A does not play a role in chromatin mobility. However, it does not rule out the possibility that other transcription factors that also bind to iE μ and iE κ , such as NF κ B, function as chromatin guiders and thereby provide a function for intron enhancers in chromatin mobility, facilitating the process of ordered rearrangements.

The inaccessibility of iE κ for E2A binding in pro-B cells prevents too early rearrangement events,⁵¹ although it did not affect locus contraction (**Chapter III**). Interestingly, deletion of iE μ did not affect the *IGH* topology either.¹⁷ Thus, while the intron enhancers are crucial for rearrangement,⁴³⁻⁴⁶ these seem redundant for locus contraction. Likely, the presence of multiple binding sites for general and B-cell specific factors across the Ig loci is sufficient to maintain their 3D structure.

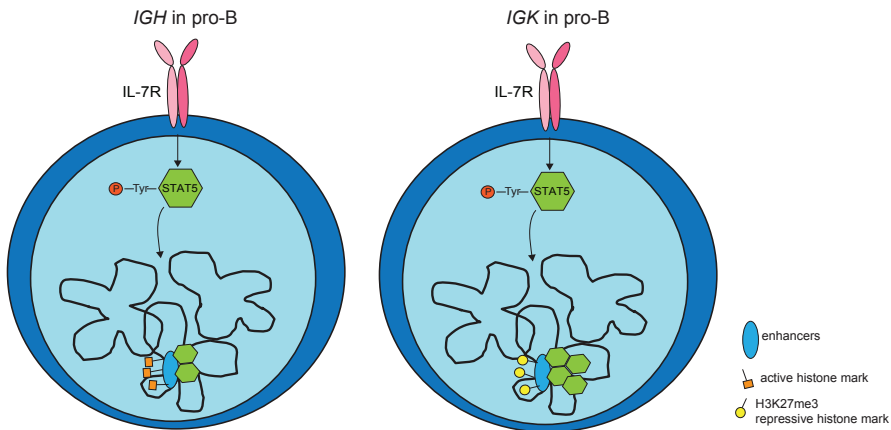


Figure 3. IL-7R signaling and STAT5. IL-7R induced STAT5 activation regulates the accessibility of Ig loci for recombination. In pro-B cells, STAT5 homodimers promote *IGH* locus accessibility to the V(D)J recombinase, whereas as a STAT5 tetramers deposited on iE κ suppress V κ to J κ gene rearrangements through induction of repressive histone marks.

Pre-BCR signaling increases *IGK* locus accessibility

Although the E2A-mediated *IGK* locus contraction increased the amount of long-range interactions between V κ genes and κ enhancers already in pro-B cells, only recruitment or further accumulation of E2A, Ikaros and IRF4 at the *IGK* enhancers following pre-BCR signaling focused the enhancer-mediated interactions on the V κ genes and thereby increased the locus accessibility for RAG proteins (**Chapters II and III**). Still, E2A and Ikaros are also expressed in pro-B cells (**Chapters II and III**). This raises the question how pre-BCR signaling increases *IGK* locus accessibility for V κ -J κ recombination.

Induction of *IGK* gene rearrangements occurs only after attenuation of IL-7R signaling and is mediated by pre-BCR signaling through SLP65 (BLNK) and BTK. SYK phosphorylates BTK and SLP65 which inhibits STAT5 phosphorylation and thereby attenuates the cell cycle. This allows the *IGK* locus to escape from the repressive histone marking supported by IL-7R signaling (**Figure 3**).⁵¹ SLP65 also activates the RAS-ERK pathway, which together induces E2A and represses the E2A inhibitor ID3.⁵² The resulting greater abundance of free nuclear E2A can now bind to the available E-boxes within iE κ and mediate the long range interactions between κ enhancers and V κ genes. Indeed, the BTK and SLP65-deficient pre-B cells showed decreased levels of specific long-range interactions at V κ genes (**Chapter II**). The pre-BCR signaling increases also chromatin accessibility for Ikaros,⁵³⁻⁵⁵ and these E2A and Ikaros-mediated interactions induce a

functional redistribution of enhancer-mediated long-range interactions within the V_{κ} region and facilitate V_{κ} to J_{κ} gene rearrangements (**Chapter II**).

Still, the mechanisms which keep the *IGK* locus inaccessible for Ikaros binding in pro-B cells remain unknown. Perhaps specific chromatin modifications attract Ikaros, or Ikaros can only perform this function in concert with E2A. Lack of E2A binding to iE_{κ} in pro-B cells prevents V_{κ} to J_{κ} gene rearrangements. iE_{κ} release from repressive marking in pre-B cells allowed for loading of E2A and Ikaros at the iE_{κ} and thereby facilitates the rearrangement. The pre-BCR could potentially release the iE_{κ} from repressive histone marking by disruption of the speculative complex between H3K27me3 and nuclear lamina or by induction of *IGK* locus movement to the nuclear center. It would thus be very interesting to study the nuclear positioning of the *IGK* locus in pre-B cells with reduced pre-BCR signaling due to BTK and/or SLP65-deficiency.

Ig gene repertoire formation in human fetal B-cell progenitors

The Ig gene repertoire in fetal B cells was skewed towards increased usage of V_{H1-2} , D_{H7-27} , J_{H2} and J_{H3} genes (**Chapter V**). It is tempting to speculate that the skewing towards proximal gene segments results from impaired Ig locus topology. The Ig locus contraction brings all Ig genes into spatial proximity which creates a stochastic environment for all genes to be recombined, albeit that during V(D)J recombination only one V, one (D) and one J genes are chosen for assembly. Impaired locus topology can therefore skew the Ig gene usage. However, *IGH* locus contraction was not altered in fetal progenitor B-cells (**Chapter V**). Thus, the skewed Ig gene usage in fetus does not seem to result from an altered global chromatin topology of *IGH*.

An alternative explanation for the skewed gene usage could be impaired opening of the *IGH* locus. Fetal derived human pro-B cells and pre-B1 cells had decreased expression of IL-7R (**Chapter V**). Studies in mouse models have indicated a role for IL-7R induced activation of STAT5 in opening of the *IGH* locus for the transcription machinery.⁵⁶ STAT5 binds to the promoters of multiple V_H genes, and STAT5^{-/-} pro-B cells show impaired induction of V_H -DJH rearrangements.^{57, 58} STAT5 did not affect the nuclear repositioning or compaction of the *IGH* locus, but regulated locus opening through germline transcription and histone acetylation of the distal V_H region in pro-B cells.⁵⁶ Thus, likely in the fetus, the DJH region was more efficiently opened at the proximal site, which increased the usage of D_{H7-27} , J_{H2} and J_{H3} genes. Subsequently, the V_H region was also more accessible at its proximal site, resulting in the increased usage of V_{H1-2} in *IGH* gene rearrangements in the fetus.

How IL-7R expression is regulated in B cells remains unknown. In invariant natural killer (NK)T cells, IL-7R expression is under control of the transcription factor lymphoid

enhancer factor 1 (LEF1).⁵⁹ Interestingly, LEF1 was highly expressed in progenitor-B cells of pediatric BM,⁶⁰ while in fetal progenitor-B cells the transcript level of LEF1 was decreased (**Chapter V**). Thus, the low expression of LEF1 in fetal precursor-B cells corresponds with the lower IL-7R expression and decreased STAT5 activation leading to the impaired *IGH* locus opening (**Figure 4**). Furthermore, the Ig gene repertoire in fetal precursor-B cells was characterized by shorter IgH-CDR3 regions due to less amount of N-nucleotides (**Chapter V**).⁶¹⁻⁶⁸ The shorter junction formation was caused by altered *IGH* junction processing due to decreased TdT expression which, as suggested by the ingenuity pathway analysis, was related to decreased IL-7R expression (**Chapter V**). Thus, the formation of the skewed fetal Ig gene repertoire is very likely controlled by decreased IL-7R signaling. It would be interesting to confirm that decreased IL-7R signaling directly causes decreased TdT expression and consequently reduced insertion of N-nucleotides in the Ig gene repertoire of B cells from IL-7R-deficient patients.

The expression of LEF1 in fetal derived precursor-B cells could be controlled by external factors such as antigens. Fetuses develop in a sterile host with limited amounts of pathogens. The skewed fetal Ig repertoire could thus be considered as a basic Ig repertoire. This Ig repertoire already changes prior to birth as evidenced from the less skewed *IGH* gene repertoire in neonatal cord blood (**Chapter V**). It is tempting to speculate that this is caused by exposure to external antigens, which can already cross the placenta at low concentrations, but will especially affect the neonate upon direct exposure to the environment. How the presence of antigens within fetuses would result in upregulation of LEF1 and IL-7R, remains subject of further studies.

Ig gene repertoire formation in postnatal aging BM

Aging BM produced a diverse Ig gene repertoire as compared to B cells of pediatric BM, but fewer B cells were generated with age (**Chapter IV**). The decline in B-cell production was associated with transcriptional upregulation of ID2 (**Chapter IV**). As an E2A-inhibitory protein, ID2 is assumed to have a central role in modulating the E2A-dependent transcriptional regulatory networks, and hence inhibits B-cell lineage commitment and differentiation.^{69, 70} We did not observe a block at early stages of B-cell development in adults, and the relative composition of the B-cell compartment of adult BM was normal (**Chapter IV**). Thus, ID2 upregulation might result in decreased B-cell generation, but not in inhibition of maturation. Likely, the decreased B-cell output from adult BM was caused by altered *IGH* locus contraction. The *IGH* locus contraction is established by general chromatin folding factors and B-cell specific transcription factors, including E2A (**Chapters II and III**).^{7-13, 21-25} Thus, even in the presence of normal E2A

transcript levels (**Chapter IV**), upregulation of ID2 likely suppresses E2A-mediated Ig locus contraction and reduced efficient V(D)J recombination (**Figure 4**).

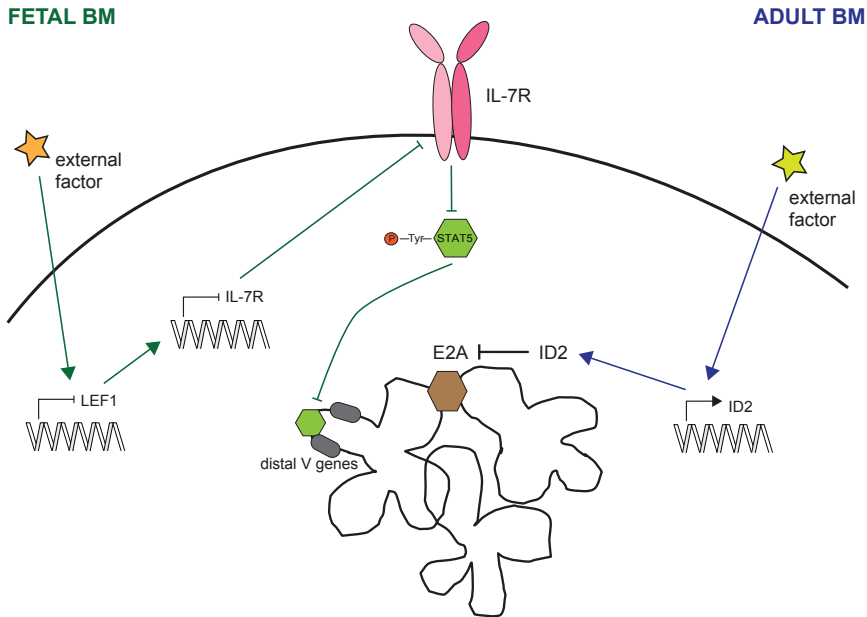


Figure 4. Bone marrow delivers different signals to developing B-cells during life. B-cell development in BM starts before birth and continues in postnatal BM. Through human life, the environmental milieu in BM undergoes physiological changes which results in providing different signals to developing B cells and thereby distinct Ig gene repertoires are generated. The fetal Ig gene repertoire is skewed towards proximal *IGH* gene usage and shorter junction formation due to decreased IL-7R signaling. IL-7R expression stays under control of the transcription factor lymphoid enhancer factor 1 (LEF1). The decreased IL-7R signaling in fetuses resulted in lower STAT5 activation and impaired *IGH* locus opening. Ig gene repertoire generated in aging BM is diverse but fewer B cells are produced due to transcriptional upregulation of ID2. ID2 inhibits E2A, the mediator of locus contraction, which causes impaired *IGH* locus contraction and less efficient V(D)J recombination.

Which factors induce the expression of ID2 in precursor-B cells is not known. Likely the expression of ID2 is regulated by cytokines produced by BM stromal cells. It was recently shown that the production of chemokine CCL5 increases with age. CCL5 is produced by BM stromal cells and supports myeloid production from HSC and inhibits lymphopoiesis.⁷¹ It is therefore possible that CCL5 or other soluble factors control ID2 expression in B-cell progenitor. Moreover, it is tempting to speculate that the cytokine levels produced by BM stromal cells are controlled by external factors, such as inflammation status. Adults have difficulties in clearing new infections and the pathways of B lymphopoiesis deviate from normal at old age as a consequence of increased inflammation locally within the BM.⁷² Another plausible mechanism could be the increased number of plasma cells and memory B-cells with age. It was previously shown that expansion of

the memory-B cell compartment with age negatively affects B-cell development.⁷³ If the presence of large numbers of memory-B-cells and plasma cells affects ID2 expression, this would be reversed when these cells are depleted. Thus, it would be interesting to unravel whether adults following B-cell depletion therapy show normal ID2 expression and normal *IGH* locus contraction. Such studies could e.g. be performed in adults who have replenished their B-cell compartment, but still have reduced memory B cell frequencies following rituximab treatment.

Distinct hematopoietic stem cells (HSC) within prenatal and postnatal bone marrow

The apparent quantity and diversity of Ig molecules generated from fetal, childhood and adult BM (**Chapters IV and V**) could alternatively result from intrinsic properties of HSC. It is suggested based on studies in mouse models that the HSCs in fetuses differentiate mainly into B-1 cells, while in postnatal BM the B-2 cell fate dominates.⁷⁴ A striking distinction between these two B-cell populations is the less diverse Ig gene repertoire of B-1 cells as compared to B-2 cells and this, in turn, is reflected in the capacity of these two populations to respond to antigens.^{75,76} Indeed, antibody responses towards certain antigens are impaired in neonates,^{64,65,77} which is partially related to the pre-mature diversity of the fetal Ig repertoire (**Chapter V**) and thus supports a different origin of fetal B cells.

However, the presence of B-1 cells in humans is still controversial and has not been definitively demonstrated,⁷⁸⁻⁸⁰ and adult-derived precursor-B cells were found to generate a diverse *IGH* gene repertoire in NOD-SCID mice.⁸¹ In addition, *in vivo* reciprocal adoptive transfers of either young or aged BM cells into irradiated young or aged recipients indicated that reconstitution of B lymphopoiesis was influenced by the host microenvironment.⁸² Thus, Ig gene repertoire formation in B-cell progenitors seems more dependent on the distinct signals delivered by BM stromal cells during life rather than distinct HSC properties.

Ig gene repertoire and Ig reactivity

B cells in the human thymus were more reactive to protein auto-antigens than BM-derived B cells, despite their seemingly similar Ig gene repertoires (**Chapter VI**). By contrast, fetal B cells carried a skewed Ig gene repertoire (**Chapter V**), and displayed only a marginal increase in reactivity to dsDNA (**Chapter VI**). This raises a question how the Ig gene repertoire and accordingly the Ig reactivity is shaped during B-cell development in distinct niches.

B cells that develop in distinct niches have been found to play different functions. Fetal B cells are suggested to clear common pathogens and cell debris produced during extensive hematopoiesis.⁸³⁻⁸⁵ Therefore, the Ig produced by fetal B cells had mostly natural antibody properties with a skewed Ig gene repertoire. Still, fetal Ig molecules did not recognize more frequently cellular antigens, insulin, dsDNA or epitopes expressed on apoptotic cells such as MDA (**Chapter VI**). Thus, the exact function of fetal B cells remains unknown. Due to shorter *IGH* junctions and thereby smaller antigen-binding loops, the fetal antibodies are likely less specific and recognize more general foreign structures. This would make sense, as *in utero* infections are rare, and the fetus is also protected by maternal IgG antibodies that have crossed the placenta.^{86, 87} To better elucidate the role of fetal antibodies, more extensive panels of antigens with different properties would need to be studied.

By contrast, the thymic B cells were enriched in autoreactive clones that are capable to take up auto-antigens and present these to developing T-cells during negative selection.⁸⁸⁻⁹⁰ This was confirmed by greater amount of anti-nuclear antibodies (ANA) in thymus than in pediatric BM (**Chapter VI**). Still, we did not find evidence of skewed V, D and J gene usage in ANA, although we do not exclude that subtle differences may exist in gene usage that will only be detectable with next-generation sequencing analysis. More importantly, however, both pediatric BM and thymus-derived ANA carried longer IgH-CDR3 and IgL-CDR3. Thus, the auto-reactivity of B cells in the human thymus does not seem to be based on a unique Ig gene repertoire, but rather enrichment for autoreactive B cells with similar sequence properties as BM-derived autoreactive B cells.

Concluding remarks

During life, B-cells differentiate in BM in consecutive stages to rearrange their Ig genes and ultimately generate a broad Ig repertoire. Studies described in this thesis provide better understanding how the Ig gene repertoire formation is regulated. The step-wise V(D)J recombination process is tightly controlled by transcriptional and epigenetic mechanisms which must cooperate to provide the stepwise developmental increase in Ig loci accessibility for rearrangement. Furthermore, the formation of a diverse Ig gene repertoire is differentially regulated during ontogeny. Through life, the BM milieu is modified by external factors. This provides different signals to developing B cells and consequently results in formation of Ig gene repertoires with different reactivity. Which environmental factors modify the Ig loci accessibility for the V(D)J recombinase and thereby control the Ig repertoire formation remains a subject for future studies. This knowledge could then potentially be applied to help shape an optimal Ig repertoire in patients with inherited immune diseases or patients following B-cell depletion treatment.

REFERENCES

1. Jhunjhunwala, S., M. C. van Zelm, M. M. Peak, S. Cutchin, R. Riblet, J. J. van Dongen, F. G. Grosveld, T. A. Knoch, and C. Murre. 2008. The 3D structure of the immunoglobulin heavy-chain locus: implications for long-range genomic interactions. *Cell* 133:265-279.
2. Jhunjhunwala, S., M. C. van Zelm, M. M. Peak, and C. Murre. 2009. Chromatin architecture and the generation of antigen receptor diversity. *Cell* 138:435-448.
3. Parelho, V., S. Hadjur, M. Spivakov, M. Leleu, S. Sauer, H. C. Gregson, A. Jarmuz, C. Canzonetta, Z. Webster, T. Nesterova, B. S. Cobb, K. Yokomori, N. Dillon, L. Aragon, A. G. Fisher, and M. Merkenschlager. 2008. Cohesins functionally associate with CTCF on mammalian chromosome arms. *Cell* 132:422-433.
4. Phillips, J. E., and V. G. Corces. 2009. CTCF: master weaver of the genome. *Cell* 137:1194-1211.
5. Wood, A. J., A. F. Severson, and B. J. Meyer. 2010. Condensin and cohesin complexity: the expanding repertoire of functions. *Nat Rev Genet* 11:391-404.
6. Handoko, L., H. Xu, G. Li, C. Y. Ngan, E. Chew, M. Schnapp, C. W. Lee, C. Ye, J. L. Ping, F. Mulawadi, E. Wong, J. Sheng, Y. Zhang, T. Poh, C. S. Chan, G. Kunarso, A. Shahab, G. Bourque, V. Cacheux-Rataboul, W. K. Sung, Y. Ruan, and C. L. Wei. 2011. CTCF-mediated functional chromatin interactome in pluripotent cells. *Nat Genet* 43:630-638.
7. Ebert, A., S. McManus, H. Tagoh, J. Medvedovic, G. Salvagiotto, M. Novatchkova, I. Tamir, A. Sommer, M. Jaritz, and M. Busslinger. 2011. The distal V(H) gene cluster of the Igh locus contains distinct regulatory elements with Pax5 transcription factor-dependent activity in pro-B cells. *Immunity* 34:175-187.
8. Guo, C., T. Gerasimova, H. Hao, I. Ivanova, T. Chakraborty, R. Selimyan, E. M. Oltz, and R. Sen. 2011. Two forms of loops generate the chromatin conformation of the immunoglobulin heavy-chain gene locus. *Cell* 147:332-343.
9. Guo, C., H. S. Yoon, A. Franklin, S. Jain, A. Ebert, H. L. Cheng, E. Hansen, O. Despo, C. Bossen, C. Vettermann, J. G. Bates, N. Richards, D. Myers, H. Patel, M. Gallagher, M. S. Schlissel, C. Murre, M. Busslinger, C. C. Giallourakis, and F. W. Alt. 2011. CTCF-binding elements mediate control of V(D)J recombination. *Nature* 477:424-430.
10. Degner, S. C., J. Verma-Gaur, T. P. Wong, C. Bossen, G. M. Iverson, A. Torkamani, C. Vettermann, Y. C. Lin, Z. Ju, D. Schulz, C. S. Murre, B. K. Birshtein, N. J. Schork, M. S. Schlissel, R. Riblet, C. Murre, and A. J. Feeney. 2011. CCCTC-binding factor (CTCF) and cohesin influence the genomic architecture of the Igh locus and antisense transcription in pro-B cells. *Proc Natl Acad Sci U S A* 108:9566-9571.
11. Degner, S. C., T. P. Wong, G. Jankevicius, and A. J. Feeney. 2009. Cutting edge: developmental stage-specific recruitment of cohesin to CTCF sites throughout immunoglobulin loci during B lymphocyte development. *J Immunol* 182:44-48.
12. Lin, Y. C., C. Benner, R. Mansson, S. Heinz, K. Miyazaki, M. Miyazaki, V. Chandra, C. Bossen, C. K. Glass, and C. Murre. 2012. Global changes in the nuclear positioning of genes and intra- and interdomain genomic interactions that orchestrate B cell fate. *Nat Immunol* 13:1196-1204.

13. Liu, H., M. Schmidt-Suppran, Y. Shi, E. Hobeika, N. Barteneva, H. Jumaa, R. Pelanda, M. Reth, J. Skok, and K. Rajewsky. 2007. Yin Yang 1 is a critical regulator of B-cell development. *Genes Dev* 21:1179-1189.
14. Ribeiro de Almeida, C., R. Stadhouders, M. J. de Bruijn, I. M. Bergen, S. Thongjuea, B. Lenhard, W. van Ijcken, F. Grosveld, N. Galjart, E. Soler, and R. W. Hendriks. 2011. The DNA-binding protein CTCF limits proximal V κ recombination and restricts kappa enhancer interactions to the immunoglobulin kappa light chain locus. *Immunity* 35:501-513.
15. Dixon, J. R., S. Selvaraj, F. Yue, A. Kim, Y. Li, Y. Shen, M. Hu, J. S. Liu, and B. Ren. 2012. Topological domains in mammalian genomes identified by analysis of chromatin interactions. *Nature* 485:376-380.
16. Lieberman-Aiden, E., N. L. van Berkum, L. Williams, M. Imakaev, T. Ragoczy, A. Telling, I. Amit, B. R. Lajoie, P. J. Sabo, M. O. Dorschner, R. Sandstrom, B. Bernstein, M. A. Bender, M. Groudine, A. Gnirke, J. Stamatoyannopoulos, L. A. Mirny, E. S. Lander, and J. Dekker. 2009. Comprehensive Mapping of Long-Range Interactions Reveals Folding Principles of the Human Genome. *Science* 326:289-293.
17. Medvedovic, J., A. Ebert, H. Tagoh, I. M. Tamir, T. A. Schwickert, M. Novatchkova, Q. Sun, P. J. Huis In 't Veld, C. Guo, H. S. Yoon, Y. Denizot, S. J. Holwerda, W. de Laat, M. Cogne, Y. Shi, F. W. Alt, and M. Busslinger. 2013. Flexible long-range loops in the VH gene region of the Igh locus facilitate the generation of a diverse antibody repertoire. *Immunity* 39:229-244.
18. Roldan, E., M. Fuxa, W. Chong, D. Martinez, M. Novatchkova, M. Busslinger, and J. A. Skok. 2005. Locus 'decontraction' and centromeric recruitment contribute to allelic exclusion of the immunoglobulin heavy-chain gene. *Nat Immunol* 6:31-41.
19. Sayegh, C. E., S. Jhunjhunwala, R. Riblet, and C. Murre. 2005. Visualization of looping involving the immunoglobulin heavy-chain locus in developing B cells. *Genes Dev* 19:322-327.
20. Nodland, S. E., M. A. Berkowska, A. A. Bajer, N. Shah, D. de Ridder, J. J. van Dongen, T. W. LeBien, and M. C. van Zelm. 2011. IL-7R expression and IL-7 signaling confer a distinct phenotype on developing human B-lineage cells. *Blood* 118:2116-2127.
21. Fuxa, M., J. Skok, A. Souabni, G. Salvagiotto, E. Roldan, and M. Busslinger. 2004. Pax5 induces V-to-DJ rearrangements and locus contraction of the immunoglobulin heavy-chain gene. *Genes Dev* 18:411-422.
22. Bain, G., E. C. Maandag, D. J. Izon, D. Amsen, A. M. Kruisbeek, B. C. Weintraub, I. Krop, M. S. Schlissel, A. J. Feeney, M. van Roon, and et al. 1994. E2A proteins are required for proper B cell development and initiation of immunoglobulin gene rearrangements. *Cell* 79:885-892.
23. Lin, H., and R. Grosschedl. 1995. Failure of B-cell differentiation in mice lacking the transcription factor EBF. *Nature* 376:263-267.
24. Reynaud, D., I. A. Demarco, K. L. Reddy, H. Schjerven, E. Bertolino, Z. S. Chen, S. T. Smale, S. Winandy, and H. Singh. 2008. Regulation of B cell fate commitment and immunoglobulin heavy-chain gene rearrangements by Ikaros. *Nature Immunology* 9:927-936.
25. Verma-Gaur, J., A. Torkamani, L. Schaffer, S. R. Head, N. J. Schork, and A. J. Feeney. 2012. Noncoding transcription within the Igh distal V-H region at PAIR elements affects the 3D structure of the Igh locus in pro-B cells. *P Natl Acad Sci USA* 109:17004-17009.

26. Lin, Y. C., S. Jhunjhunwala, C. Benner, S. Heinz, E. Welinder, R. Mansson, M. Sigvardsson, J. Hagman, C. A. Espinoza, J. Dutkowski, T. Ideker, C. K. Glass, and C. Murre. 2010. A global network of transcription factors, involving E2A, EBF1 and Foxo1, that orchestrates B cell fate. *Nat Immunol* 11:635-U109.
27. Goldmit, M., Y. Ji, J. Skok, E. Roldan, S. Jung, H. Cedar, and Y. Bergman. 2005. Epigenetic ontogeny of the Igk locus during B cell development. *Nat Immunol* 6:198-203.
28. Jensen, K., M. B. Rother, B. S. Brusletto, O. K. Olstad, H. C. D. Aass, M. C. van Zelm, P. Kierulf, and K. M. Gautvik. 2013. Increased ID2 Levels in Adult Precursor B Cells as Compared with Children Is Associated with Impaired Ig Locus Contraction and Decreased Bone Marrow Output. *J Immunol* 191:1210-1219.
29. Bredemeyer, A. L., B. A. Helmkink, C. L. Innes, B. Calderon, L. M. McGinnis, G. K. Mahowald, E. J. Gapud, L. M. Walker, J. B. Collins, B. K. Weaver, L. Mandik-Nayak, R. D. Schreiber, P. M. Allen, M. J. May, R. S. Paules, C. H. Bassing, and B. P. Sleckman. 2008. DNA double-strand breaks activate a multi-functional genetic program in developing lymphocytes. *Nature* 456:819-823.
30. Kosak, S. T., J. A. Skok, K. L. Medina, R. Riblet, M. M. Le Beau, A. G. Fisher, and H. Singh. 2002. Subnuclear compartmentalization of immunoglobulin loci during lymphocyte development. *Science* 296:158-162.
31. Skok, J. A., K. E. Brown, V. Azuara, M. L. Caparros, J. Baxter, K. Takacs, N. Dillon, D. Gray, R. P. Perry, M. Merckenschlager, and A. G. Fisher. 2001. Nonequivalent nuclear location of immunoglobulin alleles in B lymphocytes. *Nat Immunol* 2:848-854.
32. Reddy, K. L., J. M. Zullo, E. Bertolino, and H. Singh. 2008. Transcriptional repression mediated by repositioning of genes to the nuclear lamina. *Nature* 452:243-247.
33. Osborne, C. S., L. Chakalova, K. E. Brown, D. Carter, A. Horton, E. Debrand, B. Goyenechea, J. A. Mitchell, S. Lopes, W. Reik, and P. Fraser. 2004. Active genes dynamically colocalize to shared sites of ongoing transcription. *Nature Genetics* 36:1065-1071.
34. Peric-Hupkes, D., W. Meuleman, L. Pagie, S. W. Bruggeman, I. Solovei, W. Brugman, S. Graf, P. Flicek, R. M. Kerkhoven, M. van Lohuizen, M. Reinders, L. Wessels, and B. van Steensel. 2010. Molecular maps of the reorganization of genome-nuclear lamina interactions during differentiation. *Mol Cell* 38:603-613.
35. Zullo, J. M., I. A. Demarco, R. Pique-Regi, D. J. Gaffney, C. B. Epstein, C. J. Spooner, T. R. Luperchio, B. E. Bernstein, J. K. Pritchard, K. L. Reddy, and H. Singh. 2012. DNA sequence-dependent compartmentalization and silencing of chromatin at the nuclear lamina. *Cell* 149:1474-1487.
36. Zink, D., M. D. Amaral, A. Englmann, S. Lang, L. A. Clarke, C. Rudolph, F. Alt, K. Luther, C. Braz, N. Sadoni, J. Rosenecker, and D. Schindelhauer. 2004. Transcription-dependent spatial arrangements of CFTR and adjacent genes in human cell nuclei. *J Cell Biol* 166:815-825.
37. de Graaf, C. A., and B. van Steensel. 2013. Chromatin organization: form to function. *Curr Opin Genet Dev* 23:185-190.
38. Lucas, J. S., Y. Zhang, O. K. Dudko, and C. Murre. 2014. 3D trajectories adopted by coding and regulatory DNA elements: first-passage times for genomic interactions. *Cell* 158:339-352.
39. Kouzarides, T. 2007. Chromatin modifications and their function. *Cell* 128:693-705.

40. Saha, A., J. Wittmeyer, and B. R. Cairns. 2006. Chromatin remodelling: the industrial revolution of DNA around histones. *Nat Rev Mol Cell Biol* 7:437-447.
41. van Attikum, H., and S. M. Gasser. 2005. ATP-dependent chromatin remodeling and DNA double-strand break repair. *Cell Cycle* 4:1011-1014.
42. Neumann, F. R., V. Dion, L. R. Gehlen, M. Tsai-Pflugfelder, R. Schmid, A. Taddei, and S. M. Gasser. 2012. Targeted INO80 enhances subnuclear chromatin movement and ectopic homologous recombination. *Genes Dev* 26:369-383.
43. Inlay, M. A., T. X. Lin, H. H. Gao, and Y. Xu. 2006. Critical roles of the immunoglobulin intronic enhancers in maintaining the sequential rearrangement of IgH and Igk loci. *Journal of Experimental Medicine* 203:1721-1732.
44. Inlay, M. A., H. Tian, T. X. Lin, and Y. Xu. 2004. Important roles for E protein binding sites within the immunoglobulin kappa chain intronic enhancer in activating V(kappa)J(kappa) rearrangement. *Journal of Experimental Medicine* 200:1205-1211.
45. Perlot, T., F. W. Alt, C. H. Bassing, H. Suh, and E. Pinaud. 2005. Elucidation of IgH intronic enhancer functions via germ-line deletion. *Proc Natl Acad Sci U S A* 102:14362-14367.
46. Chen, J., F. Young, A. Bottaro, V. Stewart, R. K. Smith, and F. W. Alt. 1993. Mutations of the intronic IgH enhancer and its flanking sequences differentially affect accessibility of the JH locus. *EMBO J* 12:4635-4645.
47. Xu, C. R., and A. J. Feeney. 2009. The Epigenetic Profile of Ig Genes Is Dynamically Regulated during B Cell Differentiation and Is Modulated by Pre-B Cell Receptor Signaling. *Journal of Immunology* 182:1362-1369.
48. Liu, Y., R. Subrahmanyam, T. Chakraborty, R. Sen, and S. Desiderio. 2007. A plant homeodomain in Rag-2 that binds hypermethylated lysine 4 of histone H3 is necessary for efficient antigen-receptor-gene rearrangement. *Immunity* 27:561-571.
49. Matthews, A. G. W., A. J. Kuo, S. Ramon-Maiques, S. M. Han, K. S. Champagne, D. Ivanov, M. Gallardo, D. Carney, P. Cheung, D. N. Ciccone, K. L. Walter, P. J. Utz, Y. Shi, T. G. Kutateladze, W. Yang, O. Gozani, and M. A. Oettinger. 2007. RAG2 PHD finger couples histone H3 lysine 4 trimethylation with V(D)J recombination. *Nature* 450:1106-U1118.
50. Ji, Y., W. Resch, E. Corbett, A. Yamane, R. Casellas, and D. G. Schatz. 2010. The in vivo pattern of binding of RAG1 and RAG2 to antigen receptor loci. *Cell* 141:419-431.
51. Mandal, M., S. E. Powers, M. Maienschein-Cline, E. T. Bartom, K. M. Hamel, B. L. Kee, A. R. Dinner, and M. R. Clark. 2011. Epigenetic repression of the Igk locus by STAT5-mediated recruitment of the histone methyltransferase Ezh2. *Nat Immunol* 12:1212-1220.
52. Kee, B. L., M. W. Quong, and C. Murre. 2000. E2A proteins: essential regulators at multiple stages of B-cell development. *Immunol Rev* 175:138-149.
53. Heizmann, B., P. Kastner, and S. Chan. 2013. Ikaros is absolutely required for pre-B cell differentiation by attenuating IL-7 signals. *Journal of Experimental Medicine* 210:2823-2832.

54. Schwickert, T. A., H. Tagoh, S. Gultekin, A. Dakic, E. Axelsson, M. Minnich, A. Ebert, B. Werner, M. Roth, L. Cimmino, R. A. Dickins, J. Zuber, M. Jaritz, and M. Busslinger. 2014. Stage-specific control of early B cell development by the transcription factor Ikaros. *Nat Immunol* 15:283-293.
55. Ferreira-Vidal, I., T. Carroll, B. Taylor, A. Terry, Z. Liang, L. Bruno, G. Dharmalingam, S. Khadayate, B. S. Cobb, S. T. Smale, M. Spivakov, P. Srivastava, E. Petretto, A. G. Fisher, and M. Merkenschlager. 2013. Genome-wide identification of Ikaros targets elucidates its contribution to mouse B-cell lineage specification and pre-B-cell differentiation. *Blood* 121:1769-1782.
56. Bertolino, E., K. Reddy, K. L. Medina, E. Parganas, J. Ihle, and H. Singh. 2005. Regulation of interleukin 7-dependent immunoglobulin heavy-chain variable gene rearrangements by transcription factor STAT5. *Nat Immunol* 6:836-843.
57. Corcoran, A. E., A. Riddell, D. Krooshoop, and A. R. Venkitaraman. 1998. Impaired immunoglobulin gene rearrangement in mice lacking the IL-7 receptor. *Nature* 391:904-907.
58. Hesslein, D. G., D. L. Pflugh, D. Chowdhury, A. L. Bothwell, R. Sen, and D. G. Schatz. 2003. Pax5 is required for recombination of transcribed, acetylated, 5' IgH V gene segments. *Genes Dev* 17:37-42.
59. Carr, T., V. Krishnamoorthy, S. Yu, H. H. Xue, B. L. Kee, and M. Verykokakis. 2015. The transcription factor lymphoid enhancer factor 1 controls invariant natural killer T cell expansion and Th2-type effector differentiation. *J Exp Med* 212:793-807.
60. van Zelm, M. C., M. van der Burg, D. de Ridder, B. H. Barendregt, E. F. de Haas, M. J. Reinders, A. C. Lankester, T. Revesz, F. J. Staal, and J. J. van Dongen. 2005. Ig gene rearrangement steps are initiated in early human precursor B cell subsets and correlate with specific transcription factor expression. *J Immunol* 175:5912-5922.
61. Rechavi, E., A. Lev, Y. N. Lee, A. J. Simon, Y. Yinon, S. Lipitz, N. Amariglio, B. Weisz, L. D. Notarangelo, and R. Somech. 2015. Timely and spatially regulated maturation of B and T cell repertoire during human fetal development. *Sci Transl Med* 7:276ra225.
62. Schroeder, H. W., Jr., J. L. Hillson, and R. M. Perlmutter. 1987. Early restriction of the human antibody repertoire. *Science* 238:791-793.
63. Schroeder, H. W., G. C. Ippolito, and S. Shiokawa. 1998. Regulation of the antibody repertoire through control of HCDR3 diversity. *Vaccine* 16:1383-1390.
64. Schroeder, H. W., Jr., F. Mortari, S. Shiokawa, P. M. Kirkham, R. A. Elgavish, and F. E. Bertrand, 3rd. 1995. Developmental regulation of the human antibody repertoire. *Ann NY Acad Sci* 764:242-260.
65. Schroeder, H. W., Jr., L. Zhang, and J. B. Philips, 3rd. 2001. Slow, programmed maturation of the immunoglobulin HCDR3 repertoire during the third trimester of fetal life. *Blood* 98:2745-2751.
66. Shiokawa, S., F. Mortari, J. O. Lima, C. Nunez, F. E. Bertrand, P. M. Kirkham, S. G. Zhu, A. P. Dasanayake, and H. W. Schroeder. 1999. IgM heavy chain complementarity-determining region 3 diversity is constrained by genetic and somatic mechanisms until two months after birth. *J Immunol* 162:6060-6070.
67. Souto-Carneiro, M. M., G. P. Sims, H. Girschik, J. Lee, and P. E. Lipsky. 2005. Developmental changes in the human heavy chain CDR3. *J Immunol* 175:7425-7436.

68. Zemlin, M., R. L. Schelonka, K. Bauer, and H. W. Schroeder, Jr. 2002. Regulation and chance in the ontogeny of B and T cell antigen receptor repertoires. *Immunol Res* 26:265-278.
69. Greenbaum, S., and Y. Zhuang. 2002. Regulation of early lymphocyte development by E2A family proteins. *Semin Immunol* 14:405-414.
70. Kee, B. L. 2009. E and ID proteins branch out. *Nat Rev Immunol* 9:175-184.
71. Ergen, A. V., N. C. Boles, and M. A. Goodell. 2012. Rantes/Ccl5 influences hematopoietic stem cell subtypes and causes myeloid skewing. *Blood* 119:2500-2509.
72. Riley, R. L. 2013. Impaired B lymphopoiesis in old age: a role for inflammatory B cells? *Immunol Res* 57:361-369.
73. Keren, Z., S. Naor, S. Nussbaum, K. Golan, T. Itkin, Y. Sasaki, M. Schmidt-Suppran, T. Lapidot, and D. Melamed. 2011. B-cell depletion reactivates B lymphopoiesis in the BM and rejuvenates the B lineage in aging. *Blood* 117:3104-3112.
74. Dorshkind, K., and E. Montecino-Rodriguez. 2007. Fetal B-cell lymphopoiesis and the emergence of B-1-cell potential. *Nat Rev Immunol* 7:213-219.
75. Hardy, R. R., C. E. Carmack, S. A. Shinton, R. J. Riblet, and K. Hayakawa. 1989. A single VH gene is utilized predominantly in anti-BrMRBC hybridomas derived from purified Ly-1 B cells. Definition of the VH11 family. *J Immunol* 142:3643-3651.
76. Baumgarth, N., J. W. Tung, and L. A. Herzenberg. 2005. Inherent specificities in natural antibodies: a key to immune defense against pathogen invasion. *Springer Semin Immunopathol* 26:347-362.
77. Stein, K. E. 1992. Thymus-independent and thymus-dependent responses to polysaccharide antigens. *J Infect Dis* 165 Suppl 1:S49-52.
78. Griffin, D. O., N. E. Holodick, and T. L. Rothstein. 2011. Human B1 cells are CD3-: A reply to "A human equivalent of mouse B-1 cells?" and "The nature of circulating CD27+CD43+ B cells?". *J Exp Med* 208:2566-2569.
79. Perez-Andres, M., C. Grosserichter-Wagener, C. Teodosio, J. J. van Dongen, A. Orfao, and M. C. van Zelm. 2011. The nature of circulating CD27+CD43+ B cells. *J Exp Med* 208:2565-2566.
80. Descatoire, M., J. C. Weill, C. A. Reynaud, and S. Weller. 2011. A human equivalent of mouse B-1 cells? *J Exp Med* 208:2563-2564.
81. Kolar, G. R., T. Yokota, M. I. Rossi, S. K. Nath, and J. D. Capra. 2004. Human fetal, cord blood, and adult lymphocyte progenitors have similar potential for generating B cells with a diverse immunoglobulin repertoire. *Blood* 104:2981-2987.
82. Labrie, J. E., 3rd, A. P. Sah, D. M. Allman, M. P. Cancro, and R. M. Gerstein. 2004. Bone marrow microenvironmental changes underlie reduced RAG-mediated recombination and B cell generation in aged mice. *J Exp Med* 200:411-423.
83. Meffre, E., and J. E. Salmon. 2007. Autoantibody selection and production in early human life. *J Clin Invest* 117:598-601.
84. Merbl, Y., M. Zucker-Toledano, F. J. Quintana, and I. R. Cohen. 2007. Newborn humans manifest auto-antibodies to defined self molecules detected by antigen microarray informatics. *J Clin Invest* 117:712-718.

85. Wang, C., S. P. Turunen, O. Kummu, M. Veneskoski, J. Lehtimäki, A. E. Nissinen, and S. Horkko. 2013. Natural antibodies of newborns recognize oxidative stress-related malondialdehyde acetaldehyde adducts on apoptotic cells and atherosclerotic plaques. *Int Immunol* 25:575-587.
86. Palmeira, P., C. Quinello, A. L. Silveira-Lessa, C. A. Zago, and M. Carneiro-Sampaio. 2012. IgG placental transfer in healthy and pathological pregnancies. *Clin Dev Immunol* 2012:985646.
87. Malek, A., R. Sager, P. Kuhn, K. H. Nicolaides, and H. Schneider. 1996. Evolution of maternofetal transport of immunoglobulins during human pregnancy. *Am J Reprod Immunol* 36:248-255.
88. Dunn-Walters, D. K., C. J. Howe, P. G. Isaacson, and J. Spencer. 1995. Location and sequence of rearranged immunoglobulin genes in human thymus. *Eur J Immunol* 25:513-519.
89. Spencer, J., M. Choy, T. Hussell, L. Papadaki, J. P. Kington, and P. G. Isaacson. 1992. Properties of human thymic B cells. *Immunology* 75:596-600.
90. Tonnelle, C., C. D'Ercole, V. Depraetere, D. Metras, L. Boubli, and M. Fougereau. 1997. Human thymic B cells largely overexpress the VH4 Ig gene family. A possible role in the control of tolerance in situ? *Int Immunol* 9:407-414.



Addendum

List of abbreviations

Summary

Samenvatting

Acknowledgements

PhD Portfolio

Curriculum Vitae

List of publications

LIST OF ABBREVIATIONS

3C-Seq	circular chromosome conformation capture with high-throughput sequencing
3D FISH	3-dimensional fluorescence in situ hybridization
ATM	ataxia telangiectasia mutated
BCR	B cell antigen receptor
bHLH	basic helix loop helix
BM	bone marrow
C	constant
CBE	CTCF binding element
ChIP	chromatin immunoprecipitation
CDR	complementary determining region
CTCF	CCCTC binding factor
CyIg	cytoplasmic Ig
D	diversity gene segment
DNA-PKcs	catalytic subunit of DNA dependent protein kinase
DSB	double strand break
EBF	early B cell factor
FOXO1	forkhead box protein O1
FR	framework
HSC	hematopoietic stem cell
iE	intron enhancer
Ig	immunoglobulin
IGCR1	intergenic control region
IgH	Ig heavy chain
Ig κ	Ig kappa light chain

Ig λ	Ig lambda light chain
J	joining gene segment
LAD	lamina associated domain
LAS	lamina associated sequence
LIG4	DNA ligase IV
Mb	megabases
MLS	multi-loop subcompartment
NHEJ	nonhomologous end joining
N-nucleotide	random nucleotide
PAIR	Pax5-activated intergenic elements
P-nucleotide	palindromic nucleotide
RAG	recombinase activating gene
RQ-PCR	real-time quantitative polymerase chain reaction
RSS	recombination signal sequence
SiS	silencer in the intervening sequence
SmIg	surface membrane Ig
STAT5	signal transducer and activator of transcription 5
TAD	topologically associated domain
TCR	T cell receptor
TdT	terminal deoxynucleotidyl transferase
TF	transcription factor
CB	cord blood
V	variable gene segment
YY1	Yin Yang 1

SUMMARY

Precursor-B cells develop in bone marrow (BM) from hematopoietic stem cells (HSC) with the ultimate goal to generate mature B-cells with unique immunoglobulins (Ig), whereby all B cells together provide an enormous Ig repertoire diversity. Formation of the Ig occurs through somatic V(D)J recombination of the Ig heavy chain (*IGH*) and the Ig light chain (*IGK* or *IGL*) loci that contain multiple variable (V), diverse (D) and joining (J) coding elements. Random assembly of these elements creates the highly diverse Ig repertoire. The Ig loci recombine in an ordered manner. The *IGH* locus rearranges before the Ig light chain loci and functional Ig rearrangements are generally restricted to one allele. Although the V(D)J recombination machinery is expressed in both B cells and T cells, complete V_H - D J_H rearrangements occur in B cells. Thus, the ordered accessibility of Ig loci for rearrangements is tightly controlled. Studies described in this thesis aimed to better understand the mechanisms underlying the stage-specific regulation of V(D)J recombination and the generation of a diverse Ig repertoire during precursor-B-cell development.

During B-cell development, the precursor-B cell receptor (pre-BCR) signaling is thought to increase the *IGK* locus accessibility to the V(D)J recombinase enzyme system. However, it remains unknown how the pre-BCR-induced signals regulate the *IGK* locus accessibility. In **Chapter II**, we identified the effects of pre-BCR signaling on germline $V\kappa$ transcription and on the expression of transcription factors implicated in the regulation of *IGK* gene rearrangement. We found that the decrease in pre-BCR signaling capacity from wild-type to BTK-deficient, and to SLP65-deficient and BTK/SLP65 double-deficient pre-B cells was paralleled by a progressively decreased expression of many transcription factors including Ikaros, Aiolos, IRF4 and (to a lesser extent) E2A, as well as by a decreased *IGK* locus accessibility for recombination. Several of these factors can mediate long-range chromatin interactions and are known to occupy κ regulatory elements that regulate locus accessibility. We therefore analyzed the effect of pre-BCR signaling on the higher-order chromatin structure organized by these regulatory sequences at the *IGK* locus. To this end, we performed chromosome conformation capture and sequencing (3C-seq) analyses on pro-B cells, and pre-B cells from mice single or double deficient for BTK or SLP65 to evaluate the effects of different levels of pre-BCR signaling on *IGK* locus topology. These 3C-seq experiments demonstrated that already in pro-B cells the κ enhancers robustly interact with the $V\kappa$ region and its flanking sequences, and that pre-BCR signaling induces accessibility by a functional redistribution of enhancer-mediated chromatin interactions within the $V\kappa$ region.

Committed B-cell progenitors show large-scale Ig locus contraction to provide a diverse Ig repertoire. Initially, Ig locus contraction was thought to occur only at the stage of locus rearrangement, however, recent observations question whether Ig locus

contraction is decisive for V(D)J recombination. In **Chapter III**, we have examined how Ig locus contraction and nuclear positioning are associated with the stepwise control of V(D)J recombination. We analyzed locus contraction, long-range chromatin interactions and nuclear positioning of the germline *IGH* and *IGK* alleles in three consecutive progenitor-B-cell subsets with 3D-DNA FISH and 3C-Seq. This integrated approach enabled us to identify that both Ig loci were already contracted in the earliest committed pro-B-cell stage and retained this configuration in pre-B cells. In contrast, positioning away from the nuclear lamins was tightly regulated for *IGH* in pro-B cells and for *IGK* in pre-B cells, and correlated with germline transcription. Thus, nuclear localization rather than Ig locus topology is closely linked with the developmental regulation of *IGH* and *IGK* locus assembly.

After birth, B cell generation in human BM continues throughout life, although the total pool of precursor-B cells decreases with age. The effects of aging on human precursor-B-cell development have been scarcely studied so far. In **Chapter IV**, we analyzed precursor-B-cell subsets and their gene expression profiles in BM from healthy young children and adults. We characterized the differences in transcriptional activity of precursor-B cells in adults and children, and identified differences in V(D)J recombination factors, ID2, and cell cycle genes that could underlie the marked age-related reduction in the human precursor-B-cell compartment. Functional analysis of potentially involved mechanisms indicated that upregulation of ID2 in adults inhibited E2A-mediated Ig locus contraction. This caused reduction in efficiency of V(D)J recombination and precursor-B-cell differentiation leading to decline in B-cell output from BM.

B cell generation starts already before birth in fetal liver and fetal BM providing the neonate with a diverse Ig repertoire. Still, antibody responses towards certain antigens are impaired in neonates and this initial inability to mount such antibody responses is underlined by “pre-mature” diversity of the Ig repertoire. In **Chapter V**, we studied the differences in formation of the Ig repertoire between fetal and pediatric B-cell precursors at 4 levels, i.e. cellular composition of the precursor-B-cell compartment in BM, epigenetic organization of the *IGH* locus, genetic composition of Ig gene rearrangements, and expression of factors involved in V(D)J recombination. With this approach, we demonstrated that fetuses generated a diverse Ig gene repertoire. Still, this repertoire showed skewed V, D, and J gene usage and was restricted to shorter CDR3 regions in *IGH*. This restriction was the result of limited N-nucleotides in the junctions and more frequent usage of the relatively short D_H7-27, J_H3 and J_H4 genes. The paucity of N-nucleotide additions in *IGH* gene rearrangements resulted from altered V(D)J recombination rather than Ig repertoire selection. These rearrangements were formed in a different molecular environment with reduced XRCC4, TdT and ATM, as well as IL7R and FLT3.

The major site of postnatal human B-cell differentiation is the BM. Still, B cells are present in the thymus, and these cells were suggested to present self-antigens during negative selection of T cells. In **Chapter VI**, we studied the Ig gene repertoires of single-sorted B cells from fetal BM, pediatric BM and pediatric thymus, and cloned these genes to assess their ability to bind self-antigens. B cells from human thymus displayed an Ig gene repertoire that was similar to pediatric BM and did not show typical skewing in V_H , D_H and J_H gene usage, nor short IgH-CDR3 regions that are characteristic for fetal BM B cells. Still, thymic B cells were enriched for autoreactive clones that showed increased specificity to peptide autoantigens, and not towards dsDNA as seen for fetal B cells. Although, the majority of B cell progenitors in BM generate an autoreactive Ig, these were previously found to be counterselected resulting in only 20% autoreactive circulating B cells. Thus, autoreactive thymic B cells might either develop in the thymus or in a distinct BM niche with selection mechanisms allowing for formation of self-reactive Ig gene repertoire. Alternatively, the autoreactive BM-derived B cells can home specifically to the thymus.

The studies described in this thesis provide better understanding of mechanisms controlling the stage-specific regulation of V(D)J recombination and the generation of a diverse Ig repertoire during precursor-B-cell development. The stepwise V(D)J recombination process is controlled by transcriptional and epigenetic mechanisms which must cooperate together to provide the developmental increase in Ig loci accessibility for rearrangement. The formation of the broad Ig repertoire is dependent on the B-cell developmental niche. The BM niche undergoes physiological changes during life and therefore provides different signals to developing B cells, resulting in distinct Ig gene repertoires with distinct reactivity. Future studies should reveal which environmental factors modify the Ig loci accessibility for the V(D)J recombinase and thereby control the Ig repertoire and reactivity. Such knowledge might be applicable for shaping the Ig repertoire in immune deficient patients.

SAMENVATTING

Voorloper B-cellen ontwikkelen in het beenmerg (BM) vanuit hematopoietische stamcellen (HSC). Het ultieme doel is het genereren van mature B-cellen die elk een unieke immuunglobuline (Ig) tot expressie brengen. Op deze manier zorgen alle B-cellen tezamen voor een enorme hoeveelheid verschillende antistoffen; Ig repertoire diversiteit. Vorming van deze Ig vindt plaats door herschikking van 'variable' (V), 'diversity' (D) en 'joining' (J) gensegmenten op DNA niveau in de genen die coderen voor de Ig zware (*IGH*) en de Ig lichte ketens (*IGK* of *IGL*). De willekeurige samenvoeging van een van elk van deze elementen, zgn. V(D)J-recombinatie, zorgt voor een zeer divers Ig repertoire. De Ig loci worden herschikt in een stapsgewijs proces. Het *IGH* locus herschikt vóór de Ig lichte keten loci en functionele herschikkingen blijven in het algemeen beperkt tot één allel. Hoewel alle V(D)J-recombinatie elementen aanwezig zijn in zowel B-cellen als T-cellen, vinden complete V_H - D J_H herschikkingen alleen plaats in B-cellen. De stapsgewijze toegankelijkheid van de Ig loci voor herschikkingen wordt dus strikt gereguleerd. De studies beschreven in dit proefschrift hadden als doel het beter begrijpen van het mechanisme dat ten grondslag ligt aan de fase-specifieke regulatie van V(D)J-recombinatie en het genereren van een divers Ig repertoire tijdens de ontwikkeling van voorloper B-cellen.

Er wordt verondersteld dat tijdens voorloper-B-cel ontwikkeling signalering door de pre-B-cel-receptor (pre-BCR) het *IGK* locus toegankelijk maakt voor het V(D)J-recombinase enzym-systeem. Echter, het is nog steeds niet bekend hoe de pre-BCR geïnduceerde signalen de toegankelijkheid van het *IGK* locus reguleren. In **Hoofdstuk II** identificeerden wij de effecten van pre-BCR signalering op transcriptie van nog niet herschikte *IGK* allelen en op de expressie van transcriptiefactoren die *IGK* genherschikkingen reguleren. Wij vonden een stapsgewijze afname in pre-BCR signalering van voorloper B-cellen van wild type naar BTK-deficiënte, naar SLP65-deficiënte en tenslotte naar BTK/SLP65-dubbel deficiënte muizen. Deze stapsgewijze afname liep parallel met een progressief verlaagde expressie van de transcriptiefactoren Ikaros, Aiolos, IRF4 en (in mindere mate) E2A, alsmede met een verlaagde *IGK* locus toegankelijkheid voor recombinatie. Deze effecten hadden gevolgen voor de interacties tussen V segmenten en enhancers in het *IGK* locus, zoals bleek uit 'chromosome conformation capture' (3C-) sequencing analyses. Deze 3C-seq experimenten demonstreerden dat reeds in pro-B-cellen de *IGK* enhancers een robuuste interactie vertonen met de V_κ regio en de omliggende sequenties, en dat pre-BCR-signalering verdere toegankelijkheid induceert door een functionele herverdeling van enhancer-gemedieerde chromatine interactie binnen de V_κ regio.

Voor efficiënte V(D)J-recombinatie ondergaan Ig loci in voorloper-B-cellen contractie. Eerder werd gedacht dat Ig locus contractie alleen plaatsvindt in het stadium waarin

het betreffende locus herschikt wordt, maar meer recente observaties lijken dit tegen te spreken. In **Hoofdstuk III** hebben wij bestudeerd hoe locuscontractie en positionering van de celkern geassocieerd zijn met de stapsgewijze regulatie van V(D)J-recombinatie. Hiervoor analyseerden wij *IGH* en *IGK* locuscontractie, intra-locus chromatine interacties en positionering binnen de celkern in 3 opeenvolgende stadia van voorloper-B-cellen in de muis door middel van 3D-DNA FISH en 3C-Seq. Door middel van deze geïntegreerde aanpak konden wij aantonen dat beide Ig loci al gecontraheerd waren in het vroege pro-B-cel stadium waarin normaal gesproken *IGH* wordt herschikt en deze configuratie behielden als pre-B-cellen waarin *IGK* herschikt wordt. In de vroegste pre-pro-B-cellen waren beide loci niet gecontraheerd en gepositioneerd aan de rand van de celkern, dichtbij de lamina. In pro-B-cellen bevonden de *IGH* allelen zich in het centrum van de celkern, weg van de lamina, en waren *IGH* transcripten verhoogd. *IGK* was specifiek in het centrum gelokaliseerd in pre-B-cellen, die ook verhoogde *IGK* transcripten lieten zien. Hier kan uit geconcludeerd worden dat niet de topologie, maar specifieke lokalisatie binnen de celkern van het Ig locus geassocieerd lijkt te zijn met de regulatie van toegankelijkheid voor V(D)J-recombinatie.

In zowel de muis als de mens worden gedurende het hele leven nieuwe B-cellen aangemaakt vanuit hematopoietische stamcellen in het beenmerg. Met toenemende veroudering nemen de aantallen voorloper-B-cellen in het beenmerg af, maar de oorzaak hiervan is tot op heden niet bekend. In **Hoofdstuk IV** analyseerden wij de voorloper-B-cel stadia in het beenmerg van gezonde jonge kinderen en volwassenen. Uit genexpressie analyses bleek dat de voorloper-B-cellen van volwassenen verhoogde aantallen transcripten hadden van het *ID2* gen ten opzichte van kinderen. *Id2* blokkeert de functie van *E2A*, een transcriptiefactor die een rol speelt in Ig locus contractie. Voorloper-B-cellen van volwassenen bleken minder sterke contractie van het *IGH* locus te hebben dan bij kinderen het geval was. Hieruit concludeerden wij dat de verhoogde *ID2* transcripten zorgen voor verminderde *E2A* activiteit en Ig locus contractie. Dit zou een belangrijke rol kunnen spelen in de efficiëntie van de V(D)J-recombinatie en voorloper-B-cel differentiatie, leidend tot een afname in de B-cel output vanuit het beenmerg in volwassenen.

De aanmaak van B-cellen begint al voor de geboorte in de foetale lever en foetale BM waardoor een pasgeborene al een divers Ig repertoire heeft. Toch zijn pasgeborenen niet in staat om voldoende sterke antistof responsen te vormen tegen bepaalde antigenen en hebben de B-cellen een afwijkend, onderontwikkeld (“pre-mature”) Ig repertoire. In **Hoofdstuk V** hebben wij bestudeerd hoe het komt dat de vorming het Ig repertoire zo verschilt tussen foetussen en jonge kinderen. Hiervoor zijn voorloper-B-cellen uit beenmerg geïsoleerd en bestudeerd op 4 niveaus: de cellulaire samenstelling, de 3D vouwing van het *IGH* locus, de gevormde Ig genherschikkingen en expressie van factoren die betrokken zijn bij V(D)J-recombinatie. Met deze aanpak hebben wij aangetoond dat

foetale voorloper-B-cellen in staat zijn om een divers Ig gen repertoire te vormen. Echter, in *IGH* genherschikkingen werden de proximale V, D en J gensegmenten relatief vaak gebruikt en waren de CDR3 regio's korter dan in jonge kinderen. De kortere CDR3 regio's waren het resultaat van verminderde aantallen N-nucleotiden in de juncties, en het frequente gebruik van de relatief korte D_{H7-27} , J_{H3} en J_{H4} gensegmenten. De verminderde aantallen N-nucleotiden waren niet beïnvloed door Ig repertoire selectie, maar een direct gevolg van verminderde expressie van *XRCC4* en TdT. Bovendien waren de receptoren *IL7R* en *FLT3* verlaagd op foetale voorloper-B-cellen, en leidt een *IL7R*-deficiëntie tot verminderde TdT expressie en N-nucleotide inserties in D-J juncties.

De belangrijkste locatie voor postnatale humane B-celdifferentiatie is het beenmerg. B-cellen bevinden zich echter ook in de thymus. Tijdens de negatieve selectie van T-cellen zouden deze B-cellen in de thymus rol spelen in de presentatie in MHC klasse II van autoantigenen, die zijn opgenomen door herkenning via de membraangebonden Ig. In **Hoofdstuk VI** hebben wij het Ig repertoire bestudeerd van B-cellen uit foetaal beenmerg, en beenmerg en thymus van kinderen. Wij hebben individuele B-cellen geïsoleerd om het Ig genrepertoire te bestuderen en om de Ig genen te kloneren. Van deze gekloneerde genen hebben we vervolgens in vitro antistoffen geproduceerd om te testen of ze autoantigenen kunnen binden. Wij vonden dat het Ig repertoire van B-cellen in de thymus vergelijkbaar was met dat van B-cellen in het beenmerg van kinderen. Er was geen verschuiving in V_H , D_H en J_H gengebruik zichtbaar, noch zagen wij de voor foetale BM B-cellen karakteristieke korte IgH-CDR3 regio's. Wel zagen wij dat B-cellen uit de thymus meer autoreactieve klonen bevatten. Deze autoreactieve klonen waren veelal specifiek voor peptide autoantigenen en juist niet voor dsDNA, zoals foetale B-cellen. Aangezien we geen voorloper-B-cellen konden aantonen in de thymus is het waarschijnlijk dat autoreactieve B-cellen die geproduceerd zijn in het beenmerg specifiek migreren naar de thymus, of specifiek in de thymus overleven, waardoor deze cellen relatief frequent aanwezig zijn.

De studies beschreven in dit proefschrift geven inzicht in de controlerende mechanismes voor de strikte regulatie van V(D)J-recombinatie en de ontwikkeling van een divers Ig repertoire tijdens de voorloper B-cel ontwikkeling. Het stapsgewijze V(D)J-recombinatie proces wordt gecontroleerd door transcriptionele en epigenetische mechanismes. Deze mechanismes moeten samenwerken om te zorgen dat de Ig loci beter toegankelijke worden voor V(D)J recombinatie tijdens een specifiek stadium van ontwikkeling. De vorming van een breed Ig repertoire is afhankelijk van de niche waar deze B-cellen zich ontwikkelen. De niche in het beenmerg ondergaat fysiologische veranderingen gedurende het leven en verzorgt op die manier verschillende signalen voor ontwikkelende B-cellen. Dit resulteert in een karakteristiek Ig repertoire met een specifieke reactiviteit tijdens verschillende fasen van het leven. Vervolgstudies moeten meer inzicht geven welke omgevingsfactoren de Ig loci toegankelijkheid voor de V(D)J-recombinase beïnvloeden en op

die manier het Ig repertoire en reactiviteit bepalen. Deze kennis zou toegepast kunnen worden om het beperkte Ig repertoire van immuundeficiëntie patiënten te verbreden zonder problemen te krijgen met autoreactiviteit.

ACKNOWLEDGEMENTS

Finally, the time has come to write the most important part of the book, the acknowledgements. I could not do this thesis alone and here I would like to thank the people that help me during my PhD journey. The journey began 5 years ago when as a foreigner coming from Poland, I stepped into the Immunology Department at Erasmus MC. Over the last years, I had a pleasure to work with many great people who helped me to grow and develop my scientific skills.

My dear promoter Jacques and co-promoter Menno, thank you for believing in me 5 years ago and that you gave me the chance to explore my passion in science. The last years have been extremely fruitful and during this period I learnt a lot from both of you. I am grateful for all your scientific support which undoubtedly shaped me as a scientist, who I am now. Dear Menno, although sometimes we had different opinion about things which led us to little arguments, I sincerely appreciate that you always stood by my side and supported me at every step of the PhD. I hope that my thesis defense is not the end of our relationship.

I also would like to thank my Doctoral Committee members. Dear Kees, Rudi, Tom, Prof. dr. Ellen van der Schoot, Prof. dr. Frank Staal and Dr. Heinz Jacobs, thank you for agreeing to become my Committee members and for your useful comments on my thesis. I am very glad that you participate in this important day to me.

I am very grateful to all co-authors of my papers. I could not write these manuscripts without your useful commentaries and constructive criticism. Dear Mirjam, next to the scientific support which you provided to me during writing the “fetal manuscript”, I also want to thank you for your kindness, sympathy and great understanding.

Dziękuję również Pani Joannie Strzelczyk i Panu Profesorowi Wiczkowskiemu za pomoc na samym początku mojej drogi naukowej. Bez Waszej pomocy, nie byłoby mnie tu dziś.

I would like to thank all the current and former members of my BCD group for their help with the experiments and support with the daily small things as well as unusual big things. Dear Diana, Christina, Britt, Jorn, Benjamin, Magda B., Katharina, Halima, Ruud, Marieke and Edwin, I think we created a very nice team of friends who always protected and supported each other in the good and bad times. I am very honored that I could be part of the team. I am sure that all of you will manage to pursue your scientific life further and I wish you all the best. Britt, thank you for translating my summary to Dutch. Diana, we started the PhDs together and we will finish together. You were the closest friend to me and I want to thank you for all the evening discussions about my papers and little chats about the life. Thanks to you, I didn't become insane.

I can not forget about my beloved students. Dear Kevin, Sanne and Roel, it was a pleasure to work with you and you contributed enormously to shape this thesis. Thank you for your hard work and friendship.

My dear roommate Karin, we shared the room at 9th floor of the old Erasmus MC faculty building for around 2 years. These were the funniest and nicest years of my PhD. You showed me how important it is to keep the balance between personal and professional life and I appreciate your relaxed attitude and distance to life. Thank you for all the pleasure talks accompanied by burgers and beers. Alice, Prisca and Fabian, my subsequent roommates, thank you for the nice atmosphere in the room which we shared after movement to the new building. Fabian, thank you for all the pleasure evening chats about science and that you agreed to become my paranymph.

I also want to thank the PhDs, now mainly Postdocs and Medical Doctors, with whom I spent most of my studies. Dear Hanna, Jeroen, Sita, Chris, Mati, Zana, Naomi, Nicole, Kim, I am very pleased that I could work with you and learn from you.

I also had the pleasure to work with many people outside the Immunology Department. Dear friends from Cell Biology Department, Robert-Jan, Anita and Ralph, it was a great fun to work with you and observe how enormously Departments can differ within the same Institute. I entered your field as a complete newbie but you thought me everything about the Seq procedures. I also would like to thank Eddy from Pediatrics Department for organizing the fetal samples and that you always remembered that I might need some more. Dear microscope experts, Gert and Gert-Jan, thank for your assistance with the microscopes, data acquisition and analysis.

I could not finish this PhD without a support from my family and friends. Kochani rodzice i siostra dziękuję Wam za całe wsparcie, którym mnie obdarzyliście, że zawsze akceptowaliście moje szalone pomysły wakacyjnych wyjazdów zagranicznych, aż wreszcie, że poparliście mój kilkuletni wyjazd do Holandii. Bez Waszej pomocy nie udałooby mi się zorganizować przeprowadzki i zaaklimatyzować w nowym kraju. Dziękuję również, że zawsze witacie mnie z otwartymi ramionami w domu.

Kochani przyjaciele w Holandii i w Polsce, Andrzej, Sylwia, Piotrek, Bartek, Paulina, dziękuję za wszystkie szalone imprezy i wycieczki, że pamiętamy o sobie pomimo codziennego zabiegania. Bartek, dziękuję, że zgodziłeś się zostać moją paranymph. Dear Reinier and Marsha thank you for creating such a nice working atmosphere for Mariusz, for being our personal bookkeeper, for the nice trip to Hanover and all the evening dinners.

Last but not least, to my husband. Mojemu mężowi chciałabym podziękować właściwie za wszystko. Dziękuję, że przyjechałeś za mną do Holandii, mimo, że musiałeś zostawić wiele w Polsce, że zawsze mogę na Ciebie liczyć, za spokój i opanowanie, gdy ja wpadam w panikę, że zawsze wiesz, co trzeba zrobić i nie ma takich problemów, których byśmy razem nie rozwiązali. Dziękuję, że po prostu przy mnie jesteś.

Approaching the end of my PhD, I am sure that my scientific journey is not over. It will last for many more years because the curiosity seed has been planted thanks to all of you.

PHD PORTFOLIO

Name PhD student	Magdalena Beata Rother
Erasmus MC Department	Immunology
Research School	Molecular Medicine
PhD period	September 2010 – November 2015
Promoter	Prof.dr. J.J.M. van Dongen
Co-promoter	Dr. M.C. van Zelm

PHD TRAINING

In-depth courses

2010	Leica Confocal Introduction
2010	Biomedical Research Technique
2011	Laboratory Animal Science
2011	Molecular Medicine
2011	Molecular Immunology
2012-2013	Biomedical English Writing and Communication
2014	Basic Introduction Course on SPSS

Seminars and minisymposia

2010-2013	Journal club at the Department of Immunology
2010-2014	Seminars and minisymposia at the Department of Immunology

Teaching

2011-2014	Histology for 1 st and 2 nd year Medicine Students
2011-2012	Bachelor thesis supervision
2012-2013	Master thesis supervision
2013-2014	Bachelor thesis supervision

National Conferences

- 2010 Dutch Society for Immunology (NVVI) Annual Meeting, Noordwijkerhout, the Netherlands
- 2011 15th Molecular Medicine Day, Rotterdam, the Netherlands; *poster presentation*
- 2011 Dutch Society for Immunology (NVVI) Annual Meeting, Noordwijkerhout, the Netherlands; *poster presentation*
- 2012 16th Molecular Medicine Day, Rotterdam, the Netherlands; *poster presentation*
- 2012 Dutch Society for Immunology (NVVI) Annual Meeting, Noordwijkerhout, the Netherlands; *poster presentation*
- 2013 17th Molecular Medicine Day, Rotterdam, the Netherlands; *poster presentation*
- 2013 Dutch Society for Immunology (NVVI) Annual Meeting, Noordwijkerhout, the Netherlands; *poster presentation*
- 2014 18th Molecular Medicine Day, Rotterdam, the Netherlands; *poster presentation*

International Conferences

- 2013 ‘Epigenetics & Chromatin: Interactions and processes’, Boston, MA, USA; *poster presentation*

Awards and funds

- 2013 Fund for conference attendance from the Dutch Society for Immunology (NVVI)
- 2014 Poster award from the Molecular Medicine Postgraduate School, Erasmus MC, Rotterdam, the Netherlands for the poster ‘Seemingly normal B-cell development with skewed immunoglobulin (Ig) repertoire formation in fetal bone marrow’.

CURRICULUM VITAE

Name	Magdalena Beata Rother
Date of birth	6 September 1985
Place of birth	Bytom, Poland
Nationality	Polish

Education

2010 – 2015	PhD studies; Erasmus MC, University Medical Center, Rotterdam, the Netherlands, Immunology Department
2004 – 2009	Master in Biotechnology; Medical University of Silesia, Katowice, Poland, Faculty of Pharmacy and Division of Laboratory Medicine, Proteomics Department
2007 – 2009	Student Scientific Group; Medical University of Silesia, Katowice, Poland, Faculty of Medicine and Division of Dentistry, General Biology Department
July 2007	Master internship; Cancer Center and Institute of Oncology, Gliwice, Poland, Molecular Biology Department
2000 – 2004	Secondary School No 4, Bytom, Poland

LIST OF PUBLICATIONS

1. Stadhouders R, de Bruijn MJW, **Rother MB**, Yuvaraj S, Ribeiro de Almeida C, Kolovos P, van Zelm MC, van Ijcken WFJ, Grosveld F, Soler E, Hendriks RW. Pre-B cell receptor signaling induces immunoglobulin κ locus accessibility by functional redistribution of enhancer-mediated chromatin interactions. *PLoS Biol* 2014; 12: e1001791
2. Jensen K, **Rother MB**, Brusletto BS, Olstad OK, Aass HCD, van Zelm MC, Kierulf K, Gautvik KM. Increased ID2 levels in adult precursor B cells as compared with children is associated with impaired Ig locus contraction and decreased bone marrow output. *J Immunol* 2013; 191:1210-1219
3. **Rother MB**, Palstra RJ, Jhunjhunwala S, van Kester KAM, van Ijcken WFJ, Hendriks RW, van Dongen JJM, Murre C, van Zelm MC. Nuclear positioning rather than contraction controls ordered rearrangements of immunoglobulin loci. *Manuscript accepted at Nucleic Acids Research*
4. **Rother MB**, Jensen K, van der Burg M, van den Bovenkamp FS, Kroek R, van Ijcken WFJ, van der Velden VHJ, Cupedo T, Olstad OK, van Dongen JJM, van Zelm MC. Altered V(D)J recombination underlies the skewed immunoglobulin repertoires in normal and malignant B-cell precursors from fetal origin. *Submitted*
5. **Rother MB**, Schreurs MWJ, Kroek R, Bartol SJW, van Dongen JJM, van Zelm MC. The human thymus is enriched for autoreactive B cells. *Submitted*